

BIOANALYTICAL DEVELOPMENT OF CHARGED CYCLODEXTRIN
CAPILLARY ELECTROKINETIC CHROMATOGRAPHY AND
MICROPERFUSION SAMPLING TO STUDY ENDOGENOUS D-SERINE AND
L-GLUTAMATE EFFLUX IN BRAIN

A
THESIS

Presented to the Faculty
of the University of Alaska Fairbanks
in Partial Fulfillment of the Requirements
for the Degree of
DOCTOR OF PHILOSOPHY

By

Daniel L. Kirschner, B.S.

Fairbanks, Alaska

May 2009

UMI Number: 3374162

INFORMATION TO USERS

The quality of this reproduction is dependent upon the quality of the copy submitted. Broken or indistinct print, colored or poor quality illustrations and photographs, print bleed-through, substandard margins, and improper alignment can adversely affect reproduction.

In the unlikely event that the author did not send a complete manuscript and there are missing pages, these will be noted. Also, if unauthorized copyright material had to be removed, a note will indicate the deletion.

UMI[®]

UMI Microform 3374162
Copyright 2009 by ProQuest LLC
All rights reserved. This microform edition is protected against
unauthorized copying under Title 17, United States Code.

ProQuest LLC
789 East Eisenhower Parkway
P.O. Box 1346
Ann Arbor, MI 48106-1346

BIOANALYTICAL DEVELOPMENT OF CHARGED CYCLODEXTRIN
CAPILLARY ELECTROKINETIC CHROMATOGRAPHY AND
MICROPERFUSION SAMPLING TO STUDY ENDOGENOUS D-SERINE AND
L-GLUTAMATE EFFLUX IN BRAIN

By

Daniel L. Kirschner

RECOMMENDED:

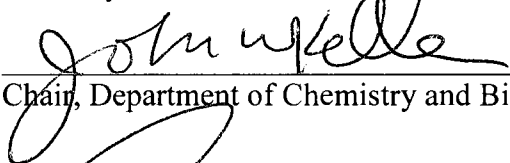









Advisory Committee Chair

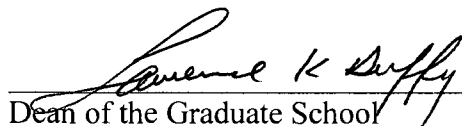


Chair, Department of Chemistry and Biochemistry

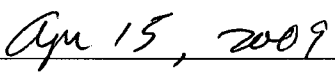
APPROVED:



Dean, College of Natural Science and Mathematics



Dean of the Graduate School



Date

Abstract

A multitude of studies have revealed specific biological mechanisms that contribute to D-amino acid action and regulation in the mammalian central nervous system. The remarkable increase in our understanding of D-amino acid function and distribution in mammals is in many ways a result of the development of sensitive enantioselective separation strategies that allow for quantification in real biological samples. In capillary electrokinetic chromatography (cEKC) the most powerful chiral resolving agents are anionic cyclodextrins (CDs), yet these have not previously been investigated for chiral bioanalysis of amino acids. The focus of this dissertation research was to investigate for the first time the feasibility of and application of anionic cyclodextrins as resolving agents in bioanalytical chiral separations of amino acids. This dissertation encompasses 1) the development of a new bioanalytical separation utilizing capillary electrophoresis laser induced fluorescence (CE-LIF) with sulfated- β -cyclodextrin for analysis of D-serine (D-ser) and L-glutamate (L-glu) in mammalian brain, 2) the first synthesis and characterization of 6 members of a new family of single isomer sulfoalkyl cyclodextrins, 3) initial studies on chiral analysis of amino acids using single isomer sulfoalkyl CDs, and 4) development and application of a novel microperfusion sampling approach for acute brain slices and coupling of this method to the developed chiral CE-LIF for studying magnitude and timing of D-ser and L-glu efflux from acute hippocampus in response to modeled cerebral ischemia. The results of these studies demonstrate that 1) anionic CDs are powerful chiral selectors for amino acids and can be applied for

sensitive bioanalysis of D-amino acids including D-ser, D-glu, and D-asp in brain samples; 2) single isomer sulfoalkyl CDs can be synthesized by regioselective reaction chemistry; 3) single isomer sulfoalkyl CDs are excellent resolving agents for amino acid analysis and may be valuable for bioanalytical chiral applications; and 4) microperfusion sampling coupled to CE-LIF can be used to analyze dynamic changes in the magnitude and timing of neurochemical efflux from single acute hippocampus slices exposed to modeled ischemia. Results of these latter studies suggest that D-ser and L-glu efflux occurs simultaneously in acute hippocampus with similar timing but differing magnitudes.

Table of Contents

	Page
Signature Page.....	i
Title Page.....	ii
Abstract.....	iii
Table of Contents.....	v
List of Figures.....	x
List of Tables.....	xvii
List of Manuscripts.....	xviii
Acknowledgements.....	xix
Chapter 1. Introduction.....	1
1.1 Biological significance of D-amino acid and regulation in CNS.....	1
1.2 Sensitive analytical approaches for D-amino acid quantification.....	10
1.2.1 Enzyme linked assays.....	10
1.2.2 Separation and detection of D-amino acids.....	12
1.3 Cyclodextrins in electrokinetic chromatography.....	24
1.4 Summary of research aims.....	35
Chapter 2. Development and application of S- β -CD cEKC for D-ser and L-glu analysis in microdialysates.....	37
2.1 Overview of study.....	37
2.2 Methods.....	39
2.2.1 Chemicals and reagents.....	39
2.2.2 Capillary electrophoresis apparatus.....	40

	Page
2.2.3 Derivatization procedure for separation and stacking studies.....	41
2.2.4 Capillary electrophoresis and enantioseparation studies.....	42
2.2.5 Construction of standard curves and analysis of microdialysates.....	43
2.2.6 ¹³ C NMR titration of ser and CBI-ser.....	44
2.3 Results.....	45
2.3.1 Chiral separation of CBI-derivatives.....	45
2.4 Stacking of dilute amino acid solutions with S-β-CD.....	59
2.5 Analysis of D-ser, DL-asp, and DL-glu in hippocampus of arctic ground squirrel.....	69
2.6 Summary of S-β-CD as chiral selector for CBI-amino acids.....	72
Chapter 3. Synthesis and characterization of single isomer sulfoalkyl cyclodextrins.....	73
3.1 Overview of study.....	73
3.2 Materials and methods.....	78
3.2.1 General methods.....	78
3.2.2 NMR spectral analysis.....	78
3.2.3 Indirect UV detection CE.....	79
3.3 Synthesis and characterization.....	79
3.3.1 Heptakis(6- <i>O-tert</i> -butyldimethylsilyl)cyclomaltoheptaose (2A) and Hexakis(6- <i>O-tert</i> -butyldimethylsilyl)cyclomaltohexaose (2B)	81
3.3.2 Heptakis(2,3-di- <i>O</i> -methyl-6- <i>O-tert</i> -butyldimethylsilyl)cyclomaltoheptaose (3A) and Hexakis(2,3-di- <i>O</i> -methyl-6- <i>O-tert</i> -butyldimethylsilyl)- cyclomaltohexaose (3B).....	85

	Page
3.3.3 Heptakis(2,3-di-O-ethyl-6-O- <i>tert</i> -butyldimethylsilyl)cyclomaltoheptaose (3C) and Hexakis(2,3-di-O-ethyl-6-O- <i>tert</i> -butyldimethylsilyl)-cyclomaltohexaose (3D).....	89
3.3.4 Heptakis(2,3-di-O-methyl)cyclomaltoheptaose (4A) and Hexakis(2,3-di-O-methyl)cyclomaltohexaose (4B).....	92
3.3.5 Heptakis(2,3-di-O-ethyl)cyclomaltoheptaose (4C) and Hexakis(2,3-di-O-ethyl)cyclomaltohexaose (4D).....	96
3.3.6 Heptakis(2,3-di-O-methyl-6-O-sulfopropyl)cyclomaltoheptaose (5A) and (5A').....	100
3.3.7 General Procedure for the synthesis of potassium salts of (5B), (5C), (5D), (5E), (5F).....	114
3.3.8 Characterization of heptakis(2,3-di-O-methyl-6-O-sulfobutyl)-cyclomaltoheptaose (5B).....	117
3.3.9 Characterization of hexakis(2,3-di-O-methyl-6-O-sulfopropyl)-cyclomaltohexaose (5C).....	121
3.3.10 Characterization of hexakis(2,3-di-O-methyl-6-O-sulfobutyl)-cyclomaltohexaose (5D).....	125
3.3.11 Characterization of hexakis(2,3-di-O-ethyl-6-O-sulfopropyl)-cyclomaltohexaose (5E).....	129
3.3.12 Characterization of heptakis(2,3-di-O-ethyl-6-O-sulfopropyl)-cyclomaltoheptaose (5F).....	133
3.4 Investigation of inclusion complex formation.....	138
3.5. Summary of findings on single isomer sulfoalkyl CD synthesis.....	141
Chapter 4. Chiral separation of CBI-amino acids with single isomer sulfoalkyl β -CDs.....	143
4.1 Overview of study.....	143
4.2 General methods.....	144

	Page
4.3 Results with single isomer sulfoalkyl CDs for chiral analysis.....	144
4.4 Summary of findings for enantioselectivity of KSPDM- β -CD, KSBMD- β -CD, and KSPDE- β -CD.....	167
Chapter 5. Simultaneous efflux of endogenous D-ser and L-glu from single acute hippocampus slices during oxygen glucose deprivation.....	169
5.1 Overview of study.....	169
5.2 Methods.....	171
5.2.1 General.....	171
5.2.2 Microperfusion chamber.....	171
5.2.3 Acute hippocampus slices.....	174
5.2.4 CE-LIF analysis.....	175
5.2.5 Monitoring treatment profile.....	176
5.2.6 Statistics.....	177
5.3 Results.....	177
5.4 Discussion.....	185
5.4.1 D-ser efflux from hippocampal slices during OGD.....	185
5.4.2 Validity of microperfusion chamber.....	186
5.4.3 Significance of L-thr efflux.....	187
5.4.4 Significance of L-gln efflux.....	188
5.4.5 Advantages of microperfusion/CE-LIF technique.....	189
5.5 Summary on microperfusion sampling with CE-LIF.....	190
Chapter 6. Conclusions.....	192

	Page
6.1 Overview.....	192
6.2 Conclusions on reverse polarity CD cEKC with S- β -CD.....	193
6.3 Conclusions on synthesis of selectively modified sulfoalkyl CDs.....	194
6.4 Conclusion on single isomer CDs as resolving agents for CBI-amino acids.....	195
6.5 Conclusions on Microperfusion/CE-LIF for D-ser and L-glu analysis during oxygen glucose deprivation.....	197
6.6 Final Remarks.....	198
References.....	200

List of Figures

	Page
Figure 1.1. Top view chemical structure of α -, β -, and γ -CD.....	25
Figure 1.2. Side view of cyclodextrin structure illustrating toroidal shape.....	26
Figure 1.3. Illustration of CD host:guest inclusion complex formation.....	27
Figure 1.4. Illustration of a typical capillary electrophoresis instrument with separation mechanism for ionic analyte.....	29
Figure 1.5. Illustration of CE modes of chiral recognition of fluorescently labeled amino acids published in bioanalytical methods.....	31
Figure 1.6. Illustration of reversed polarity CD-cEKC with anionic CDs.....	34
Figure 2.1. Reaction scheme for fluorescent labeling of amino acids with NDA.....	38
Figure 2.2. Absorbance and emission spectrum of CBI-tyr in water.....	42
Figure 2.3. Dependence of chiral resolution of CBI-ser on pH of the BGE.....	46
Figure 2.4. Effect of BGE pH on chiral resolution of CBI-amino acids.....	47
Figure 2.5. ^{13}C NMR titration of L-ser and CBI-L-ser.....	49
Figure 2.6. Comparison of electropherograms of CBI-L-ser in the presence and absence of S- β -CD at pH 3.....	51
Figure 2.7. Electropherogram of a mixture of CBI-DL-amino acids arg, ala, ser, and glu at 2 wt % S- β -CD.....	53
Figure 2.8. Effect of S- β -CD concentration on the migration time of CBI-amino acids.....	54
Figure 2.9. CBI-DL-arg migration time as a function of buffer pH at 2 wt % S- β -CD.....	55
Figure 2.10. Influence of phosphate buffer concentration on chiral resolution of a series of CBI-amino acids.....	56

Figure 2.11. Chiral separation of 14 CBI-amino acids with 2 wt % S- β -CD in 25 mM phosphate, pH 2.00.....	57
Figure 2.12. Stacking of dilute solutions of CBI-DL-ser and CBI-DL-glu using S- β -CD.....	60
Figure 2.13. Detection by hydrodynamic stacking of 1 nM each of CBI-DL-ser and CBI-DL-glu using S- β -CD.....	62
Figure 2.14. Stacking of a complex dilute sample of 11 CBI-amino acids with S- β -CD.....	63
Figure 2.15. Schematic diagram of the pH-mediated stacking/ sweeping-S- β -CD of chiral CBI-amino acids.....	64
Figure 2.16. Electropherograms from experiment demonstrating both pH mediated stacking and sweeping as mechanisms for S- β -CD.....	66
Figure 2.17. Linear regression calibration curves for CBI-amino acid standards for bioanalysis with S- β -CD.....	70
Figure 2.18. Typical electropherogram of a microdialysate from the hippocampus of an arctic ground squirrel	71
Figure 3.1. Comparison of the chiral separation of a mixture of CBI-DL-ser, CBI-DL-glu, CBI-L-asp using different synthetic batches of S- β -CD.....	75
Figure 3.2. General reaction scheme for the selective synthesis of single isomer sulfoalkylated cyclodextrins.....	80
Figure 3.3. ^1H NMR of heptakis(6-O- <i>tert</i> -butyldimethylsilyl)cyclomaltoheptaose (2A) in CDCl_3	82
Figure 3.4. ^{13}C NMR of heptakis(6-O- <i>tert</i> -butyldimethylsilyl)cyclomaltoheptaose (2A) in CDCl_3	83
Figure 3.5. ^1H NMR of hexakis(6-O- <i>tert</i> -butyldimethylsilyl)cyclomaltohexaose (2B) in CDCl_3	84
Figure 3.6. ^{13}C NMR of hexakis(6-O- <i>tert</i> -butyldimethylsilyl)cyclomaltohexaose (2B) in CDCl_3	85

	Page
Figure 3.7. ^1H NMR of heptakis(2,3-di-O-methyl-6-O- <i>tert</i> -butyldimethylsilyl)-cyclomaltoheptaose (3A) in acetone- d_6	86
Figure 3.8. ^{13}C NMR of heptakis(2,3-di-O-methyl-6-O- <i>tert</i> -butyldimethylsilyl)-cyclomaltoheptaose (3A) in acetone- d_6	87
Figure 3.9. ^1H NMR of hexakis(2,3-di-O-methyl-6-O- <i>tert</i> -butyldimethylsilyl)-cyclomaltohexaose (3A) in acetone- d_6	88
Figure 3.10. ^{13}C NMR of hexakis(2,3-di-O-methyl-6-O- <i>tert</i> -butyldimethylsilyl)-cyclomaltohexaose (3A) in acetone- d_6	89
Figure 3.11. ^1H NMR of heptakis(2,3-di-O-ethyl-6-O- <i>tert</i> -butyldimethylsilyl)-cyclomaltoheptaose (3C) in CDCl_3	90
Figure 3.12. ^1H NMR of hexakis(2,3-di-O-ethyl-6-O- <i>tert</i> -butyldimethylsilyl)-cyclomaltohexaose (3D) in CDCl_3	91
Figure 3.13. ^1H NMR of heptakis(2,3-di-O-methyl)cyclomaltoheptaose (4A) in acetone- d_6	93
Figure 3.14. ^{13}C NMR of heptakis(2,3-di-O-methyl)cyclomaltoheptaose (4A) in acetone- d_6	94
Figure 3.15. ^1H NMR of hexakis(2,3-di-O-methyl)cyclomaltohexaose (4B) in acetone- d_6	95
Figure 3.16. ^{13}C NMR of hexakis(2,3-di-O-methyl)cyclomaltohexaose (4B) in acetone- d_6	96
Figure 3.17. ^1H NMR of heptakis(2,3-di-O-ethyl)cyclomaltoheptaose (4C) in CDCl_3	97
Figure 3.18. ^{13}C NMR of heptakis(2,3-di-O-ethyl)cyclomaltoheptaose (4C) in CDCl_3	98
Figure 3.19. ^1H NMR of hexakis(2,3-di-O-ethyl)cyclomaltohexaose (4D) in CDCl_3	99
Figure 3.20. ^{13}C NMR of hexakis(2,3-di-O-ethyl)cyclomaltohexaose (4D) in CDCl_3	100

Figure 3.21. Indirect UV detection of heptakis(2,3-di-O-methyl-6-O-sulfopropyl)cyclomaltoheptaose (KSPDM- β -CD).....	103
Figure 3.22. ^1H NMR spectrum of KSPDM- β -CD (5A'), DS_{CE} 4.1 in D_2O	104
Figure 3.23. ^1H NMR reaction monitoring spectrum of (5A) from reaction using 18-crown-6 immediately after formation of gummy layer but prior to addition of excess propane sultone.....	106
Figure 3.24. ^1H NMR reaction monitoring spectrum of (5A) from reaction using 18-crown-6 after addition of excess 1,3-propane sultone.....	107
Figure 3.25. ^1H NMR spectra of acetone and ultrafiltration waste showing selective removal of impurities.....	108
Figure 3.26. ^1H NMR spectrum of pure heptakis(2,3-di-O-methyl-6-O-sulfopropyl)cyclomaltoheptaose (5A), DS_{CE} 6.9 in D_2O	110
Figure 3.27. ^{13}C NMR spectrum of pure heptakis(2,3-di-O-methyl-6-O-sulfopropyl)cyclomaltoheptaose (5A), DS_{CE} 6.9 in D_2O	111
Figure 3.28. ^1H NMR spectrum in DMSO-d_6 of heptakis(2,3-di-O-methyl-6-O-sulfopropyl)cyclomaltoheptaose (5A).....	112
Figure 3.29. ^1H NMR spectrum obtained for the crude acid of heptakis-(2,3-di-O-ethyl-6-O-sulfopropyl)cyclomaltoheptaose (5E) in D_2O	116
Figure 3.30. ^1H NMR spectrum of heptakis(2,3-di-O-methyl-6-O-sulfobutyl)cyclomaltoheptaose (5B), DS_{CE} 6.8 in D_2O	118
Figure 3.31. ^{13}C NMR spectrum of heptakis(2,3-di-O-methyl-6-O-sulfobutyl)cyclomaltoheptaose (5B), DS_{CE} 6.8 in D_2O	119
Figure 3.32. gCOSY NMR spectrum of heptakis(2,3-di-O-methyl-6-O-sulfobutyl)cyclomaltoheptaose (5B), DS_{CE} 6.8 in D_2O	120
Figure 3.33. gHSQC NMR spectrum of heptakis(2,3-di-O-methyl-6-O-sulfobutyl)cyclomaltoheptaose (5B), DS_{CE} 6.8 in D_2O	121
Figure 3.34. ^1H NMR spectrum of hexakis(2,3-di-O-methyl-6-O-sulfopropyl)cyclomaltohexaose (5C), DS_{CE} 6.0 in D_2O	122

Figure 3.35. ^{13}C NMR spectrum of hexakis(2,3-di-O-methyl-6-O-sulfopropyl)cyclomaltohexaose (5C), DS_{CE} 6.0 in D_2O	123
Figure 3.36. gCOSY NMR spectrum of hexakis(2,3-di-O-methyl-6-O-sulfopropyl)cyclomaltohexaose (5C), DS_{CE} 6.0 in D_2O	124
Figure 3.37. gHSQC NMR spectrum of hexakis(2,3-di-O-methyl-6-O-sulfopropyl)cyclomaltohexaose (5C), DS_{CE} 6.0 in D_2O	125
Figure 3.38. ^1H NMR spectrum of hexakis(2,3-di-O-methyl-6-O-sulfobutyl)cyclomaltohexaose (5D), DS_{CE} 5.8 in D_2O	126
Figure 3.39. ^{13}C NMR spectrum of hexakis(2,3-di-O-methyl-6-O-sulfobutyl)cyclomaltohexaose (5D), DS_{CE} 5.8 in D_2O	127
Figure 3.40. gCOSY NMR spectrum of hexakis(2,3-di-O-methyl-6-O-sulfobutyl)cyclomaltohexaose (5D), DS_{CE} 5.8 in D_2O	128
Figure 3.41. gHSQC NMR spectrum of hexakis(2,3-di-O-methyl-6-O-sulfobutyl)cyclomaltohexaose (5D), DS_{CE} 5.8 in D_2O	129
Figure 3.42. ^1H NMR spectrum of hexakis(2,3-di-O-ethyl-6-O-sulfopropyl)cyclomaltohexaose (5E), DS_{CE} 6.0 in D_2O	130
Figure 3.43. ^{13}C NMR spectrum of hexakis(2,3-di-O-ethyl-6-O-sulfopropyl)cyclomaltohexaose (5E), DS_{CE} 6.0 in D_2O	131
Figure 3.44. gCOSY NMR spectrum of hexakis(2,3-di-O-ethyl-6-O-sulfopropyl)cyclomaltohexaose (5E), DS_{CE} 6.0 in D_2O	132
Figure 3.45. gHSQC NMR spectrum of hexakis(2,3-di-O-ethyl-6-O-sulfopropyl)cyclomaltohexaose (5E), DS_{CE} 6.0 in D_2O	133
Figure 3.46. ^1H NMR spectrum of heptakis(2,3-di-O-ethyl-6-O-sulfopropyl)cyclomaltoheptaose (5F), DS_{CE} 6.8 in D_2O	134
Figure 3.47. ^{13}C NMR spectrum of heptakis(2,3-di-O-ethyl-6-O-sulfopropyl)cyclomaltoheptaose (5F), DS_{CE} 6.8 in D_2O	135
Figure 3.48. gCOSY NMR spectrum of heptakis(2,3-di-O-ethyl-6-O-sulfopropyl)cyclomaltoheptaose (5F), DS_{CE} 6.8 in D_2O	136

Figure 3.49. gHSQC NMR spectrum of heptakis(2,3-di-O-ethyl-6-O-sulfopropyl) cyclomaltoheptaose (5F), DS_{CE} 6.8 in D_2O	137
Figure 3.50. 2D ROESY spectrum of inclusion complex of KSPDM- β -CD:CBI-ser (molar ratio 2:1).....	139
Figure 3.51. Inclusion Complex of KSPDM- β -CD with CBI-ser in D_2O	140
Figure 4.1. Comparison of mobility and selectivity of KSPDM- β -CD and S- β -CD at low pH reversed polarity.....	145
Figure 4.2. Chiral separation of 9 CBI-amino acids using KSPDM- β -CD.....	147
Figure 4.3. Effect of KSPDM- β -CD concentration on chiral resolution of CBI-amino acids at low pH reversed polarity.....	149
Figure 4.4. Chiral separation of CBI-ser at 0.2 mM (~0.05 wt %) KSPDM- β -CD in the BGE.....	150
Figure 4.5. Chiral separation of 9 CBI-amino acids using KSBDM- β -CD.....	153
Figure 4.6. Effect of decreasing concentration of KSBDM- β -CD in the BGE on chiral resolution of CBI-amino acids at low pH reversed polarity.....	155
Figure 4.7. Comparison of CBI-glu enantioseparation in the presence and absence $\leq 100 \mu M$ KSBDM- β -CD in the BGE.....	157
Figure 4.8. Comparison of cationic CBI-his migration time with weakly acidic anionic CBI-amino acids.....	158
Figure 4.9. Effect of pH and anionic chiral selector on resolution of CBI-ser enantiomers.....	160
Figure 4.10. Chiral separation of 9 CBI-amino acids using KSPDE- β -CD.....	162
Figure 4.11. Comparison of chiral separation of CBI-glu and CBI-asp at pH 2.15 with 5.0 mM KSPDE- β -CD in the BGE.....	164

Figure 4.12. Reversal of EMO for 22:78 CBI-ala dependent on concentration of KSPDE- β -CD in the BGE.....	165
Figure 5.1. Custom Microperfusion chamber for single acute brain slices.....	172
Figure 5.2. Impact of narrow pH range on migration order and run time for CBI-amino acids for bioanalysis with S- β -CD.....	178
Figure 5.3. OGD treatment profile determined using trace D-glu perfusion across slices.....	180
Figure 5.4. Comparison of typical electropherograms from basal and OGD perfusate samples.....	181
Figure 5.5. Efflux profiles for amino acids from single acute hippocampus slices in response to OGD.....	182

List of Tables

	Page
Table 2.1. Migration and R_s values for CBI-DL-amino acids at 2 and 6% wt % S- β -CD.....	58
Table 2.2. Signal to Noise (S/N) Ratio, Resolution (R_s), and Estimated Concentration Limits of Detection (CLOD) for CBI-Ser and CBI-Glu.....	61
Table 2.3. Comparison of Full-Capillary Sample Stacking /Sweeping-MEKC and pH Mediated Stacking/Sweeping-S- β -CD of dilute CBI-amino acids.....	68
Table 2.4. Quantitative analysis of amino acids in microdialysate from hippocampus of arctic ground squirrel.....	72
Table 3.1. Effect of 18-crown-6 in reaction medium on the average degree of substitution of KSPDM- β -CD, (5A).....	113
Table 4.1. Summary of enhanced enantioresolution of CBI-amino acids at low (< 0.8 mM) concentrations of KSBDM- β -CD in the BGE.....	156
Table 5.1. Linear regression results for concentration determinations of amino acids in perfusate medium.....	179

List of Manuscripts

1. Kirschner D, Green T (2009) Separation and Sensitive Detection of D-amino acids in Biological Matrices. *J Sep Sci* (In Press).
2. Kirschner DL, Wilson AL, Drew KL, Green TK (2009) Simultaneous efflux of endogenous D-ser and L-glu from single acute hippocampus slices during oxygen glucose deprivation. *J Neurosci Res* (In Press).
3. Kirschner D, Jaramillo M, Green T, Hapiot F, Leclercq L, Bricout H, Monflier E (2008) Fine tuning of sulfoalkylated cyclodextrin structures to improve their mass-transfer properties in an aqueous biphasic hydroformylation reaction *J Mol Catal A Chem* 286:11-20.
4. Kirschner DL, Jaramillo M, Green TK (2007) Enantioseparation and stacking of Cyanobenz[f]isindole-amino acids by reverse polarity capillary electrophoresis and sulfated beta-cyclodextrin. *Anal Chem* 79:736-743.
5. Kirschner D, Green T, Hapiot F, Tilloy S, Leclercq L, Bricout H, Monflier E (2006) Heptakis(2,3-di-O-methyl-6-O-sulfopropyl)-beta-cyclodextrin: A Genuine Supramolecular Carrier for Aqueous Organometallic Catalysis. *Advanced Synthesis & Catalysis* 348:379-386.
6. Kirschner DL, Green TK (2005) Nonaqueous synthesis of a selectively modified, highly anionic sulfopropyl ether derivative of cyclomaltoheptaose (beta-cyclodextrin) in the presence of 18-crown-6. *Carbohydr Res* 340:1773-1779.

Acknowledgements

Firstly, I thank my wife Tammie for all her support throughout my education. I would like to express my sincere gratitude to the Department of Chemistry and Biochemistry and the Institute of Arctic Biology for research space, faculty support, and financial support. A large portion of this research was supported in part by funding through U.S. Army Research Office (W911NF-05-1-0280), U.S. Army Medical Research and Materiel Command (05178001) and NS041069-06 (National Institute of Neurological Disorders and Stroke, National Institute of Mental Health).

Several individuals at UAF have had a hand in one or more aspects of this research. I am thankful to members of the Green Research Lab (Analytical/Organic Chemistry) and Drew Research Lab (Neuroscience/Neurochemistry) for valuable insights and direct contributions. Specifically I would like to express thanks to Michael Jaramillo for his participation in scaling up the cyclodextrin synthesis for catalytic studies. Mike additionally participated in some of the early analytical method development for DL-ser chiral separations where he investigated a variety of neutral cyclodextrins under various normal polarity electrophoresis separation modes. Mike was frequently available throughout the early analytical studies to discuss ideas with. The NMR titration study described in Chapter 2 for L-ser was carried out by an undergraduate organic chemistry laboratory under the supervision of Mike Jaramillo. I am also grateful to Ann Wilson for providing brain slices and Jeanette Moore for help around the neuroscience lab. Also, I'd like to thank Dr. Eric Monflier from the University D'Artois for his collaboration in catalytic studies where his group carried out organometallic catalysis studies using single

isomer CDs developed here. Eric Johansen and Ned Manning from the UAF Engineering Department were very helpful aiding in the construction of the microchambers developed in this thesis. I am thankful to my committee members, and especially indebted to Dr. Kelly Drew for investing so much of her time and support in my research and education. Finally, I would like to express a deep gratitude to my thesis advisor, Dr. Tom Green, for teaching me a great deal about chemistry and offering me much more than simply space in his lab.

Chapter 1

Introduction

1.1 Biological significance of D-amino acids and regulation in CNS

Chirality is a pervasive feature of biological systems. Of the 20 common α -amino acids found in biology, only glycine lacks a stereocenter. The 19 L-amino acids are widespread in nature and critical for life processes. In contrast, until recently the presence of D-isomers of amino acids was accepted only in lower organisms such as bacteria where they predominately play structural roles in peptidoglycan layers of cell walls (Bhattacharyya and Banerjee, 1974). Essentially all bacteria have been shown to produce, metabolize, and store D-amino acids; the presence of D-amino acids in mammalian brain and other tissue was thought to indicate bacterial contamination of samples (Corrigan, 1969). In 1987, Man et al. identified age dependent levels of D-aspartate in hydrolyzed protein samples from human white brain matter (Man et al., 1987). Their approach relied on isolating tissue samples, liberating amino acids, concentrating, labeling with fluorinated agents to increase volatility, and quantifying amino acid enantiomers by chiral gas chromatography mass spectrometry (GC-MS). Around the same time, Dunlop et al. identified significant levels of free D-aspartate in brain and other tissue of mammals (Dunlop et al., 1986) using high performance liquid chromatography (HPLC) with fluorescence detection. This latter approach allowed for the study of free aspartate in newborn rat brain tissue where they found high levels of D-aspartate that decrease systematically with aging. Other related studies with chick embryos demonstrated that

free D-asp increases with development in the egg (a closed system) then decreases during postnatal stages (Neidle and Dunlop, 1990). Today, D-asp is known to be produced in mammalian brain with particular localization to glandular structures involved in hormone regulation including the pituitary and pineal glands (Schell et al., 1997a). Among its effectors, D-asp may act in glandular structures in the CNS to regulate release of prolactin and melatonin (Furuchi and Homma, 2005; D'Aniello, 2007).

In 1992, Hashimoto and associates utilized chiral HPLC coupled to amino acid derivatization and sensitive fluorescence detection and confirmed several of the earlier studies on D-asp localization and developmental changes. Importantly, these newer studies demonstrated high levels of free D-serine (D-ser) in the central nervous system (CNS) with particular localization in forebrain regions (Hashimoto et al., 1992b; Hashimoto et al., 1992a; Hashimoto et al., 1993b; Hashimoto et al., 1993a). Typical levels of D-ser in the CNS are as much as one-third that of the corresponding L enantiomer making free D-ser overall the most abundant D-amino acid in the brain. In forebrain regions the concentration of free D-ser is commonly higher than many L-isomers. In contrast to D-asp, Hashimoto demonstrated that free D-ser remains in high levels in the CNS from developmental stages throughout adulthood. The localization of D-ser in CNS is consistent with a regulatory role on the N-methyl-D-aspartate receptor (NMDAR) (Hashimoto et al., 1993a; Schell et al., 1997b).

The NMDAR is a glutamatergic ligand gated ion channel with permeability for Na^+ , K^+ , and Ca^{2+} (Hille, 2001). A functional channel is a heterodimer of NR1 and NR2 subunits.

NR3 subunits have also been identified and co-expressed with NR1 though their physiological relevance in the CNS is not well known; NR1-NR3 channels are not activated by glutamate (Chatterton et al., 2002; Nilsson et al., 2007; Yao et al., 2008). In contrast to ionotropic glutamate receptor channels, α -amino-3-hydroxyl-5-methyl-4-isoxazole-propionate receptors (AMPA) and Kainate receptors (KAR), the NMDAR shows greater permeability for Ca^{2+} (Iino et al., 1990; Jonas, 1993). It is expressed throughout the CNS with high levels in forebrain regions and studies demonstrate NMDAR plays critical roles in a variety of physiological functions and disorders ranging from cell excitability to learning and memory to necrotic and apoptotic cell death (Wolosker, 2007). The NMDAR is known to contain at least 7 distinct binding domains for endogenous regulators. This suggests its activity is highly controlled in the CNS. The receptor is unique among known neurotransmitter receptors in its requirement for coagonist activation. Simultaneous binding of L-glu and coagonist typically identified as glycine (gly) at their distinct binding domains on the NR2 and NR1 subunits respectively, is required for channel activation (Wroblewski et al., 1989; Dingledine et al., 1990).

Prior to the work of Hashimoto, the notion that D-ser can regulate the glutamatergic NMDAR was well established. Both D-ser and D-alanine (D-ala) bind with high affinity to the strychnine insensitive glycine site on the NR1 subunit with as much as 100-fold more potency than their corresponding L-isomers (Kleckner and Dingledine, 1988; McBain et al., 1989; Dingledine et al., 1990). These early studies were considered

'nonphysiological' responses since D-amino acids were not believed to exist in significant levels in the CNS.

The early work by Hashimoto and the advent of sensitive chiral HPLC suggested a physiological role for D-ser and provided a common sensitive analytical tool to investigate D-amino acid dynamics in addition to several important L-isomers simultaneously. Over the next couple of years, multiple studies were undertaken that provided clues as to what physiological role D-ser might play in the CNS. Polyclonal antibodies were initially developed for D-ser allowing for selective detection and studies on regional localization, uptake, and release in brain tissue (Schell et al., 1995).

Dunlop and Neidle investigated the fate of L-ser in CNS and provided strong evidence for the endogenous origin of D-ser in mammals (Dunlop and Neidle, 1997). They utilized microdialysis for administering glucose, glycine, and ^3H -L-ser. In addition, they quantified pools of free D-ser in response to administration of these metabolites. Their results show that ^3H -D-ser is produced in CNS after administration of the L-isomer providing evidence for racemization of D-ser in the CNS. In 1999, Snyder and colleagues provided definitive proof for D-ser regulation in the CNS by isolating its synthetic enzyme from glia cultures (Wolosker et al., 1999a; Wolosker et al., 1999b). Serine racemase (SR) selectively catalyzes the conversion of L-ser to D-ser in the mammalian CNS. Incubation of glial cultures with exogenous L-ser was shown to increase production of D-ser. The enzyme is pyridoxyl phosphate dependent and in addition to racemization activity, has been shown to catalyze α,β -elimination to form hydroxypyruvate.

Immunohistochemistry demonstrates that SR is expressed in glia near glutamatergic neurons (Wolosker et al., 1999a). Initially this strict localization to glia was confirmed by staining techniques which did not stain neurons as determined by co-staining with neuronal markers. Recently however, newer antibodies and staining techniques demonstrate high levels of SR in neurons (Kartvelishvily et al., 2006). Purified neuron cultures from cortex of rat and mice were shown to contain high levels of SR and these cultures produce D-ser when L-ser is exogenously supplied. A recent study which utilized novel serine racemase knockout mice suggests that SR is primarily expressed in neurons in the rat CNS (Miya et al., 2008).

The regional distribution of D-ser in the CNS as determined by immunostaining and quantitative HPLC is consistent with the notion that D-amino acid oxidase (DAAO) is responsible for catabolism. DAAO was first identified in mammals in by Hans Krebs (Krebs, 1935) though little significance was given to the mammalian oxidase since it was believed that higher mammals did not utilize D-amino acids. Immunostaining studies suggest the enzyme is expressed exclusively in glia with a regional distribution in the CNS which is opposite to immunohistochemical staining for D-ser; increased staining of DAAO in brainstem and cerebellum is consistent with low D-ser staining in these regions (Horiike et al., 1994; Nagata et al., 1994).

Several studies have provided evidence for regulated release of D-ser in to extracellular space from both glia and neurons. A mechanism of controlled release suggests that D-ser dynamically regulates NMDAR function. Early work by Schell and Snyder suggested a glutamate receptor dependent efflux of D-ser from glial cultures (Schell et al., 1995).

Immunostaining of glial cells loaded with ^3H -D-ser decreases when cells are incubated with ionotropic glutamate receptor agonists kainate, AMPA, and glutamate; the effect is blocked by co-application of selective antagonists of AMPA and Kainate receptors. These studies were supported by Ribeiro and colleagues who demonstrated a kainate concentration dependent increase in ^3H -D-ser efflux from glial cultures that was blocked with the selective antagonist DNQX (Ribeiro et al., 2002). Mothet et al. investigated rapid efflux of D-ser from glial cultures using a unique luminol based double enzyme linked assay (Mothet et al., 2005). Application of 100 μM glutamate, AMPA, kainate, or metabotropic receptor nonselective agonist (1S,3R)-1-aminocyclopentane-1,3-dicarboxylic acid (t-ACPD) for 5 s elicited rapid efflux of D-ser over a $\sim 10\text{s}$ period which was blocked by selective antagonists of the ionotropic and metabotropic receptors. The mechanism of glu dependent release in glia was demonstrated to be Ca^{2+} dependent and apparently vesicular since various modifiers of calcium systematically altered release and potent blockers of vesicular loading (vesicular H^+ -ATPase inhibitors) and docking (vesicular SNARE protease tetanus neurotoxin) abolished glu receptor dependent D-ser release in these glia cultures.

Support for compartmentalization of D-ser into vesicles comes from two separate studies. Williams et al. investigated D-ser immunoreactivity in glial cells using a new antibody that allows for superior co-localization studies with fixation-sensitive antigens than previously available (Williams et al., 2006). They demonstrate that D-ser immunoreactivity is punctate in glial processes rather than being uniformly distributed throughout. They suggest that to achieve this nonuniform distribution D-ser must be

compartmentalized. They further noted that many immunoreactive glial puncta were localized near cell walls suggesting the possibility of vesicular-like storage in glia. Martineau et al. used confocal imaging with co-localization quantification to track exocytotic routes of D-ser and provide morphological evidence for Ca^{2+} and SNARE protein-dependent D-ser release from astrocytes (Martineau et al., 2008). They reveal that D-ser immunoreactivity in glia co-localizes with vesicular protein markers, that D-ser loading in to vesicles occurs directly from the cytosol, and that stimulus induced calcium elevation causes recruitment of labeled synaptic vesicles to the plasma membrane with a concomitant loss of D-ser immunoreactivity as it is released from the cell. Taken together, recent studies on D-ser cytochemical localization and regulated release provides compelling evidence that D-ser is stored in and released from glial secretory vesicles through calcium dependent exocytosis after ionotropic glutamate receptor activation.

Future studies will be required to determine definitively if D-ser can be released from neurons by a similar mechanism as seen in glia. Kartvelishvily and coworkers provide evidence that D-ser synthesized in pure cortical neuron cultures can be released by ionotropic glutamate receptor activation (Kartvelishvily et al., 2006). Furthermore, they demonstrate that release of D-ser is Ca^{2+} dependent in these cultures. Despite this they suggest that the release may not be vesicular since attempts to block release through blockade of vesicle loading (vesicular H^+ -ATPase inhibitor) did not decrease evoked D-ser release. In addition, synaptic vesicles isolated from these neuron cultures did not take up D-ser under conditions that are optimal for L-glu uptake.

Two distinct transporters have been implicated for D-ser uptake in the CNS and while both operate based on heteroexchange of small neutral amino acids; they are functionally and structurally quite distinct. The alanine serine cysteine 1 (ASC-1) transporter was identified by Fukasawa and colleagues after isolation of the cDNA from mouse brain and shown to transport D-ser with a K_m of 52 μM when expressed in *Xenopus Oocytes*. The human isoform transports D-ser with a K_m of 21 μM . ASC-1 shows up to 65% structural homology with members of the L-amino acid transporter (LAT) family and requires co-expression of type II membrane glycoprotein 4F2 heavy chain for activity. The transporter is Na^+ independent and pH independent and operates primarily by amino acid exchange though also to a lesser degree by facilitated diffusion. It transports small neutral amino acids with preference for L-isomers. Particular affinity is demonstrated for gly, L-ala, L-ser, L-cys, and L-thr, and D-ser. Helboe and colleagues developed a polyclonal antibody against ASC-1 in mouse to determine its expression in the CNS (Helboe et al., 2003). They found that ASC-1 is distributed throughout the CNS including cortex, hippocampus, striatum, thalamic structures, cerebellum, and brain stem. Ultrastructurally, ASC-1 appears to be expressed exclusively in neurons and primarily at presynaptic terminals suggesting its functional expression may allow for D-ser clearance from synaptic space. A similar finding at this structural level for ASC-1 in neurons was confirmed in rat CNS using polyclonal antibodies against the rat isoform (Matsuo et al., 2004).

A recent study utilizing synaptosomes isolated from ASC-1 gene knockout mice suggests ASC-1 is the primary transporter of D-ser in the CNS (Rutter et al., 2007). ^3H -

D-ser uptake in cerebellar and forebrain synaptosomes was reduced to ~30% of wildtype levels in knockout mice and further omission of Na^+ reduced this to <10% of wildtype levels. This suggests that the Na^+ independent transporter ASC-1 mediates the majority of D-ser uptake in the CNS. The remaining uptake in knockout mice synaptosomes is primarily low affinity (approaching millimolar value) Na^+ dependent transport. The alanine serine cysteine transporter 2 (ASCT-2) is a heteroexchange neutral amino acid transporter with structural homology placing it in the excitatory amino acid transporter (EAAT) superfamily. ASCT-2 most likely mediates low affinity Na^+ dependent transport of D-ser and other small neutral amino acids in the CNS (Utsunomiya-Tate et al., 1996; Broer et al., 2000). Ribeiro and colleagues demonstrated that astrocyte rich primary cortical cultures from rat, take-up D-ser by low affinity Na^+ dependent heteroexchange (Ribeiro et al., 2002). A low affinity component of D-ser transport was verified recently by studies investigated high affinity ASC-1 dependent D-ser transport (Rutter et al., 2007).

In 2005, ASC-1 knockout mice were generated and behavioral phenotype was established (Xie et al., 2005). These mice displayed tremors, ataxia, seizures, and early postnatal death. Seizures and tremors were significantly reduced using NMDAR antagonist MK-801 suggesting that D-ser uptake by ASC-1 may be critical for normal physiological function. Studies are awaited on development of SR knockout mice which would be incapable of producing endogenous D-ser.

1.2 Sensitive analytical approaches for D-amino acid quantification

The discoveries of D-amino acids in biological samples and the physiological significance, particularly D-ser and D-asp, have stimulated new efforts to develop quantitative chiral selective bioanalytical techniques to measure physiological levels and study dynamics in brain. Sensitive approaches are either enzyme-linked assays or separation and detection based. Enzyme-linked assays can offer unique selectivity and sensitivity without the need for sample cleanup and separation. The limitation of these approaches is due to the fact that they are selective only as single component assays and in addition few enzymes for D-isomers of amino acids are available. Multiple distinct enzyme assays would be required in parallel preparations if multiple components were to be analyzed by this approach alone.

1.2.1 Enzyme linked assays

Due to the predominance of L-amino acids in CNS, only a few select enzymes have been identified that show D-amino acid specificity. DAAO reacts with D-ser in the presence of molecular O_2 to form hydroxypyruvate and H_2O_2 . The enzyme is not selective to D-ser alone however, and catalyzes α -keto acids formation from many D-isomers. Despite this, the production of H_2O_2 by this enzyme has been used to estimate D-ser levels in mammalian brain by several approaches which indirectly detect peroxide generation. Enzyme assays can be adapted to study a variety of biological tissues including CNS tissue *in vivo*. Recently, Pernot et al. developed a yeast D-amino acid oxidase microbiosensor (enzyme microelectrode) that is highly selective for D-ser compared

with L-amino acids and offers a mean response time of 2 s and detection limit of 16 nM *in vivo* (Pernot et al., 2008). A platinum microelectrode is initially coated with a membrane layer of poly-m-phenylene-diamine (PPD) that prevents oxidation of common metabolites such as ascorbic acid, uric acid, serotonin, and dopamine by the electrode. A layer of DAAO enzyme follows the PPD coating. When a potential is applied, free D-ser in the vicinity of the enzyme electrode is converted to hydroxypyruvate and H₂O₂ by DAAO with the latter product being oxidized at an applied potential of + 500 mV versus the Ag/AgCl reference electrode. The current recorded from oxidation is used to determine [D-ser] based on calibration curves. The approach was used to assay D-ser in cortex of live anesthetized rats. From a selectivity standpoint, the approach is sensitive only to total D-amino acids. The selectivity observed for D-ser compared to other D-isomers was primarily due to the apparent low abundance of other D-amino acids in the CNS relative to D-ser.

DAAO enzyme linked assays have also been adapted *in vitro*. One approach investigated dynamic changes in D-ser in extracellular space from glial cells in culture by linking peroxide generation from DAAO to peroxide reduction through oxidation of luminol catalyzed by horse radish peroxidase (HRP) (Mothet et al., 2005). In this double enzyme linked assay, DAAO, HRP, and luminol are added to cultures and luminescence is quantified. The assay provides detection limits approaching 40 pM for D-ser.

1.2.2 Separation and detection of D-amino acids

The vast majority of bioanalytical approaches for chiral amino acid analysis rely on separation and detection strategies after derivatization of the native metabolite. Derivatization plays one or more functional roles depending on the analytical approach including 1) increasing detection limits by introducing chromophores and/or fluorophores for spectrophotometric detection, 2) increasing volatility of amino acids for GC based separations, and 3) conversion of enantiomers to diastereomers. High performance liquid chromatography (HPLC), gas chromatography (GC), and capillary electrophoresis (CE) have all been used to analyze derivatized DL-amino acids in the CNS and a multitude of approaches are available.

A fundamental distinction for chiral separation strategies in LC, GC, and CE is whether the chiral resolving mechanism is direct or indirect with respect to diastereomer formation. Direct methods for diastereomer formation are the most common approach in chromatographic techniques and involve chemically derivatizing the enantiomers using optically pure chiral reagents. Most commonly this reagent is linked to a fluorophore for sensitive detection though in GC it is commonly perfluorinated to alter vapor pressure. The derivatized pair of diastereomers can then be directly separated using standard separation approaches. Care must be taken with respect to optical purity and reaction kinetics since long reaction times can lead to differential rates of diastereomer production. Indirect methods for diastereomer formation (direct chiral recognition) involve noncovalent reversible diastereomer formation through interaction of the chiral solute with a chiral phase. A variety of chiral columns are commercially available for

HPLC and GC as are chiral and achiral derivatization agents. In CE the chiral selector is most commonly added directly to the separation buffer (Weinberger, 2000).

GC was one of the first approaches for quantifying D-amino acids such as D-asp (Man et al., 1987) and D-ser (Hashimoto et al., 1992b) in the mammalian brain. It has proven valuable for quantitative D-isomer determinations in bulk tissue and media but is currently not applicable to small volume samples such as microdialysates due to sample preparation requirements. These generally include successive cumbersome steps after deproteination including sample extraction, evaporation, and re-suspension, prior to derivatization at high temperature (~100 °C). After derivatization samples are commonly extracted and dried to remove residual water which interferes with GC-MS analysis. In some cases amino acids are first isolated by cation exchange prior to these steps (Bruckner and Hausch, 1993). Ultimately, precolumn derivatization is required to increase volatility of amino acids. For analysis of biological samples one of the more successful approaches is achiral derivatization with pentafluoropropionic anhydride (PFPA) followed by chiral separation on a Chirasil L-valine ((N-2-methylpropionyl-L-valine-t-butylamide)-methylpolysiloxane immobilized) fused silica column. Separation is dependent on formation of multiple hydrogen bonds with the stationary phase (Gubitz and Schmid, 2001; Schurig, 2001). Hashimoto et al. used this approach to quantify D-ser distribution in mammalian neural tissue for the first time (Hashimoto et al., 1992b). The approach has been used to analyze D-ser and gly levels in serum with an analysis time of 11 min (Fuchs et al., 2008). One of the advantages of GC-MS with Chirasil L-valine is the high peak capacity in temperature gradient mode which under optimal

conditions allows for quantification of most DL-isomers including D-asp and D-ala in a single analysis. Brückner and colleagues have extensively used this approach to evaluate relative and absolute levels of 13 D-isomer in mammalian tissue homogenates, serum, urine, and feces from a variety of species (Bruckner and Hausch, 1993; Schieber et al., 1997; Bruckner and Schieber, 2001; Patzold et al., 2005).

HPLC is widely used for analysis of chiral compounds though the technique has several limitations in this respect when applied to biological samples. Sample throughput is often limiting in chiral HPLC of amino acids since retention times for most typical bioanalytical methods are generally > 20 min and most enantioselective analysis times range from 20-70 min. Separation efficiency is less than GC and CE (Dong, 2006). Chiral HPLC columns are expensive and their selection and subsequent appropriate method development may not be straight forward. In addition, sample volumes are typically quite large (5-50 μL), which can limit the nature of the tissue samples being analyzed for trace metabolites. This becomes especially important with *in vivo* microdialysis studies (Benveniste et al., 1984), and especially where low volume sampling probes can collect extracellular neurotransmitters in a near-real time (Lada et al., 1997). Temporal resolution of neurochemical events such as stimulated increases or decreases of neurotransmitters is limited by the volume of sample that must be pooled for a given LC analysis. Typically microdialysis flow rates range from 0.5 to 3.0 $\mu\text{L}/\text{min}$ for analysis of amino acid neurotransmitters, thus anywhere from 5-20 minutes may be required for each fraction analyzed by most HPLC approaches. Nonetheless, HPLC techniques are widely utilized for the separation of D-ser and other amino acid

neurochemicals both *in vitro* and *in vivo*. Most HPLC methods offer excellent precision and accuracy.

One of the first sensitive HPLC methods identifying D-ser in CNS was developed by Hashimoto et al. for D-ser, D-asp, and D-ala quantification in neural tissue and cerebral spinal fluid (Hashimoto et al., 1992a). Analysis time was optimized at 29 min for D-ser and ~75 min to quantify 18 amino acids (excluding column re-equilibration time). Derivatization using *ortho*-phthalaldehyde (OPA) and the chiral thiol *N-tert*-butyloxycarbonyl-L-cysteine (BOC-L-cys) in combination with gradient elution allowed for fluorescence detection of the isoindole diastereomer products with excitation at 344 nm and emission 443 nm. Detection limits for the assay were in the low picomolar range per injection (~25 nM free amino acid LOD calculated based on reported injection and calibration curves). Due to the diastereomeric products formed in the derivatization step, the use of standard octadecyl silane (C-18) reversed phase column is sufficient for separation. This initial approach is still widely used for analysis of D-ser, D-asp and/or D-ala along with several L-amino acids without significant alterations (Dunlop and Neidle, 1997; Takahashi et al., 1997; Morikawa et al., 2001; De Miranda et al., 2002; Shleper et al., 2005; Panizzutti et al., 2006) despite criticism of the stability of the OPA derivative (Jacobs et al., 1986) as well as a prerequisite in some assays to ‘prove’ the D-ser peak by DAAO catabolism for each analysis. This latter prerequisite was required in cell culture assays where the D-ser OPA derivative partially overlapped a preceding major metabolite (Shleper et al., 2005).

Alternative chiral thiols have been used with OPA to alter selectivity and stability of the isoindole DL-amino acid derivatives (Lo et al., 1998; Grant et al., 2006). Selectivity appears to be the primary concern with assays being developed to allow D-ser quantification in neural samples in conjunction with major metabolites including L-glu, L-asp, L-ser, gly, taurine, and phosphoethanolamine.

Several studies utilize achiral fluorescent labeling reagents in conjunction with chiral bonded HPLC columns. Following deproteination of serum and brain tissue homogenates, sensitive determination of D-ala, D-lys, and D-ser was obtained by HPLC with precolumn fluorescent labeling using 4-fluoro-7-nitro-2,1,3-benzoxadiazole (NBD-F) with excitation at 470 nm and emission at 530 nm and a Sumichiral OA-2500 column (Fukushima et al., 1995). The separation was successful for baseline resolving DL-isomers though in several cases the isomers partially overlapped unknown components when studied in serum and brain tissue. The achiral NBD-F labeling reagent displays superior stability compared to OPA, requires elevated temperature and longer reaction time compared with OPA, and offers sufficient quantum yields for fluorescence detection of biological samples.

Naphthalene-2,3-dicarboxaldehyde (NDA) was developed as an alternative reagent to OPA which offers higher quantum yields and better stability for primary amine derivatization (De Montigny et al., 1987). The reagent was recently reviewed (Rammouz et al., 2007) but significant progress in chiral amino acid bioanalytical methods development by HPLC is lacking. Duchateau et al. investigated enantioseparation of DL-amino acids by HPLC using β -cyclodextrin bonded stationary phases (Duchateau et al.,

1992). Ammonium nitrate/methanol mobile phase compositions were studied and a dramatic effect of pH and buffer concentration on retention times was noted. The method was capable of separating several neutral NDA derivatized DL-amino acids but was not studied for enantioseparations in biological samples.

A column switching HPLC approach has been valuable for determining trace DL-amino acid levels in the CNS and was recently reviewed in part (Hamase, 2007). Column switching HPLC with fluorescence detection using a variety of individualized protocols has been successful for the quantification of trace D-isomers of amino acids in neural tissue, plasma, and urine. Levels of DL-ser (Fukushima et al., 2004), DL-asp (Long et al., 2001), DL-ala (Morikawa et al., 2003; Morikawa et al., 2008), DL-leu (Inoue et al., 2000; Hamase et al., 2001), DL-val (Hamase et al., 2007), DL-isoleucine (Hamase et al., 2007), DL-pro (Hamase et al., 2001; Hamase et al., 2006; Tojo et al., 2008), and DL-thr and *D-allo*-thr (Zhao et al., 2004) have been determined in biological samples. Generally, precolumn derivatization with NBD-F or an alternative fluorescent reagent that produces stable derivatives is followed by reversed phase HPLC on C-18 column and fractionation of the respective mixed DL-isomer band of interest. The enantiomer ratio of the fractionated band is then determined subsequently by timed online post-column switching with separation and detection using a chiral bonded column and fluorescence detector. The first separation step with achiral RP-HPLC is capable of baseline resolving a large number of amino acids which can be valuable for biological studies if certain amino acids are known to exist overwhelmingly in one form. The chiral component of interest can then be determined through online column coupling and

detection. When micro-RP-HPLC is used for the first separation step, optimal sensitivity can be obtained for the fractionated band (Hamase, 2007). Major limitation relates to the cost of operating the system which requires two fluorescent detectors and multiple LC columns as well as analysis times which generally exceed 50 min per sample. The system is capable of quantifying one chiral pair at a time.

Song and colleagues recently developed a micro-HPLC approach with electrospray ionization tandem mass spectrometry (ESI-MS/MS) to analyze DL-ser, DL-glu, and DL-asp in neural tissue from *Aplysia* ganglia (Song et al., 2006; Song et al., 2007) and rat (Song et al., 2006; Song et al., 2008). Detection was by selective reaction monitoring (SRM) for the precursor-to-product ion transitions for NBD-labeled amino acids. A quadrupole linear ion trap (Q-trap) MS operated in positive ion mode was used for detection. This was the first approach for sensitive D-amino acid analysis in biological samples by tandem MS techniques. Precolumn derivatization with NBD-F followed by sample enrichment by stacking on a C-18 extraction microcolumn was required prior to separation for optimal sensitivity. Samples were loaded directly by switching valve from the extraction column to a micro-HPLC column consisting of chiral antibiotic (Teicoplanin aglycon) bonded stationary phase. The use of tandem MS with SRM allowed for elimination of chromatographic interferences and the application of co-eluting ^3H -labeled DL-amino acid isotopes as internal standards. Detection limits for D-isomers were ~ 100 ng/mL by this approach. Taking into account the microextraction step, an injection cycle time of ~ 50 min was optimized for the separation. The technique was used to investigate differences in DL-asp, DL-glu, and DL-ser levels in total brain

extracts from rats as well as regional variations in these D-amino acids in *Aplysia* ganglia neural processes.

Berna et al. recently developed a rapid and sensitive HPLC-ESI-MS/MS approach for DL-ser quantification in microdialysates after chiral derivatization using fluorodinitrophenyl-L-alanine amide (DNPA-F, “Marfey’s reagent”) and diastereomer separation using RP-HPLC (Berna and Ackermann, 2007). An injection cycle time of 3.5 min is reported. The approach utilized a Q-trap in negative ion mode for detection and a 2.1 mm I.D. C-18 column for separation. The offline derivatization step was carried out in microplate format and followed by evaporation of the medium to dryness and resuspension of the residue in separation buffer. Quantification was carried out by MS/MS in SRM mode with a reported 10.3 ng/mL LOD. The approach was recently adapted to triple quadrupole by Fuchs and colleagues in negative ion spray mode and selective ion monitoring (SIM) and included quantification of glycine in addition to DL-ser (Fuchs et al., 2008).

High Performance Capillary Electrophoresis (HPCE) coupled with laser induced fluorescence detection (CE-LIF) has been established as an efficient approach for D-amino acid analysis in biological samples. Chiral CE-LIF has many advantages over GC and LC approaches and can provide high sensitivity for amino acid analysis in biological samples. Like HPLC and GC, CE is capable of monitoring multiple components which is often of significant value in biological studies. The technique is cheap to maintain, requiring small quantities (<60mM) of chiral selector dissolved in small volumes of aqueous background electrolyte (BGE). Chiral method development is, in principle,

much simpler than HPLC since chiral selectors and various other pseudostationary phases can be easily adjusted. Chiral recognition by various CE approaches has recently been reviewed (Gubitz and Schmid, 2008). CE-LIF is especially suited for neurochemical studies where small sample volumes (nL- μ L) are often encountered. Typical CE injection volumes are in the nanoliter range and attomole detection limits can be readily achieved with appropriate LIF detection. LIF requires derivatization of amino acids and several chiral and achiral reagents that have been developed for HPLC approaches are directly applicable to CE-LIF. Bioanalytical chiral CE-LIF approaches generally use either micellar electrokinetic chromatography (MEKC) as a separation mode or chiral capillary electrokinetic chromatography (cEKC).

Chiral amino acid separations by CE-LIF has been extensively studied and recently reviewed (Iadarola et al., 2008) in part. Many chiral techniques were not optimized for biological samples initially by their investigators. These include chiral separations of amino acids derivatized with OPA (Tivesten and Folestad, 1995, 1997; Yang et al., 2001), NDA (Ueda et al., 1991; DeSilva and Kuwana, 1997), 5-dimethylamino-naphthalene-1-sulphonyl chloride (DNS) (Gozel et al., 1987; Yang and Yuan, 1999), fluorescein isothiocyanate (FITC) (Jin et al., 1999; Lu and Chen, 2002), and the achiral reagents such as (+)- and (-)-1-(9-anthryl)-2-propyl chloroformate (APOC) (Thorsen et al., 1997). Several of these methods laid the groundwork for later application to real samples.

OPA derivatization which continues to be popular for HPLC has been adapted for CE-LIF chiral analysis of D-ser. Thompson and colleagues developed a rapid CE-LIF

approach to quantify OPA/ β -mercaptoethanol derivatized DL-asp in brain homogenates from rats using online microdialysis CE-LIF (Thompson et al., 1999). Separation was accomplished using CD-cEKC at pH 10 with 7.5 mM β -CD as chiral selector. A separation time of \sim 3 s was reported. The microdialysis probe was inserted directly into a 50 μ L sample of rat brain homogenate diluted 3-fold. Despite a microdialysis probe recovery for D-asp of only 20 %, the reported detection limit for the online microdialysis CE-LIF assay was 905 nM. O'Brien et al. developed a CE-LIF approach to analyze OPA β -mercaptoethanol derivatized D-ser in salamander retina (O'Brien et al., 2003). Chiral recognition was achieved using hydroxypropyl- γ -cyclodextrin (HP- γ -CD) dissolved in a high pH BGE. Separation time using an online microdialysis CE-LIF approach was 9 s with a theoretical plate count per meter of 400,000. A variety of amino acids including DL-asp, L-glu, L-ser, GABA, and taurine could be analyzed in addition to D-ser. The approach was used to characterize D-ser in salamander retina (O'Brien et al., 2003; O'Brien et al., 2004), cortical brain slice (O'Brien and Bowser, 2006), and rat striatum *in vivo* (Ciriacks and Bowser, 2006).

Tsunoda and colleagues developed the first method of DL-amino acid bioanalysis by CE-LIF with precapillary derivatization using the reagent NBD-F (Tsunoda et al., 1999). Enantioseparation was achieved under slightly acidic conditions (pH 4) using trimethyl- β -cyclodextrin (TM- β -CD) as a chiral selector. DL-asp levels were investigated in pineal glands of rats to demonstrate application of the approach. This appears to be the first application of capillary electrophoresis for the analysis of D-amino acids in mammals. Zhao and colleagues utilized CE-LIF with NBD-F derivatization to analyze

D-ser in rat cerebrum tissue homogenates after protein precipitation (Zhao et al., 2005b). Chiral separation was achieved at high pH with HP- β -CD as chiral selector. The method clearly separated DL-ser without interferences in 40 min. They suggested that decreasing capillary length and diameter could significantly increase sample throughput. Around the same time O'Brien et al. developed a faster approach than Zhao with similar derivatization and identical BGE components though with slight differences in concentrations of the components in the BGE (O'Brien et al., 2005). In addition, capillary length was reduced 43 % resulting in a voltage gain from 214 V/cm to 357 V/cm (~40%). This allowed for analysis of D-ser, L-glu, GABA, and gly in retinal perfusion media with a run time of 14 min. Furthermore, the approach was recently adapted for online microdialysis CE-LIF of D-ser (Klinker and Bowser, 2007). The final BGE was similar to Zhao with slight increase in pH (0.5 units) and decrease concentration of HP- β -CD (2-fold). Using online microdialysis CE-LIF, excellent resolving power was demonstrated by analyzing 16 amino acid derivatives including important neurochemicals L-glu, GABA, gly, D-ser, and taurine in 21.5 seconds. The approach was used to investigate DL-isomer changes *in vivo* after local K⁺ infusion in rat striatum by microdialysis.

Thorsen et al. used achiral APOC derivatization and found D-ala, D-asp, and D-gln in CSF and D-glu in urine (Thorsen and Bergquist, 2000). This was the first micellar electrokinetic chromatography (MEKC) method for analysis of D-amino acids in mammals.

Precapillary derivatization with 3-(4-carboxybenzoyl)-2-quinoline-carboxaldehyde (CBQCA) in conjunction with chiral CD-MEKC using β -CD allowed for the separation of D-asp and D-ser along with 15 additional amino acids commonly found in CSF (Thongkhao-On et al., 2004). Quantification of D-ser along with 11 L-amino acids in rat brain vitreous perfusates was demonstrated with a run time of 10 min. Detection limits were 0.21 μ M and 0.38 μ M for D-ser and D-asp, respectively.

Zhao and colleagues quantified free D-ala in human plasma using FITC labeling and CD-MEKC with 18 mM β -CD as chiral selector (Zhao et al., 2006). Detection was by optical fiber light-emitting diode-induced fluorescence. D-ala detection limit was \sim 8 nM with a separation time of < 9 min.

NDA has been extensively studied for analysis of DL-amino acids in biological fluids by CE-LIF using high pH BGEs. Zhao and colleagues used precapillary derivatization with NDA and CD-MEKC with methanol additive to analyze free DL-asp in rat brain homogenates at different ages of CNS development (Zhao et al., 2001). A similar approach without methanol was used for the analysis of DL-asp, DL-phe, DL-leu concentration and distribution in single cells of *Aplysia californica*, a sea mollusk commonly used in model neuronal studies (Zhao and LifuYm, 2001). The presence of DL-trp in human urine, CSF, rat brain homogenates, and *Aplysia* ganglia neurons was investigated using CD-MEKC with HP- γ -CD in the BGE at pH 9 (Zhao and Liu, 2001). Quan and Liu analyzed DL-glu derivatized with NDA in rat brain, ganglia, and single neurons of *Aplysia californica* with a detection limit of 0.54 μ M (Quan and Liu, 2003). The approach used CD-MEKC with β -CD and methanol (25%) for baseline separation

of DL-glu in ~42 min. Altering selectivity by removing micelles and using saccharide enhanced dual chiral selection with HP- γ -CD and D-(+)-glucose allowed for separation and quantification of D-ser in rat brain homogenates, microdialysates, and *Aplysia californica* neuronal processes (Quan et al., 2005). D-ser analysis was optimized with a run time of ~30 min and detection limit of 100 nM in this study. Zhao et al. analyzed D-ser labeled with NDA in homogenates of *Aplysia* ganglia using dual chiral selector CD-MEKC with sodium taurocholate and β -CD (Zhao et al., 2005a). A 30 nM detection limit was reported with a run time of ~30 min for D-ser. Miao et al. developed NDA derivatization of chiral amino acids with CD-MEKC using 15% methanol and 20 mM β -CD for analysis of D-asp in neural samples (Miao et al., 2005). Analysis time was optimized at 30 min. They investigated D-asp in neuronal processes from individual neurons. The approach was further used to investigate D-asp synthesis and distribution in specific neuronal clusters of *Aplysia californica* (Miao et al., 2006). Within some neuronal clusters of this Californian sea slug as much as 85% of the total asp levels were determined to be in the D-isomer form.

1.3 Cyclodextrins in electrokinetic chromatography

Cyclodextrins (CDs) are a family of naturally occurring macrocyclic oligosaccharide rings composed of D-glucose subunits connected by α -1,4-glycosidic linkages. The three most common cyclodextrins consist of 6, 7, and 8 glucose subunits and are designated α , β , and γ -CD. A top view of the CD structures is given in Figure 1.1.

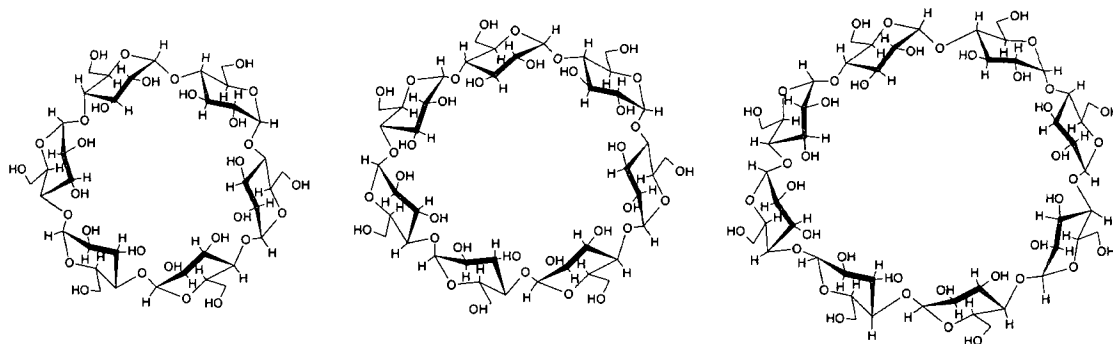
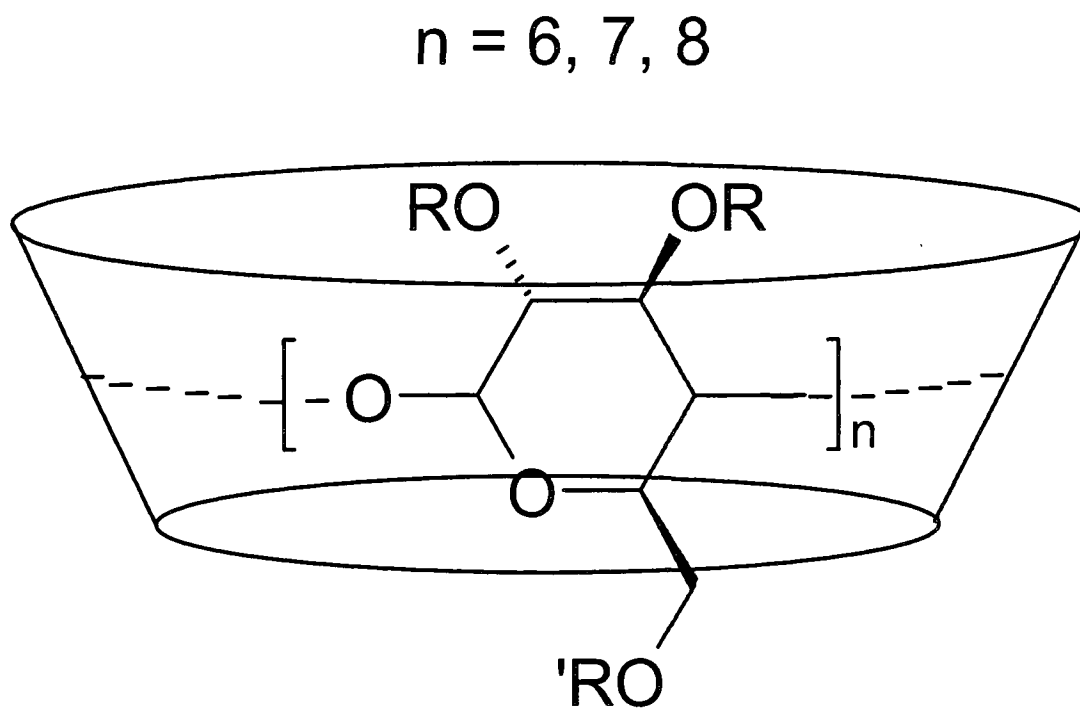


Figure 1.1. Top view chemical structure of α -, β -, and γ -CD. A top view of the CDs shows the linkage of α -D-glucose subunits combined to form macrocyclic rings. Shown from left to right are α -, β -, and γ -CD.

The result is a macrocyclic ring of toroidal shape (or truncated conical cylinder). The upper rim of the truncated cone (commonly referred to as CD torus) is defined by the secondary hydroxyls of the glucose units, while the lower rim contains primary hydroxyls. A side view depiction of a CD showing the toroidal structure is given in Figure 1.2.



$R = H$, (native CDs)

Figure 1.2. Side view of cyclodextrin structure illustrating toroidal shape. The orientation of 1,4-glycosidic linked α -D-glucose units are such that primary and secondary hydroxyls extend out away from CD torus at the upper (secondary) and lower (primary) torus rims.

The numerous hydroxyl groups on the native CDs periphery (18, 21, 24 for α , β , and γ -CD respectively) give the exterior of the CD hydrophilic characteristics. They are also the site for synthetic modification. In contrast to the polar exterior, the cavity (or annulus) of CD is considered moderately hydrophobic, due to a high electron density resulting from nonbonding π -electrons of the glycoside linkages and the also from the hydrophobic backbone of the glucose units (Easton and Lincoln, 1999). The number of glucose subunits will determine the internal cavity volume. The combination of

hydrophilic exterior and hydrophobic chiral interior gives rise to unique and useful host-guest complexation ability. An illustration of host-guest complex formation through interaction in solution between hydrophobic guest and CD is shown in Figure 1.3.

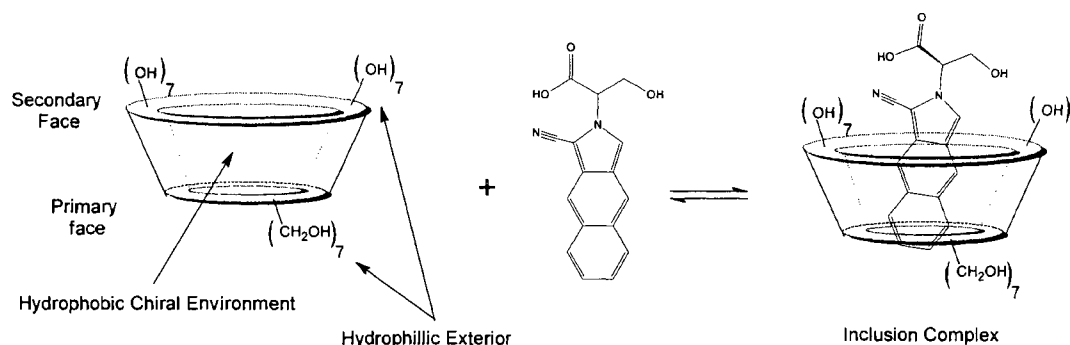


Figure 1.3. Illustration of CD host:guest inclusion complex formation. The diagram illustrates the equilibrium where a hydrophobic derivatized amino acid, NDA labeled D-ser, forms an inclusion complex in solution with the cyclodextrin (β -CD) through interaction with the hydrophobic cavity.

Cyclodextrins are the most widely utilized chemicals that form host-guest inclusion complexes (Weinberger, 2000). Complex formation is the basis for application in analytical chemistry where CDs find extensive use as chiral selectors. They offer the broadest selectivity of any chiral selector in analytical chromatographic and electrophoretic separations (Juvancz et al., 2008).

The analytical separation of enantiomers is of primary importance in pharmaceutical and biochemical research. Direct chiral separation (indirect diastereomer formation) is achieved when a pair of enantiomers exhibit differential rates of adsorption (chromatography) or partitioning (capillary electrophoresis) with a chiral phase as they migrate through a column. CDs bonded on stationary phases act as chiral selectors in

GC, LC, and capillary electrochromatography (CEC) to alter enantiomer adsorption rates through differential chiral interactions with the solute species. Alternatively, CDs can be dissolved in solution and through partitioning of chiral solute into the chiral cavity from the bulk phase, differentially alter migration (CE) or retention (LC with CD in mobile phase) of enantiomers. In this latter case, the effective physiochemical properties (lipophilicity, effective mass/size, charge) of each enantiomer is altered as it interacts in the column.

CE is a powerful analytical tool originally used primarily for the separation of charged analytes. When coupled with the use of chiral reagents such as cyclodextrins, this technique is especially useful for enantiomeric separations. CE is based on the migration of charged analytes in solution through a small diameter liquid filled capillary (typically ≤ 0.1 mm) under the influence of an electric field (typically 5-30 kV). The size of the analyte and its charge are principle factors influencing migration. With an appropriate buffer, voltage, capillary, etc., high separation efficiencies can be realized (up to several hundred thousand theoretical plates/meter is common). A schematic illustrating the basic principle of capillary electrophoresis separation and detection is shown in Figure 1.4.

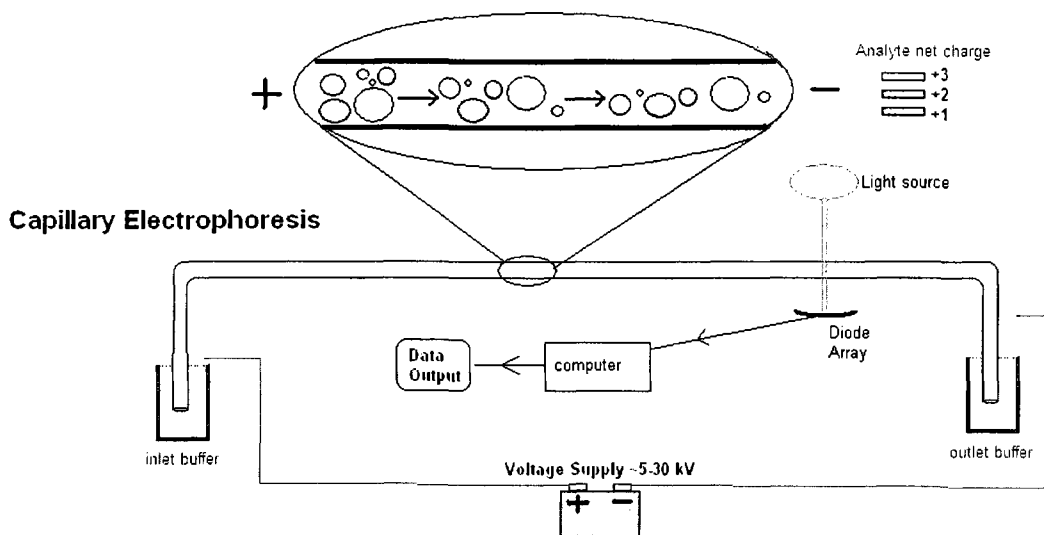


Figure 1.4. Illustration of a typical capillary electrophoresis instrument with separation mechanism for ionic analyte. A small diameter (≤ 0.1 mM) buffer filled capillary is immersed at either end in buffer reservoirs containing high voltage leads of opposite polarity. After injection of ionic analytes, an electric field is generated by a high voltage power supply and ionic species migrate based on their intrinsic ionic electrophoretic mobilities, μ_i , with constant electrophoretic velocity, $v_{e,i}$, proportional to the strength of the electric field, E , or $v_{e,i} = \mu_i E$. For the illustration shown above, cationic species display net mobility toward the cathode and are separated according to their size/charge ratios and detected in-capillary by spectrophotometric techniques. Note that the pH dependent electrophoretic pumping mechanism, electroosmotic flow (EOF), is not included in this simple illustration. A comprehensive mathematical treatment of mobility parameters is described elsewhere (Khaledi, 1998).

One of several distinct advantages of CE over many chiral chromatography techniques is the simplicity with which the separation is carried out. Chiral secondary equilibria can be achieved simply by dissolving a chiral solute such as a CD at an appropriate concentration in an appropriate separation buffer. If a given CD proves insufficient in providing chiral resolution then a multitude of native and derivatized CDs are commercially available that can potentially alter selectivity.

Cyclodextrins are the most widely used chiral selectors in CE and a variety of strategies can be employed for bioanalytical analysis of amino acids as referenced in Section 1.1. Regardless of which strategy is used, the addition of CDs to electrophoretic buffers results in a separation mode termed cyclodextrin capillary electrokinetic chromatography (CD-cEKC) (Chankvetadze, 2007). In a recent 2008 CD literature review covering the past 8 years, it was estimated that as much as 50% of all cyclodextrin related analytical studies were carried out using CD-cEKC with CDs containing charged functional groups (Juvancz et al., 2008). Interestingly, these CDs are the least studied for DL-amino acid analysis in biological matrices though they are the focus of this dissertation research. The most common CE-LIF approaches in bioanalytical analysis of fluorescently labeled amino acids as referenced in section 1.1 are illustrated mechanistically in Figure 1.5 below.

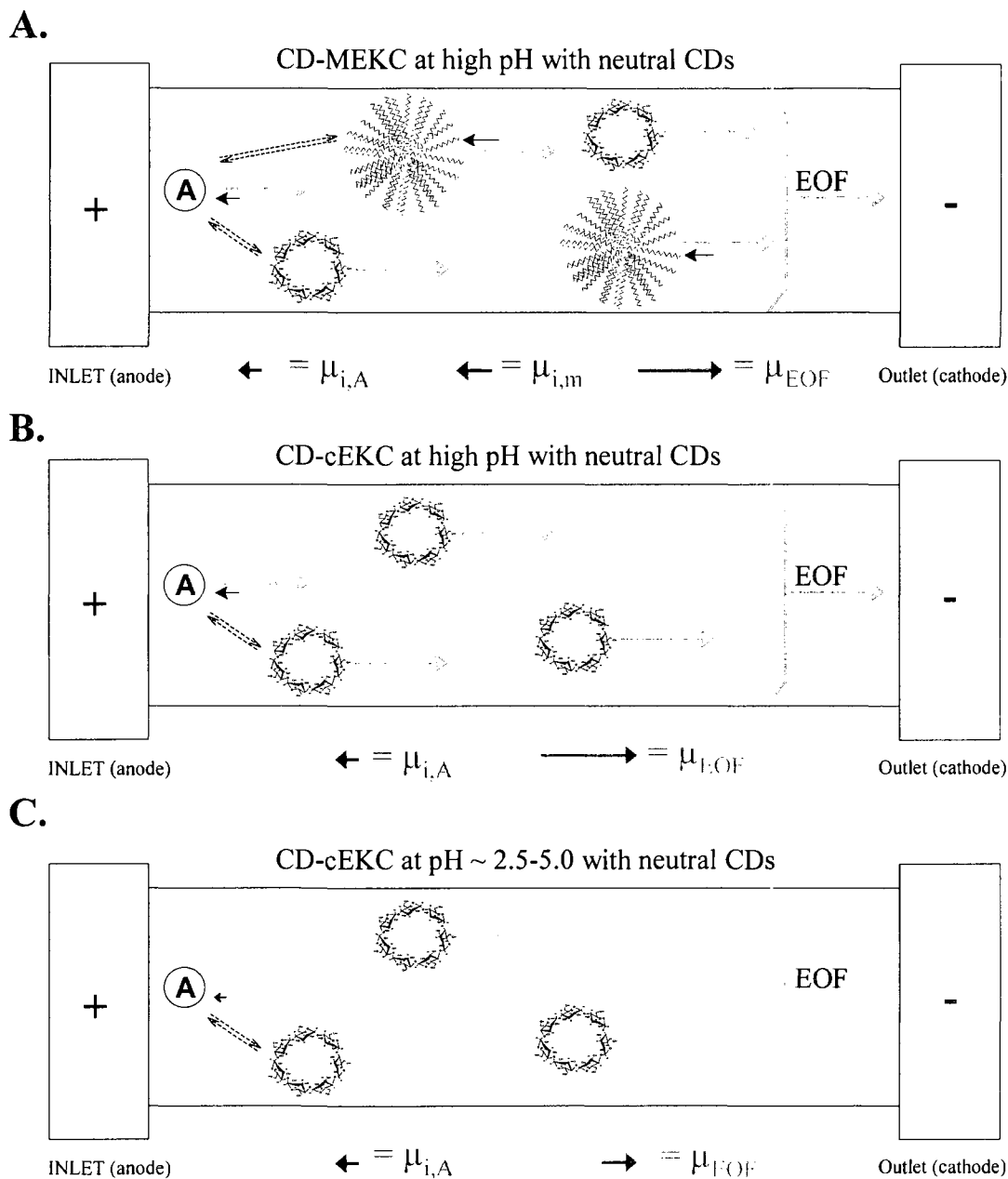


Figure 1.5. Illustration of CE modes of chiral recognition of fluorescently labeled amino acids published in bioanalytical methods. These modes represent methods applied for chiral analysis of biological samples. Alternative modes not applied to biological samples are omitted here. Note that species A represents all analytes including enantiomers. The most common CE-LIF approaches are represented in (A) and (B). (A) CD-MEKC at high pH with neutral CDs. EOF drives A towards detector despite

opposing mobility to EOF for both A and micelle. The CD is added to induce secondary equilibria and allow for chiral separation of A. The micelle provides additional hydrophobic interaction and mobilizes charged and neutral analytes increasing separation window. (B) CD-cEKC at high pH. Chiral separation is based on inclusion complex formation with CD and is applicable only to charged A species as uncharged A will coelute at μ_{EOF} . Separation depends on μ_i for each A species. (C) CD-cEKC at low pH. Separation is same as high pH but with reduced EOF and pH approaching pK_a of acidic species A.

MEKC is a powerful separation approach which has been extensively used for analysis of small biomolecules and particularly derivatized amino acids (Figure 1.5A). The application to amino acid analysis was recently reviewed (Iadarola et al., 2008) in part. The technique operates at high pH in normal polarity mode (cathode at outlet) where strong electroosmotic flow (EOF) is directed toward the cathode. Anionic micelles and anionic solutes migrate toward the anode (inlet) based on their electrophoretic mobility, μ_i , but EOF results in bulk flow of micelles and solutes toward the detector. The interior of the micelle is lipophilic which results in partitioning of hydrophobic solute between the bulk solution and the micelle. One advantage of MEKC compared with zone electrophoresis is the ability to differentiate closely related species (such as fluorescently labeled amino acids) based on minute lipophilic differences. Furthermore, the mode is amenable to charged and neutral solutes. Neutral native and derivatized CDs can easily be added as a second pseudostationary phase for chiral resolution (CD-MEKC). In this case, the partitioning of solute into the chiral cavity of the CD is in competition with partitioning into the micelle. Typically the ratio of the micellar agent to CD can dramatically influence separation and is finely tuned for a given analysis. Sodium dodecyl sulfate (SDS) is the most common ionic micellar agent used in conjunction with

CDs though chiral bile salts such as sodium deoxycholate also find use in bioanalytical DL-amino acid analysis (Zhao et al., 2005a).

CD-cEKC at high pH (>8) with neutral CDs is also a popular approach for the analysis of amino acids in biological samples (Figure 1.5B). In CD-cEKC migration times for a given set of solutes, capillary, buffer, and voltage conditions will always be less than the identical separation using CD-MEKC. The exception is the use of multiply charged CDs in high pH CD-cEKC which has not been used for bioanalytical approaches of amino acids. Derivatized amino acids migrate based on unique electrophoretic mobility for each analyte. Chiral resolution is achieved through differential partitioning into the CD cavity. Strong EOF opposing anionic analyte migration results in bulk mobility toward the detector. A variety of native and neutral CDs have been utilized for high pH cEKC.

When the pH of the BGE approaches the pK_a of the charged solute, enantioresolution can often be obtained (Weinberger, 2000). Low pH CD-cEKC (Figure 1.5C) with neutral CDs is not well studied for chiral amino acid analysis in biological samples. Low pH would be required to approach the pK_a region of several derivatized amino acids, either the α -COOH and/or the terminal -COOH (aspartate and glutamate). One study by Tsunoda et al. investigated NBD-DL-asp enantioseparation in biological samples in the pH range of 2.5-4.7 (Tsunoda et al., 1999). A variety of native and derivatized neutral CDs were tested. Separation was achieved with neutral trimethyl- β -CD at pH 4.0 and the approach was applied to study D-asp in CNS. This is the only low pH normal polarity (cathode at outlet) approach that has been applied to DL-amino acids in biological samples.

An alternative to the modes described above is the use of anionic cyclodextrins at low pH (minimal EOF) under reversed polarity (RP, anode at detector) to sweep neutral and weakly ionic species towards the detector as represented in Figure 1.6 below.

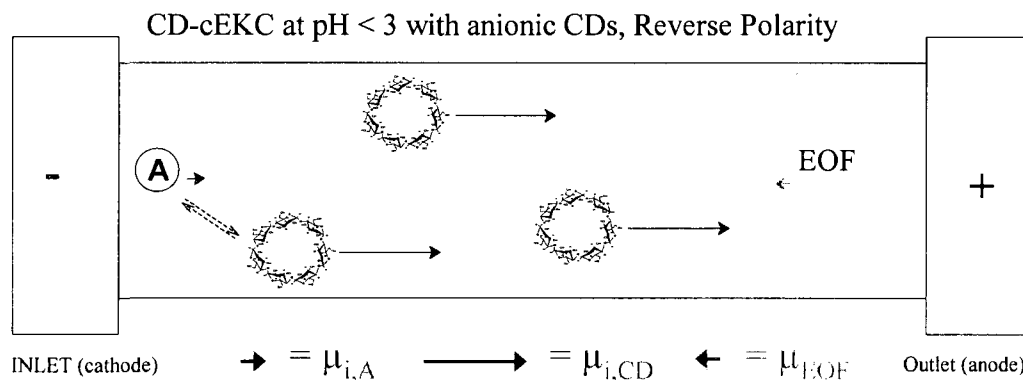


Figure 1.6. Illustration of reversed polarity CD-cEKC with anionic CDs. The anionic CDs possess strong μ_i towards the anode which exceeds that of μ_{EOF} . Significant inclusion complex formation results in sweeping of ionic and neutral A toward the detector. While weakly acidic analytes approach their pK_a in this pH range, cationic analytes are capable of forming additional interactions (electrostatic).

With this approach an anionic CD would migrate toward the detector while the derivatized amino acids (protonated carboxylic acid at low pH, derivatized on amine) will be swept toward the detector based upon the strength of their interaction with the cyclodextrin as well as any inherent electrophoretic mobility of the weakly acidic analyte. Cationic amino acids derivatives such as those produced from lys, his, and arg may additionally exhibit electrostatic interactions with anionic CDs.

This approach is referred to as RP-CD-cEKC and, as of the writing of this dissertation, only Piehl and coworkers have used it for fluorescently labeled amino acids (Piehl et al.,

2004). With microchip electrophoresis and fluorescence detection, they achieved subsecond chiral separations of dansylated amino acids (DNS-AA) by utilizing highly sulfated γ -CD at pH 2.5. They did not report on the separation of DNS-ser nor was the approach applied to biological samples or complex multicomponent mixtures.

1.4 Summary of research aims

The focus of this dissertation was to demonstrate for the first time the capabilities of anionic CDs in cEKC bioanalysis of amino acids and take advantage of sensitive bioanalytical approaches with these chiral selectors for quantifying D-amino acids in the CNS. Selective separation and sensitive detection of D-ser, the dominant coagonist of the NMDAR, in CNS samples, was a central focus of this work. This research represents the first application of an ionic CD for bioanalysis of a chiral amino acid. Because of this there is particular emphasis placed on developing an understanding of the advantages and disadvantages of using this type of chiral selector in cEKC bioanalysis. Studies over the past few years stress the importance of single isomer CDs for robust chiral separations; this thesis research also focuses on design and synthesis of a new family of single isomer selectively modified sulfoalkyl anionic CDs and investigations on their application for D-amino acid analysis. Sensitive separation and quantification is only one aspect of bioanalytical chemistry. This dissertation additionally includes the development of a novel microperfusion brain slice chamber for rapid sampling of neurochemical efflux dynamics including D-ser and L-glu from single acute hippocampus slices. Studies with this approach coupled to anionic CD based

chiral separations are carried out for investigating timing and magnitude of D-ser and L-glu efflux in response to modeled cerebral ischemia.

Chapter 2

Development and application of S- β -CD cEKC for D-ser and L-glu analysis in microdialysates

2.1 Overview of study

Research in amino acid neurochemistry reveals that D-ser is an important neuromodulator responsible for coagonist regulation of the glutamatergic NMDA receptor. Therefore the ability to monitor D-ser and L-glu dynamics simultaneously is an important attribute in a bioanalytical technique used to study NMDA receptor function.

Sensitive amino acid analysis requires derivatization. Naphthalene-2,3-dicarboxaldehyde (NDA) is an efficient fluorogenic reagent for amino acids which reacts with primary amines in the presence of sodium cyanide in a condensation reaction to form fluorescent cyanobenz(f)isoindole (CBI) derivatives, according the reaction scheme and proposed mechanism given in Figure 2.1.

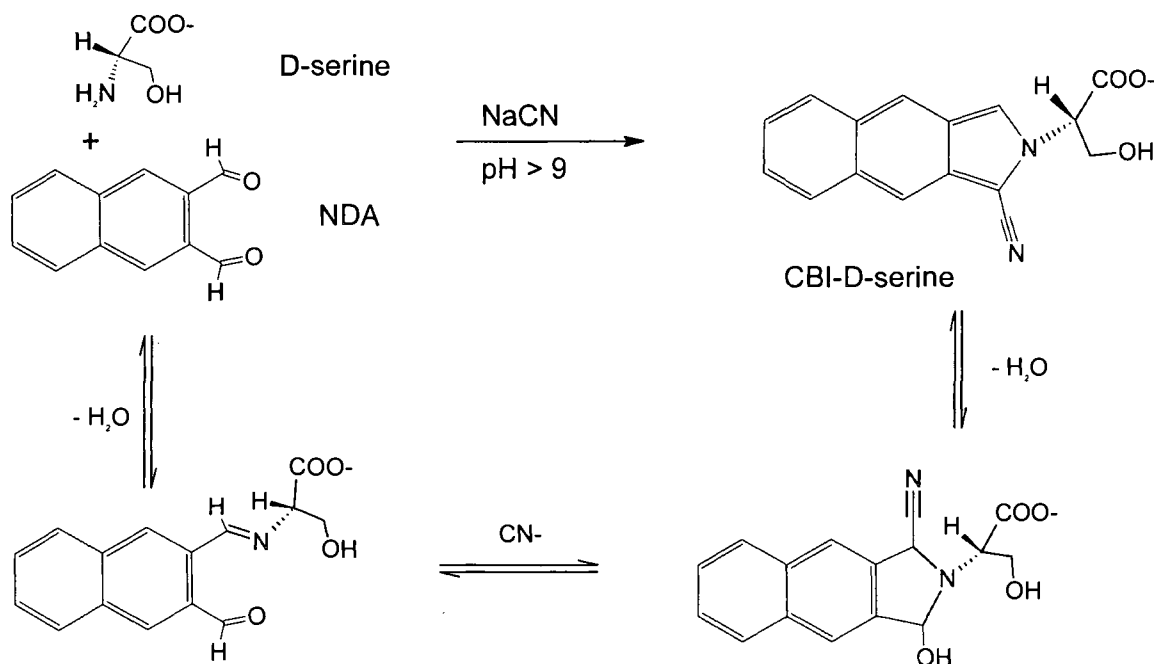


Figure 2.1. Reaction scheme for fluorescent labeling of amino acids with NDA. NDA reacts with primary amines in the presence of cyanide to form highly fluorescent cyanobenz[f]isoindoles. The possible key intermediates in mechanism for condensation of NDA and α -amino is also illustrated. Mechanism is adapted and modified from the scheme proposed by De Montigny et al. for key intermediates in the analogous OPA reaction (De Montigny et al., 1987).

Few CE-LIF approaches have been successful resolving CBI-DL-ser. There are currently no reports for the development of a bioanalytical method utilizing anionic sulfated cyclodextrins for quantification of fluorescently labeled amino acids in complex biological matrices. This is perhaps surprising considering this class of chiral selectors is considered one of the more powerful resolving agents available in CE.

This dissertation research describes the development of the first bioanalytical method utilizing anionic cyclodextrins for sensitive chiral analysis of amino acids in a biological matrix. We (Kirschner et al., 2007) utilized commercially available S- β -CD in reversed polarity CD-cEKC for the quantification of D-ser, L-glu, and L-asp in microdialysates

obtained from hippocampus of arctic ground squirrel. The chiral separation was optimized for CBI-DL-ser and then applied to other CBI-amino acids. Baseline resolution of 13 CBI-amino acids was achieved using a single buffer formulation. We demonstrate an important dependence of chiral separation on buffer pH. At 2 wt % S- β -CD, CBI-ser enantiomers are baseline-resolved at pH 2.00 but no resolution is obtained at pH 3.00. Furthermore, we demonstrate that dilute solutions of CBI-amino acids can be stacked by hydrodynamic injection with a 100-fold improvement in signal-to-noise ratio without loss of chiral resolution. The mechanism proposed for stacking is described.

2.2 Methods

2.2.1. Chemicals and reagents.

All chemicals were analytical reagent grade unless otherwise stated. NDA and sodium cyanide were purchased from Sigma-Aldrich. All amino acids were purchased from Aldrich Chemical Company unless otherwise noted. Water was prepared from a Millipore Milli Q ultrapure water purification system with 18 M Ω -cm resistivity. Sulfated- β -CD was purchased from Fluka (Lot # 1148973, reported as 7-11 moles per mol β -CD). Phosphoric acid and sodium monohydrogen phosphate were obtained from Fisher Scientific. Background electrolytes (BGEs) typically consisted of 25 mM phosphate adjusted to a desired pH by mixing equal concentrations of aqueous 25 mM sodium monophosphate and 25 mM phosphoric acid solutions.

2.2.2. Capillary electrophoresis apparatus.

The capillary electrophoresis instrument was in-house built using an Olympus BH2 microscope (Olympus, Center Valley, PA, USA). A high-voltage power supply (0-30 kV, Spellman CZE 1000R) was used to drive the electrophoresis. The bare silica capillary (Polymicro Technologies Inc., Phoenix, AZ, USA) was focused with an oil immersion 100x 1.3 na, 0.17 working distance Olympus UVFL fluorite microscope objective. A 420-nm blue diode laser (Power Technology Inc., Little Rock, AR, USA), adjusted to 5 mW power, was used for excitation. The laser beam passed initially through a D425, 40x bandpass exciter filter (Chroma Technologies Corp., Rockingham, VT, USA) followed by reflection of 90° by a dichroic filter (460DCLP, Chroma Technologies) prior to focusing on the capillary. Fluorescent emission passed back through the dichroic filter and then through a bandpass emission filter (D490/40m) to a photomultiplier tube (PMT) (R1527, Hamamatsu Photonics, Hamamatsu City, Shizuoka, JAP) housed in a Photon Technology Instrument DB104 photometer. The analog signal was converted to digital signal, stored, and processed using LabView software (National Instruments Corp., Austin, TX, USA). The signal was collected at 200 Hz and signal averaged to 20 Hz. Injection was accomplished by computer-controlled application of vacuum at the outlet side of the capillary for a specified time. Applied vacuum injection ranged from 300-400 Torr as measured with Baratron[®] Type 221AD pressure transducer (MKS Instruments Inc., Andover, MA, USA). PeakFit[®] software (SeaSolve Software Inc., Framingham, MA, USA) was used to fit the peaks to a Gaussian line shape to determine resolution values, R_s , and noise levels to the 95% confidence interval.

Furthermore, Peakfit[®] was valuable for determining the separation efficiency of an analyte for a given electrophoretic condition. The efficiency of a separation is an indication of the sharpness of the peaks relative to the separation time; an efficient separation produces sharp peaks in a short amount of time. Separation efficiency is defined as the number of theoretical plates or plate number (N) for a given electrophoretic condition. The number of theoretical plates can be calculated as the square of the ratio of migration time (t_m) divided by the standard deviation (σ) of the peak (Dong, 2006). For Gaussian peaks, width at base (w_b) is approximately 4σ , so $N=16(t_m/w_b)^2$.

2.2.3. Derivatization procedure for separation and stacking studies.

CBI-amino acids were prepared for separation and stacking studies by reacting equal volumes of amino acid (1 mM), NDA (1 mM in methanol), and NaCN (1 mM in 60 mM borate buffer, pH 9.3) and allowed to react for a minimum of 15 min. CBI-amino acids were diluted to 10 μ M with water. The use of equal molar quantities of amino acid, NDA, and NaCN were used to minimize NDA side products for the separation and stacking studies. For derivatization of microdialysates and standards for calibration curves, see below. CBI-amino acids absorb strongly in the visible region at 405, 422, and 442 nm with a broad emission band at 490-530 nm. The absorption and emission spectra of CBI-tyrosine in water is shown in Figure 2.2.

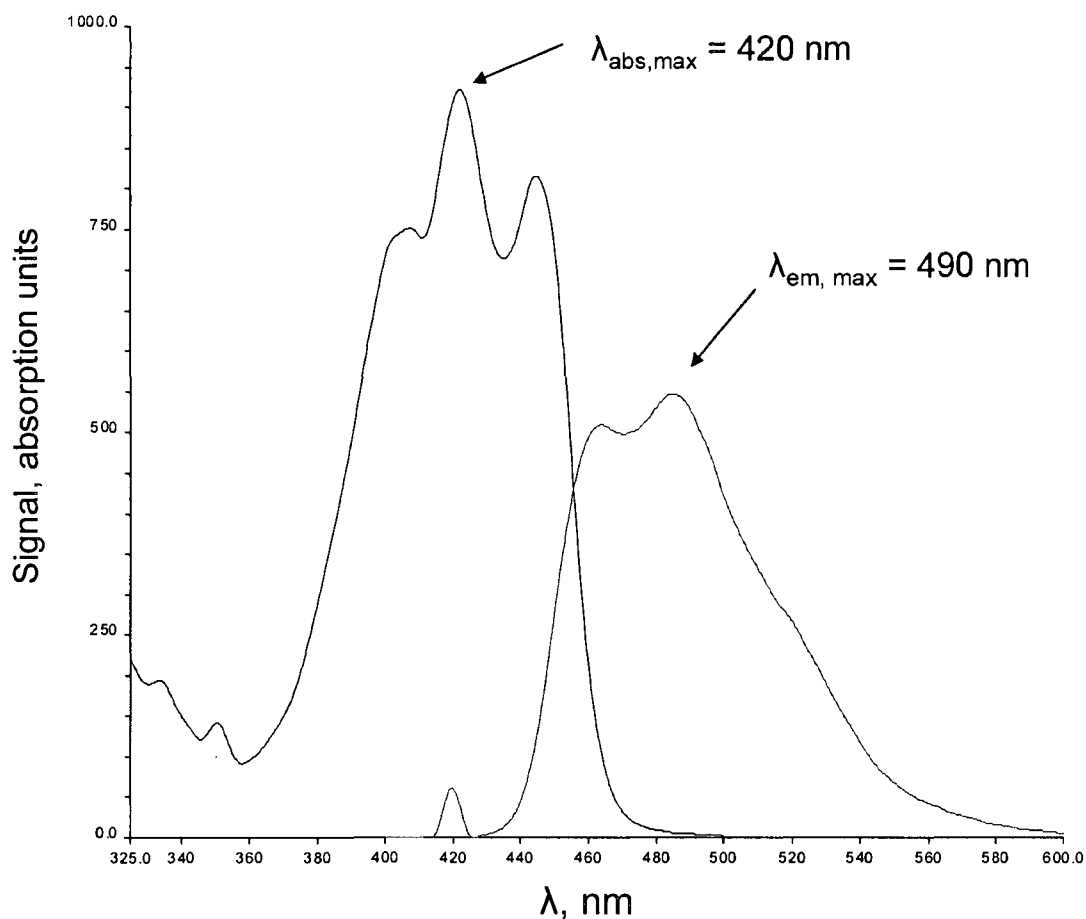


Figure 2.2. Absorbance and emission spectrum of CBI-tyr in water. Absorbance spectrum is shown in blue (360-480 nm) and emission spectrum in red (430-600 nm) for a 10 μM solution of CBI-tyr. The characteristic absorbance wavelengths, λ_{abs} , of 405, 420, 442 nm demonstrate that the 420 nm blue diode laser maximally excites CBI-tyr. The emission spectrum scanned after excitation at 420 nm demonstrates that maximum emission is collected at 490 nm corresponding to the selected bandpass filter for the above described CE instrumentation. Absorption/fluorescence instrumentation: Perkin Elmer LS-50B Spectrofluorimeter with 4-sided 1-cm quartz cuvettes. Sample was prepared according to Section 2.23.

2.2.4. Capillary electrophoresis and enantioseparation studies.

All electrophoresis experiments were operated with reverse polarity (anode at detector).

For separation studies, the capillary was bare fused-silica of dimensions 70 x 45.0 cm x 25 μm . Injection was accomplished by vacuum injection at the detector end. Typical

currents ranged from 20 to 60 μA . Typical injection times were 1 s, but ranged from 2 to 180 s for stacking experiments. Injection vacuum was 380 mbar, which gave an injection plug of 19.5 cm for 180-s injection. New capillaries were conditioned once for 8 min with 1 M NaOH, then for 2 min with 0.1 M NaOH, and 2 min with BGE between each experiment. Resolution (R_s) of CBI-amino acid enantiomers was calculated by dividing the difference in migration times (Δt_m) of eluting peaks by the average peak width at base (w_b). An Ohm's law plot for the capillary (70 cm x 25 μm) with the optimized BGE consisting of 25 mM phosphate adjusted to pH 2.0 and containing 2 wt % S- β -CD gave a linear relationship (Correlation coefficient, $R^2 = 0.991$) in the region of 5-30 kV suggesting maximum voltage (30kV) could be used without loss of resolution through joule heating (Weinberger, 2000).

2.2.5. Construction of standard curves and analysis of microdialysates.

All biological samples and standards were analyzed using a bare fused-silica capillary of dimensions 48 x 45 cm x 25 μm . Voltage was reduced to 21 kV to allow for similar applied field conditions as described for separation studies. Five standards were prepared for CBI-D-ser, CBI-DL-asp, and CBI-DL-glu with concentrations of 0.3, 0.8, 1.4, 2.4, and 5.0 μM by dilution of a 2 mM stock amino acid solution with artificial cerebral spinal fluid (aCSF, containing in mM; 124 NaCl, 2.7 KCl, 1 CaCl₂, 0.85 MgCl₂, 24 NaHCO₃, 1.4 D-glucose, pH 7.4). Standards and samples were reacted by equal volume dilutions with NDA (1 mM in methanol) and NaCN (1 mM in 60 mM tetraborate with 9 μM L-homoarginine as the internal standard). Capillary was preconditioned and the

standards/samples were injected using 1-s vacuum injection (380 mbar). Using peak areas, the CBI-amino acid/internal standard ratio was plotted versus [CBI-amino acid]. A five-point calibration curve was constructed for each amino acid ($n > 4$ at each concentration) using a weighted least-squares analysis. For microdialysis, typically 1-2 μL of dialysate was reacted. Samples and standards were reacted a minimum of 15 min prior to analysis. Identities of CBI-amino acids in the microdialysates were confirmed by spiking with known CBI-amino acids. Triplicate analyses were conducted on all microdialysates. Concentrations of amino acids were determined from calibration curves using a weighted least-squares analysis, with uncertainty reported as $\pm s$, where s is the standard deviation. The average and standard deviation in peak area ratios (CBI-amino acid/ internal standard) for nine injections of 2.4 μM CBI-amino acid were as follows; CBI-L-glu, 0.461 ± 0.070 ; CBI-D-ser, 0.400 ± 0.085 , CBI-L-asp, 0.358 ± 0.036 .

2.2.6. ^{13}C NMR titration of ser and CBI-ser.

All ^{13}C NMR measurements were made with a Varian Mercury FT-NMR at 75 MHz. Ser titration: 15 mL of 60 mM borate buffer, pH 9.3, was mixed with 5 mL of methanol- d_4 and then 0.50 g of L-ser in 15 mL of D_2O . The pH was 8.70 using a H_2O -calibrated pH meter. The solution was titrated incrementally with 1.0 mM HCl followed by measurement of the ^{13}C NMR chemical shift of the carboxyl carbon referenced to methanol- d_4 (49.9 ppm). CBI-ser titration: The same procedure was used except 15 mL of 60 mM borate buffer, pH 9.3, containing 15 mM NaCN was mixed with 15 mM NDA in 15 mL of methanol and then with 15 mL of (C 1)- ^{13}C enriched L-ser in D_2O . The pK_a

H^* , which was determined in D_2O using an H_2O -calibrated pH meter, was determined by plotting the first derivative of the chemical shift in ppm against pH^* .

2.3 Results

2.3.1. Chiral separation of CBI-derivatives

Literature suggests that CBI-ser enantiomers are difficult to resolve at high pH using conventional neutral chiral selectors. Therefore we chose reverse polarity CD-cEKC with commercially available Sulfated- β -CD (S- β -CD) at low pH. Stalcup and Gahm have demonstrated excellent resolving power of this chiral selector for a variety of chiral analytes (Stalcup and Gahm, 1996). Conditions are typically carried out under reversed polarity (anode at detector) in a pH range of 2.00-3.50. Under these conditions, EOF would be minimized and the highly charged anionic S- β -CD would migrate toward the detector. CBI-amino acids could interact with S- β -CD through their hydrophobic naphthalene group to form inclusion complexes in solution with S- β -CD. Strong complex formation would result in sweeping of the CBI-amino acid solute toward the detector.

We find pH to be the most critical factor controlling chiral resolution of CBI-ser enantiomers using S- β -CD in the range of 2-6 wt % as shown in Figure 2.3.

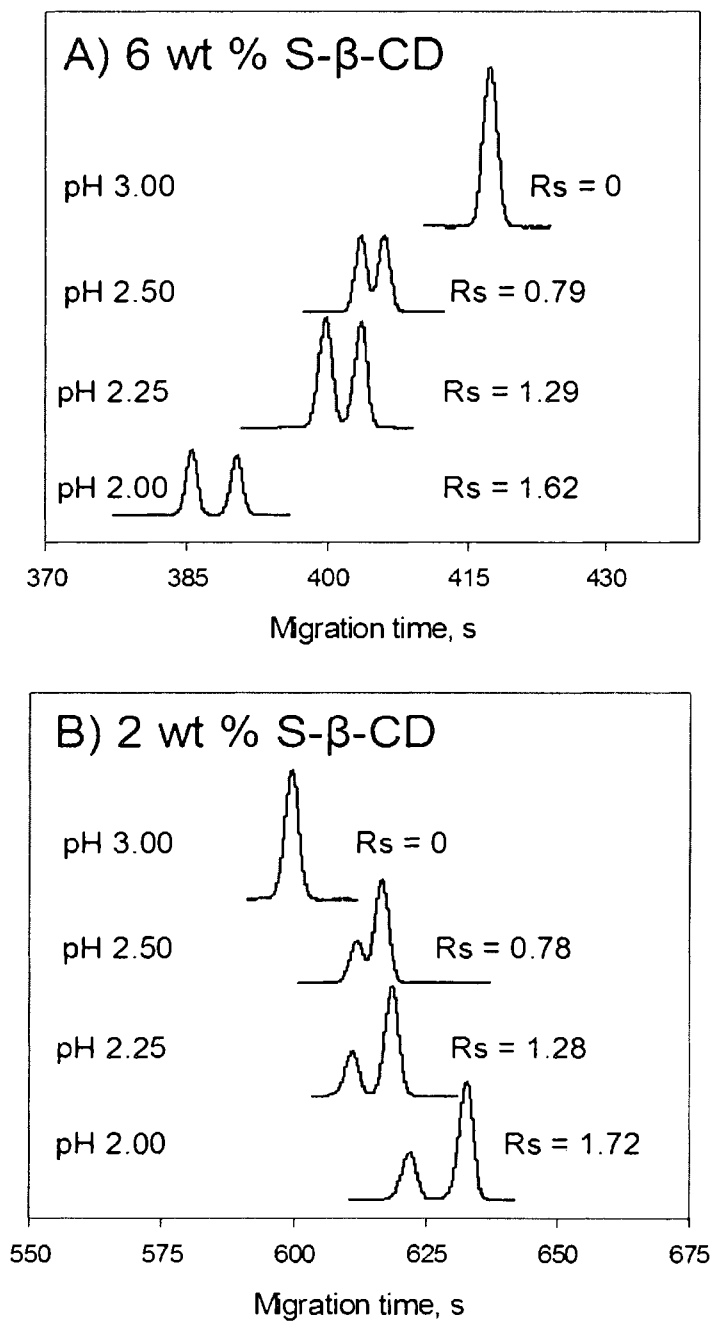


Figure 2.3. Dependence of chiral resolution of CBI-ser on pH of the BGE. A) BGE: 6 wt % S-β-CD, 25 mM phosphate, B) 2 wt % S-β-CD, 25 mM phosphate.

Resolution dramatically decreases as the pH of the BGE is raised from 2 to 3 irrespective of the concentration of CD. Indeed, CBI-ser enantiomers are baseline resolved at pH 2.00 ($R_s = 1.62, 1.72$ for 6 and 2 wt % respectively), but resolution completely vanishes at pH 3.00. Additionally, migration time is not significantly altered by BGE pH; an observation not altogether surprising given the reduced EOF over this range.

Studies on resolution versus pH were also conducted on CBI-ala, CBI-glu, and CBI-arg and a plot is given in Figure 2.4.

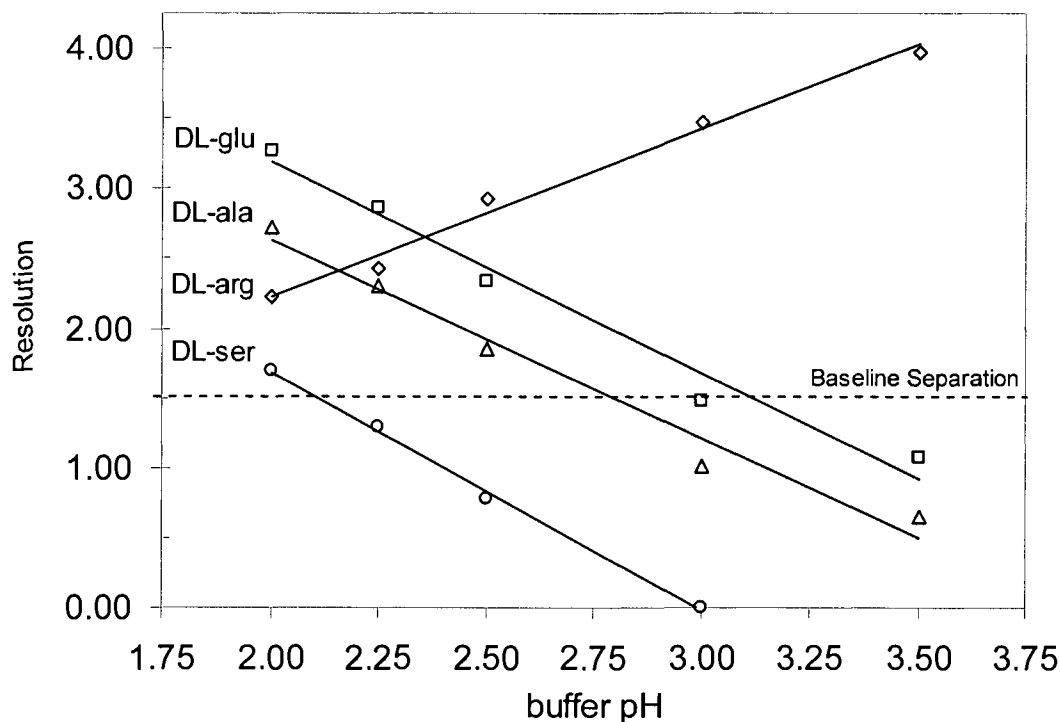


Figure 2.4. Effect of BGE pH on chiral resolution of CBI-amino acids. BGE: 2 wt % S- β -CD, 25 mM phosphate. Each R_s value represents an average ($n = 3$).

CBI-glu and CBI-ala show a similar pH dependent response as seen for CBI-ser with a linear decrease in resolution with increasing pH. This suggests a similar mechanism of chiral recognition between these analytes and S- β -CD. In contrast, CBI-arg resolution increases linearly with increasing pH.

CBI-amino acids possess carboxylic functional groups that may influence chiral recognition and migration time by interacting with S- β -CD during inclusion complex formation. The degree of ionization could play an important role by influencing electrostatic, hydrogen bonding, and/or hydrophobic interactions with the anionic CD. It has been demonstrated that anionic CDs are poor chiral resolving agents for anionic substrates due to electrostatic repulsion. The lower pH (2.00) in our study may minimize these undesirable interactions. To our knowledge, the pK_a values of CBI-amino acids have not been determined. To investigate the nature of the interaction of CBI-amino acids with S- β -CD, we utilized ^{13}C NMR titration to determine the pK_a value of CBI-ser. The chemical shift of the carboxyl carbon of ^{13}C -enriched CBI-L-ser (99.0 atom % at C-1) was determined over the pH* range 1-6 as shown in Figure 2.5.

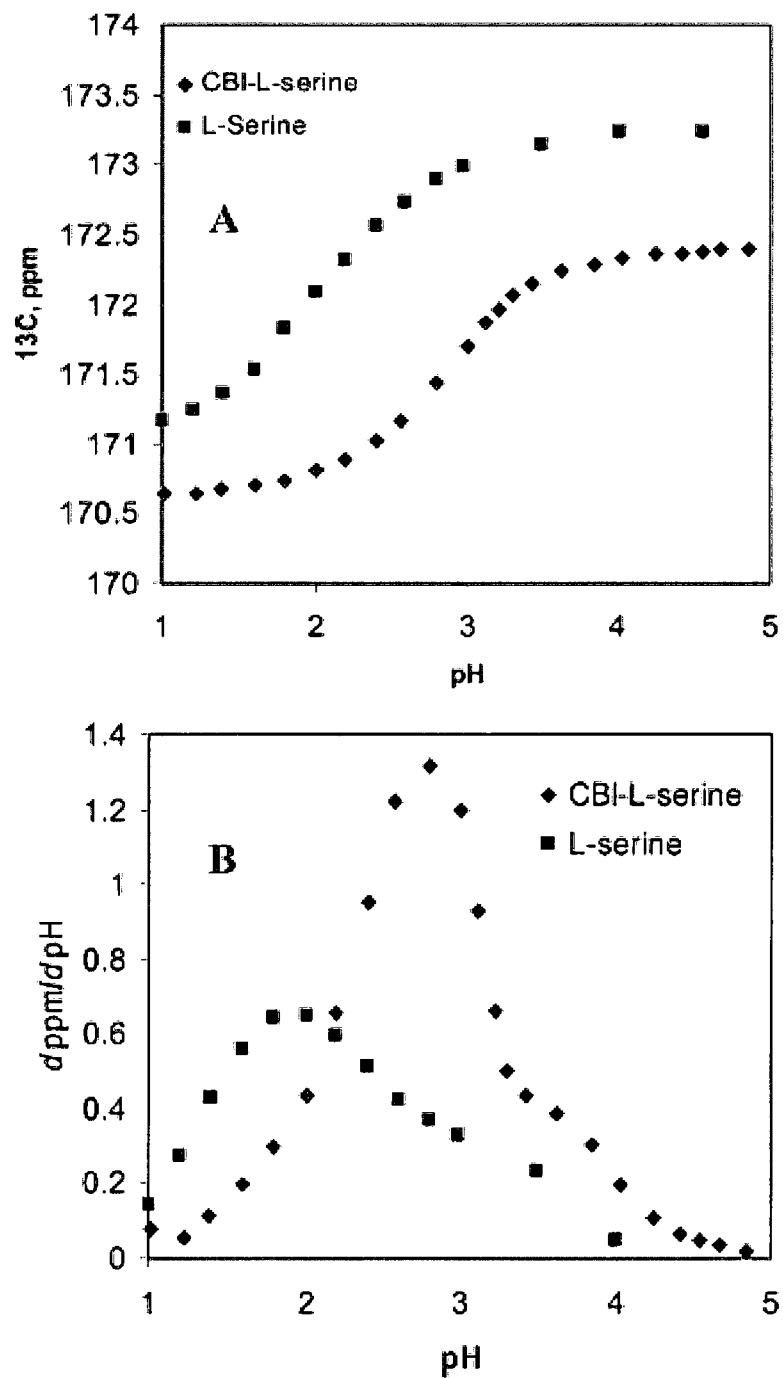


Figure 2.5. ^{13}C NMR titration of L-ser and CBI-L-ser. (A) ^{13}C NMR titration of L-ser and CBI-L-ser. ^{13}C chemical shift of carboxyl group monitored. (B) First derivative of titration curve. Peak maximums for (B) yield $\text{pK}_a^{\text{H}^*}$ which is used to determine pK_a^{H} for L-ser and CBI-L-ser.

pH^* is the direct reading of the D_2O /methanol solution used in the titration with an H_2O calibrated pH meter. The titration curves are shown in Figure 2.5A, along with results on L-ser. The first-derivative curves for these titrations are shown in Figure 2.5B. The $\text{pK}_a^{\text{H}^*}$ values for L-ser and CBI-L-ser are determined to be 1.9 and 2.8, respectively, according to the peak maxima in Figure 2.5B. A recently published equation allows for converting these $\text{pK}_a^{\text{H}^*}$ values determined in D_2O into an H_2O equivalent, thus yielding pK_a^{H} of 2.2 for L-ser and 3.0 for CBI-L-ser. The accepted pK_a of L-ser is 2.2. These results demonstrate that incorporation of the amino function into the NDA molecule substantially decreases the acidity of the carboxyl group of L-ser.

At pH 3 when enantioresolution is lost (Figure 2.3), CBI-ser is substantially ionized (50%, see Figure 2.5) and thus likely exhibits significant electrostatic repulsion with S- β -CD. It is possible that at pH 3 chiral resolution is lost for the weakly acidic CBI-ser due significant lack of interaction with the anionic CD at this pH. A comparison of migration times for CBI-L-ser in the presence and absence of S- β -CD at pH 3 is shown in Figure 2.6.

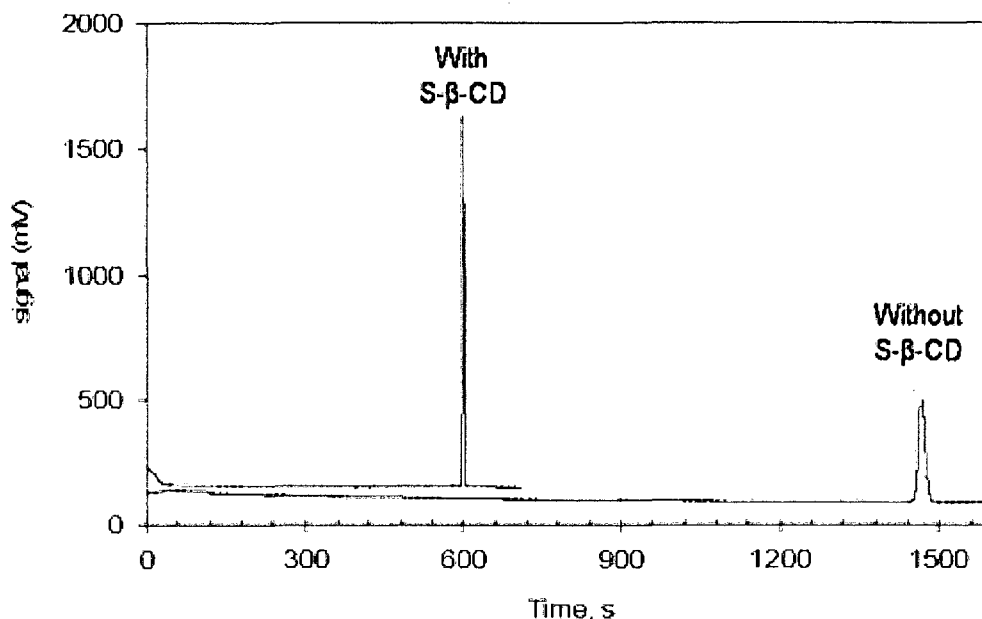


Figure 2.6. Comparison of electropherograms of CBI-L-ser in the presence and absence of S- β -CD at pH 3. BGE: 25 mM phosphate pH 3.00 with and without 2 wt % S- β -CD.

It is apparent that CBI-ser migrates with its own electrophoretic mobility in the absence of S- β -CD at pH 3. This is in agreement with the pK_a data demonstrating its ionization at this pH. Addition of 2 wt % S- β -CD then results in a > 2-fold decrease in CBI-ser migration time. Thus, despite repulsion, CBI-ser continues to show a strong interaction at pH 3 with S- β -CD. This suggests that the loss of chiral recognition at this pH is more probably related to a change in the nature of interaction with the chiral resolving agent. The anionic moiety of CBI-ser may be positioned above the CD cavity and exhibit electrostatic repulsion which limits the depth of penetration into the hydrophobic CD cavity. In contrast, the more protonated CBI-ser at pH 2 (10% ionized) may exhibit greater depth of penetration of the naphthyl group into the CD cavity. This effect could allow for greater enantioselectivity by bringing the chiral α -carbon of CBI-ser in closer

proximity to the chiral cavity. It is also plausible that hydrogen bonding interactions between the carboxyl group of CBI-ser and the hydroxyl and sulfato groups of S- β -CD becomes more important for the more protonated CBI derivative. A similar explanation may likely explain the parallel linear decreases in resolution with pH shown in Figure 2.4 for CBI-ala and CBI-glu.

CBI-arg resolution increases with increasing pH (positive slope) with nearly 2-fold resolution improvement when pH is increased from 2.0 to 3.5 as shown in Figure 2.4. The guanidine R-group of CBI-arg is fully protonated over the pH range investigated here. At low pH (2.00), CBI-arg would be expected to be significantly cationic, due to protonation of both the α -COOH and guanidine R-group. Electrostatic attraction of the CBI-arg and S- β -CD would be expected and is likely the primary cause of the fast electromigration of CBI-arg relative to other amino acids at pH 2.0, as shown in Figure 2.7.

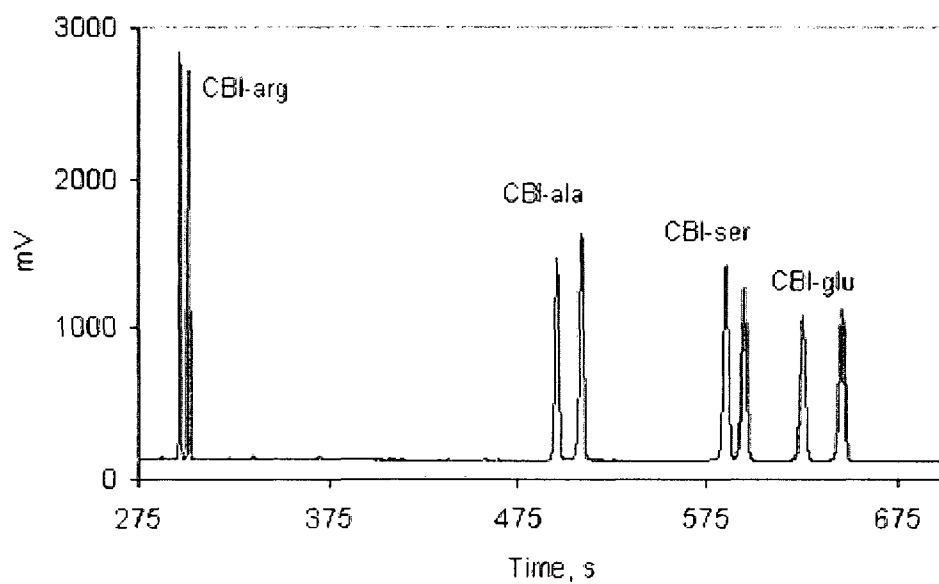


Figure 2.7. Electropherogram of a mixture of CBI-DL-amino acids arg, ala, ser, and glu at 2 wt % S- β -CD. BGE: 25 mM phosphate pH 2.00 with 2 wt % S- β -CD. The cationic CBI-arg displays the fastest migration time in the presence of S- β -CD.

Strong interaction must play an important role for CBI-arg since in the absence of S- β -CD migration would be directed toward the inlet (cathode). Evidence further implicating an electrostatic interaction for CBI-arg is shown when plotting concentration of S- β -CD as a function of the average chiral pair migration time as shown in Figure 2.8.

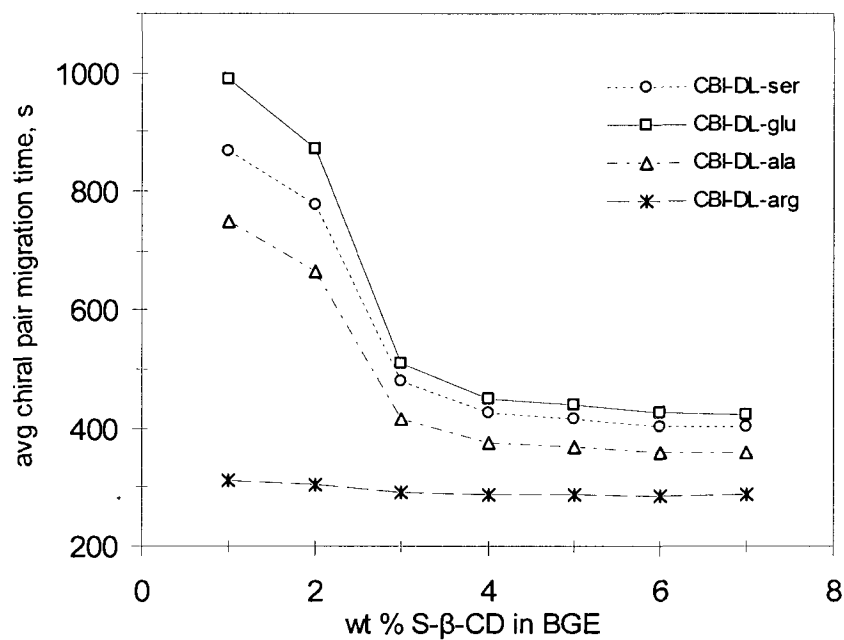


Figure 2.8. Effect of S- β -CD concentration on the migration time of CBI-amino acids. BGE: 25 mM phosphate pH 2.00. Each chiral pair migration time represents an average (n=3).

CBI-arg electromigration does not appreciably change over the S- β -CD concentration investigated whereas CBI-ser, CBI-glu, and CBI-ala all show appreciable change. Finally, as pH is increased, CBI-arg migration time dramatically increases, in contrast to the nonbasic CBI-amino acids (Figure 2.9).

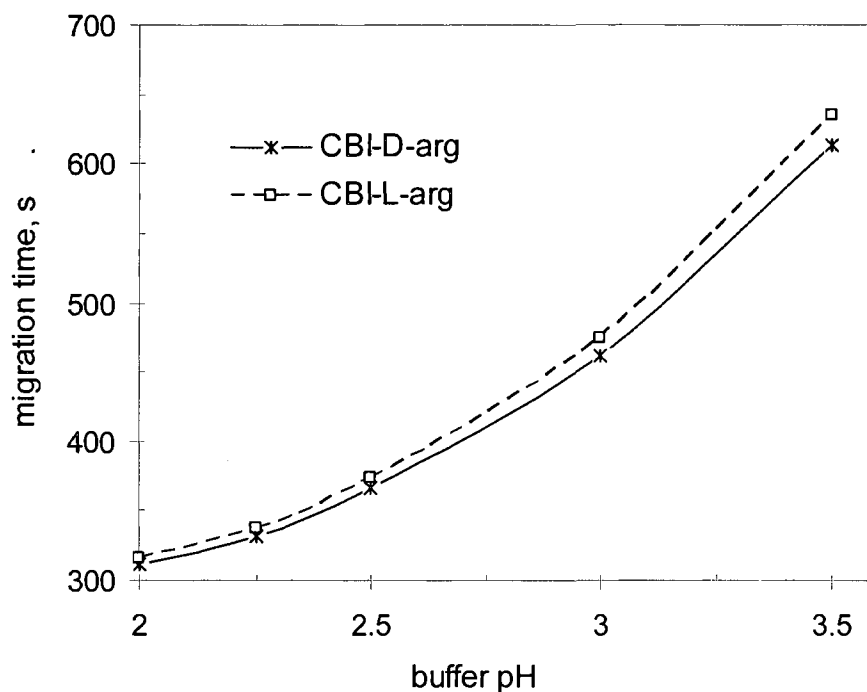


Figure 2.9. CBI-DL-arg migration time as a function of buffer pH at 2 wt % S- β -CD. BGE: 25 mM phosphate with 2 wt % S- β -CD.

This increase in migration time with pH can be attributed to changes in the degree of ionization of the CBI-arg carboxylic acid group with increasing pH. Indeed, at pH 3.5, CBI-arg is approaching a neutral, zwitterionic form with decreased electrostatic interaction with S- β -CD, and its migration time approaches that of nonbasic CBI-amino acids at pH 2.00.

The impact of phosphate buffer concentration on resolution of a series of CBI-amino acids is shown in Figure 2.10.

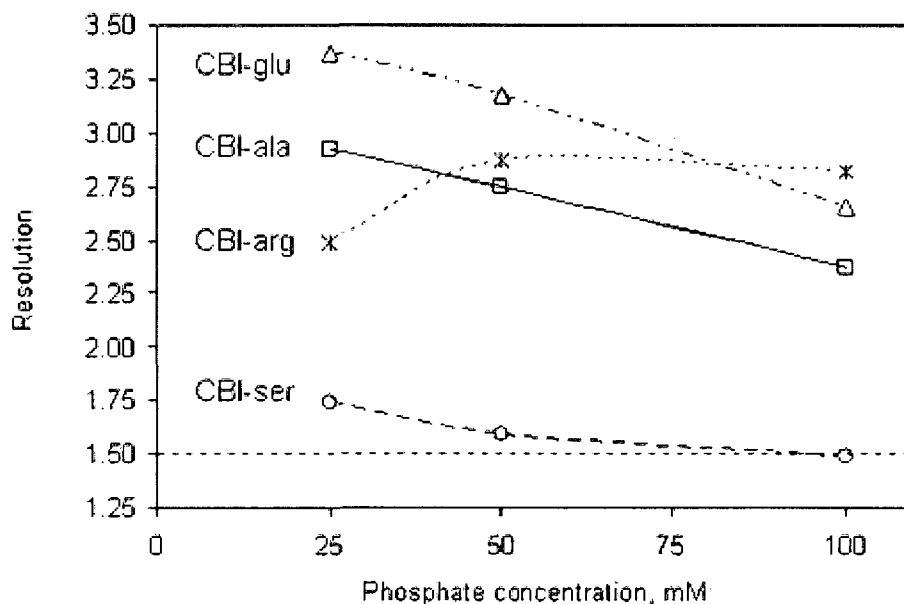


Figure 2.10. Influence of phosphate buffer concentration on chiral resolution of a series of CBI-amino acids. BGE: 2 wt % S- β -CD, pH 2.00. Each resolution value is an average ($n=3$).

Optimal chiral resolution is found for CBI-ser, CBI-glu, and CBI-ala at low phosphate concentration. While phosphate plays a lesser role than other variables investigated, increasing phosphate beyond 25 mM appears detrimental for resolution of CBI-ser, CBI-glu, and CBI-ala.

The chiral resolution of a larger group of CBI-amino acids is shown in Figure 2.11 and represented numerically in Table 2.1. An optimized buffer consisting of 25 mM phosphate at pH 2.00 with 2 wt % S- β -CD was used to investigate these chiral separations. Table 2.1 additionally contains numeric data for the same analytes except using 6 wt % S- β -CD for comparison.

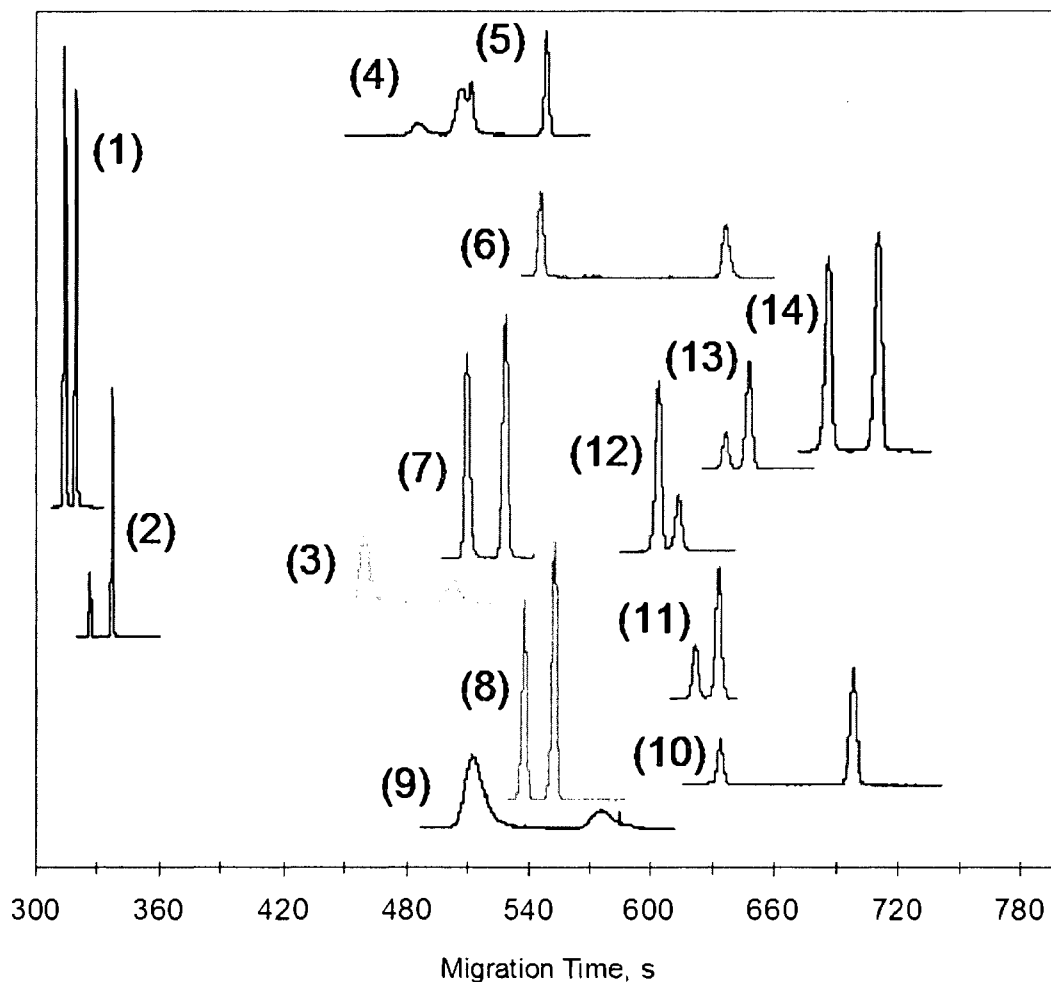


Figure 2.11. Chiral separation of 14 CBI-amino acids with 2 wt % S- β -CD in 25 mM phosphate, pH 2.00. Peak identities: (1) CBI-DL-arg; (2) CBI-DL-his; (3) CBI-DL-phe; (4) CBI-DL-ile; (5) CBI-DL-asg; (6) CBI-DL-tyr; (7) CBI-DL-met; (8) CBI-DL-ala; (9) CBI-DL-trp; (10) CBI-DL-thr; (11) CBI-DL-ser; (12) CBI-DL-gln; (13) CBI-DL-asp; (14) CBI-DL-glu. Migration times for a given analyte varied by as much as 5% per run (Table 2.1) and thus this illustration does not absolutely represent positions of CBI-amino acids relative to one another.

Table 2.1. Migration and R_s values for CBI-DL-amino acids at 2 and 6% wt % S- β -CD^a

CBI-amino acid	Migration time (s)	Resolution
	2 wt % S- β -CD D / L	2 wt % S- β -CD R_s
tyrosine	636 / 509	15.74
threonine	639 / 704	8.89
asparagine	512 / 549	7.15
phenylalanine	504 / 460	3.95
histidine	325 / 336	4.88
glutamic acid	690 / 677 \pm 39 / 37	3.29 \pm 0.08
methionine	545 / 527	3.02
alanine	525 / 539 \pm 24 / 25	2.79 \pm 0.11
arginine	307 / 312 \pm 8 / 8	2.37 \pm 0.15
aspartic acid	637 / 648	1.79
isoleucine	485 / 506	3.16
serine	621 / 632 \pm 31 / 32	1.69 \pm 0.05
tryptophan	576 / 513	2.74
glutamine	580 / 571	1.45
valine	492	0
leucine	462	0
lysine	289	0
	6 wt % S-β-CD	6 wt % S-β-CD
CBI-amino acid	D / L	R_s
tyrosine	411 / 361	17.66
threonine	402 / 428	8.2
asparagine	358 / 374	6.02
phenylalanine	347 / 328	5.17
histidine	306 / 313	3.22
glutamic acid	421 / 413	2.67
methionine	367 / 360	2.55
alanine	353 / 358	1.92
arginine	287 / 290	1.89
aspartic acid	403 / 408	1.86
isoleucine	331 / 341	1.77
serine	392 / 397	1.58
tryptophan	392 / 366	1.91
glutamine	371	0
valine	334 / 335	0.51
leucine	344	0
lysine	291	0

^a BGE: 25 mM phosphate, pH 2.00. All CBI-amino acids pairs were diluted 10 μ M total (1:2 D/L). 6 wt % S- β -CD, n = 1; 2 wt %, n =3 except for CBI-glu, CBI-arg, CBI-ala, and CBI-ser where n=9.

It is apparent from Table 2.1 that the concentration of S- β -CD plays a lesser role than pH on chiral resolution for CBI-amino acids. In fact, with the exception of CBI-phe, CBI-tyr, and CBI-val, all CBI-amino acids show either no change or a slight decrease in resolution at high concentration of S- β -CD. Nearly half the CBI-amino acids (6 of 14 at 2 wt % S- β -CD) demonstrate a reversed migration order compared to CBI-ser with the L-isomer exhibiting the greater electrophoretic mobility. These include CBI-met, CBI-gln, and CBI-glu in addition to all 3 of the aromatic side chain CBI-amino acids. These latter aromatic amino acid derivatives all show excellent enantioresolution ($R_s > 2.5$) at 2 wt % S- β -CD. CBI-tyr demonstrated remarkable enantioresolution using S- β -CD with the L-isomer eluting >2 min prior to D-isomer over the course of an 11 min separation.

2.4 Stacking of dilute amino acid solutions with S- β -CD

Stacking is an important feature of CE which under the proper conditions allows for enhanced detection of trace analytes through substantial increase in volume and/or mass injected into the capillary. For hydrodynamic injection, stacking mechanisms are important for injections > 2 % of the capillary volume (Weinberger, 2000).

We found that CBI-ser and CBI-glu standards diluted in water could be substantially stacked using vacuum injection as demonstrated in Figure 2.12, where injection time ranges from 2 to 120 s (380 mbar) for a 0.05 μ M solution of each enantiomer.

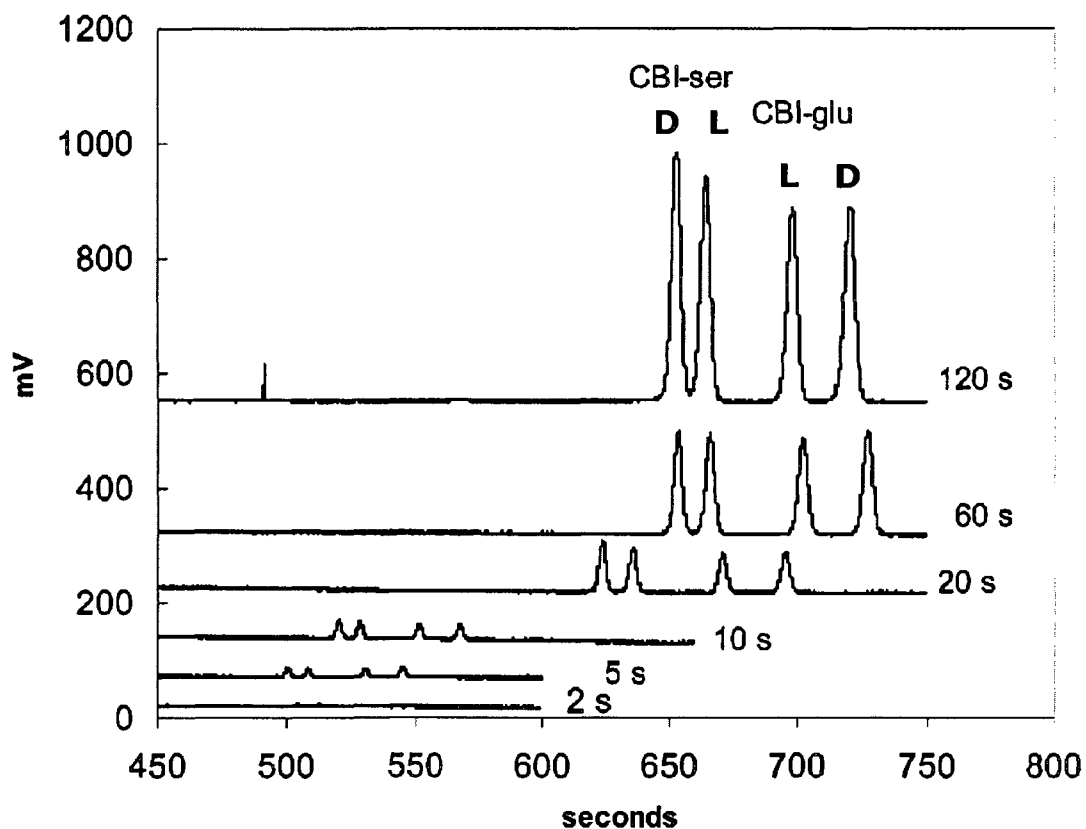


Figure 2.12. Stacking of dilute solutions of CBI-DL-ser and CBI-DL-glu using S- β -CD. CBI-amino acids were prepared at 0.05 μ M in water. Stacking is demonstrated by comparison of separate electropherograms obtained from vacuum injections ranging from 2-120 s (380 mbar). BGE: 25 mM phosphate pH 2.00 with 3 wt % S- β -CD.

An enhancement of signal-to-noise of \sim 100-fold for a 120 s versus 2s injection is realized without substantial loss of chiral resolution, as shown numerically in Table 2.2.

Table 2.2. Signal to Noise (S/N) Ratio, Resolution (R_s), and Estimated Concentration Limits of Detection (CLOD) for CBI-Ser and CBI-Glu.

injection, s ^a	S/N ^b	CLOD (nM) ^c	R_s
	CBI-ser, CBI-glu	CBI-ser, CBI-glu	CBI-ser, CBI-glu
2	2.6, 2.3	57.4, 65.7	1.92, 3.26
5	17.0, 15.8	8.8, 9.5	1.77, 3.32
10	31.4, 27.2	4.8, 5.5	1.78, 3.41
20	60.9, 51.9	2.5, 2.9	1.91, 3.38
60	135, 130	1.1, 1.2	1.57, 2.82
120	226, 186	0.66, 0.81	1.34, 2.46
180	14.9, 10.2	0.20, 0.30	1.72, 2.20

^a 50 nM of each enantiomer hydrodynamically vacuum injected except 180-s injection, which was 1 nM each enantiomer (see Figure 2.13). ^b Noise was estimated at the 95% CI by PeakFit. ^c CLOD were estimated at S/N = 3.

Furthermore, good signal-to-noise was achieved for a 180 s injection of 1 nM of each enantiomer of CBI-ser and CBI-glu as shown in Figure 2.13.

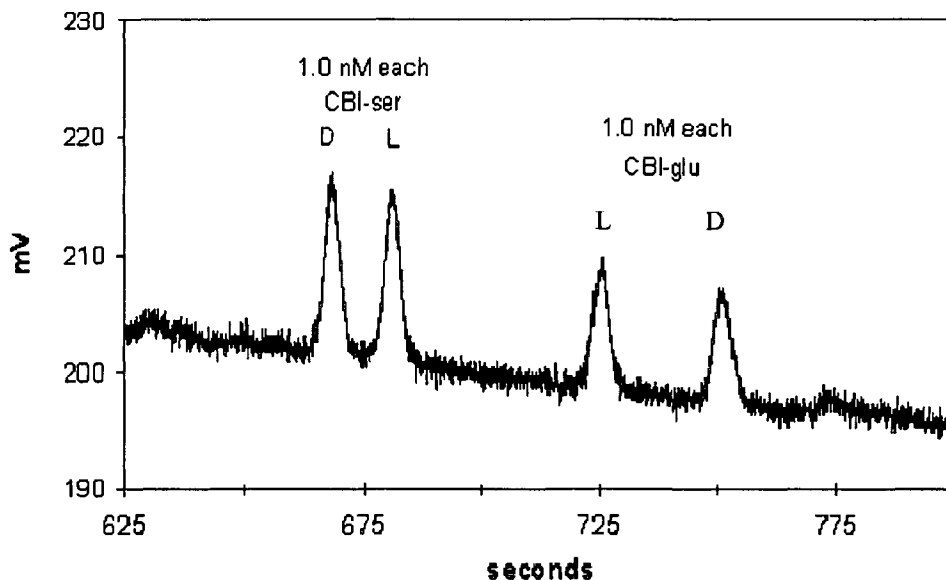


Figure 2.13. Detection by hydrodynamic stacking of 1 nM each of CBI-DL-ser and CBI-DL-glu using S- β -CD BGE. Stacking is represented by an electropherogram showing typical S/N obtained for low ionic strength solutions of racemic CBI-ser and CBI-glu. Injection was 180 s (capillary filled 19.5 cm). BGE: 25 mM phosphate pH 2.00 with 3 wt % S- β -CD. Estimated LOD; CBI-ser, 0.20 nM; CBI-glu, 0.30 nM (S/N = 3).

The baseline resolution of CBI-ser and CBI-glu enantiomers at 1 nM each demonstrates that significant stacking occurs in addition to chiral separation without significant resolution loss. A detection limit of 0.2 nM of CBI-ser and 0.3 nM CBI-glu is calculated (S/N = 3) from this electropherogram. The volume injected was determined using long injections of Brilliant Blue dye (FD&C Blue No. 1) solution. This dye was visible under 10X microscope without removal of capillary polyimide coating. This approach gives a 19.5 cm injection (~28% of capillary volume) for a 180 s vacuum injection (380 mbar) which corresponds to ~96 nL of solute. Hydrodynamic vacuum injection can also be used for stacking more complex samples, as shown in Figure 2.14, for a mixture of 11 amino acids (including 4 chiral pairs).

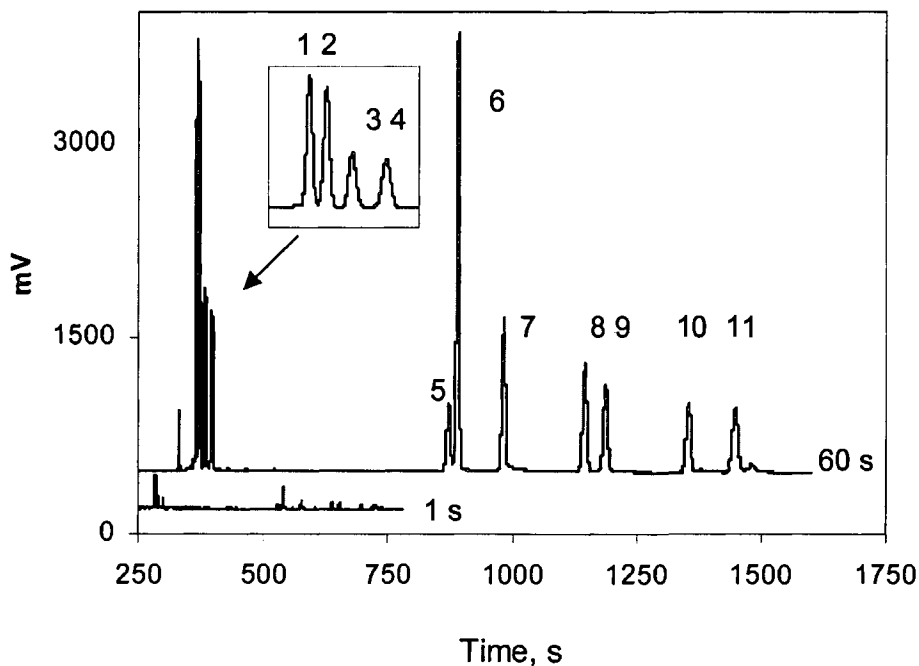


Figure 2.14. Stacking of a complex dilute sample of 11 CBI-amino acids with S- β -CD. Injection time corresponds to 380 mbar vacuum. Amino acids were prepared at $\sim 0.5 \mu\text{M}$ each. Peak identities: (1) CBI-D-arg; (2) CBI-L-arg; (3) CBI-D-his; (4) CBI-L-his; (5) CBI-gly; (6) CBI-L-tyr; (7) CBI-L-gln; (8) CBI-D-ser; (9) CBI-L-ser; (10) CBI-L-glu; (11) CBI-D-glu. BGE: 25 mM phosphate, pH 2.00 with 2 wt % S- β -CD.

The mechanism for stacking is proposed herein to involve a combination of field amplified stacking, pH mediated stacking, and sweeping by S- β -CD. A schematic of this proposed mechanism is given in Figure 2.15.

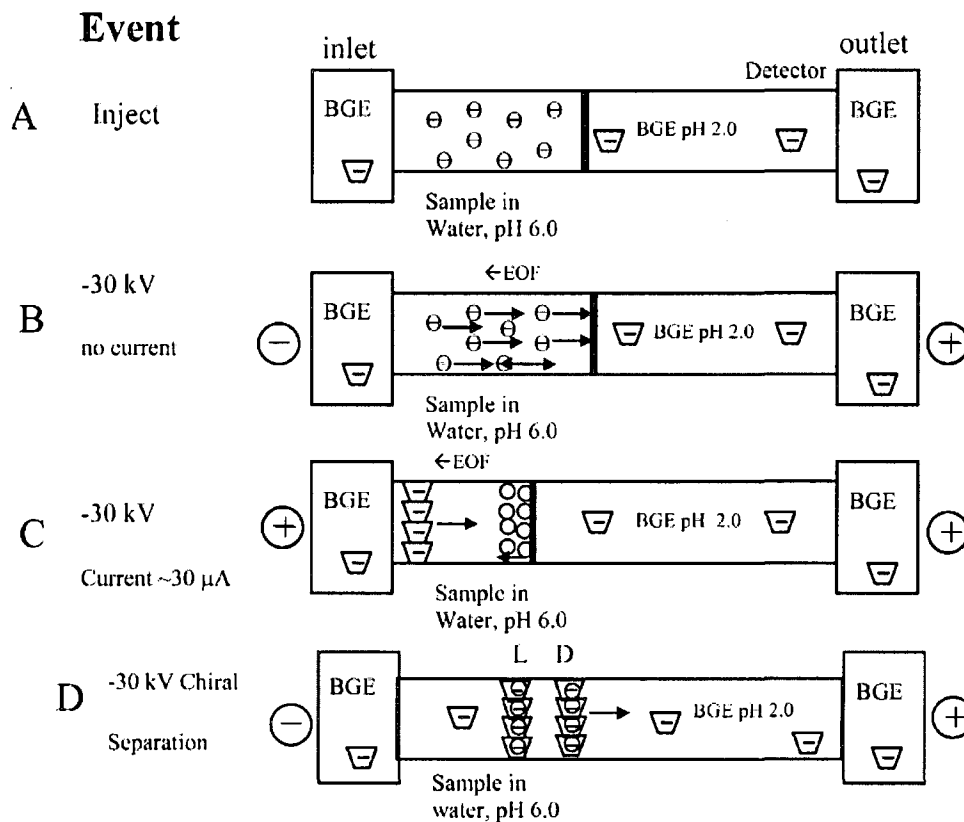


Figure 2.15. Schematic diagram of the pH-mediated stacking/ sweeping- $S\text{-}\beta\text{-CD}$ of chiral CBI-amino acids.

The dilute CBI-amino acids are anionic when initially injected at $\sim 1/3$ of the capillary volume due to the carboxylic acid groups which are substantially ionized when dissolved in water at pH 6. The exceptions are CBI-amino acids with basic side chains as mentioned above for CBI-arg. When a negative potential of -30 kV is applied (B), the current initially starts out at zero (observed) and the dilute anionic CBI-amino acids experience field amplified migration, with mobility toward the anode. This mobility is ultimately interrupted by a pH junction formed by the boundary between the injection plug and BGE at pH 2. At the pH junction (C), the dilute injection plug is substantially

stacked as CBI-amino acids are ~neutralized by the low pH BGE. This stops their electromigration. Around the same time, (D) an EOF is generated in the aqueous plug that drives the pH 6 solution out of the capillary via the inlet. Eventually the current increases as anionic S- β -CD migrates into the stacked plug and sweeps the CBI-amino acids toward the detector. It is important to note that under this mechanism, S- β -CD must enter the capillary prior to ejection of the aqueous plug or else the CBI-amino acids would be expelled from the capillary. Thus it appears there is a combination of field amplified migration, pH mediated stacking, and sweeping of the ~ neutralized CBI-amino acid toward the detector that is responsible for the overall stacking effect.

Support for the mechanism was obtained from 2 experiments using a capillary in which the detector window was placed 3 cm from the capillary inlet as shown in Figure 2.16.

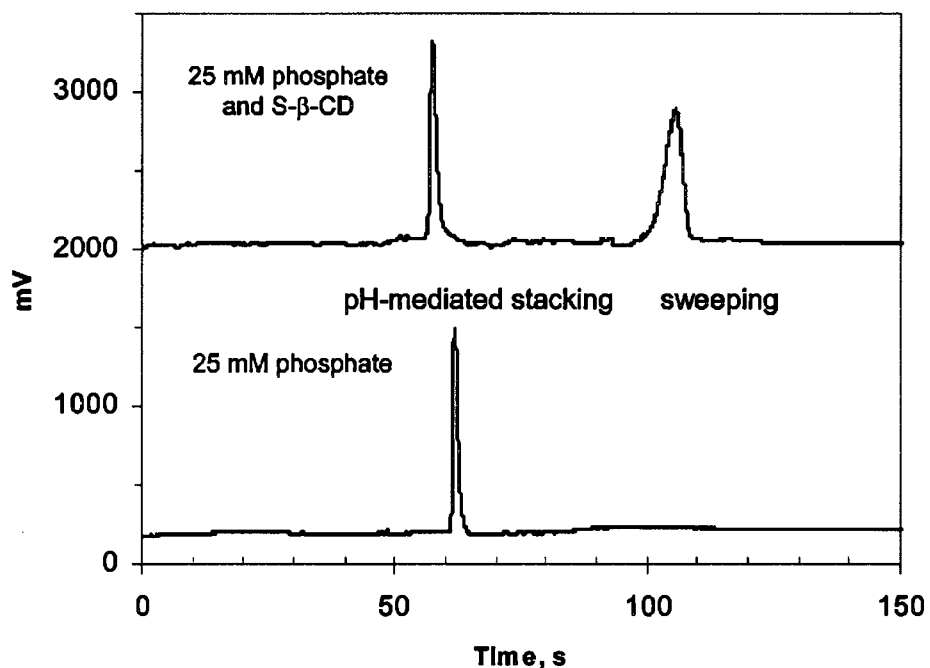


Figure 2.16. Electropherograms from experiment demonstrating both pH mediated stacking and sweeping mechanisms for S- β -CD. Lower trace: Electropherogram illustrating stacking when operating BGE without S- β -CD at low-pH reversed polarity. The capillary (70 x 3 cm x 25 μ m) was filled 19.5 cm with 0.10 μ M CBI-L-ser in water (pH 5.2), and a voltage (-30 kV) was applied. The dilute CBI-ser is stacked at the pH boundary and driven toward the inlet vial and detected prior to exiting the capillary. Upper trace: electropherogram illustrating stacking/sweeping when operating BGE with S- β -CD. Once the stacked zone nears the inlet (peak 1), it reverses direction as S- β -CD enters the capillary and sweeps the stacked CBI-ser toward the outlet vial (peak 2).

In both experiments CBI-L-ser was injected for 180 s (380 mbar) corresponding to a 19.5 cm injection. In the lower trace, a peak is observed in the absence of S- β -CD represents the field amplified, and pH mediated stacked band passing by the detector due to the EOF driving the aqueous plug back toward the inlet. Since S- β -CD is absent from the BGE, the stacked band is expelled from the capillary. In comparison, the upper trace shows an identical experiment conducted in the presence of S- β -CD. A similar pH mediated stacked band is observed from EOF driven migration back toward the inlet. In

contrast however, the upper trace demonstrates that S- β -CD enters the capillary prior to sample expulsion and sweeps the analyte back toward the detector prior to sample expulsion as represented by a second band shown at ~ 100 s. Interestingly, the pH mediated band is significantly narrower than the sweeping band suggesting some destacking occurs during migration reversal at the sweeping step (D). The cause of destacking during sweeping is currently unknown but it suggests that pH mediated stacking may be the primary mechanism responsible for stacking observed in Figures 2.12-2.16.

The proposed mechanism is similar to that proposed by Lin and Shih for CBI-amino acids using anionic SDS and low pH BGE (Shih and Lin, 2005), except their stacking/sweeping-MEKC apparently requires that initial BGE contain no SDS. After migration of the stacked analyte to nearly the inlet, the vials at both inlet and outlet are replaced to contain BGE-SDS. SDS then sweeps the stacked analyte toward the detector. Comparison of the techniques can be made and is shown in Table 2.3.

Table 2.3. Comparison of full-capillary sample stacking / sweeping-MEKC and pH mediated stacking/sweeping-S- β -CD of dilute CBI-amino acids.

Method	FCSS/ sweeping MEKC ^a	pH stacking/ sweeping S- β -CD ^b
analyte	CBI-Ile	CBI-DL-ser
injection length, cm	60 (full capillary)	19.5 (28% of length)
capillary i.d., μ m	75	25
injection volume, μ L	2.65	0.096
CLOD, M	1.1×10^{-9}	0.3×10^{-9}
mole detection limit, fmol	2900	29
switching of BGE	Yes	No
migration time, min	~30	~11
chiral separation	no	yes
plate number, N	1.2×10^5	1.8×10^5
^a Total and effective length of capillary 60/54 cm, violet LED 410 nm, 2 mW.		
^b Total and effective length of capillary 75/45 cm, violet diode laser, 420 nm, 5 mW.		

The concentration detection limits are similar for dramatically different injection volumes, with the molar detection limit for pH-mediated stacking/sweeping-S- β -CD being ~100-fold more sensitive. Given the similar separation efficiencies (N) of the two methods, it is difficult to reconcile the different molar detection limits for the two methods. The application of this stacking technique to brain microdialysates discussed below was not possible due to the high ionic strength of the sample, as discussed by Gillogly et al. (Gillogly and Lunte, 2005). Injection time of microdialysates greater than 5 s (380 mbar) results in significantly broader peaks with loss of resolution. We believe pretreatment of the sample, such as desalting, will be necessary for successful

application of this stacking technique to brain microdialysates. The promise of the technique may lie in its ability to provide low detection limits for evaluation of enantiopurity of amino acids and other chiral molecules, using either UV or fluorescence detection.

2.5 Analysis of D-ser, DL-asp, and DL-glu in the hippocampus of arctic ground squirrel.

To demonstrate application of S- β -CD at low pH reversed polarity for amino acid analysis, we chose to quantify levels of CBI-DL amino acids sampled from the brain of live arctic ground squirrels (AGS). Using a standard mixture of 22 primary amines commonly found in brain microdialysates, no interfering species were identified for CBI-D-ser, CBI-DL-asp, and CBI-DL-glu. Calibration curves were constructed for low-micromolar detection. L-homoarginine was chosen as internal standard to minimize error in quantitative analysis. The calibration curves are given in Figure 2.17.

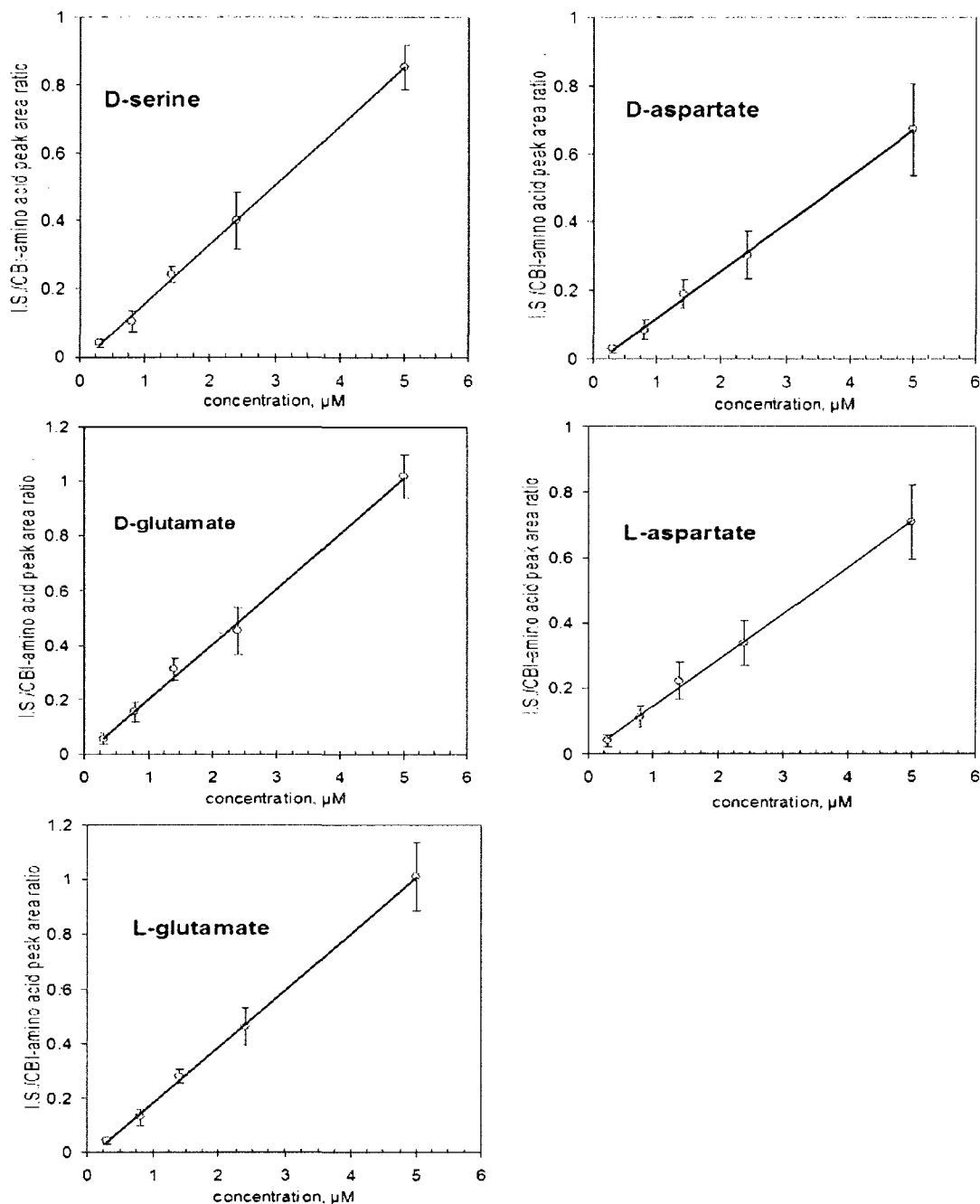


Figure 2.17. Linear regression calibration curves for CBI-amino acid standards for bioanalysis with S- β -CD. Curves were generated using an internal standard and are represented as the concentration of CBI-amino acid versus the peak area ratio of the internal standard (9 μM CBI-L-homoarginine) to CBI-amino acid. Error bars represent the standard deviation of the average I.S./CBI-amino acid peak area for the represented

concentration. Data points were constructed from at least $n > 4$ separate determinations at each known concentration.

A typical electropherogram of a microdialysate from an AGS hippocampus is illustrated in Figure 2.18.

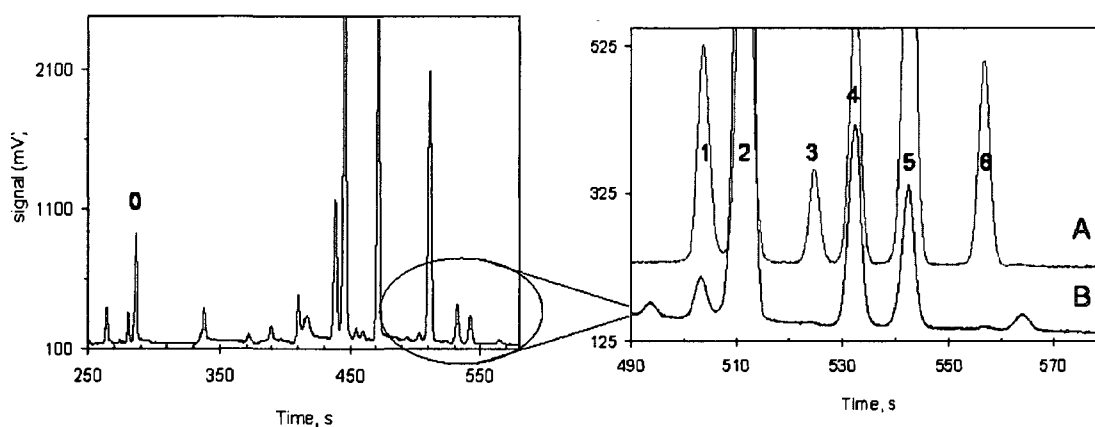


Figure 2.18. Typical electropherogram of a microdialysate from the hippocampus of an arctic ground squirrel. (A) Standard amino acid mixture including (1) CBI-D-ser; (2) CBI-L-ser + NDA side product; (3) CBI-D-asp; (4) CBI-L-asp; (5) CBI-L-glu; (6) CBI-D-glu. (B) Microdialysate from AGS obtained 40 min after probe insertion at flow rate of $0.6 \mu\text{L}/\text{min}$. The internal standard is labeled as peak (0). Identities of CBI-amino acids in microdialysates were determined by spiking with known CBI-amino acids.

Appreciable levels of D-ser, L-asp, and L-glu were observed, while D-asp and D-glu are found only as trace components below the limit of quantification (LOQ). Quantitative analysis of CBI-amino acid concentrations is shown in Table 2.4, along with equations of the weighted linear regression standard curves used for analysis.

Table 2.4. Quantitative analysis of amino acids in microdialysate from hippocampus of arctic ground squirrel.

CBI-amino acid	standard curve ^a	R ²	CLOD, nM ^b	[dialysate], uM ^c	[dialysate], uM ^d
CBI-D-ser	Y = 0.171x - 0.005	0.996	43.8 ± 0.4	0.25 ± 0.09	0.23 ± 0.09
CBI-L-asp	Y = 0.145x + 0.005	0.998	40.3 ± 0.4	1.54 ± 0.23	0.43 ± 0.11
CBI-L-glu	Y = 0.203x - 0.013	0.998	32.3 ± 0.3	0.86 ± 0.06	0.57 ± 0.15
CBI-D-asp	Y = 0.130x - 0.004	0.991	57.1 ± 0.1	trace	-
CBI-D-glu	Y = 0.203x + 0.004	0.997	41.2 ± 0.4	trace	-

^a y = mx + b. (CBI-aa/internal std) = m[CBI-aa] + b. ^b Concentration limits of detection (CLOD) calculated from response of low-concentration standard of 0.3 μM (n=4) assuming S/N = 3. ^c 20 min after probe insertion. ^d 110 min after probe insertion.

2.6 Summary of S-β-CD as chiral selector for CBI-amino acids

Commercially available S-β-CD is found to be an excellent chiral selector for CBI-amino acids using low-pH reverse polarity CD-cEKC. The strength of this CE technique lies in its ability to baseline resolve a large number of CBI-DL-amino acids with a single buffer formulation. This separation occurs best at BGE pH levels below the pK_a of the weakly acidic α-COOH of CBI-amino acids. Significant electrostatic interactions (favorable and unfavorable) were demonstrated between this CD and CBI-amino acids. D-asp, D-ser, and D-glu can all be potentially quantified in neuronal samples, if present. In our study, basal levels of D-ser, L-glu, and L-asp, all important neurotransmitters/neuromodulators, were quantified in microdialysates from the hippocampus of an arctic ground squirrel. Stacking with enantioseparation of low ionic strength solutions of CBI-amino acids was demonstrated with detection limits of 0.20 and 0.30 nM for CBI-ser and CBI-glu, respectively.

Chapter 3

Synthesis and characterization of single isomer sulfoalkyl cyclodextrins

3.1 Overview of study

Single isomer highly charged sulfated cyclodextrins have emerged as some of the most powerful chiral selectors in capillary electrophoresis. Currently the only single isomer highly charged anionic cyclodextrins are substituted with sulfato functional groups. Vigh and colleagues have designed an entire family of single isomer sulfato α -, β -, and γ -CDs for enantioresolution in CE (Vincent et al., 1997a; Vincent et al., 1997b; Cai et al., 1998; Zhu and Vigh, 2000; Maynard and Vigh, 2001; Busby et al., 2003; Li and Vigh, 2003; Zhu and Vigh, 2003; Li and Vigh, 2004b, a; Busby and Vigh, 2005a, b; North and Vigh, 2008). As of the writing of this dissertation thesis, many of these are now commercially available, offer a range of functional modifications on the primary and secondary CD rim offering alternative selectivity for chiral guests, and are thoroughly investigated for a wide range of chiral pharmaceutical compounds. The strength of the single isomer sulfato CDs as chiral selectors arises from several important structural features. Firstly, charged chiral selectors are capable of resolving charged as well as neutral chiral analytes (Chankvetadze et al., 1995). All of the anionic β -CDs synthesized by Vigh and coworkers bear at least 7 charged sulfato groups on the primary or secondary rim (α -CDs have at least 6). High charge can maximize the difference in electrophoretic mobility of free and complexed analytes, increasing resolution and separation efficiency (Skanchy et al., 1999). Secondly, CDs synthesized by Vigh and coworkers are isomerically pure

through the use of selective reaction chemistry. In contrast, nonselective synthesis of CDs often results in a wide range of regional and positional isomers with a wide range of degrees of substitution, often leading to poor batch to batch reproducibility. While they may be excellent resolving agents as isomeric mixtures for certain compounds, this heterogeneity limits robustness of developed assays. For example, the separation of CBI-ser, CBI-glu, and CBI-asp optimized in Chapter 2 is shown in Figure 3.1 below for separate synthetic batches of S- β -CD obtained from the same commercial supplier.

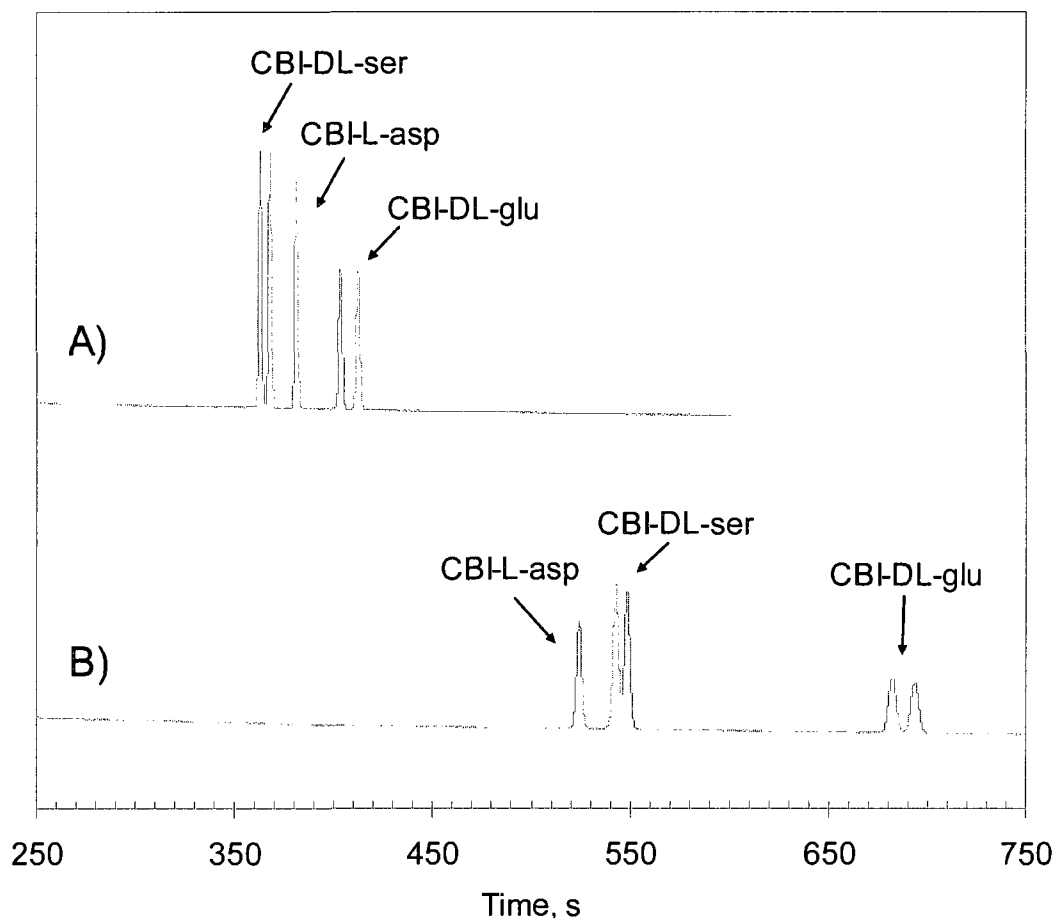


Figure 3.1. Comparison of the chiral separation of a mixture of CBI-DL-ser, CBI-DL-glu, CBI-L-asp using different synthetic batches of S- β -CD. (A) 2 wt % S- β -CD, Fluka Lot # L1148973 as optimized in Chapter 2. B) 2 wt % S- β -CD, Fluka Lot # L1348154. Separations were carried by CE-LIF as described in Chapter 2. A bare fused silica of dimensions 48 x 45 cm x 25 μ m was used in reversed polarity (21 kV). BGE was 25 mM phosphate adjusted to pH 2.15. Samples were prepared at 5 μ m each amino acid in water and injected by vacuum (380 mbar) for 1s.

While CBI-DL-glu is baseline resolved with both S- β -CD batches, CBI-DL-ser is not. Furthermore, the relative mobility of the various CBI-amino acids varies with different synthetic batches. The longer migration times shown in Figure 3.1B would additionally suggest a lower average degree of substitution (DS) of the sulfated CD mixture in this

particular synthetic batch since, under the conditions used, the migration time is related to the strength of interaction. This latter point is an important structural limitation of randomly substituted CDs since it drastically limits robustness of an analytical assay. Thirdly, CDs composed of isomeric mixtures can demonstrate marked reduction in overall resolving power since different cyclodextrin isomers within a given mixture may possess finite differences in complexation rates resulting in unavoidable kinetic band broadening (Vincent et al., 1997a). These numerous inconsistencies are entirely avoided with single isomer CDs.

Interestingly, CDs bearing sulfato groups on their primary and or secondary rim like those produced by Vigh and coworkers are not without some theoretical inclusion complexation limitations. For sulfato CDs the high charge density is in close proximity to the hydrophobic CD torus. It is reasonable that this could significantly limit the strength of interactions with hydrophobic guest molecules especially for highly charged (\geq hepta-sulfato) CDs. CDs bearing sulfoalkyl groups on the primary and secondary rim have been produced through nonselective reaction chemistry (Rajewski, 1990). These highly charged sulfoethyl, sulfopropyl, and sulfobutyl CDs are isomeric mixtures characterized by an average degree of substitution (DS) (Rajewski, 1990; Tait et al., 1992; Luna et al., 1996; Luna et al., 1997b). Zia et al. have proposed that an increase in binding potential can be realized for charged selectors by increasing the distance of the sulfonate groups from the CD torus (Zia et al., 1997). Thus for inclusion complex studies of progesterone and testosterone, a reduction of the CD alkyl chain length from sulfobutyl ether to sulfopropyl ether decreased the complexation potential. It is quite

possible therefore that single isomer sulfoalkyl CDs may exhibit enhanced complexation potential compared to single isomer sulfato CDs, and this enhancement may be important for analytical chiral separations since increased selectivity may be realized. Despite advantages, selective sulfoalkylation to produce single isomer sulfoalkylated CDs has never been achieved.

This dissertation research describes the first synthesis and characterization for an entirely new family of single isomer cyclodextrins; heptasubstituted β -CDs and hexasubstituted α -CDs with sulfoalkyl functional groups (Kirschner and Green, 2005; Kirschner et al., 2008). New single isomer β -CDs include heptakis(2,3-di-O-methyl-6-O-sulfopropyl)cyclomaltoheptaose potassium salt (KSPDM- β -CD), heptakis(2,3-di-O-methyl-6-O-sulfobutyl)cyclomaltoheptaose potassium salt (KSBDM- β -CD), and heptakis(2,3-di-O-ethyl-6-O-sulfopropyl)cyclomaltoheptaose potassium salt (KSPDE- β -CD). The single isomer sulfoalkyl derivatives of β -CD have been initially investigated as chiral resolving agents herein for CBI-amino acids including CBI-ser, CBI-asp, CBI-glu, and CBI-ala (see Chapter 4). New single isomer α -CDs include hexakis(2,3-di-O-methyl-6-O-sulfopropyl)cyclomaltohexaose potassium salt (KSPDM- α -CD), hexakis(2,3-di-O-methyl-6-O-sulfobutyl)cyclomaltohexaose potassium salt (KSBDM- α -CD), and hexakis(2,3-di-O-ethyl-6-O-sulfopropyl)cyclomaltohexaose potassium salt (KSPDE- α -CD).

3.2 Materials and methods

3.2.1. General methods

All chemicals were purchased from Aldrich Chemical Co. (Milwaukee, WI) and were of the highest purity unless otherwise noted. Native β -CD, 18-crown-6, potassium hydride, and *tert*-butyldimethylsilyl chloride were purchased from Alfa Aesar (Ward Hill, MA). All native and derivatized CD intermediates were dried under reduced pressure in a vacuum oven at 70 °C for a minimum of 24 h before subsequent reaction. THF was freshly distilled from potassium metal in the presence of benzophenone. N,N-dimethylformamide (DMF) was stirred over CaH₂, filtered, and distilled under reduced pressure (20 torr) at 57 °C onto activated 4 Å 8-12 mesh sieves. Aluminum backed silica-60 TLC plates were used to monitor reaction products and chromatography eluents. Cyclodextrin spots were imaged by charring on TLC plates after dipping plate in a solution of 2-5% concentrated sulfuric acid in ethanol and heating on a hot plate to >180 °C.

3.2.2. NMR spectral analysis

¹H, ¹³C, gCOSY, gHSQC, and ROESY NMR spectra were acquired with a Varian Mercury 300 MHz FT-NMR instrument. The ROESY spectra were acquired with 16 acquisitions in f2 and 200 increments in f1 with a mixing time of 300 ms. Assignments were made by gCOSY and gHSQC techniques. Chemical shifts are reported relative to internal sodium 3-(trimethylsilyl)-1-propanesulfonic acid (TSP) for single isomer CDs and relative to solvent peaks for CD intermediates.

3.2.3. Indirect UV detection CE

Indirect UV detection CE electropherograms of anionic cyclodextrins were obtained with an Agilent 3D CE system with diode array UV detector and with a Beckman P/ACE 2000 instrument as indicated. Separation buffer was 30 mM benzoic acid titrated to pH 6.0 with 0.1 M Tris base. CE conditions for P/ACE 2000 are as follows: wavelength, 254 nm; applied potential, 25 kV; injection, 22 mg/mL, 0.5 psi, 6 s injection. The analyses were performed in a bare, fused-silica capillary (Polymicro Technologies, Phoenix, AZ) of 50 x 59.5 cm x 50 μ m. CE conditions for Agilent were as follows: wavelength, 214nm; applied potential, 25 kV; injection 10 mg/mL, 0.5 psi 6 s injection. Capillary: 41.5 x 50.0 cm x 50 μ m bare fused silica.

3.3 Synthesis and characterization

A general reaction scheme for the selective synthesis of sulfoalkylated cyclodextrins is given in Figure 3.2.

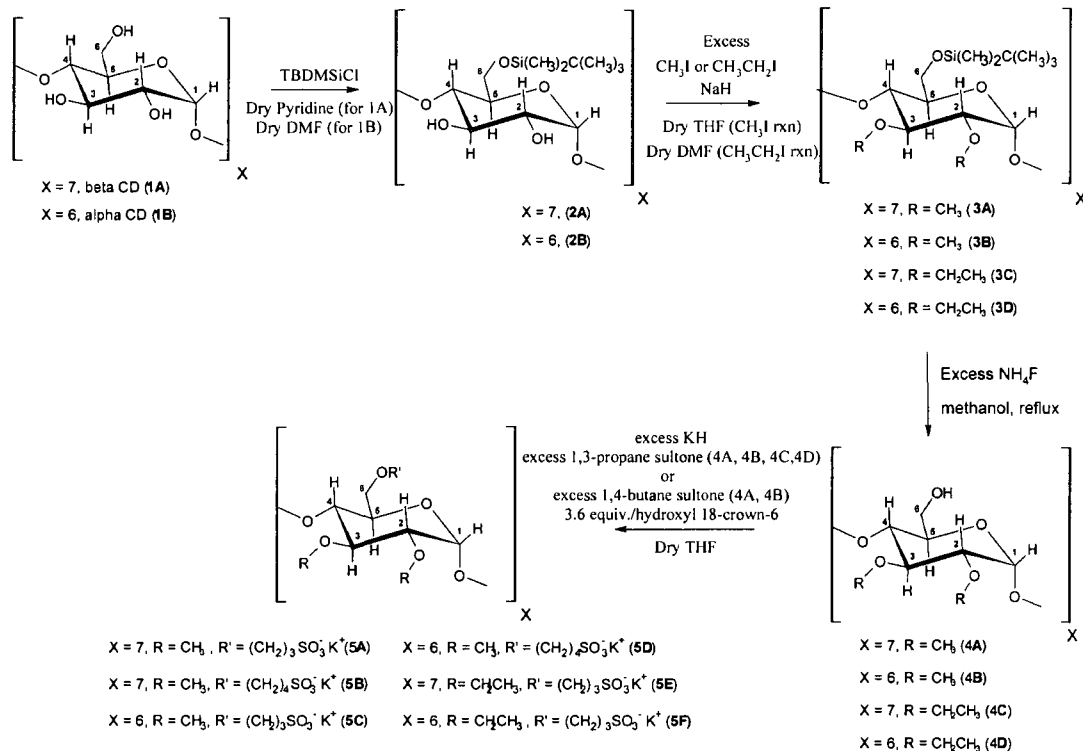


Figure 3.2. General reaction scheme for the selective synthesis of single isomer sulfoalkylated cyclodextrins. The final products are potassium salts and are labeled (5A)-(5F) depending on sulfoalkylation reagent, alkylation reagent, and α - versus β -CD.

A protection/deprotection strategy was required for regioselective synthesis of the primary (C-6) and secondary (C-2, C-3) hydroxyls to give single isomer selectively sulfoalkylated CDs. References for published procedures are given appropriately in sections 3.31-3.35 after a brief overview of the synthesis. After regioselective protection of the primary hydroxyls, the secondary hydroxyls were alkylated with either methyl iodide or ethyl iodide. The protected alkylated CDs were deprotected to give 2,3-di-O-alkyl-CDs. These CDs were then fully sulfoalkylated on the primary hydroxyl rim using the method developed and optimized as given in section 5.26.

3.3.1 Heptakis(6-*O-tert*-butyldimethylsilyl)cyclomaltoheptaose (**2A**) and Hexakis(6-*O-tert*-butyldimethylsilyl)cyclomaltohexaose (**2B**)

The C-6 primary hydroxyls of α -CD (**1A**) and β -CD (**1B**) were protected using *tert*-butyldimethylsilyl chloride (TBDMSiCl) according to a slight modification of the procedure described by Takeo for α -CD (Takeo et al., 1988) and β -CD (Takeo et al., 1989). For β -CD derivatives the C-6 hydroxyls were reacted under N₂ (g) with 1.5 equiv./hydroxyl TBDMSiCl in anhydrous pyridine cooled to ~ 0 °C. The silylation reagent was added slowly and solution was kept at ~ 0 °C for 2 h then at room temperature overnight. For α -CD derivatives, the same procedure was used with the exception that anhydrous DMF replaced pyridine as reaction solvent. After 24 h the reaction was poured over ice water and the white precipitate that formed was filtered, washed successively with ice water, and dried in vacuo. The protected β -CD derivative could often be used without further purification. The nearly pure (based on TLC and ¹H NMR) protected α -CD could be recrystallized from hot methanol/water (~ 95 %). A similar recrystallization is possible for protected β -CD. ¹H and ¹³C NMR spectra of the purified product are shown in Figure 3.3 and 3.4 for **2A** and Figure 3.5 and 3.6 for **2B**.

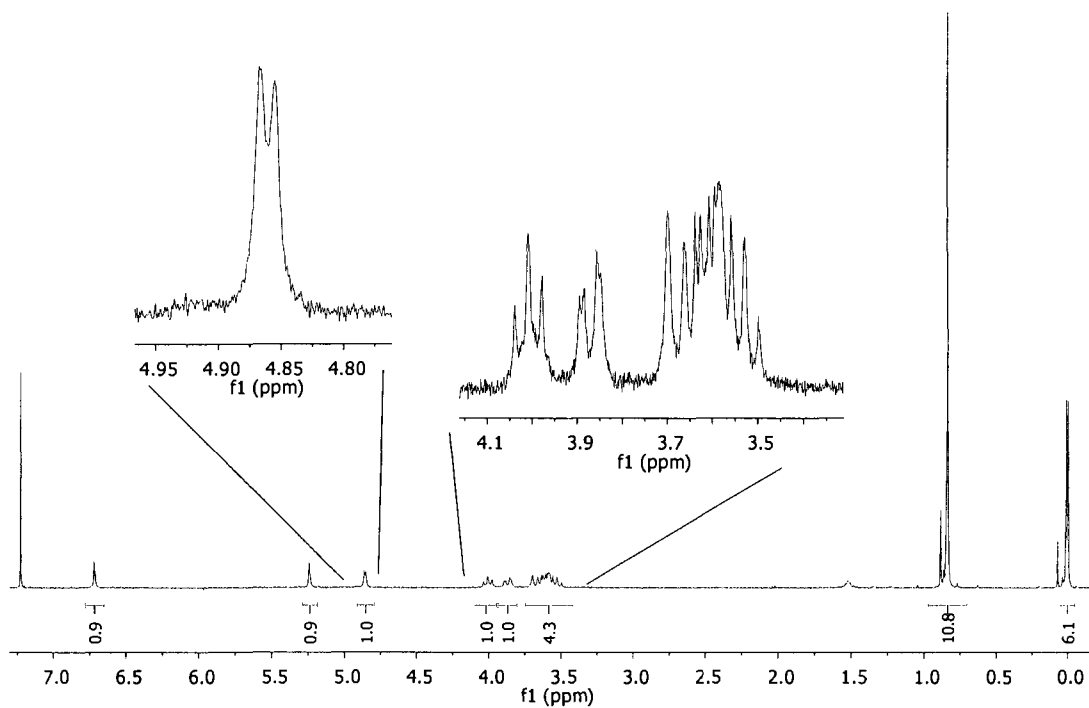


Figure 3.3. ^1H NMR of heptakis(6-O-*tert*-butyltrimethylsilyl)cyclomaltoheptaose (2A) in CDCl_3 .

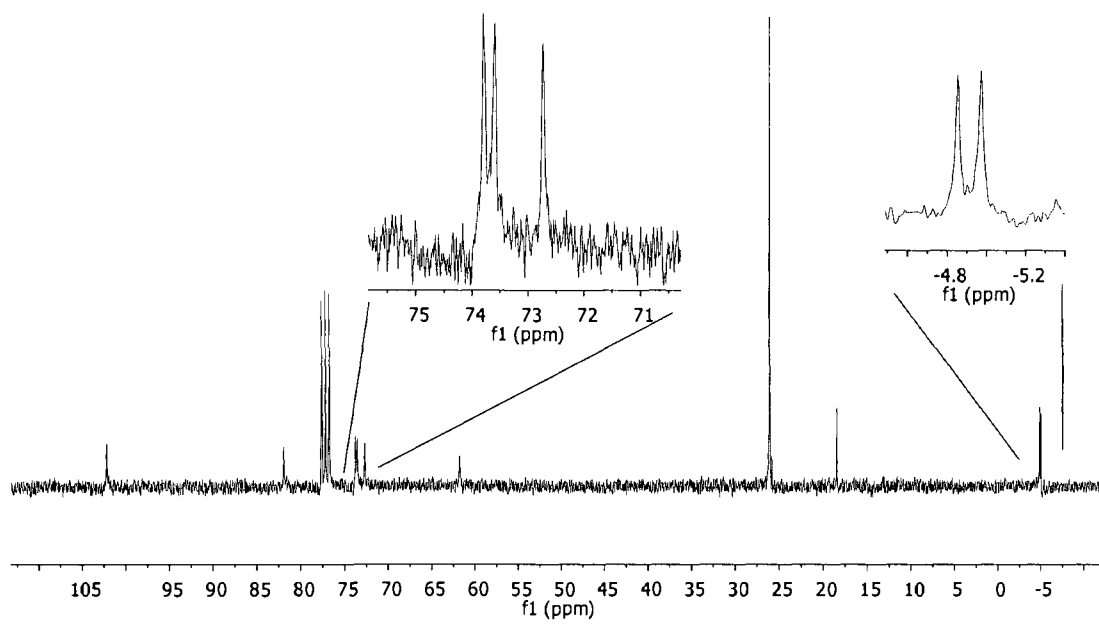


Figure 3.4. ^{13}C NMR of heptakis(6-O-*tert*-butyltrimethylsilyl)cyclomaltoheptaose (2A) in CDCl_3 .

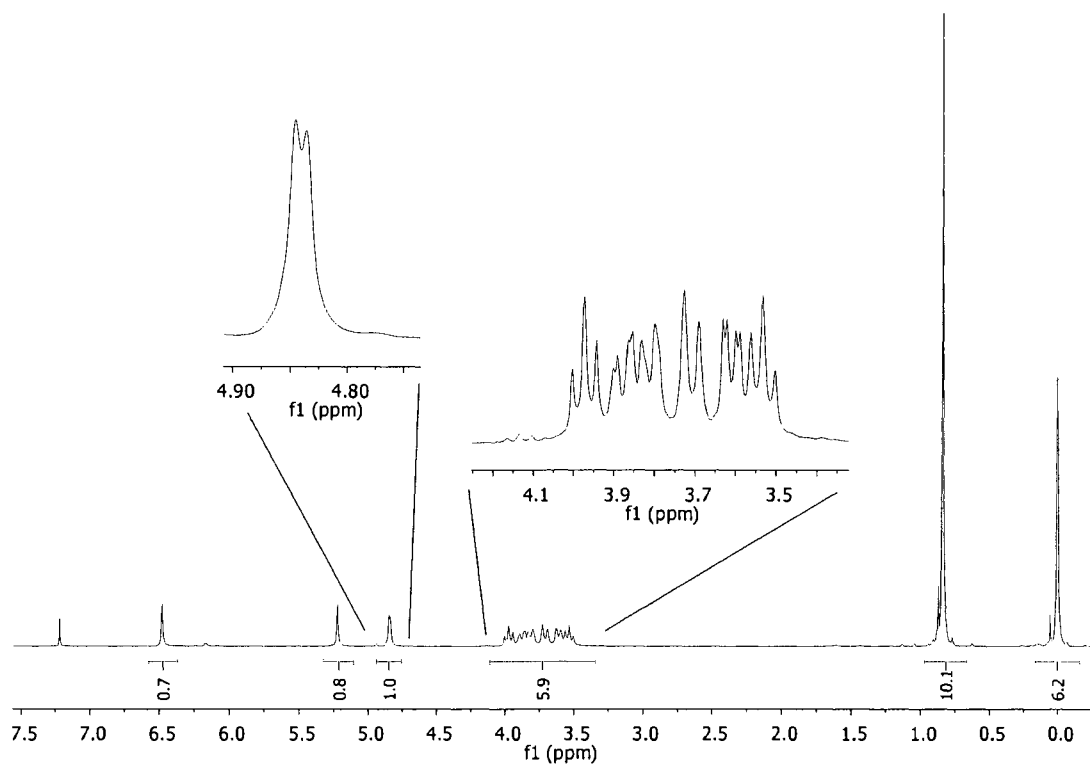


Figure 3.5. ^1H NMR of hexakis(6-O-*tert*-butyldimethylsilyl)cyclomaltohexaose (2B) in CDCl_3 .

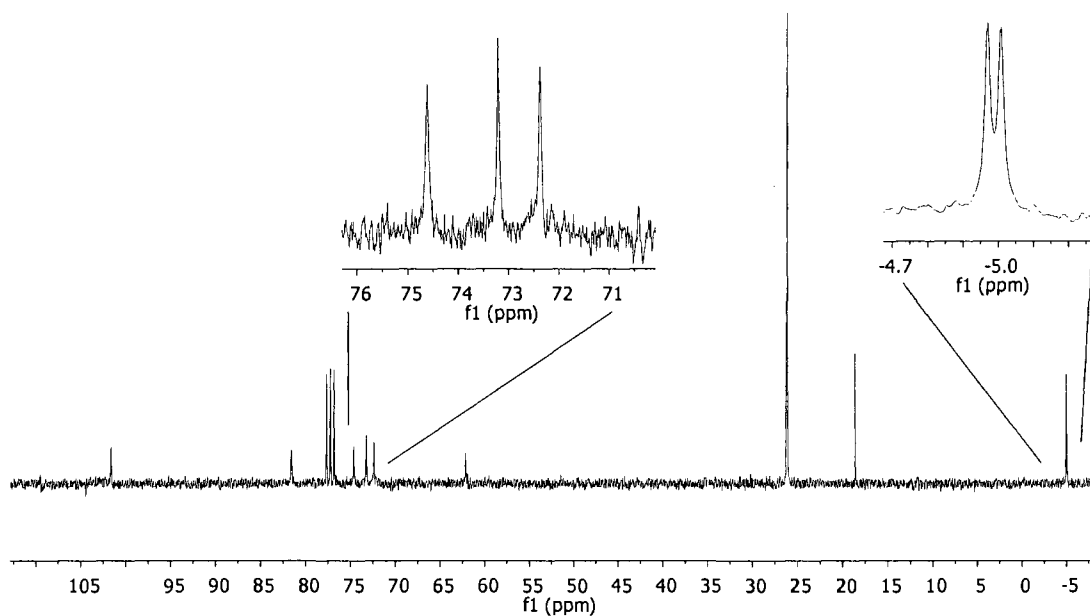


Figure 3.6. ^{13}C NMR of hexakis(6-*O*-*tert*-butyldimethylsilyl)cyclomaltohexaose (**2B**) in CDCl_3 .

Full assignments of **2A** and of **2B** were made based on comparison to literature values (Takeo et al., 1988; Takeo et al., 1989). The product NMR spectra matched well with literature and were utilized without further purification.

3.3.2 Heptakis(2,3-di-*O*-methyl-6-*O*-*tert*-butyldimethylsilyl)cyclomaltoheptaose (**3A**) and Hexakis(2,3-di-*O*-methyl-6-*O*-*tert*-butyldimethylsilyl)cyclomaltohexaose (**3B**).

The C-2 and C-3 secondary hydroxyls of **2A** and **2B** were methylated using excess methyl iodide and NaH according to the procedure described by Takeo and colleagues (Takeo et al., 1988; Takeo et al., 1989). Conditions were the same for β -CD and α -CD derivatives. Briefly, regioselective methylation was achieved by dissolving **2A** or **2B** in

anhydrous THF under N_2 and slowly adding 3 equiv./hydroxyl NaH (60 % dispersion in mineral oil, previously washed with hexane and dried under N_2) followed by 5 equiv./hydroxyl methyl iodide. The reaction was stirred for 24 h at RT. Excess NaH was quenched with methanol after 24 h and THF was removed by rotovaporization. The resultant material was partitioned between CH_2Cl_2 and water, extracted 3X, dried over Na_2SO_4 , and concentrated. 1H and ^{13}C NMR analysis is shown in Figures 3.7 and 3.8 for **3A** and 3.9 and 3.10 for **3B**.

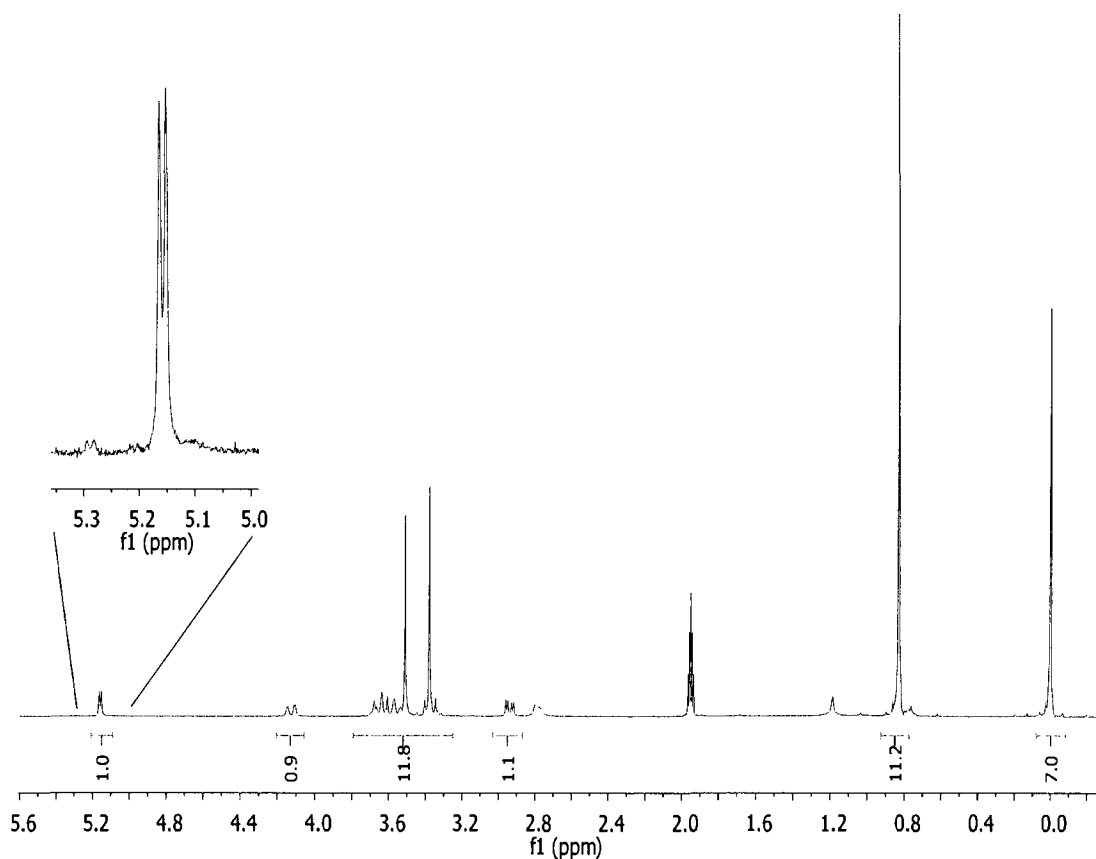


Figure 3.7. 1H NMR of heptakis(2,3-di-O-methyl-6-O-*tert*-butyl dimethylsilyl)-cyclomaltoheptaose (**3A**) in acetone- d_6 .

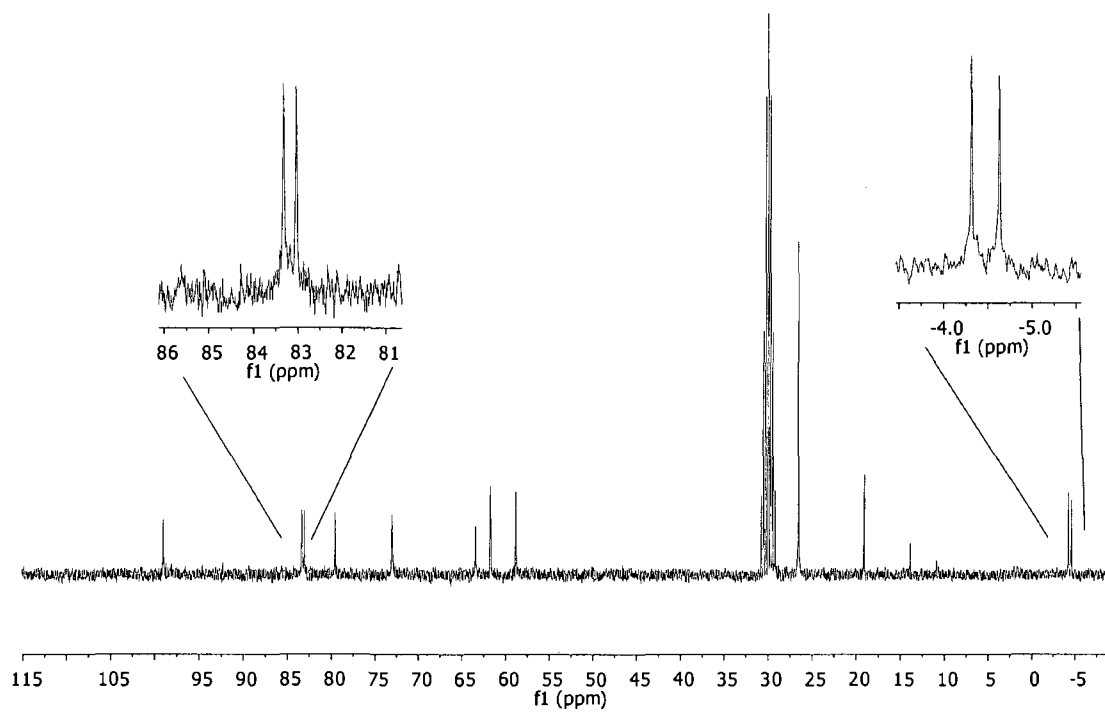


Figure 3.8. ^{13}C NMR of heptakis(2,3-di-O-methyl-6-O-*tert*-butyldimethylsilyl)-cyclomaltoheptaose (3A) in acetone- d_6 .

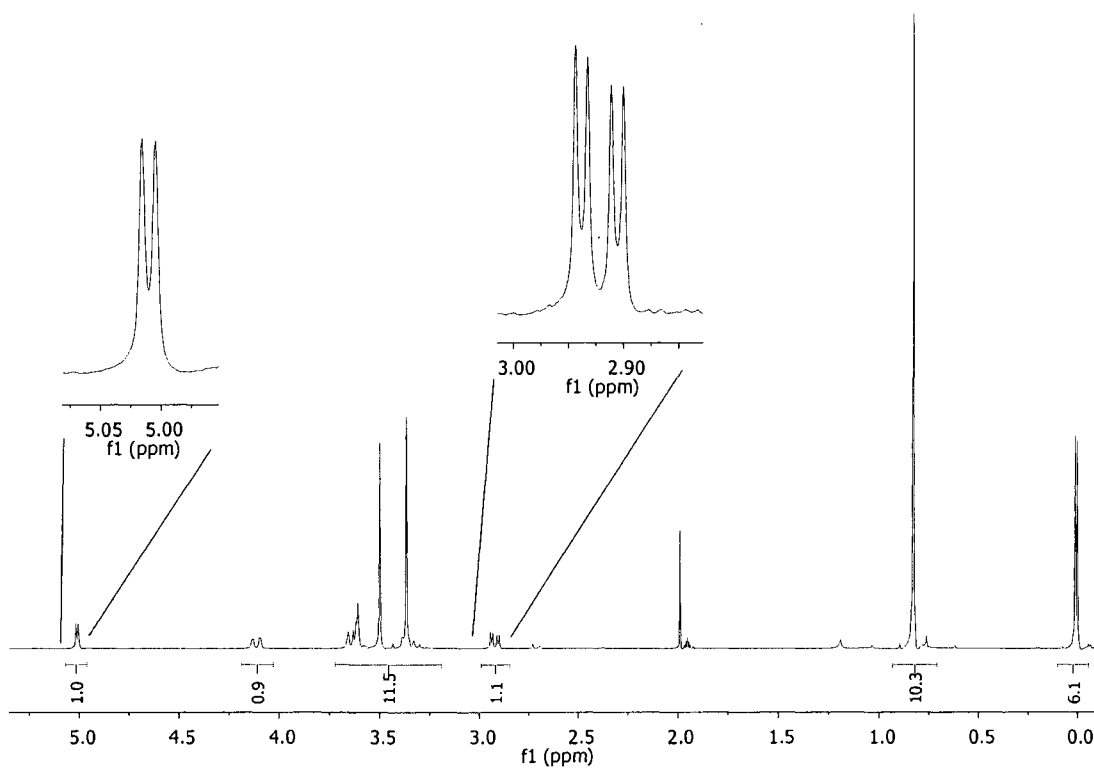


Figure 3.9. ^1H NMR of hexakis(2,3-di-O-methyl-6-O-*tert*-butyltrimethylsilyl)-cyclomaltohexaose (**3B**) in acetone- d_6 .

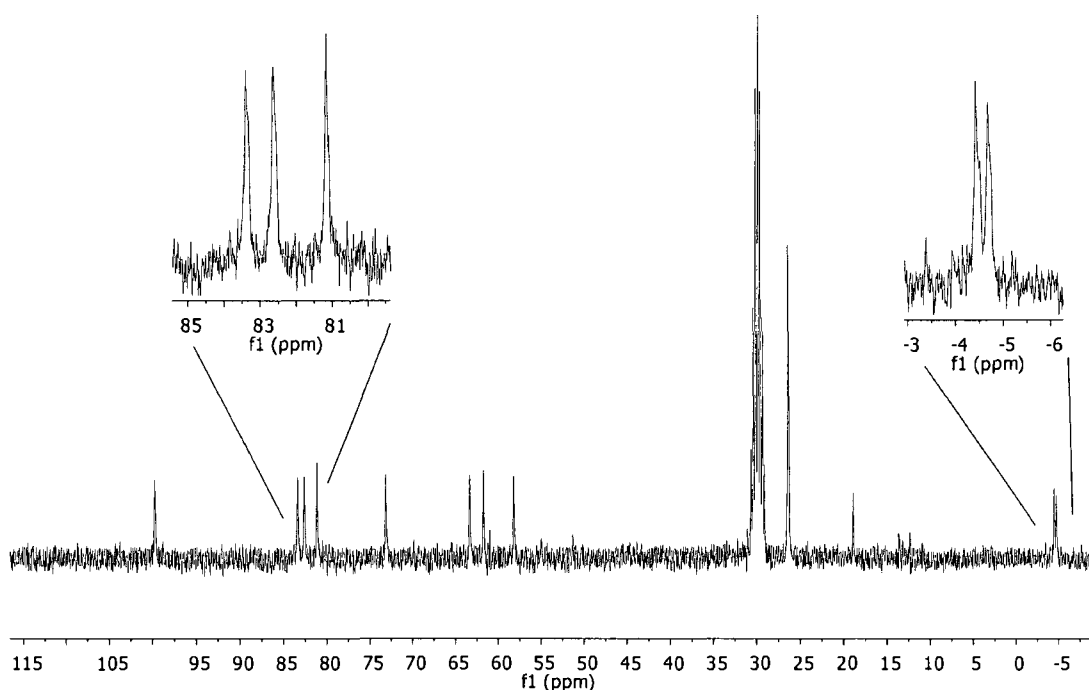


Figure 3.10. ^{13}C NMR of hexakis(2,3-di-O-methyl-6-O-*tert*-butyldimethylsilyl)-cyclomaltohexaose (**3B**) in acetone- d_6 .

Full assignments of **3A** and of **3B** were made based on comparison to literature values. The product spectra matched literature and were utilized without further purification.

3.3.3 Heptakis(2,3-di-O-ethyl-6-O-*tert*-butyldimethylsilyl)cyclomaltoheptaose (**3C**) and Hexakis(2,3-di-O-ethyl-6-O-*tert*-butyldimethylsilyl)cyclomaltohexaose (**3D**)

The C-2 and C-3 secondary hydroxyls of **2C** and **2D** were ethylated using excess ethyl iodide and NaH according to an adaptation of the procedure described by Takeo and colleagues (Takeo et al., 1988; Takeo et al., 1989). Conditions were the same for β -CD and α -CD derivatives. An identical synthetic procedure was used as for methylation

with the exception that anhydrous DMF was used instead of THF. After reaction for 24 h, the excess hydride was quenched and the product was poured over ice water and the white precipitate that formed was filtered, washed successively with ice water, and dried in vacuo. TLC of the resultant product indicated a mixture of products which was verified by ^1H NMR.

The product was purified by normal phase chromatography using a mobile phase consisting of hexane and ethyl acetate (7:1). ^1H NMR analysis of the purified material is shown in Figure 3.11 for **3C** and Figure 3.12 for **3D**.

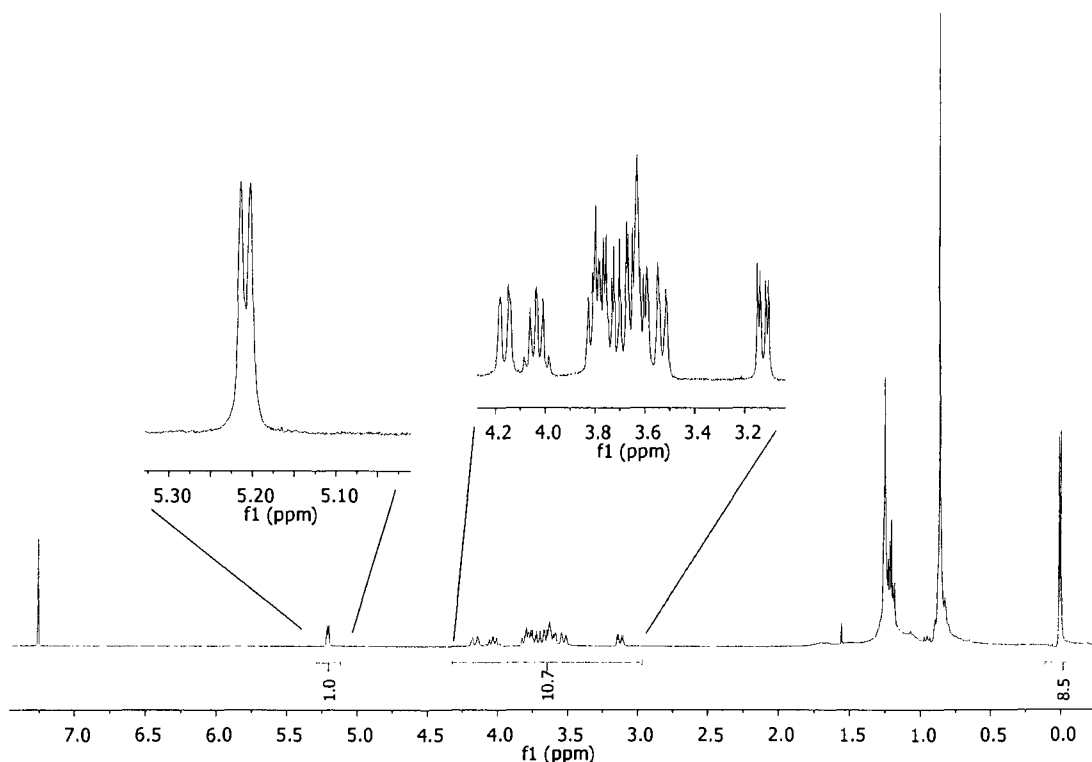


Figure 3.11. ^1H NMR of heptakis(2,3-di-O-ethyl-6-O-*tert*-butyldimethylsilyl)-cyclomaltoheptaose (**3C**) in CDCl_3 .

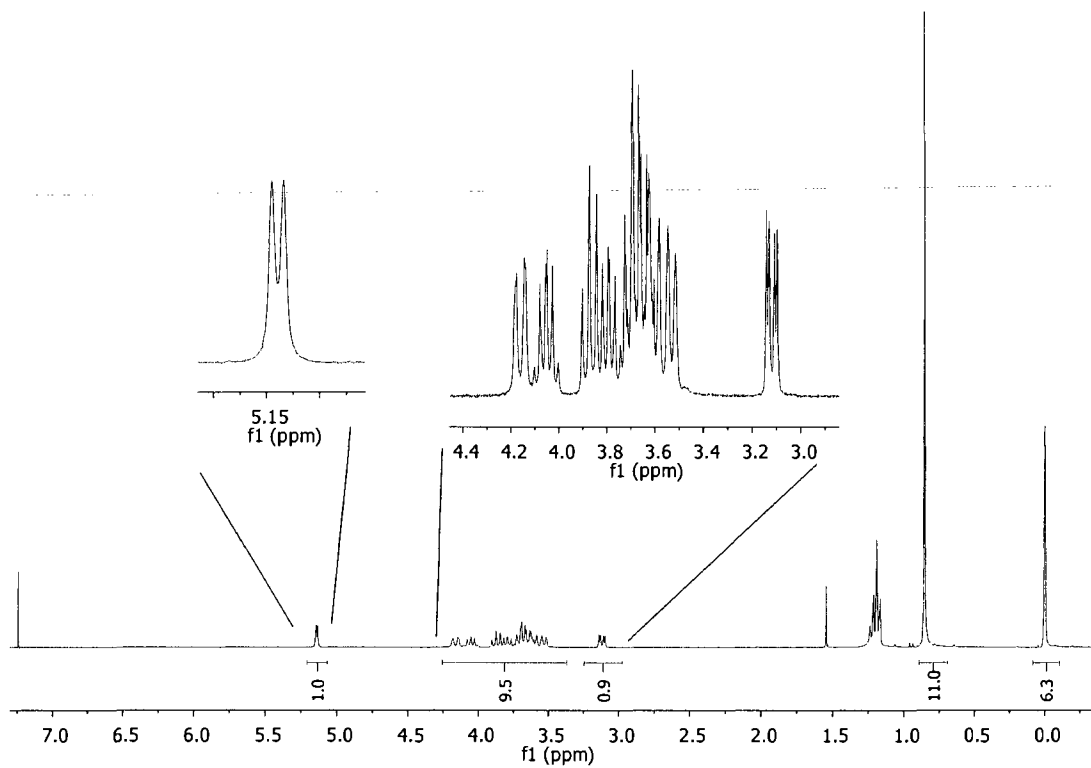


Figure 3.12. ^1H NMR of hexakis(2,3-di-O-ethyl-6-O-*tert*-butyl dimethylsilyl)-cyclomaltohexaose (**3D**) in CDCl_3 .

In **3C** the presence of mineral oil contaminant from the NaH dispersion was apparent in the purified product even after chromatography. The mineral oil was noninvasive for the follow up reaction and thus not removed from **3C**. The Assignments of the ^1H NMR spectrum for CD peaks of **3C** and **3D** were made based on comparison to literature values. The materials were used without further purification.

3.3.4 Heptakis(2,3-di-O-methyl)cyclomaltoheptaose (4A) and Hexakis(2,3-di-O-methyl)cyclomaltohexaose (4B)

O-desilylation of the C-6 protecting group of **3A** and **3B** was accomplished using a modification of the approach described by Takeo and colleagues (Takeo et al., 1988; Takeo et al., 1989). Briefly, the CD derivative was dissolved in methanol with 7 equiv./hydroxyl NH_4F instead of tetrabutylammonium fluoride. The reaction was refluxed for at least 48 h until TLC (4:1 Chloroform: methanol) indicated successful O-desilylation as indicated by a significant decrease in the retention factor compared to starting material. The reaction was stopped by cooling to room temperature and rotovaporizing methanol. The product was partitioned between CH_2Cl_2 and water, and then extracted 3X, and concentrated. ^1H NMR of the crude product suggested that nearly complete O-desilylation was achieved. The crude material was purified by flash chromatography using 4:1 chloroform methanol mobile phase. ^1H and ^{13}C NMR analysis of the purified material is shown in Figure 3.13 and 3.14 for **4A** and Figure 3.15 and 3.16 for **4B**.

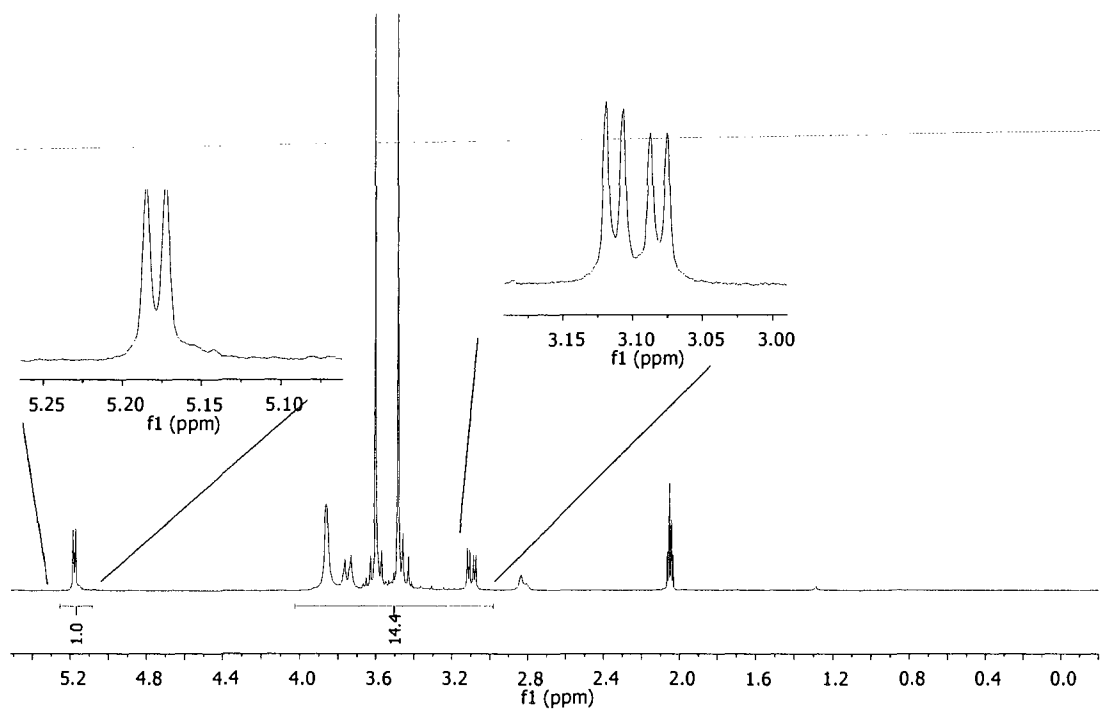


Figure 3.13. ^1H NMR of heptakis(2,3-di-O-methyl)cyclomaltoheptaose (4A) in acetone- d_6 .

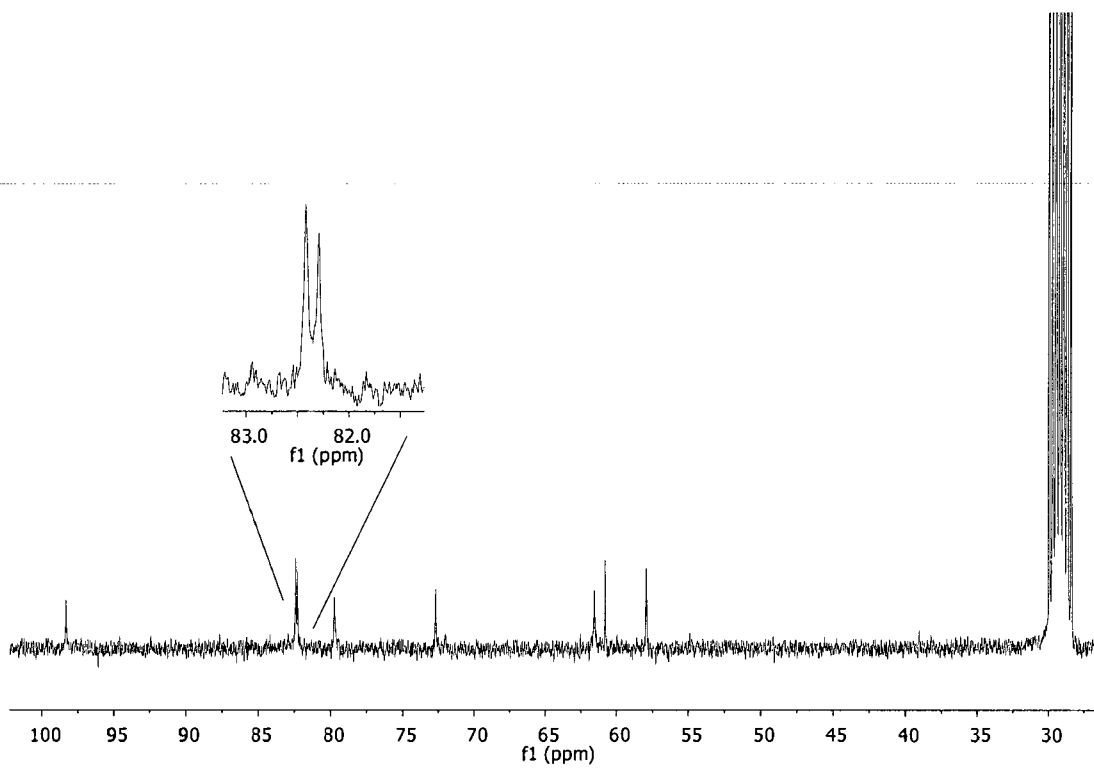


Figure 3.14. ^{13}C NMR of heptakis(2,3-di-O-methyl)cyclomaltoheptaose (4A) in acetone- d_6 .

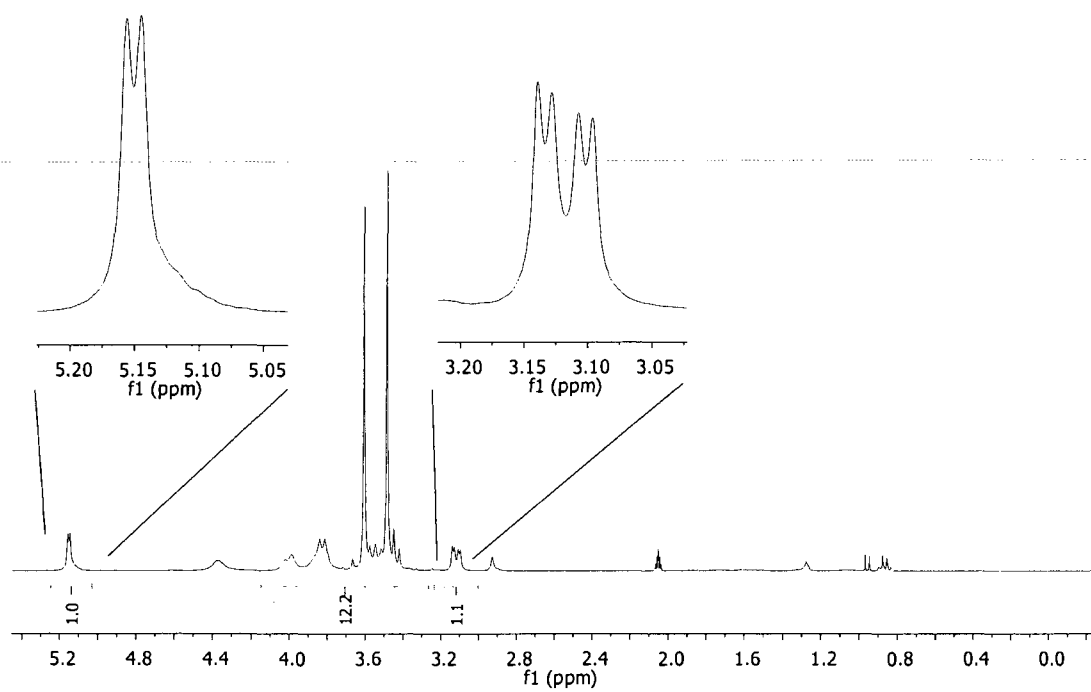


Figure 3.15. ^1H NMR of hexakis(2,3-di-O-methyl)cyclomaltohexaose (**4B**) in acetone- d_6 .

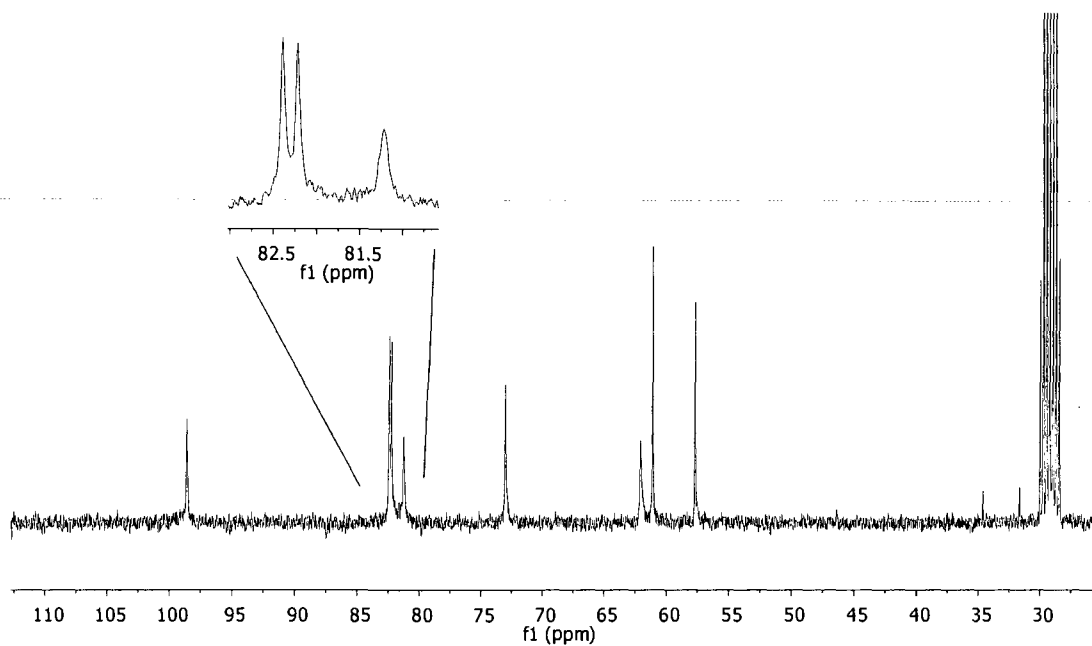


Figure 3.16. ^{13}C NMR of hexakis(2,3-di-O-methyl)cyclomaltohexaose (**4B**) in acetone- d_6 .

Full assignments of **4A** and **4B** could be made and are consistent with literature values. The product was used without further purification.

3.3.5 Heptakis(2,3-di-O-ethyl)cyclomaltoheptaose (**4C**) and Hexakis(2,3-di-O-ethyl)cyclomaltohexaose (**4D**)

O-desilylation of the C-6 protecting group of **3C** and **3D** was accomplished using an identical approach as indicated for the synthesis of **4A** and **4B**. ^1H NMR of the crude product suggested that nearly complete O-desilylation. The crude material was purified by flash chromatography using chloroform and methanol (8:1 \rightarrow 4:1 chloroform:methanol). ^1H and ^{13}C NMR analysis of the purified material is shown in Figure 3.17 and 3.18 for **4C** and Figure 3.19 and 3.20 for **4D**.

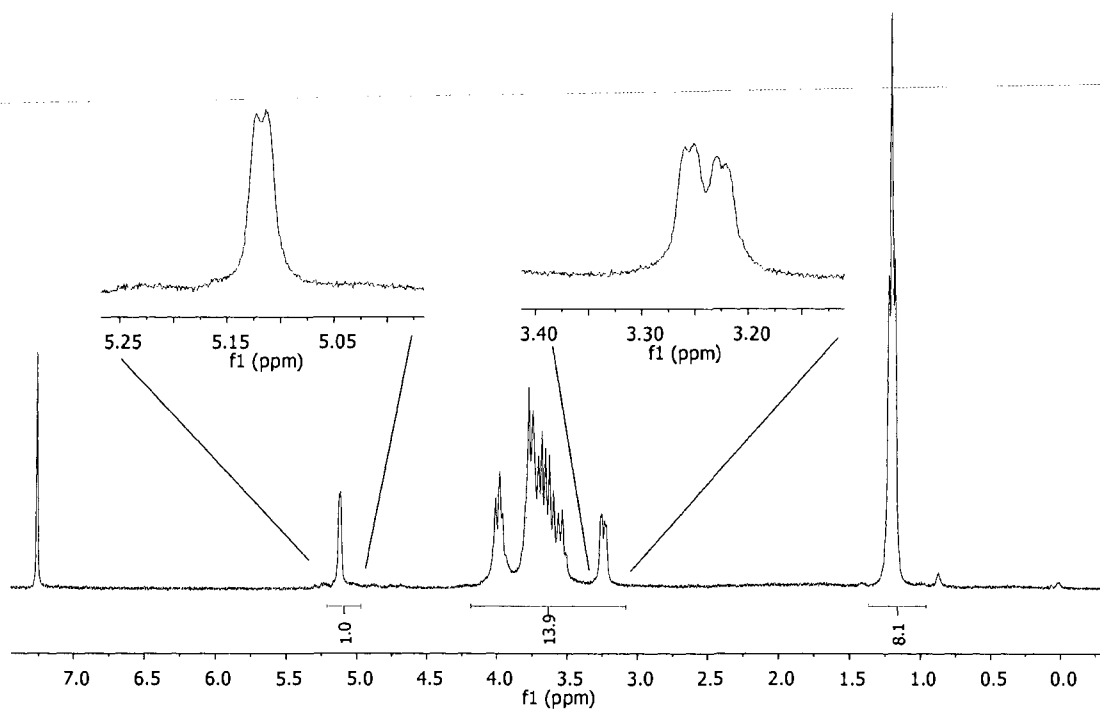


Figure 3.17. ^1H NMR of heptakis(2,3-di-O-ethyl)cyclomaltoheptaose (4C) in CDCl_3 .

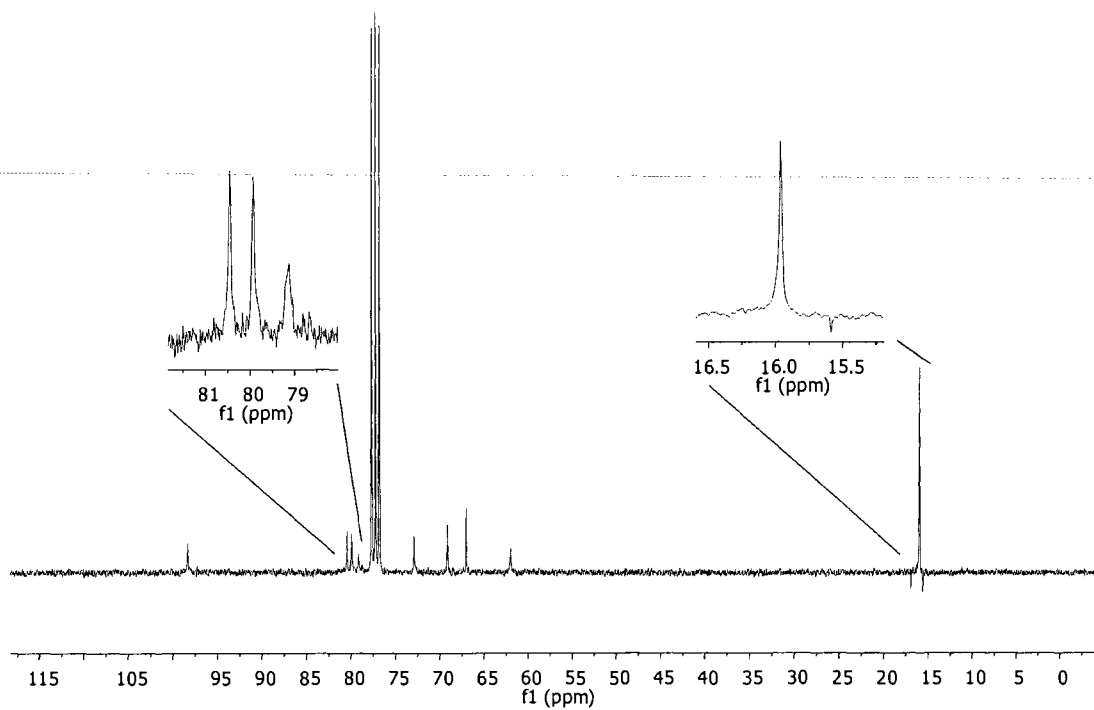


Figure 3.18. ^{13}C NMR of heptakis(2,3-di-O-ethyl)cyclomaltoheptaose (**4C**) in CDCl_3 .

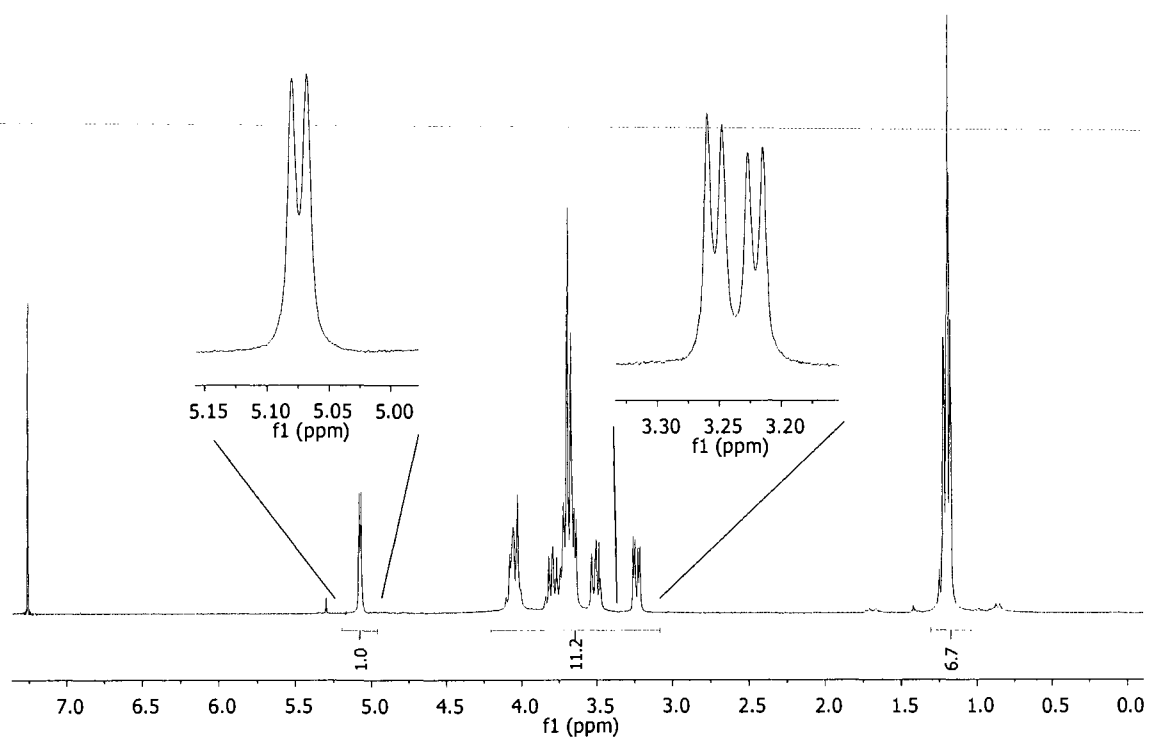


Figure 3.19. ^1H NMR of hexakis(2,3-di-O-ethyl)cyclomaltohexaose (**4D**) in CDCl_3 .

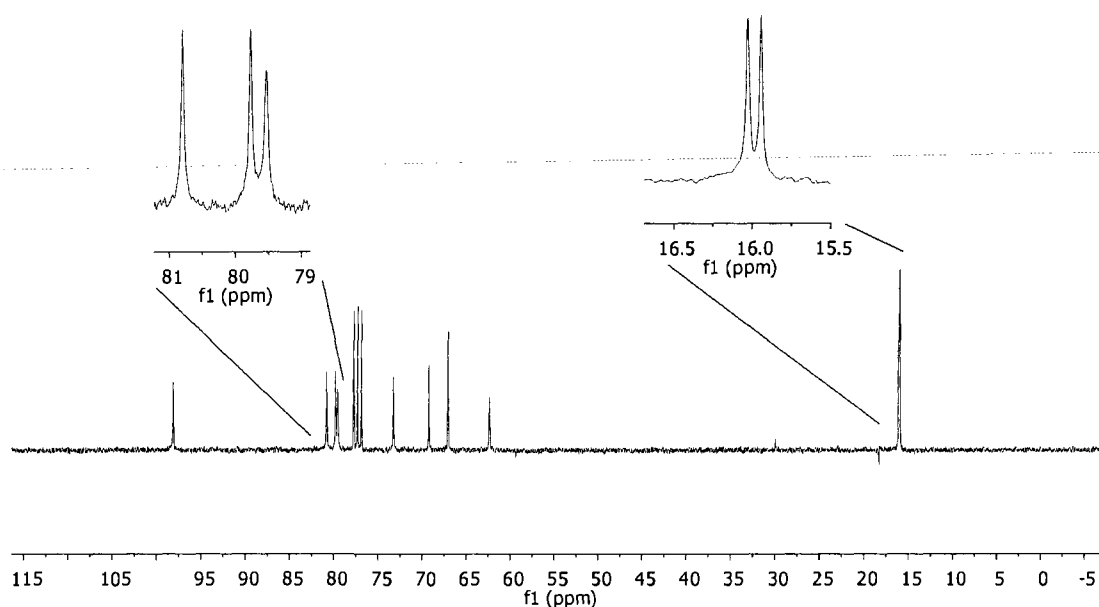


Figure 3.20. ^{13}C NMR of hexakis(2,3-di-O-ethyl)cyclomaltohexaose (**4D**) in CDCl_3 .

Full assignments of **4C** and **4D** were made and are consistent with literature values. The product was used without further purification.

3.3.6 Heptakis(2,3-di-O-methyl-6-O-sulfopropyl)cyclomaltoheptaose (**5A**) and (**5A'**)

Full regioselective sulfopropylation of the C-6 primary hydroxyls of **4A** was accomplished using 1,3-propanesultone in THF with KH/18-crown-6 as base. The reaction was carried out on mg and gram scales with a typical scaled down example given here.

Compound **4A** (0.200 g, 0.152 mmol) was added to 35 mL of anhydrous THF under nitrogen, followed by the slow addition of 0.300 g (7.48 mmol) of KH. After stirring at room temperature for 15 min, 1.02 g (3.86 mmol) of 18-crown-6 was slowly added, and

the reaction was allowed to stir for 30 min. 1,3-Propanesultone (0.520 g, 4.26 mmol) was dissolved in 4 mL of anhydrous THF and introduced dropwise over 30 min. The reaction was stirred at room temperature for 24 h. Excess KH was decomposed by cooling the reaction to 0 °C and slowly adding methanol. The solvents were removed by rotary evaporation at 70 °C, and the brown oil was dried in a vacuum oven at 70 °C for 1 h. Dry acetone (80 mL) was added to the oil, and the precipitate that formed was transferred to centrifuge tubes where successive acetone washes, followed by centrifugation removed all 18-crown-6 yielding an off-white solid. The solid was blown dry with N₂ gas, dissolved in water, and neutralized with 1 M HCl. Compound **5A** was purified by ultrafiltration through an Amicon Model 8310 Stirred Cell Ultrafiltration Unit (Millipore Corp., Billerica, MA) with a 1000 MWCO regenerate cellulose (RC) membrane to give, after concentration, 0.24 g (0.098 mmol, 61%). ¹H NMR (300 MHz, D₂O): δ 5.27 (H-1), 3.85 (H-4), 3.71 (H-3), 3.36 (H-2), 3.85 (H-5), 3.66 (OCH₂), 3.95, 3.73 (H-6), 3.63 (OCH₃), 3.53 (OCH₃), 2.99 (CH₂S), 2.05 (CH₂CH₂S). ¹³C NMR (75 MHz, D₂O): δ 100.5 (C-1), 80.7 (C-4), 83.6 (C-3), 83.0 (C-2), 73.6 (C-5), 72.4 (OCH₂), 71.6 (C-6), 62.7 (OCH₃), 60.9 (OCH₃), 51.1 (CH₂S), 27.5 (CH₂CH₂S). Anal. Calcd for K₇C₇₇H₁₃₃O₅₆S₇·7H₂O: C, 35.86; H, 5.74; S, 8.70. Found: C, 36.08; H, 5.45; S, 8.52. Inverse detection CE: Mean DS (6.9).

Partial regioselective sulfopropylation of C-6 primary hydroxyls of **4A** was accomplished to give **5A'** by following the same procedure as described above with omission of 18-crown-6. The product was worked up in an identical fashion. Yield 69%.

Inverse detection CE was employed to monitor the reaction as well as assess the average degree of substitution of the final product (Tait et al., 1992). This has become a popular approach for analysis of isomeric purity of sulfated CDs (Tait et al., 1992; Luna et al., 1996; Luna et al., 1997a; Cai and Vigh, 1998; Maynard and Vigh, 2000; Zhu and Vigh, 2000; Chen et al., 2001; Maynard and Vigh, 2001; Busby et al., 2003; Li and Vigh, 2003; Zhu and Vigh, 2003; Li and Vigh, 2004b, a; Busby and Vigh, 2005a, b). Using this method, however, Luna et al. have demonstrated that the molar response factor of sulfobutyl ether- β -CDs (SBE- β -CDs) increases with degree of substitution (DS_{CE}) (Luna et al., 1997a). Uncorrected integration of the CD bands will overestimate DS for an SBE- β -CD (DS_{CE} 4.7 from CE compared to DS_{EA} 3.6 from elemental analysis). However, the results presented here show much better agreement between DS_{CE} and DS_{EA} for these selectively modified cyclodextrins (vide infra). Typical inverse detection CE electropherograms of the purified reaction product **5A'** obtained without 18-crown-6 show a mixture of multiply charged derivatives centered on DS 4 (DS_{CE} 4.1) with 8% of the product containing CDs with DS 5 (Figure 3.21).

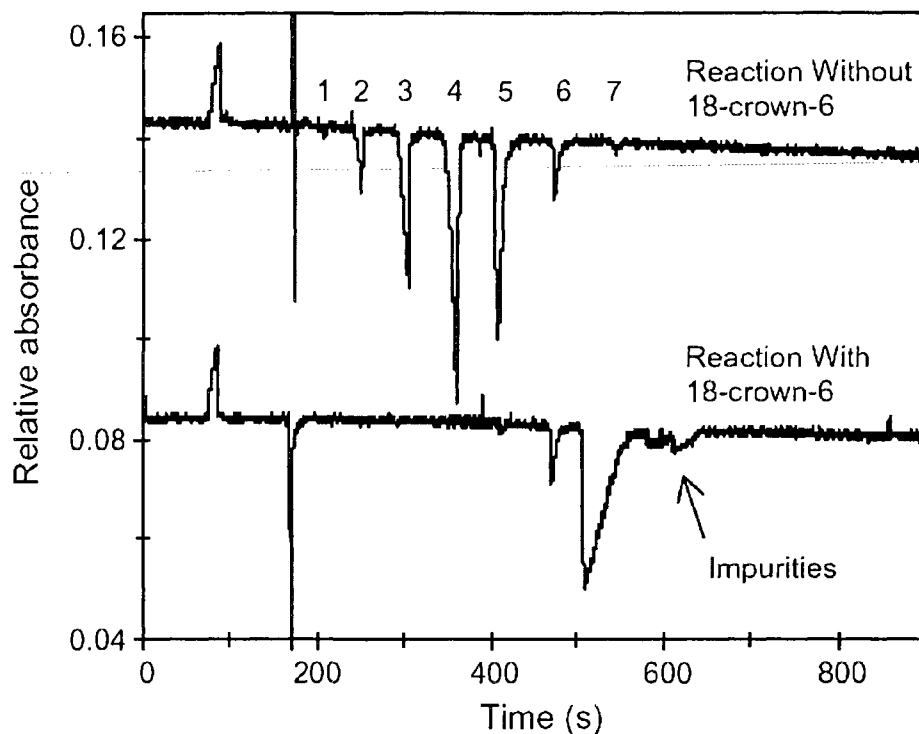


Figure 3.21. Indirect UV detection of heptakis(2,3-di-O-methyl-6-O-sulfopropyl)cyclomaltoheptaose (KSPDM- β -CD). The upper inverse detection electropherogram shows the product from the reaction without 18-crown-6 while the bottom electropherogram is the product from the reaction using 18-crown-6. The positive peak in both electropherograms is potassium ion from the CD-potassium salt. The inverse band at ~ 180 s represents electroosmotic flow. The numbers beside the top electropherogram are the different CD charged isomers which are separated uniformly due to a systematic change in their size/charge with increasing degree of substitution. BGE: 30 mM benzoic acid titrated to pH 6.0 with 0.1 M Tris base. For additional conditions see Section 3.23

Elemental analyses (C, H, S) are consistent with a DS_{EA} of 3.8. In comparison, the electropherogram of the product **5A** from the reaction incorporating 18-crown-6 indicates a predominance of DS 7 (DS_{CE} 6.9), with less than 10% of the mixture containing DS < 7 (Figure 3.21). Elemental analysis is consistent with a DS_{EA} of 6.7 in comparison.

The ^1H NMR spectrum of the purified **5A'** for the reaction omitting 18-crown-6 is shown in Figure 3.22.

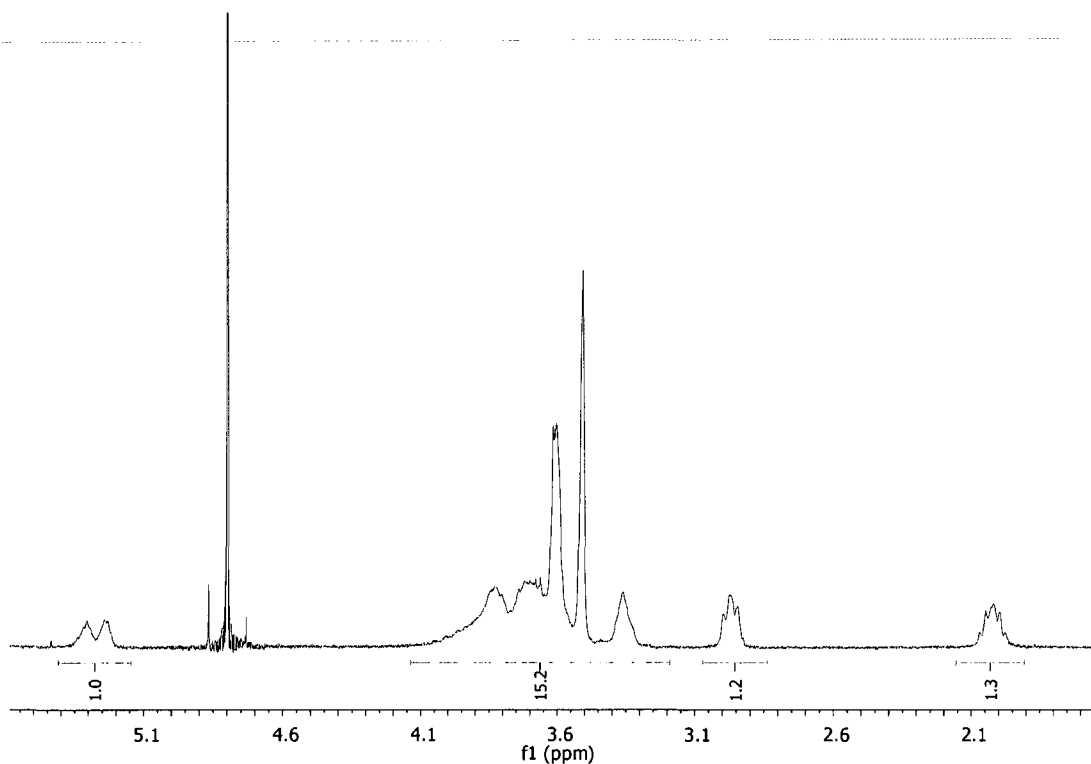


Figure 3.22. ^1H NMR spectrum of KSPDM- β -CD (**5A'**), DS_{CE} 4.1 in D_2O .

Poorly resolved H-1 anomeric signals typical of heterogeneous CD mixtures are observed. A fully substituted symmetric CD should show ^1H NMR integration ratio of 1:2 for the anomeric H-1 to sulfopropyl methylene protons, respectively. Integration of methylene units of the sulfopropyl chain (2.02, 2.97 ppm) in comparison to the anomeric signal (5.18-5.38 ppm) suggests a low DS. The poor resolution in this spectrum is undoubtedly due to the mixture of multiply charged anionic cyclodextrins that result from incomplete substitution of the primary hydroxyl groups. Additionally, a variety of

positional isomers are possible for degrees of substitution 2–5, which further adds to the heterogeneity of the product.

Due to the poor resolution of the ^1H NMR of **5A'**, the progress of the reaction under alternative conditions was monitored by ^1H NMR in addition to inverse detection CE. An aliquot of reaction mixture (~0.5% by volume) was added to 1 mL D_2O to decompose hydride. THF was removed by drying in vacuo at 70 °C for 15 min.

Of particular note in the development of the synthesis using 18-crown-6 was the generation of a viscous layer in the reaction vessel that immediately deposited after a threshold level of propane sultone was added to the reaction mixture. This gummy layer only formed when the reaction was carried out in the presence of 18-crown-6. Using ^1H NMR reaction monitoring and slowly adding sultone, the NMR of the gummy layer washed with THF immediately after it formed is shown in Figure 3.23 prior to addition of a molar excess of sultone.

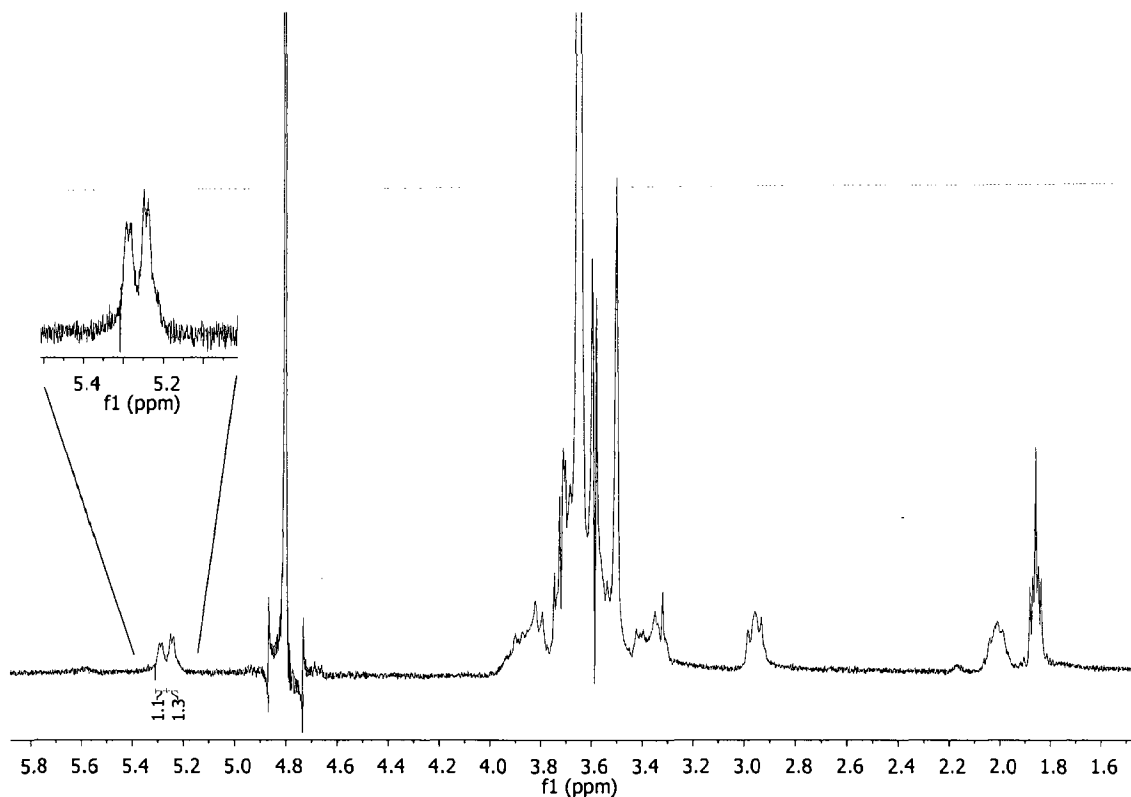


Figure 3.23. ^1H NMR reaction monitoring spectrum of (5A) from reaction using 18-crown-6 immediately after formation of gummy layer but prior to addition of excess propane sultone. The spectrum is representative of a sample obtained from the gummy layer formed in THF after rinsing with fresh THF, briefly drying, and decomposing hydride with NMR solvent.

Clearly based on resolved coupling the degree of substitution is approaching that of the single isomer (DS 7) product. Notably, the peak at 5.27 ppm is characteristic of the fully substituted Heptakis product **5A** whereas the peak at 5.23 ppm may be due to the hexakis (DS 6) product (latter not verified). This substitution pattern does not appear to have changed significantly after further reaction (data not shown). The lack of excess sultone is apparent in this spectrum due to a lack of sultone byproduct peaks. An obvious

impurity in the reaction mixture is 18-crown-6 represented by a singlet at 3.52 ppm and residual THF at 1.83 ppm.

One clear conclusion from comparison of Figure 3.23 with Figure 3.22 is that the reaction in the presence of 18-crown-6 is very rapid, since the sample from Figure 30 was obtained during the course of adding the final reagent. After 3 h following addition of 3 equiv./ hydroxyl excess sultone in this reaction, an additional aliquot of the gummy layer was obtained and a single peak showing typical well resolved coupling was noted (Figure 3.24).

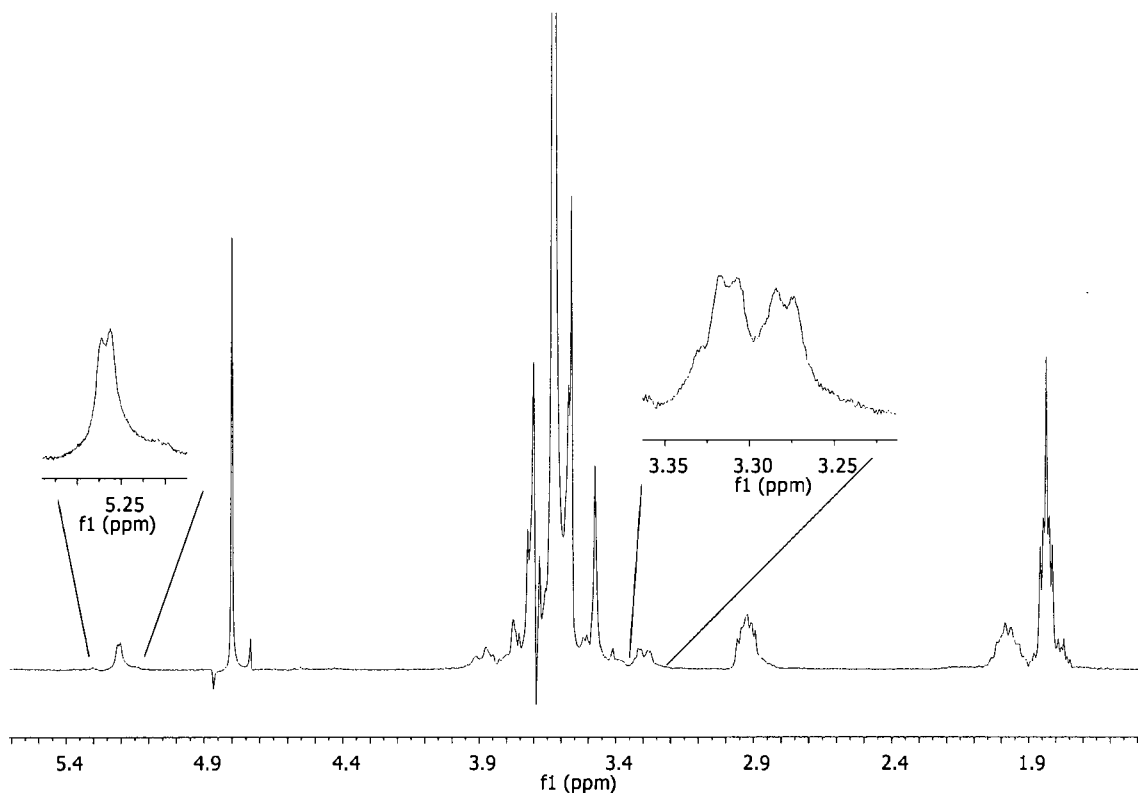


Figure 3.24. ¹H NMR reaction monitoring spectrum of (5A) from reaction using 18-crown-6 after addition of excess 1,3-propane sultone. The spectrum is representative of a sample obtained from the gummy layer formed in THF.

Clearly excess sultone pushed the reaction to completion. It is possible that this approach could be used to optimize a minimum amount of excess sultone required for full sulfoalkylation. This would simplify sample workup.

Acetone extraction and ultrafiltration steps were required for impurity removal and representative ^1H NMR spectra of the extract and ultrafiltrate eluent are shown in Figure 3.25.

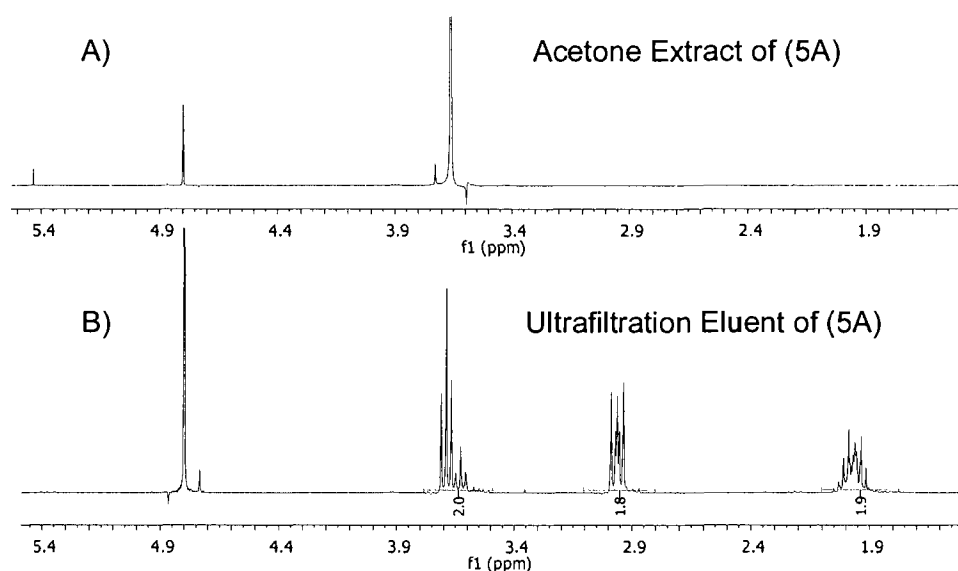


Figure 3.25. ^1H NMR spectra of acetone and ultrafiltration waste showing selective removal of impurities. A) Acetone extract and B) Ultrafiltrate eluent for the purification of heptakis(2,3-di-O-methyl-6-O-sulfopropyl)cyclomaltoheptaose (5A). The NMR of the acetone extract shows the characteristic 18-crown-6 singlet while the ultrafiltration waste shows predominately sultone byproducts. Careful examination of the baseline in the region of 3.3-5.3 ppm did not reveal the presence of any characteristic cyclodextrin peaks in either spectrum.

It is clear that acetone extraction primarily removes 18-crown-6 without concomitant loss of CD as indicated by a lack of CD signal in the ^1H NMR spectrum. In addition, ultrafiltration removes sulfone products and possibly some 18-crown-6 without loss of CD. It should be mentioned that higher levels of 18-crown-6 (>2.4 equiv./hydroxyl) during the reaction make purification more difficult by simple acetone extraction. Indeed, when 3.6 equiv./hydroxyl of 18-crown-6 is used during reaction, acetone extraction resulted in a significant loss of anionic CD into the acetone supernatant. Ultrafiltration is additionally a poor choice for removal of 18-crown-6 as attempts at extensive ultrafiltration without acetone extraction still resulted in the characteristic 18-crown-6 signal in the ^1H spectrum. For this reason 18-crown-6 was removed by an alternative procedure for other single isomer CDs during product workup.

In contrast to the poorly resolved ^1H signals for the spectrum of **5A'** shown in Figure 3.22, the ^1H NMR spectrum of purified **5A** from the reaction in the presence of 18-crown-6 (DS_{CE} 6.9) reveals a high degree of symmetry; especially sharp peaks with well-defined couplings for H-1 at 5.27 ppm (d, J 3.3 Hz) and H-2 at 3.36 ppm (dd J 3.3, 9.9 Hz) are observed (Figure 3.26).

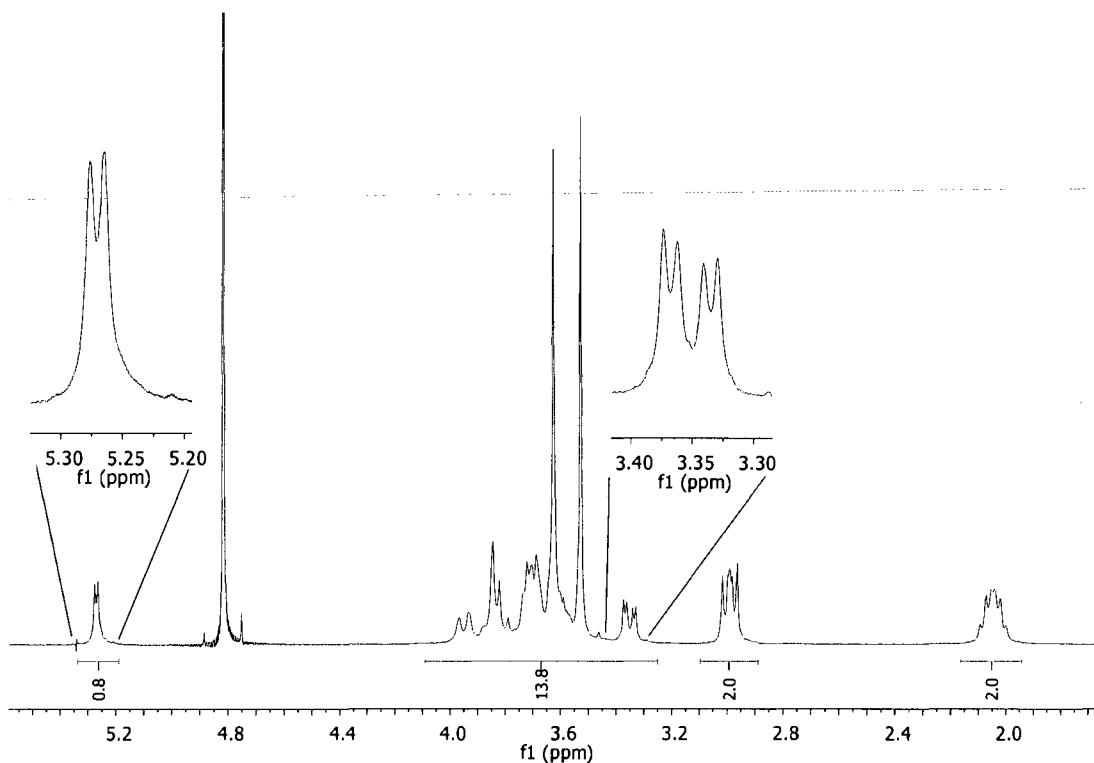


Figure 3.26. ^1H NMR spectrum of pure heptakis(2,3-di-O-methyl-6-O-sulfopropyl)-cyclomaltoheptaose (**5A**), DS_{CE} 6.9 in D_2O .

In addition, integration of the sulfopropyl methylene proton signals is in better agreement with full substitution at the C-6 primary hydroxyl sites (ratio $\sim 1:2$ for H-1 at 5.27 ppm and $-\text{CH}_2\text{S}$ at 2.98 ppm). From CE analysis, this product consists of $\sim 93\%$ of the highly symmetric heptakis-(KSPDM)- β -CD (**5A**) and $\sim 7\%$ of hexakis product (Figure 3.21). The ^{13}C NMR spectrum is given in Figure 3.27.

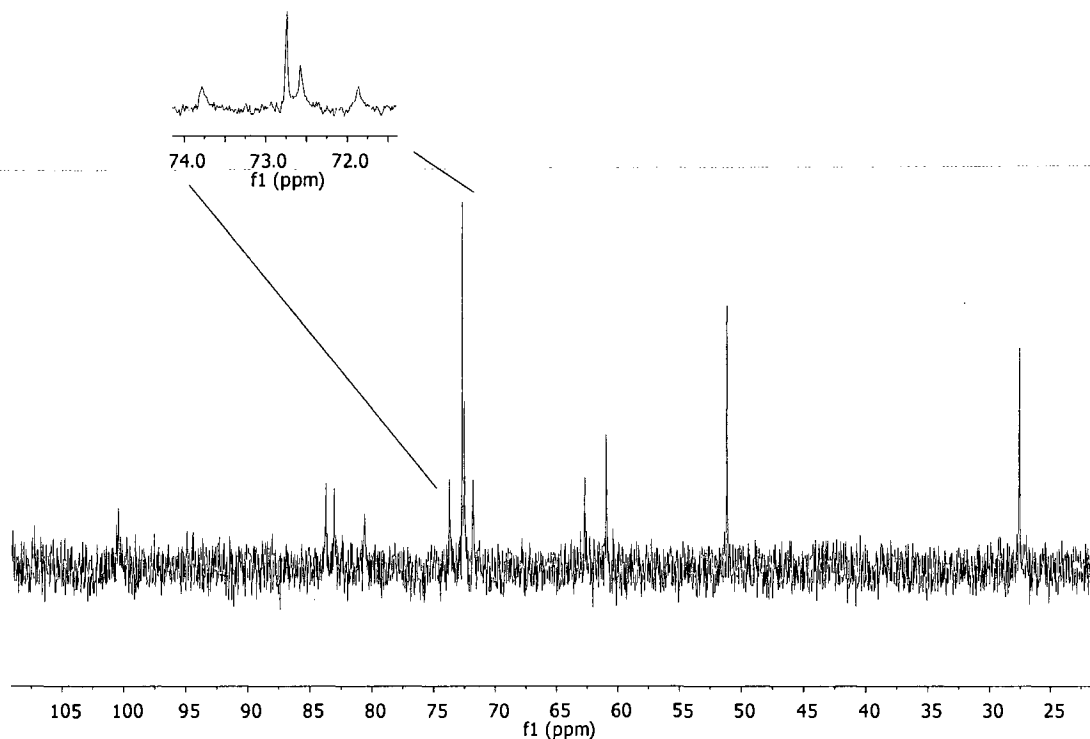


Figure 3.27. ^{13}C NMR spectrum of pure heptakis(2,3-di-O-methyl-6-O-sulfopropyl)-cyclomaltoheptaose (5A), DS_{CE} 6.9 in D_2O .

The use of DMSO-d_6 as solvent can provide additional ^1H NMR diagnostic information on the degree of sulfoalkylation of the C-6 primary hydroxyls. ^1H NMR spectroscopy with DMSO-d_6 can be used for detecting the presence of unreacted primary hydroxyl groups. This is due to the ability of DMSO to significantly reduce the rate of exchange of hydroxyl protons. The spectrum of a sulfopropylated product obtained with 1.2 equivalents/ hydroxyl 18-crown-6 (DS_{CE} 6.7) is shown in Figure 3.28.

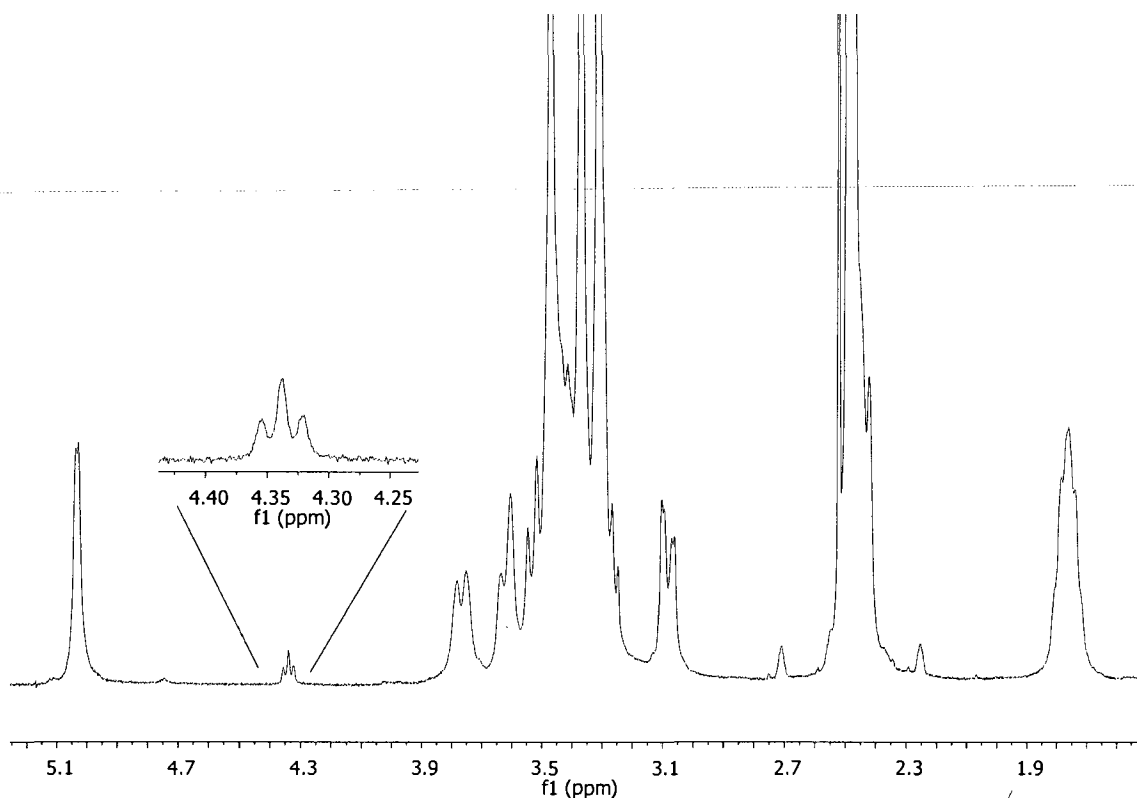


Figure 3.28. ^1H NMR spectrum in DMSO-d_6 of heptakis(2,3-di-O-methyl-6-O-sulfopropyl)cyclomaltoheptaose (**5A**). Product is from reaction using 1.2 equiv./hydroxyl 18-crown-6. The triplet at 4.34 ppm is representative of unreacted C-6 primary hydroxyl.

This spectrum reveals well-resolved H-1 and H-2 resonances, but the weak triplet at 4.36 ppm is indicative of the presence of unsubstituted primary hydroxyl. This triplet remained undetected in the product with DS_{CE} 6.9.

Increasing amounts of 18-crown-6 were required to achieve a high degree of substitution as shown in Table 3.1.

Table 3.1. Effect of 18-crown-6 in reaction medium on the average degree of substitution of KSPDM- β -CD, (5A). Percent in mixture and average DS was determined by inverse detection CE.

mmol 18-crown-6 mmol OH of (4A)	DS _{CE}	No. of added sulfopropyl groups	Percent in mixture
0	4.1	1	0.1
		2	3.9
		3	21.6
		4	37.8
		5	28.6
		6	7.1
		7	0.9
1.2	6.5	5	6.5
		6	40.5
		7	53
2.4	6.7	5	1
		6	28.9
		7	70.1
3.6	6.9	6	7
		7	93

More than 3.5 equivalents of 18-crown-6, based on the number OH groups, is required to achieve a DS_{CE} of 6.9 in 24 h at room temperature. From a practical standpoint, this amount of 18-crown-6 seems excessive, but the crown ether is recovered from the acetone wash (Figure 3.25), and can possibly be purified and reused if necessary. It is noteworthy that 18-crown-6 seems to be much more critical than time to the success of the reaction. CE and NMR of aliquots taken during the course of the reaction indicates the reaction is essentially complete within 1 h reaction time, with no detectable change during the next 23 h. Addition of more crown ether after 24 h then results in a rapid increase in the degree of substitution. 18-Crown-6 is known to effectively complex to potassium ion in THF. By doing so, the solubility of the increasingly anionic KSPDM- β -

CD **5A'** species (DS 1-7) in THF may be enhanced during the course of the reaction, leading to a more substituted product. The 18-crown-6–potassium complex may also result in a more reactive cyclodextrin oxyanion, especially if the crown ether induces some degree of potassium cation–oxyanion separation in THF. For some nucleophilic ring-opening reactions, crown ether–metal complexes also stabilize the developing negative charge on departing leaving group (Gobbi et al., 1995; Albanese et al., 2001). The precise role of the 18-crown-6 in our reaction requires further investigation.

During the development of the sulfoalkylation reaction, several alternative approaches to 18-crown-6 were investigated but not successful. The avoidance of 18-crown-6 would be beneficial by minimizing product workup and thus maximizing recovery of KSPDM- β -CD. Polar aprotic solvents are beneficial for SN2 reactions. Reactions carried out in the absence of 18-crown-6 in anhydrous DMF did not provide a highly substituted product based on ^1H NMR despite the increased polarity of DMF compared with THF. Alternatively, Monflier et al. demonstrated that repetitive additions of excess 1,3-propane sultone and KH over several days was necessary for significant sulfoalkylation of calixerene derivatives (Hapiot et al., 2004). Attempts at repetitive additions of these reagents in THF, however, did not yield highly substituted products.

3.3.7 General procedure for the synthesis of potassium salts of (5B), (5C), (5D), (5E), (5F)

Full regioselective sulfopropylation of the C-6 primary hydroxyls of **4B**, **4C**, and **4D** and sulfobutylation of **4A** and **4B** was accomplished using 1,3-propane sultone and 1,4-

butane sultone respectively in THF with KH/18-crown-6 as base. These reactions were scaled at 1-2 g of CD starting material. The same procedure as described above for the synthesis of **5A** was used. An alternative product purification strategy is described for these CDs and is recommended over the approach described above. After reaction for 24 h, the excess KH was reacted with methanol to quench reaction, and the mixture was transferred to a round bottom flask for rotary evaporization of methanol and THF. The solid was dissolved in 30 mL of water. The aqueous solution was then passed through a column of acidic cation exchange resin (Dowex 50W-X8, 25 mm dia x 350 mm length). After ion exchange, the acid form of the CD in water was extracted three times with methylene chloride, discarding the methylene chloride layer which contains almost exclusively 18-crown-6. The use of acidic ion exchange to form the CD-persulfonic acid allowed for maximal recovery of the CD as compared to acetone extraction when crown ether is in high molar excess. A ^1H NMR spectrum of the acid form of SPDE- β -CD (**5E**) after methylene chloride extraction but prior to further workup is shown in Figure 3.29.

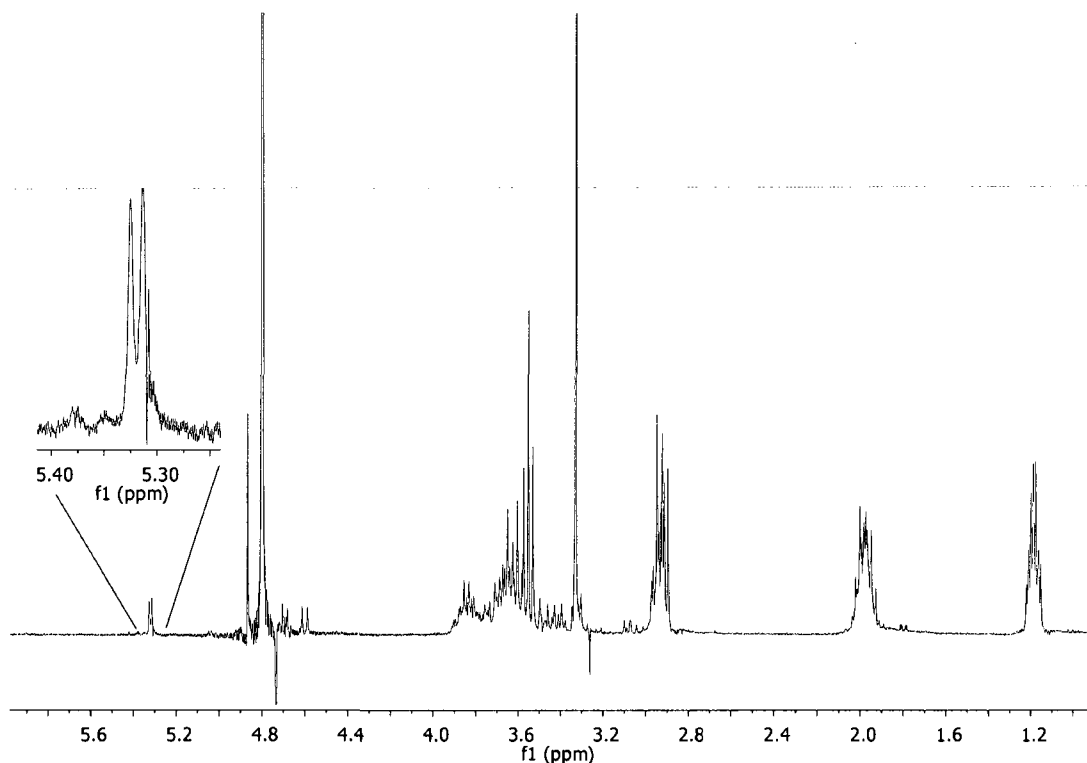


Figure 3.29. ^1H NMR spectrum obtained for the crude acid of heptakis(2,3-di-O-ethyl-6-O-sulfopropyl)cyclomaltoheptaose (**5E**) in D_2O . The spectrum demonstrates that ion exchange successfully removes 18-crown-6 (absence of a singlet, 3.52 ppm). The H-1 anomeric proton shows especially sharp coupling when the CD-acid is dissolved in D_2O .

While sulfone byproduct peaks are abundant in this spectrum, a well resolved H-1 anomeric doublet is observed for the acid form of the CD. Furthermore, a lack of significant signal at 3.52 ppm demonstrates that 18-crown-6 was successfully removed. Caution is recommended during ion exchange against prolonged formation of the acid form of the CD which may irreversibly decompose in solution if kept for an extended period. The acid form seems sufficiently stable for at least 3 h, however. After acid ion exchange, the CDs were neutralized with excess KHCO_3 (~10 g). The aqueous solution was rotary evaporated to remove trace amounts of methylene chloride, and then

subjected to continuous ultrafiltration using an Amicon Model 8400 Stirred Cell Ultrafiltration Unit. The purified CD concentrate was rotary evaporated to remove most of the water. The resulting solid was then dried in a vacuum oven (70 °C) to a constant mass. In the case of **5C** and **5D**, the purification was performed with Regenerated Cellulose 1000 MWCO ultrafiltration membranes. Lower yields obtained for these cyclodextrins were typical using these membranes compared with cellulose acetate 500 MWCO membranes used for **5B**, **5E**, and **5F**. Samples were analyzed by ^1H , ^{13}C , gCOSY, and gHSQC NMR spectroscopy, elemental analysis, inverse detection capillary electrophoresis and, for some CDs, matrix-assisted laser desorption ionization/time of flight mass spectrometry (MALDI/TOF MS). Yields are given for last step in synthesis.

3.3.8 Characterization of heptakis(2,3-di-O-methyl-6-O-sulfobutyl)cyclomaltoheptaose (5B).

Yield, 98%; ^1H NMR (300 MHz, D₂O): δ 5.19 (H-1), 3.70 (H-4), 3.57 (H-3), 3.26 (H-2), 3.73, (H-5), 3.49 (OCH₂), 3.83, 3.61 (H-6), 3.53 (OCH₃), 3.43 (OCH₃), 2.85 (CH₂S), 1.65 (CH₂CH₂O), 1.72 (CH₂CH₂S). ^{13}C NMR (75 MHz, D₂O): δ 101.8 (C-1), 85.0 (C-4), 84.2 (C-3), 82.3 (C-2), 74.8 (C-5), 74.8 (OCH₂), 73.0 (C-6), 64.1 (OCH₃), 62.1 (OCH₃), 54.9 (CH₂S), 31.9 (CH₂CH₂O), 25.3 (CH₂CH₂S). Anal. Calcd for K₇C₈₄H₁₄₇O₅₆S₇·7H₂O: C, 37.68; H, 6.06; S, 8.38. Found C, 37.42; H, 6.06; S, 8.86. Inverse detection CE: Mean ds (6.8).

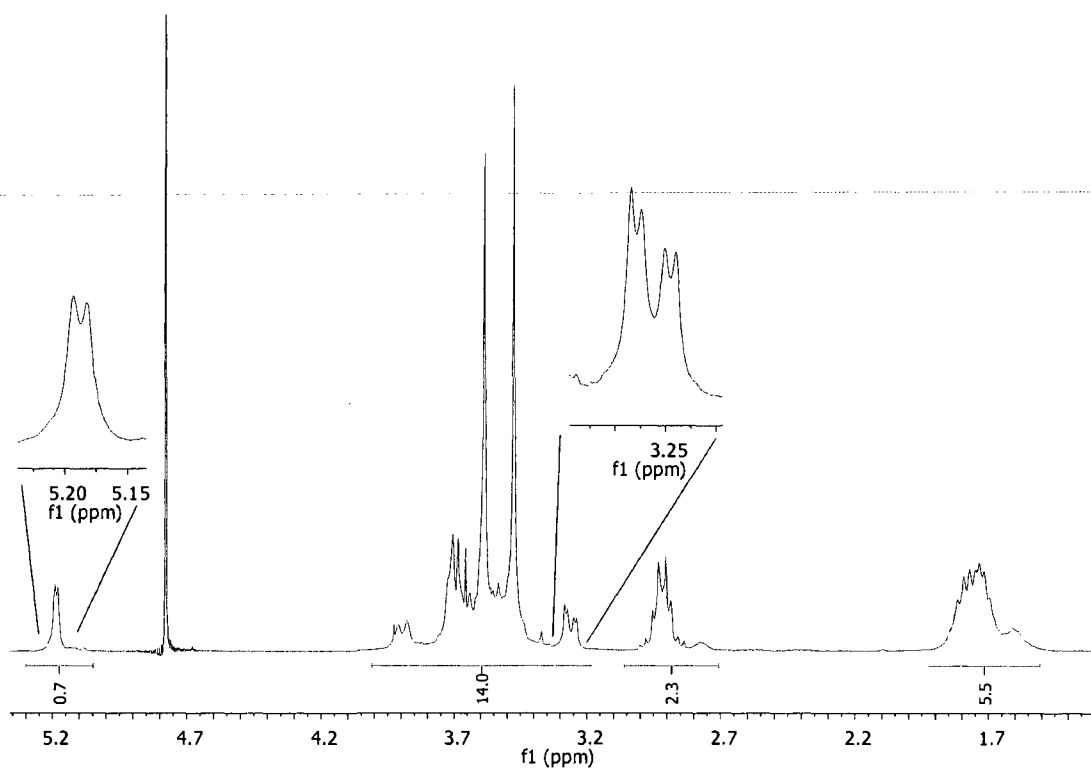


Figure 3.30. ^1H NMR spectrum of heptakis(2,3-di-O-methyl-6-O-sulfobutyl)-cyclomaltoheptaose (**5B**), DS_{CE} 6.8 in D_2O .

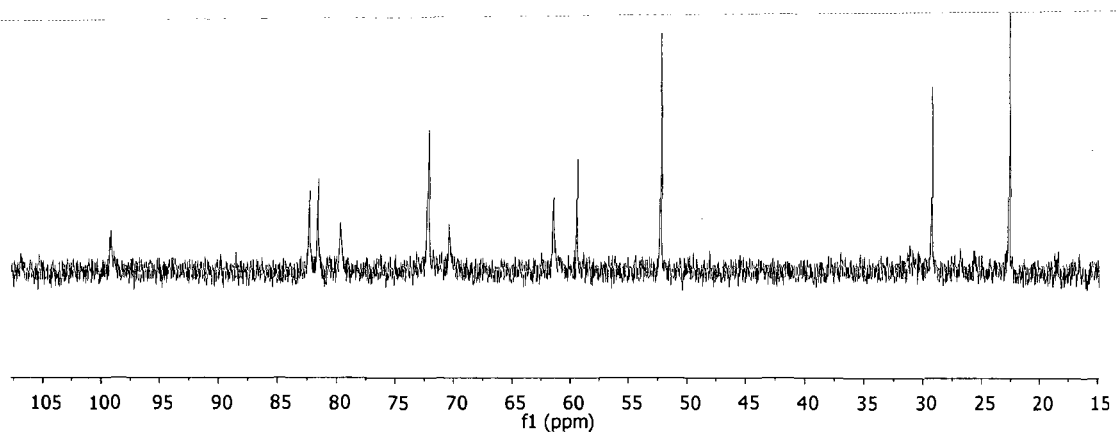


Figure 3.31. ^{13}C NMR spectrum of heptakis(2,3-di-O-methyl-6-O-sulfobutyl)-cyclomaltoheptaose (**5B**), DS_{CE} 6.8 in D_2O .

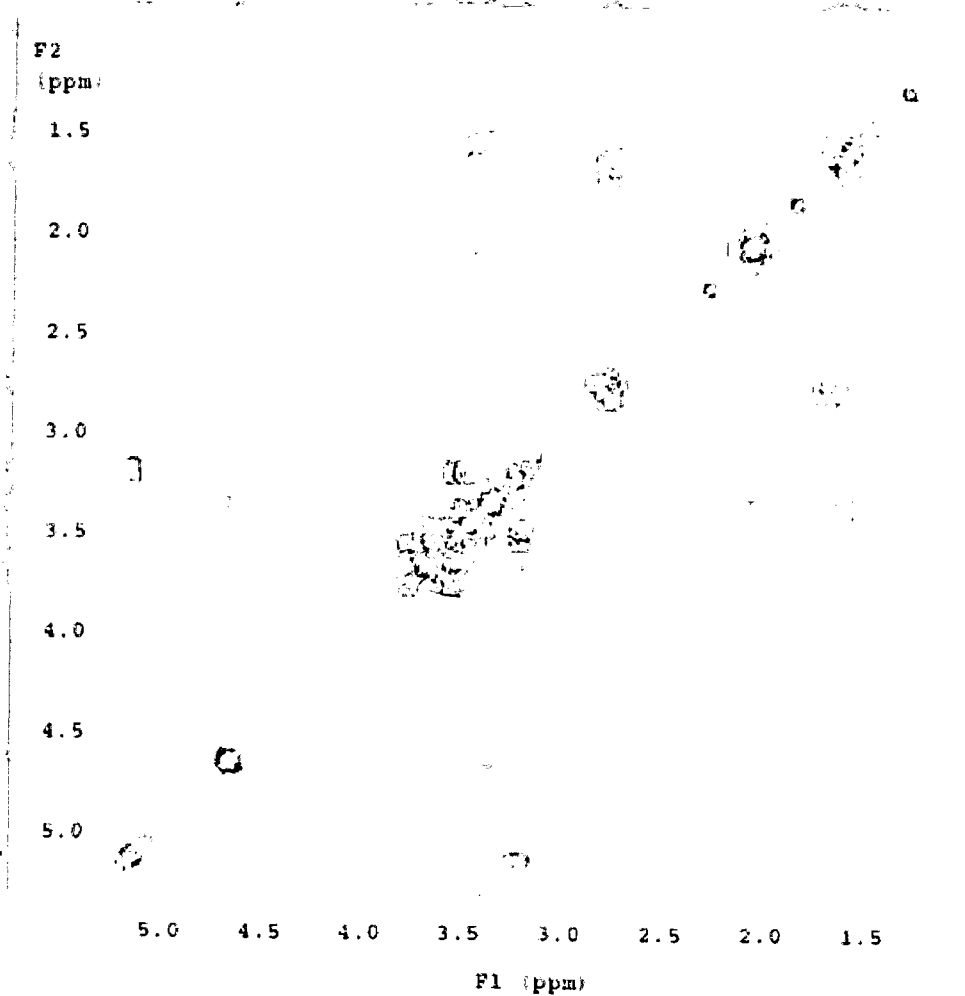


Figure 3.32. gCOSY NMR spectrum of heptakis(2,3-di-O-methyl-6-O-sulfobutyl)-cyclomaltoheptaose (**5B**), DS_{CE} 6.8 in D_2O .

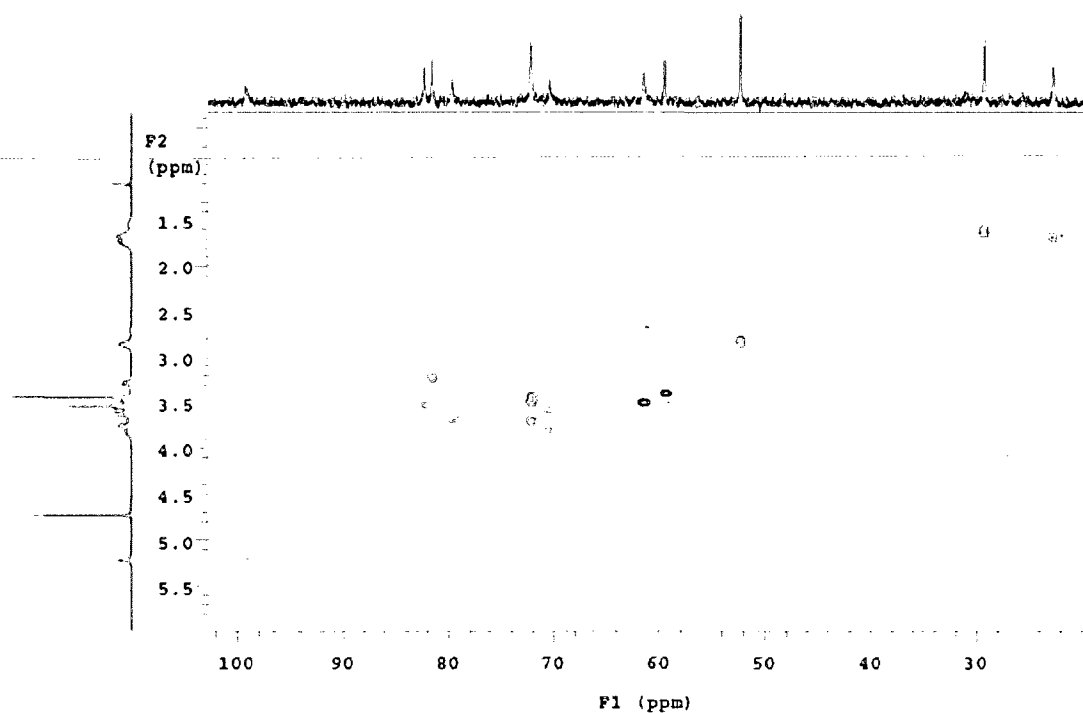


Figure 3.33. gHSQC NMR spectrum of heptakis(2,3-di-O-methyl-6-O-sulfobutyl)-cyclomaltoheptaose (**5B**), DS_{CE} 6.8 in D_2O .

3.3.9 Characterization of hexakis(2,3-di-O-methyl-6-O-sulfopropyl)cyclomaltohexaose (**5C**)

Yield, 55.0%; 1H NMR (300 MHz, D_2O): δ 5.10 (H-1), 3.69 (H-4), 3.50 (H-3), 3.19 (H-2), 3.74 (H-5), 3.53 (OCH_2), 3.84, 3.61 (H-6), 3.54 (OCH_3), 3.42 (OCH_3), 2.92 (CH_2S), 1.97 (CH_2CH_2S). ^{13}C NMR (75 MHz, D_2O): δ 101.5 (C-1), 83.4 (C-4), 83.1 (C-3), 82.8 (C-2), 72.9 (C-5), 71.6 (OCH_2), 70.8 (C-6), 62.9 (OCH_3), 59.5 (OCH_3), 50.3 (CH_2S), 26.6 (CH_2CH_2S). Anal. Calcd for $K_6C_{66}H_{114}O_{48}S_6 \cdot 6H_2O$: C, 35.86; H, 5.74; S, 8.70.

Found C, 35.98; H, 5.63; S, 8.71. Inverse detection CE: Mean ds (6.0). MS: Calcd for $K_7C_{66}H_{114}O_{48}S_6 + 2142$, Found 2141.

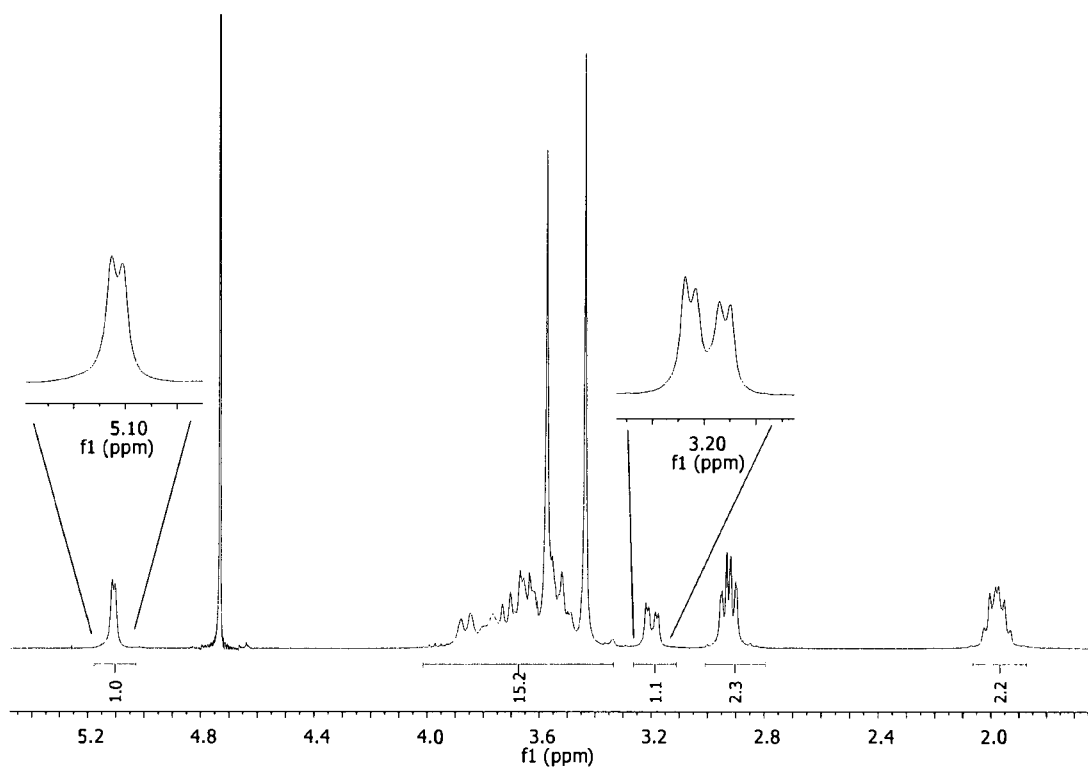


Figure 3.34. ^1H NMR spectrum of hexakis(2,3-di-O-methyl-6-O-sulfopropyl) cyclomaltohexaose (5C), DS_{CE} 6.0 in D_2O .

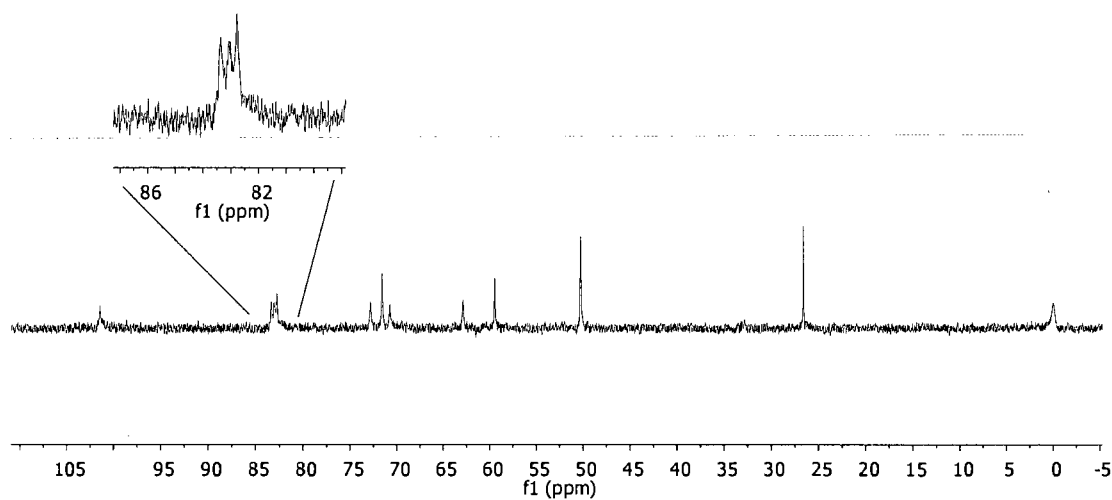


Figure 3.35. ^{13}C NMR spectrum of hexakis(2,3-di-O-methyl-6-O-sulfopropyl) cyclomaltohexaose (**5C**), DS_{CE} 6.0 in D_2O .

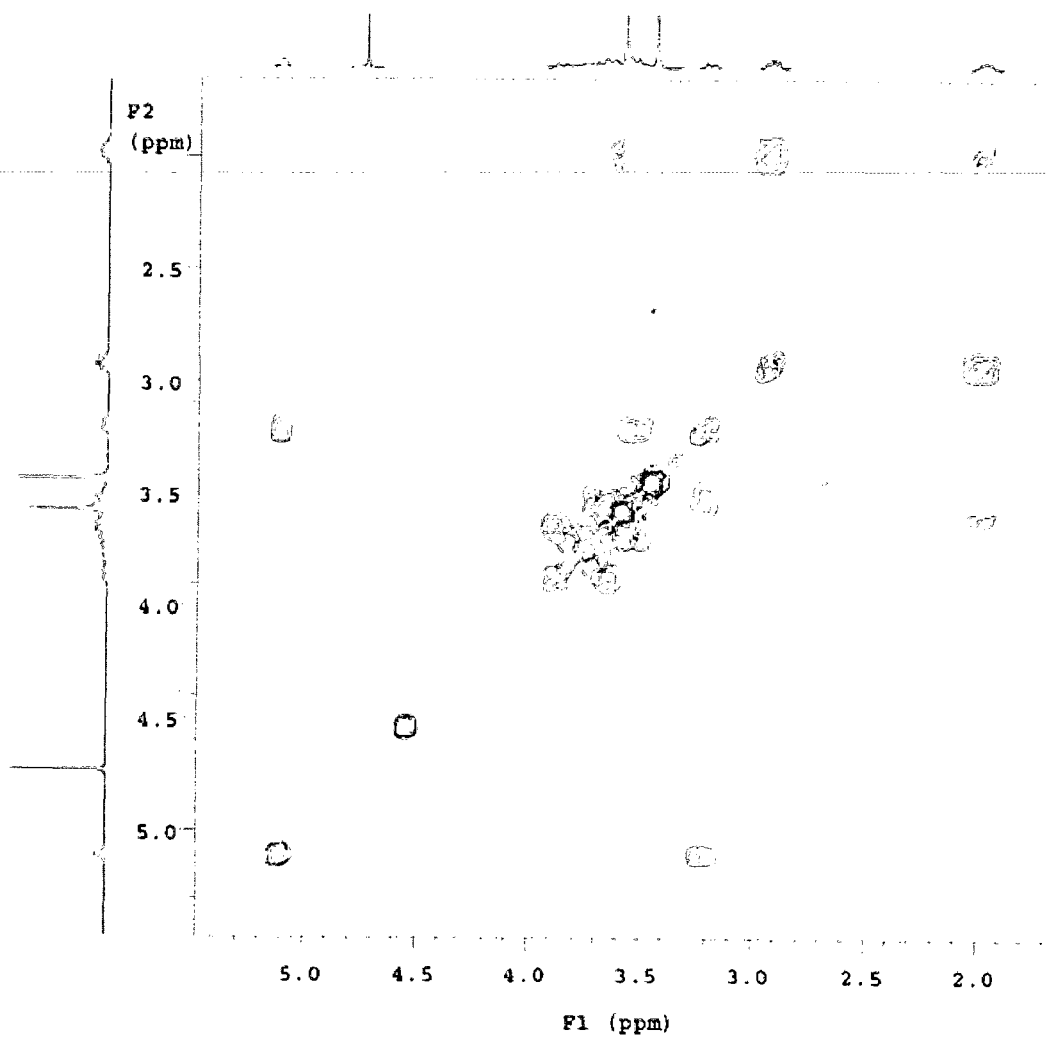


Figure 3.36. gCOSY NMR spectrum of hexakis(2,3-di-O-methyl-6-O-sulfopropyl) cyclomaltohexaose (**5C**), DS_{CE} 6.0 in D_2O .

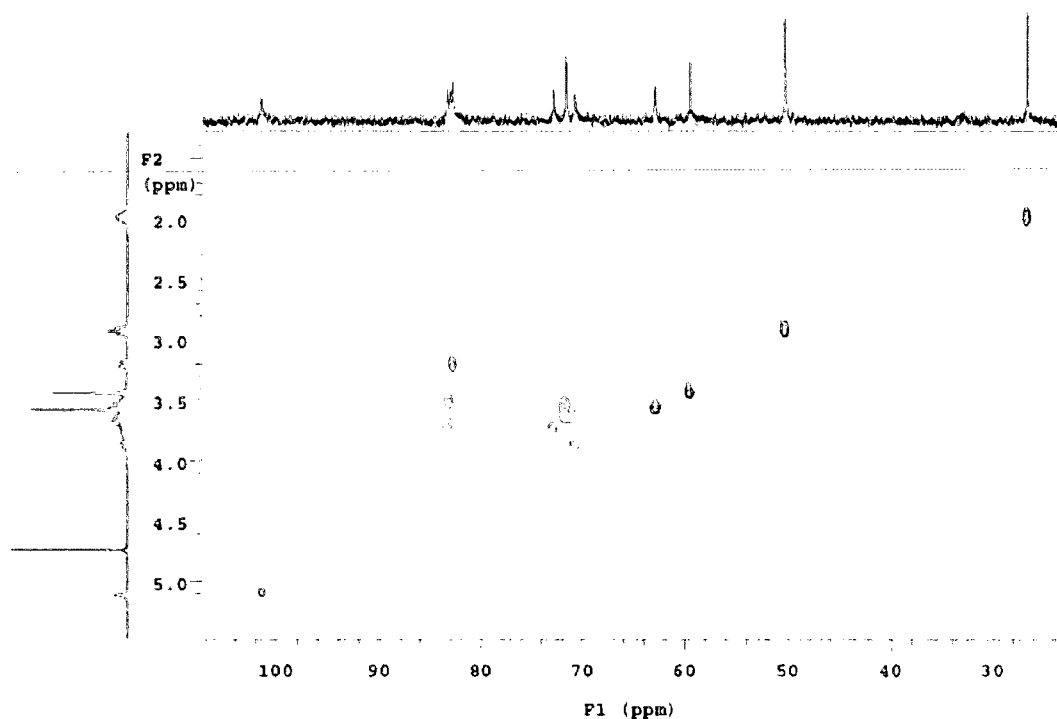


Figure 3.37. gHSQC NMR spectrum of hexakis(2,3-di-O-methyl-6-O-sulfopropyl)cyclomaltohexaose (**5C**), DS_{CE} 6.0 in D_2O .

3.3.10 Characterization of hexakis(2,3-di-O-methyl-6-O-sulfobutyl)cyclomaltohexaose (**5D**)

Yield, 54.6%; 1H NMR (300 MHz, D_2O): δ 5.12 (H-1), 3.72 (H-4), 3.52 (H-3), 3.22 (H-2), 3.75, (H-5), 3.59, 3.49 (OCH₂), 3.87, 3.61 (H-6), 3.57 (OCH₃), 3.43 (OCH₃), 2.88 (CH₂S), 1.68 (CH₂CH₂O), 1.75 (CH₂CH₂S). ^{13}C NMR (75 MHz, D_2O): δ 101.6 (C-1), 83.5 (C-4), 83.1 (C-3), 82.8 (C-2), 73.0 (C-5), 72.8 (OCH₂), 70.9 (C-6), 62.8 (OCH₃), 59.6 (OCH₃), 52.9 (CH₂S), 29.8 (CH₂CH₂O), 23.3 (CH₂CH₂S). Anal. Calcd for $K_6C_{72}H_{126}O_{48}S_6 \cdot 6H_2O$: C, 37.68; H, 6.06; S, 8.38. Found C, 38.18; H, 6.21; S, 8.98. Inverse detection CE: Mean ds (5.8).

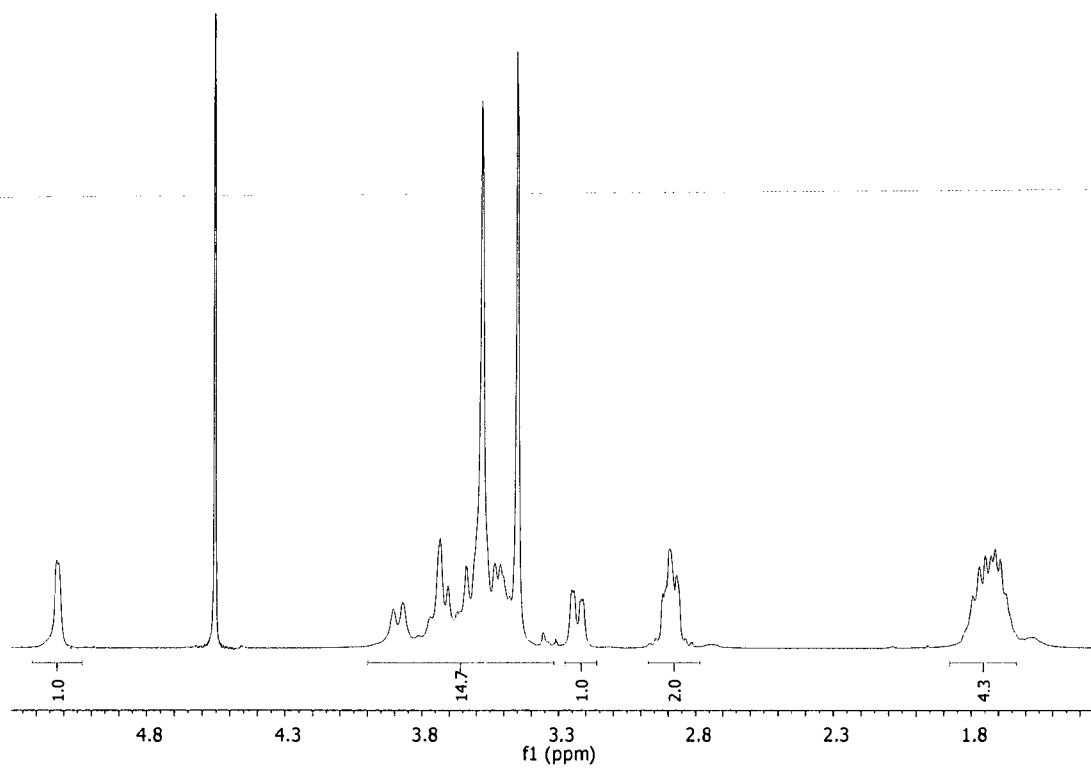


Figure 3.38. ^1H NMR spectrum of hexakis(2,3-di-O-methyl-6-O-sulfoethyl)cyclomaltohexaose (**5D**), DS_{CE} 5.8 in D_2O .

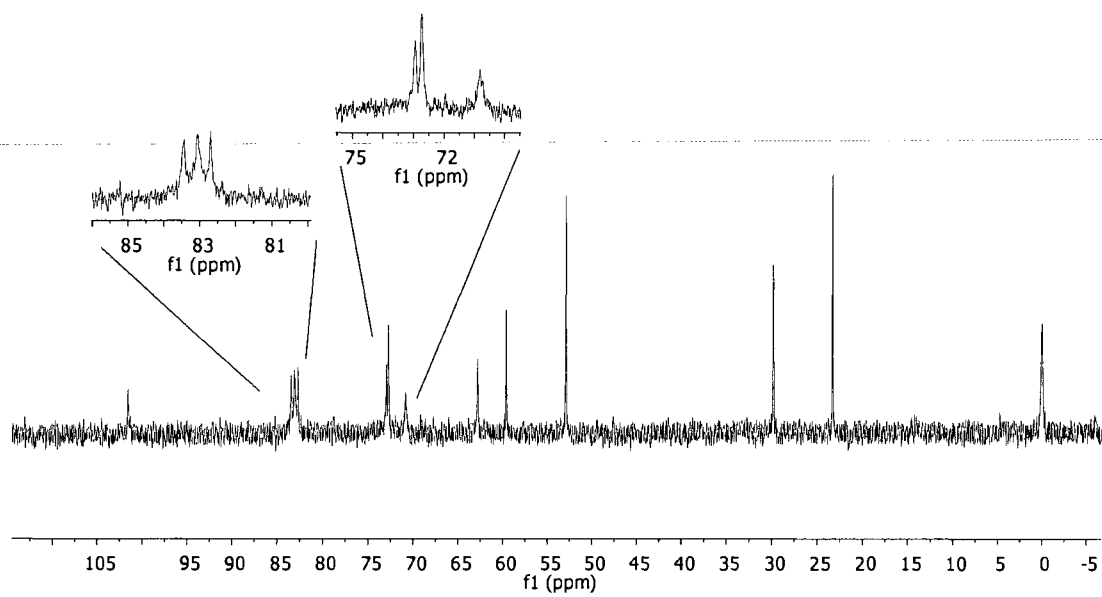


Figure 3.39. ^{13}C NMR spectrum of hexakis(2,3-di-O-methyl-6-O-sulfobutyl) cyclomaltohexaose (**5D**), DS_{CE} 5.8 in D_2O .

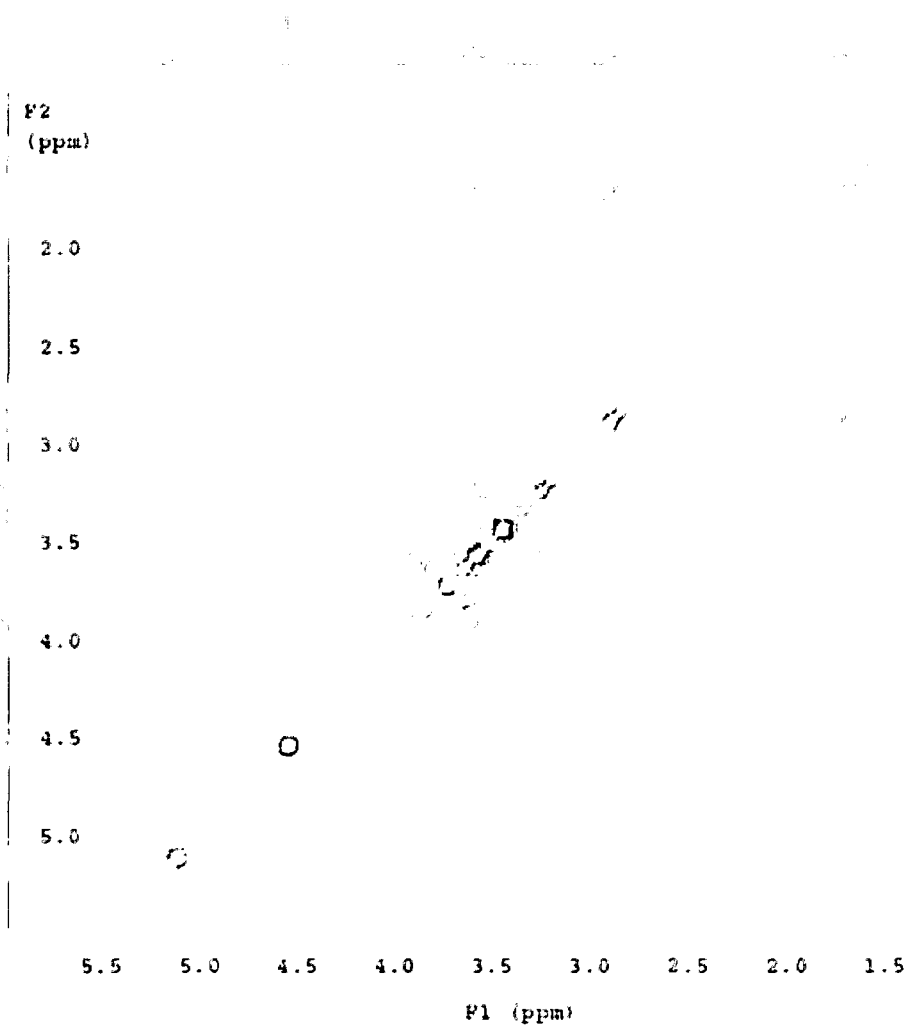


Figure 3.40. gCOSY NMR spectrum of hexakis(2,3-di-O-methyl-6-O-sulfobutyl) cyclomaltohexaose (**5D**), DS_{CE} 5.8 in D_2O .

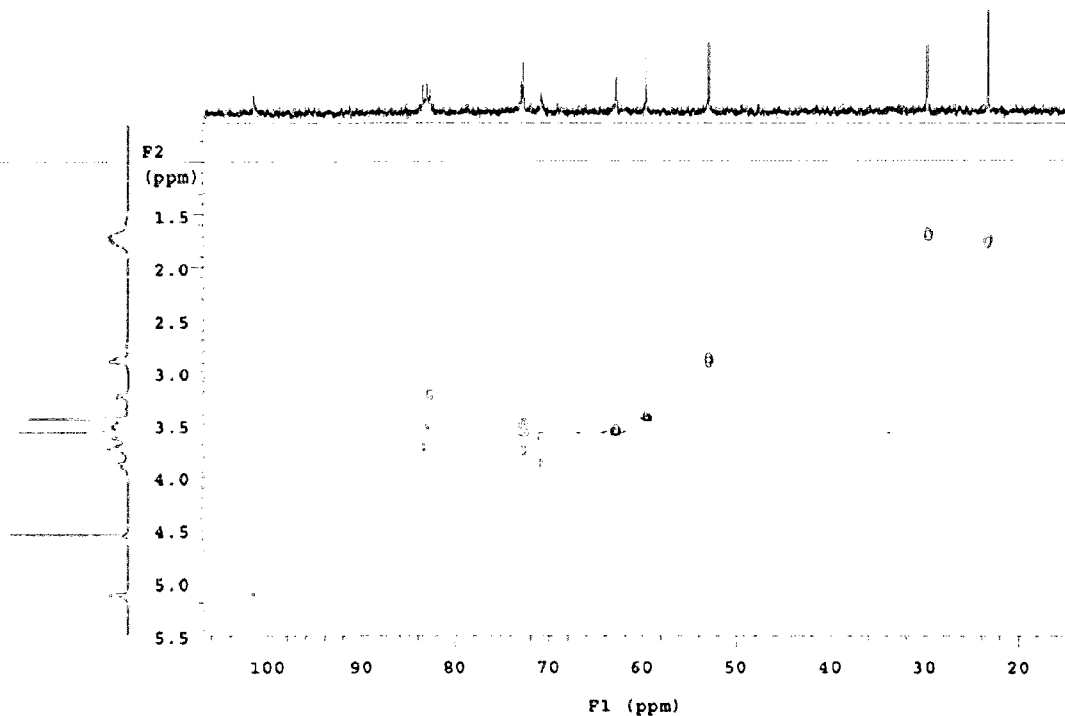


Figure 3.41. gHSQC NMR spectrum of hexakis(2,3-di-O-methyl-6-O-sulfobutyl) cyclomaltohexaose (**5D**), DS_{CE} 5.8 in D_2O .

3.3.11 Characterization of hexakis(2,3-di-O-ethyl-6-O-sulfopropyl)cyclomaltohexaose (**5E**)

Yield, 86.5%; 1H NMR (300 MHz, D_2O): δ 5.03 (H-1), 3.85, 3.68 (OCH_2CH_3), 3.57 (OCH_2CH_3), 3.83, 3.45 (H-6), 3.65 (H-5), 3.42, 3.54 (OCH_2), 3.67 (H-3, H4), 3.24 (H-2), 2.82 (CH_2S), 1.88 (CH_2CH_2S), 1.08 (2 CH_2CH_2O). ^{13}C NMR (75 MHz, D_2O): δ 100.0 (C-1), 82.0 (C-4), 80.5 (C-3), 79.8 (C-2), 73.4 (C-5), 72.0 (OCH_2), 71.5 (C-6), 70.8 (OCH_2CH_3), 69.3 (OCH_2CH_3), 50.5 (CH_2S), 26.9 (CH_2CH_2S), 17.2 (CH_3), 17.1 (CH_3). Anal. Calcd for $K_6C_{78}H_{138}O_{48}S_6 \cdot 6H_2O$: C, 39.38; H, 6.36; S, 8.09. Found C,

38.93; H, 6.27; S, 7.88. Inverse detection CE: Mean ds (6.0). MS Calcd for $K_7C_{78}H_{138}O_{48}S_6 + 2310$ Found 2309.

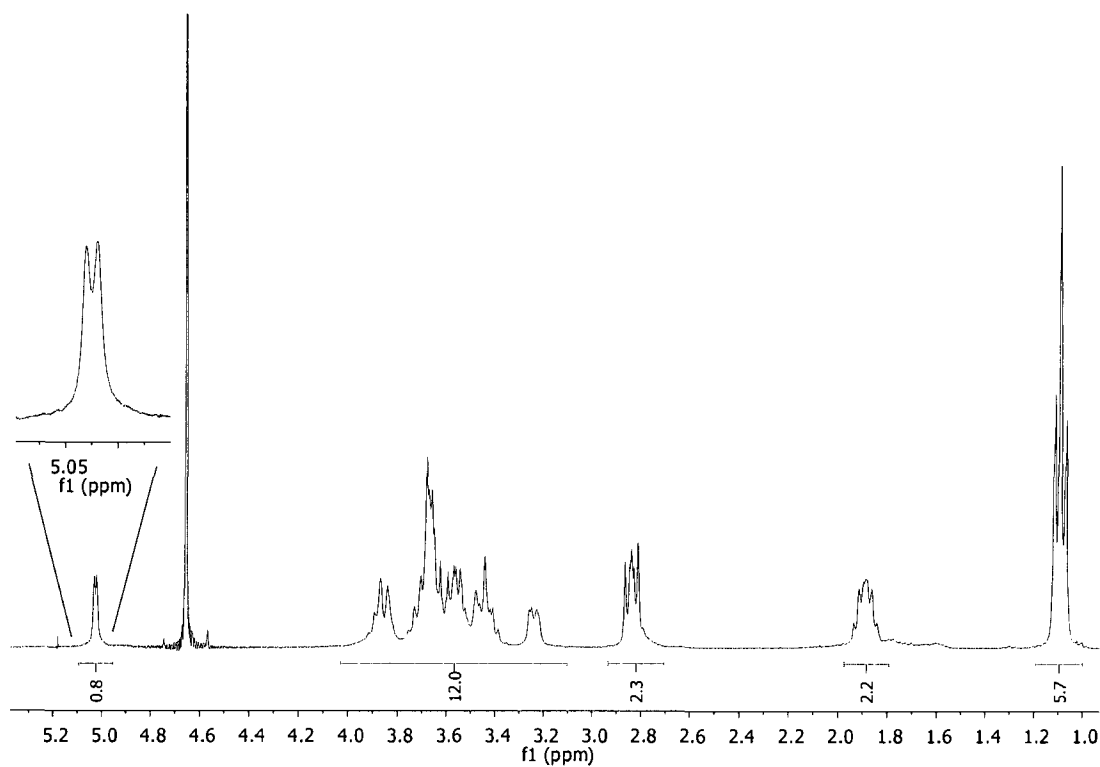


Figure 3.42. ^1H NMR spectrum of hexakis(2,3-di-O-ethyl-6-O-sulfopropyl) cyclomaltohexaose (**5E**), DS_{CE} 6.0 in D_2O .

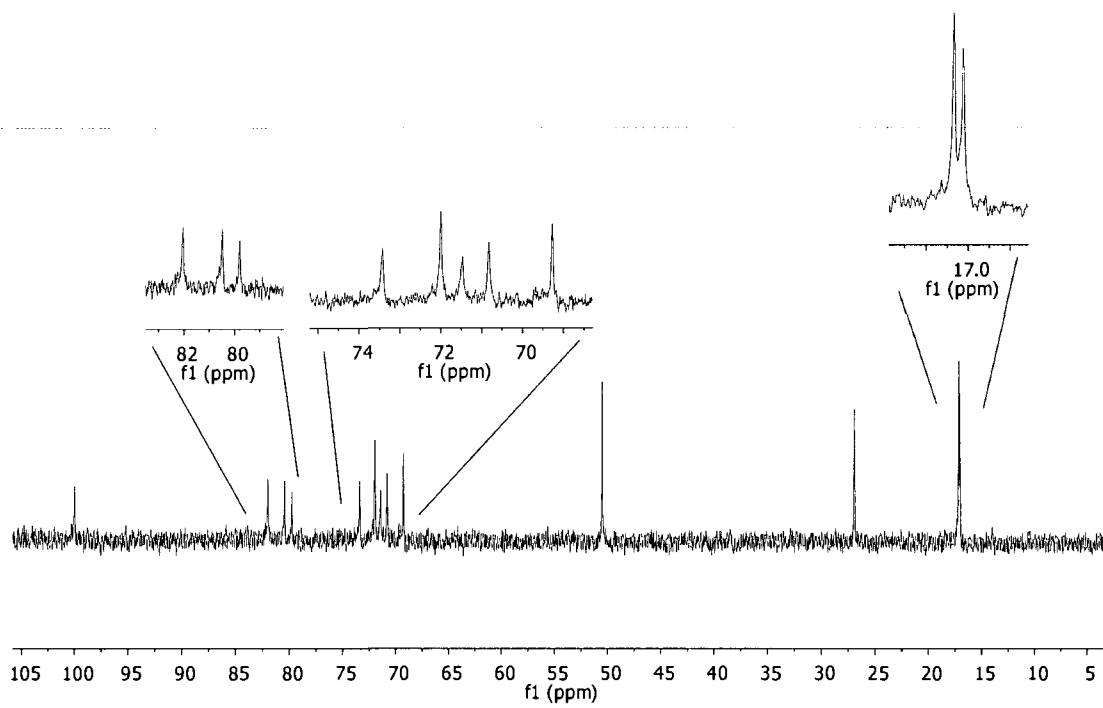


Figure 3.43. ^{13}C NMR spectrum of hexakis(2,3-di-O-ethyl-6-O-sulfopropyl) cyclomaltohexaose (**5E**), DS_{CE} 6.0 in D_2O .

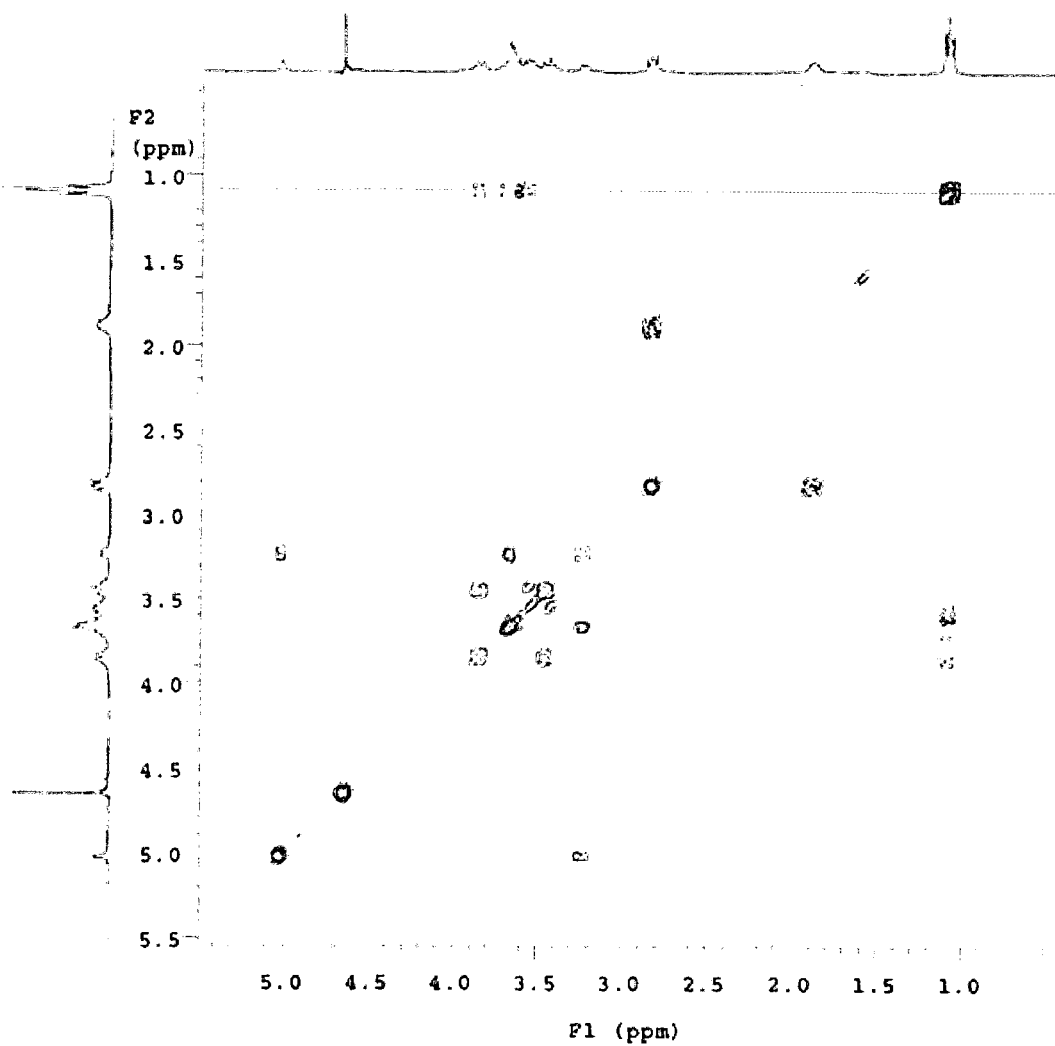


Figure 3.44. gCOSY NMR spectrum of hexakis(2,3-di-O-ethyl-6-O-sulfopropyl) cyclomaltohexaose (**5E**), DS_{CE} 6.0 in D₂O.

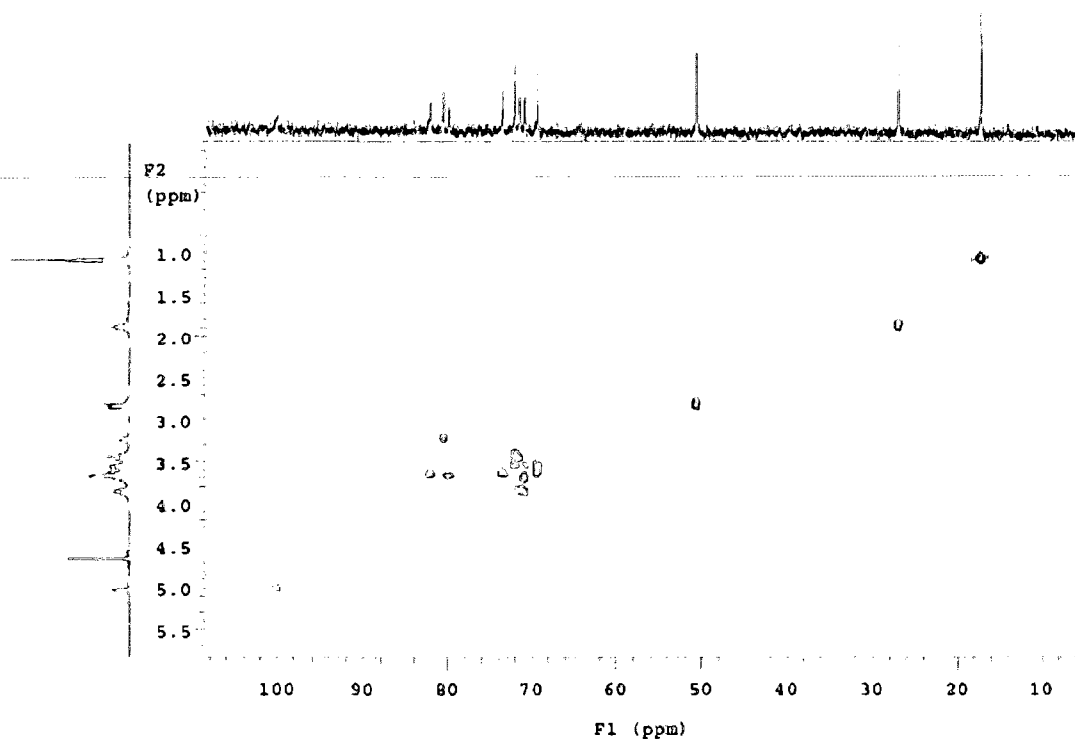


Figure 3.45. gHSQC NMR spectrum of hexakis(2,3-di-O-ethyl-6-O-sulfopropyl)cyclomaltohexaose (**5E**), DS_{CE} 6.0 in D_2O .

3.3.12 Characterization of heptakis(2,3-di-O-ethyl-6-O-sulfopropyl)cyclomaltoheptaose (**5F**)

Yield, 95.4%; 1H NMR (300 MHz, D_2O): δ 5.27 (H-1), 3.85, 3.89, 4.04 (OCH_2CH_3), 3.80 (OCH_2CH_3), 4.04, 3.70 (H-6), 3.86 (H-5), 3.64, 3.74 (OCH_2), 3.85 (H-3), 3.78 (H-4), 3.44 (H-2), 3.03 (CH_2S), 2.09 (CH_2CH_2S). 1.29 (2 CH_3). ^{13}C NMR (75 MHz, D_2O): \square 100.8 (C-1), 82.5 (C-4), 81.4 (C-3), 80.1 (C-2), 73.9 (C-5), 72.5 (OCH_2), 71.6 (C-6), 71.5 (OCH_2CH_3), 69.8 (OCH_2CH_3), 51.1 (CH_2S), 27.4 (CH_2CH_2S), 17.8, 17.6 (2 CH_3).
 Anal. Calcd for $K_7C_{91}H_{161}O_{56}S_7 \cdot 7H_2O$: C, 39.38; H, 6.36; S, 8.09. Found C, 39.33; H,

6.23; S, 8.28. Inverse detection CE: Mean ds (6.8). MS: Calcd for $K_8C_{91}H_{161}O_{56}S_7 + 2688$, Found 2688.

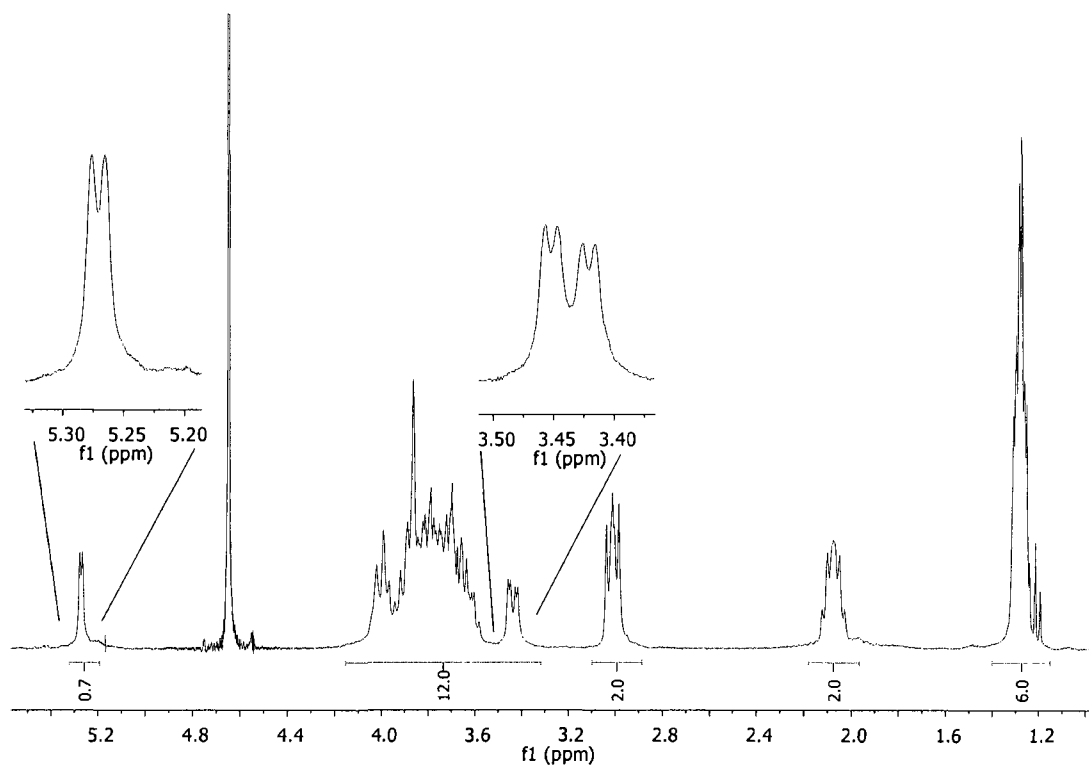


Figure 3.46. ^1H NMR spectrum of heptakis(2,3-di-O-ethyl-6-O-sulfopropyl) cyclomaltoheptaose (**5F**), DS_{CE} 6.8 in D_2O .

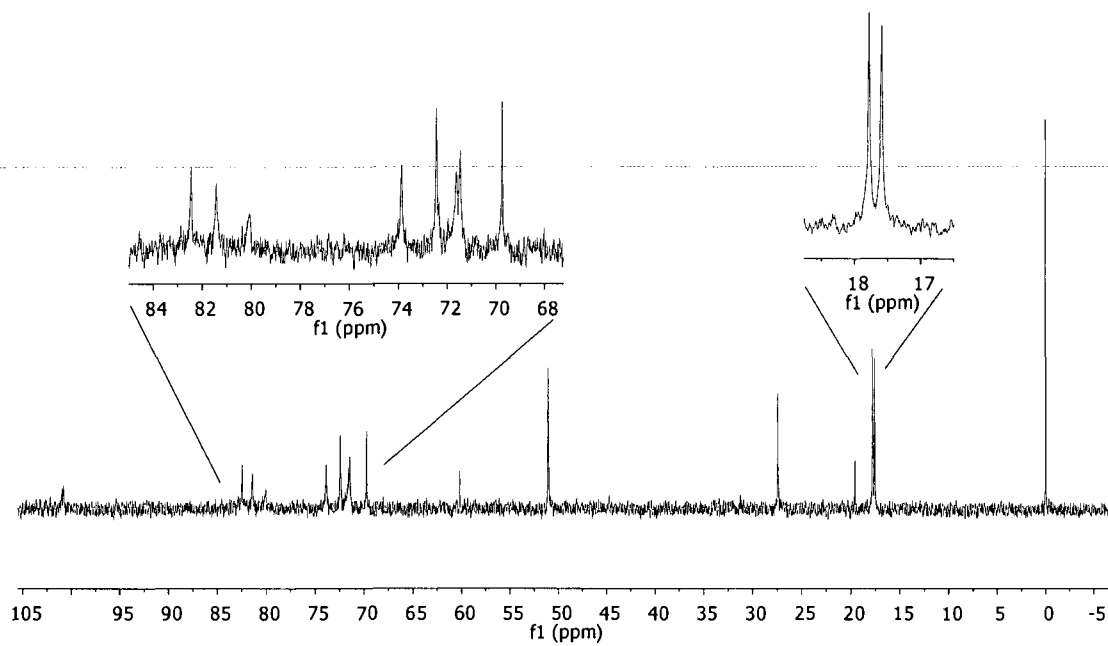


Figure 3.47. ^{13}C NMR spectrum of heptakis(2,3-di-O-ethyl-6-O-sulfopropyl) cyclomaltoheptaose (**5F**), DS_{CE} 6.8 in D_2O .

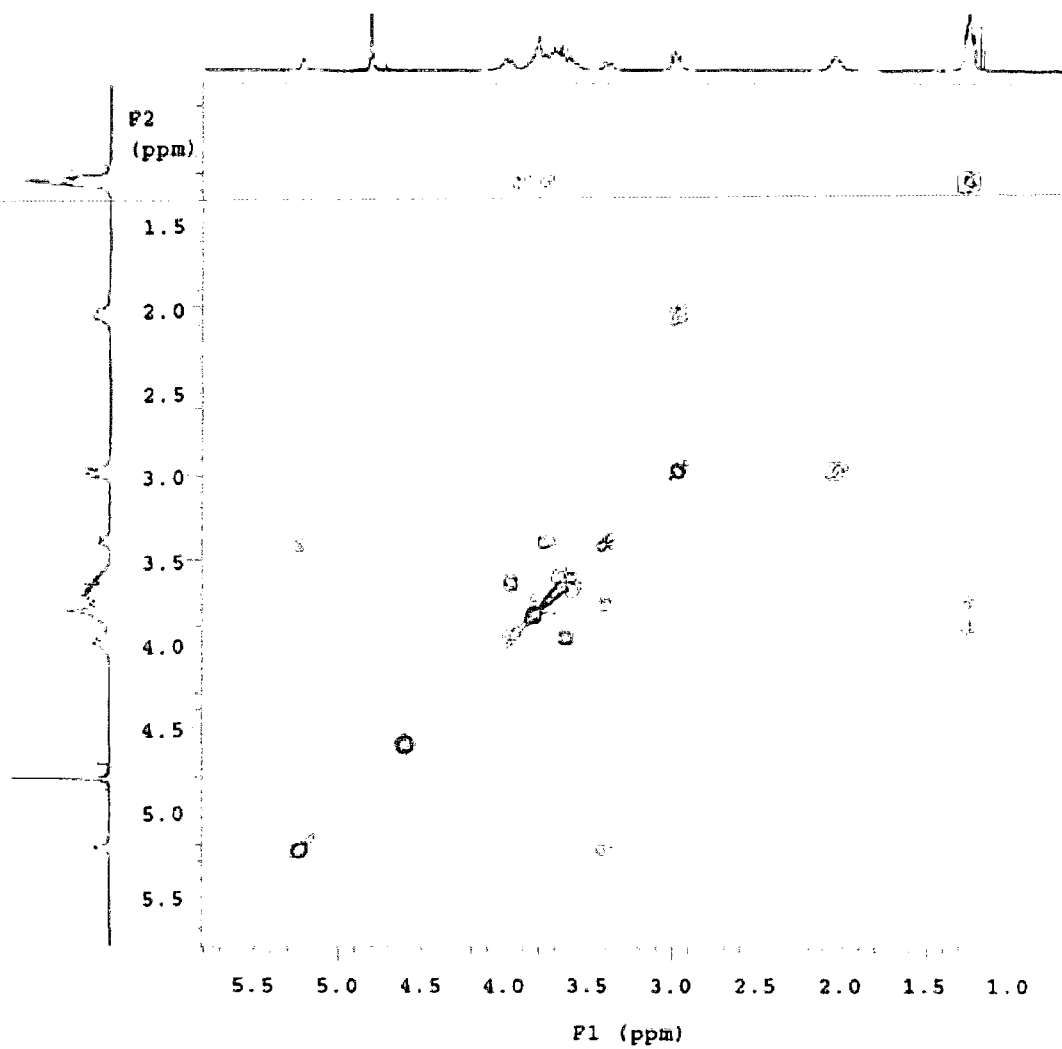


Figure 3.48. gCOSY NMR spectrum of heptakis(2,3-di-O-ethyl-6-O-sulfopropyl) cyclomaltoheptaose (**5F**), DS_{CE} 6.8 in D_2O .

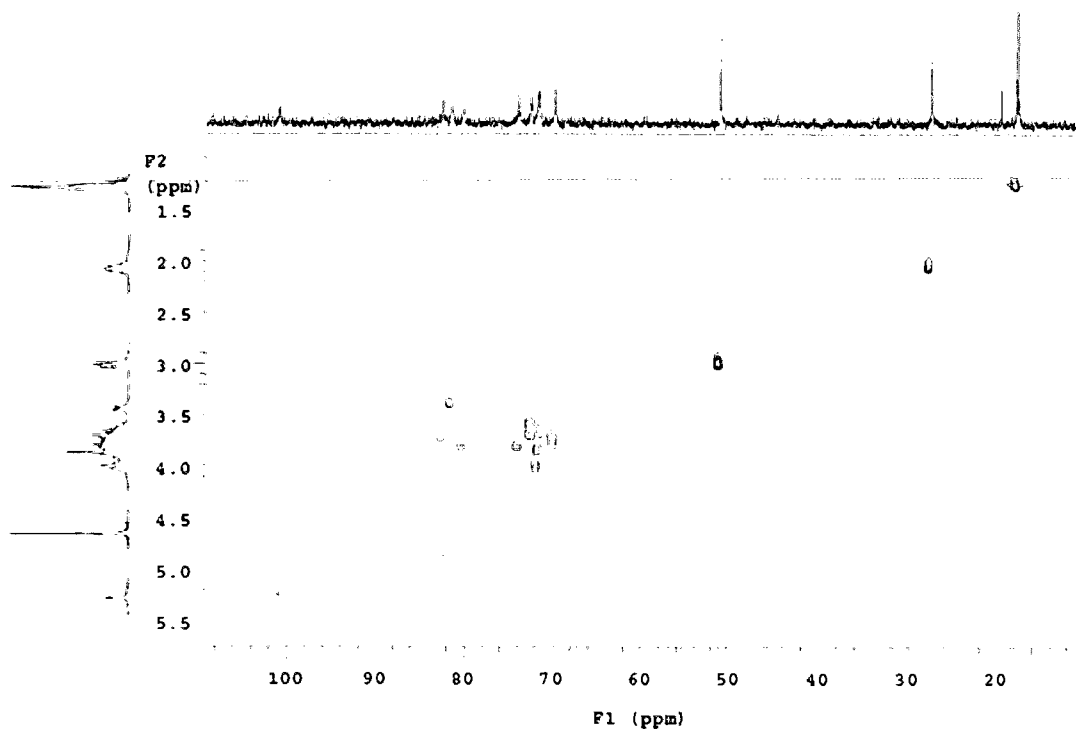


Figure 3.49. gHSQC NMR spectrum of heptakis(2,3-di-O-ethyl-6-O-sulfopropyl) cyclomaltoheptaose (**5F**), DS_{CE} 6.8 in D_2O .

3.4 Investigation of inclusion complex formation

One of the advantages of single isomer cyclodextrins like those produced here is that the ^1H resonances in the NMR spectrum are confidently assigned which allows for detailed study on the inclusion complex formed in solution between a hydrophobic guest and the CD. Upon binding, complex induced chemical shifts (CICS) can be pronounced for both guest and host ^1H resonances. Of particular note for CD inclusion complex studies are the H-3 and H-5 hydrogens on the glucose units which are directed facing the interior of the CD cavity and can show significant through space interactions (Nuclear Overhauser Effects, NOEs) with nearby hydrogens on the included guest molecule. Inclusion complex NMR data can be important for determining the orientation as well as the direction of approach of a guest molecule with the CD host. For large molecular weight (>2000 Da) species, the 2-D rotating frame NOE or ROESY experiment can be valuable for determining the orientation of the guest species. Kahle et al. were able to correlate CICS and ROESY NMR data with capillary electrophoresis chiral separation studies to provide a mechanistic explanation for pH dependent reversal of migration order of chiral dipeptides possessing aromatic amino acid side chains (Kahle et al., 2005). Chankvedetski et al. used ROESY NMR to study the inclusion complexes of the drug clenbuterol with β -CD and heptakis(2,3-diacetyl-6-O-sulfo)cyclomaltoheptaose (HDAS- β -CD) in order to investigate the mechanism of the opposite order of migration of enantiomers by CE (Chankvetadze et al., 2001). They observed significant differences in the structure of the complexes of β -CD/clenbuterol and HDAS- β -CD/clenbuterol.

As an initial study, the inclusion complex of CBI-ser with the new single isomer KSPDM- β -CD was investigated using ROESY NMR. The partial 2D-ROESY spectrum showing relevant cross peaks between CBI-ser and H3 and H5 of KSPDM- β -CD is given in Figure 3.50.

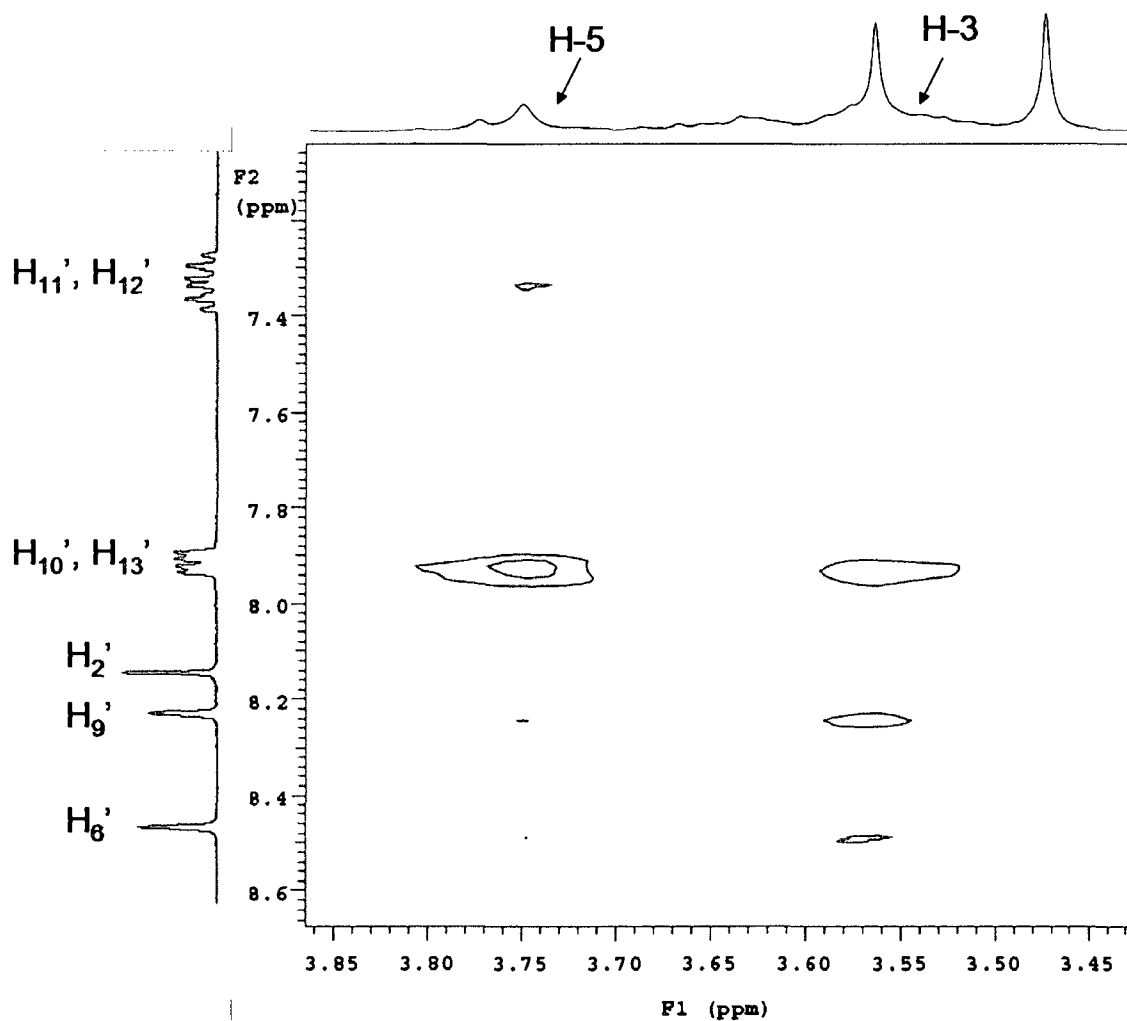


Figure 3.50. 2D ROESY spectrum of inclusion complex of KSPDM- β -CD:CBI-ser (molar ratio 2:1). Mixing time 300 ms.

Assignments of the ^1H resonances of CBI-ser were made by a combination of ^1H , gCOSY, and 1D NOE experiments and are given in Figure 3.51 for the proposed complex orientation.

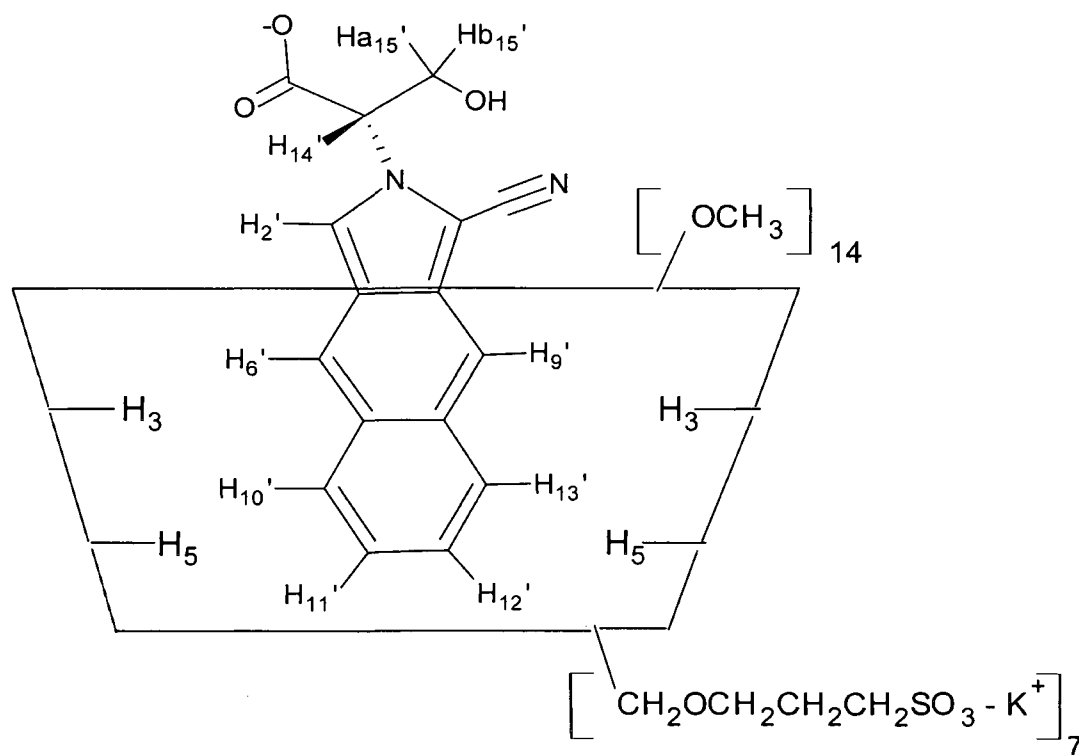


Figure 3.51. Inclusion Complex of KSPDM- β -CD with CBI-ser in D_2O .

A strong NOE crosspeak between the overlapped resonances of H_{10}' , H_{13}' of CBI-ser and H_5 of KSPDM- β -CD suggest penetration of CBI-ser deep into the cavity of the sulfoalkylated CD as represented in Figure 3.51. A weaker interaction is also observed for H_3 of KSPDM- β -CD with H_{10}' and H_{13}' of CBI-ser. Furthermore, H_5 of KSPDM- β -

CD shows a weak NOE crosspeak with the overlapped resonances of H₁₁' , H₁₂' of CBI-ser which is not observed for H₃. Finally, H₃ of KSPDM-β-CD shows NOE crosspeaks with both H₉' and H₆' of CBI-ser with the latter being slightly greater in magnitude suggesting a tilt in orientation of CBI-ser within the cavity. In contrast, very weak interactions between H₅ of the CD and H₆' and H₉' of CBI-ser are observed suggesting these protons on CBI-ser lie closer to the secondary rim of the CD. No interactions between H₂' of CBI-ser and H₃ and H₅ of KSPDM-β-CD are observed. Taken together, the data suggests complexation occurs by inclusion of CBI-ser from the secondary rim with the naphthalene group inserted deep into the cavity and the polar groups of CBI-ser oriented towards the wider secondary rim. This deep insertion into the cavity is evident despite the pH of the solution being ~ 6 which results in full ionization of CBI-ser α-COOH group (pK_a 3.0, Chapter 3). It is quite possible that at lower pH when the acid is significantly protonated (pH < 3), any electrostatic repulsion would be minimized resulting in deeper penetration of CBI-ser into the hydrophobic cavity.

3.5. Summary of findings on single isomer sulfoalkyl CD synthesis

The first members of a family of selectively modified single isomer sulfoalkylated α- and β-CDs have been synthesized through regioselective reaction chemistry. Additionally the β-derivatives have been initially investigated as chiral resolving agents for fluorescently labeled amino acids (*vide infra*). The primary challenge in the synthesis was full sulfoalkylation of the primary rim of the 2,3-di-O-alkylated (methyl or ethyl)-CD derivative. Successful sulfoalkylation was accomplished for all the derivatives

using sultone in THF with KH/18-crown-6 as base. The crown ether was demonstrated to be essential for producing the single isomer CD and was required in high molar excess compared to the CD derivative. Two steps were required to purify single isomer CDs by removing small molecule impurities. In the first step, 18-crown-6 was optimally removed by converting the CD-potassium salt to a CD-acid form, extracting away crown ether with organic solvent, and neutralizing the resultant product. In the second step sultone byproducts as well as excess salts were removed by continuous ultrafiltration using 500 MWCO membranes. All CDs were successfully characterized by NMR spectroscopy, inverse detection capillary electrophoresis, elemental analyses and, in some cases, matrix-assisted laser desorption ionization mass spectrometry (MALDI).

Chapter 4

Chiral Separations of CBI-amino acids with single isomer sulfoalkyl β -CDs

4.1 Overview of study

Single isomer sulfoalkyl CDs developed in Chapter 3 were investigated for their ability to analytically resolve CBI-amino acid enantiomers, with a particular emphasis on biologically significant separations of the enantiomers of CBI-ser, CBI-asp, CBI-glu, and CBI-ala. Separation conditions mimicked the optimized neurochemical analysis conditions described in Chapter 2 and 5, in order to make comparisons with the commercially-available S- β -CD. Briefly, separation was carried out using reversed polarity with the following β -CDs synthesized in Chapter 3: **5A**, **5B**, and **5E**. To more clearly establish nomenclature with CD structure, anionic sulfoalkyl derivatives are considered here as KSPDM- β -CD (**5A**), KSBDM- β -CD (**5B**), and KSBDE- β -CD (**5E**) according to alkyl and sulfoalkyl substituents reported in Figure 3.2 of Chapter 3. The smaller α -CD analogs were not used in any of these studies. The concentration of CD in the BGE ranged from 0.05-10 mM (~0.01-2 wt %). As mentioned in Chapter 2, under reverse polarity low pH conditions with anionic CD chiral selectors, the effective mobility of CBI-amino acids is, to a first approximation, a measure of the strength of the interaction of the analyte with the anionic CD.

4.2 General methods

All chemicals were analytical reagent grade unless otherwise stated. Reagents were described in Section 2.21 of Chapter 2. Capillary electrophoresis was performed on the instrument described in Section 2.22 of Chapter 2 using a bare fused silica capillary of dimensions 48 x 45 cm x 25 μm . CBI-amino acids were prepared for separation studies by reacting equal volumes of amino acid (1 mM), NDA (1 mM in methanol), and NaCN (5.5 mM in 60 mM borate buffer, pH 9.3) and allowed to react for a minimum of 15 min. CBI-amino acids were diluted to 5-10 μM with water. The use of equal molar quantities of amino acid, NDA, and NaCN were used to minimize NDA side products for the separation studies. The BGE was 25 mM phosphate adjusted to pH (typically 2.15) by adding appropriate volume ratios of equal molar H_3PO_4 and NaH_2PO_4 solutions. Resolution (R_s) and plate count (N) were calculated using PeakFit[®] software as described in Chapter 2.22.

4.3 Results with single isomer sulfoalkyl CDs for chiral analysis

Single isomer sulfoalkyl CDs interacted strongly with CBI-amino acids and could be utilized at much lower concentrations compared with S- β -CD as optimized in Chapter 2. A comparison of CBI-ser mobility and selectivity in the presence of ~0.2 wt % S- β -CD verses ~0.2 wt % KSPDM- β -CD demonstrates the significantly increased interaction of CBI-ser with the single isomer sulfopropyl CD (Figure 4.1).

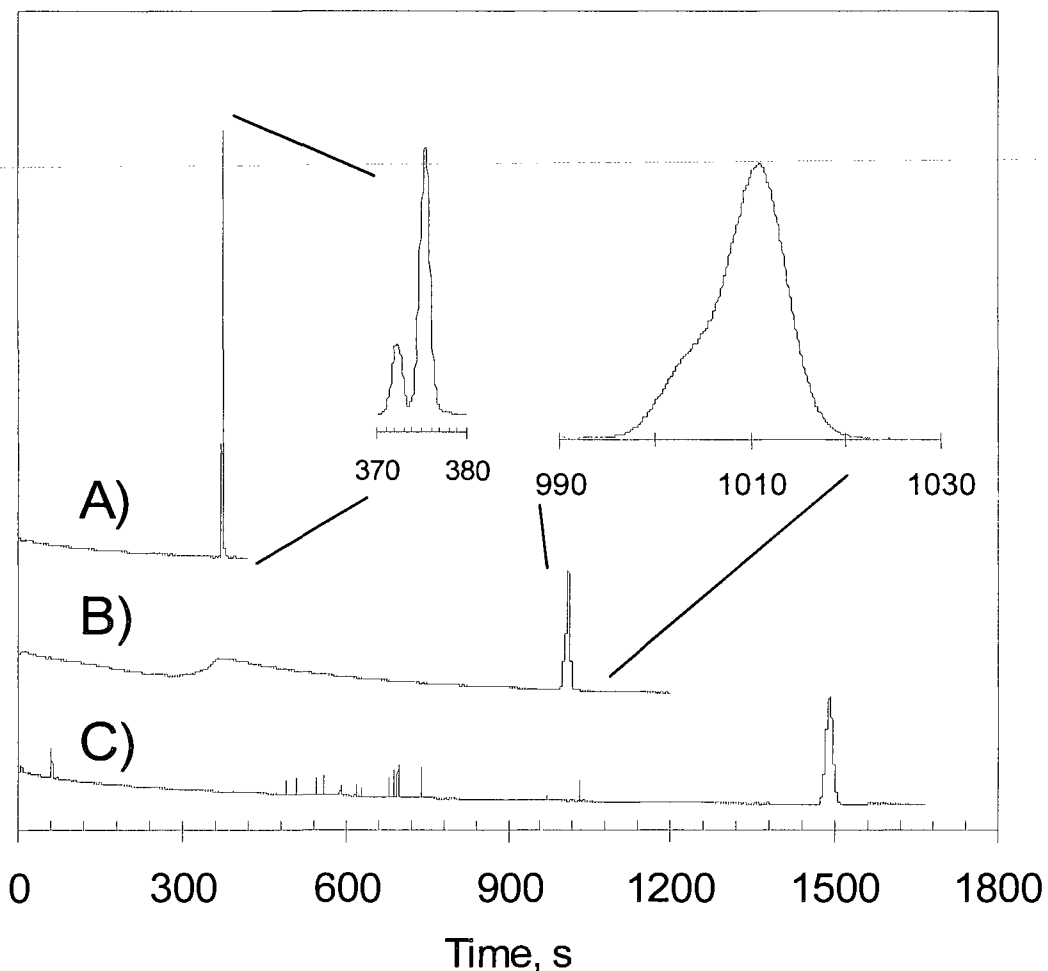


Figure 4.1. Comparison of mobility and selectivity of KSPDM- β -CD and S- β -CD at low pH reverse polarity. Both CDs were prepared to ~ 0.2 wt %. (A) CBI-DL-ser ($\sim 22:78$ D:L) with KSPDM- β -CD in BGE, (B) CBI-DL-ser with commercially available S- β -CD in BGE, (C) CBI-DL-ser in the absence of CD.

Despite its low charge at pH 2.15, the weakly acidic CBI-ser does migrate with its own electrophoretic mobility in 25 mM phosphate with a migration time of ~ 25 min (Figure 4.1C). A theoretical plate count, $N = 41,000$, is calculated. Addition of 0.2 wt % S- β -

CD then reduces migration time ~ 32% (Figure 4.1B) indicating that despite low concentration, S- β -CD does interact with CBI-ser. This interaction results in enhanced separation efficiency which approaches 78,000 plates. Additionally, partial resolution of CBI-ser enantiomers is achieved with 0.2 wt % S- β -CD. The addition of 0.2 wt % KSPDM- β -CD into the BGE results in dramatic ~75% reduction in CBI-ser migration time and additionally allows for near baseline resolution of the enantiomeric pair (Figure 4.1A). The separation efficiency reaches 328,000 plates using the single isomer KSPDM- β -CD. Thus it is apparent that the single isomer sulfoalkyl derivative, KSPDM- β -CD, forms very strong interactions with CBI-amino acids at pH 2.15 which surpass that of S- β -CD, enhances separation efficiency, and through selective chiral recognition additionally allows for analysis of CBI-amino acid enantiomers at reduced concentrations of chiral selector.

The separation of a variety of CBI-amino acids under the same conditions with KSPDM- β -CD is demonstrated in Figure 4.2.

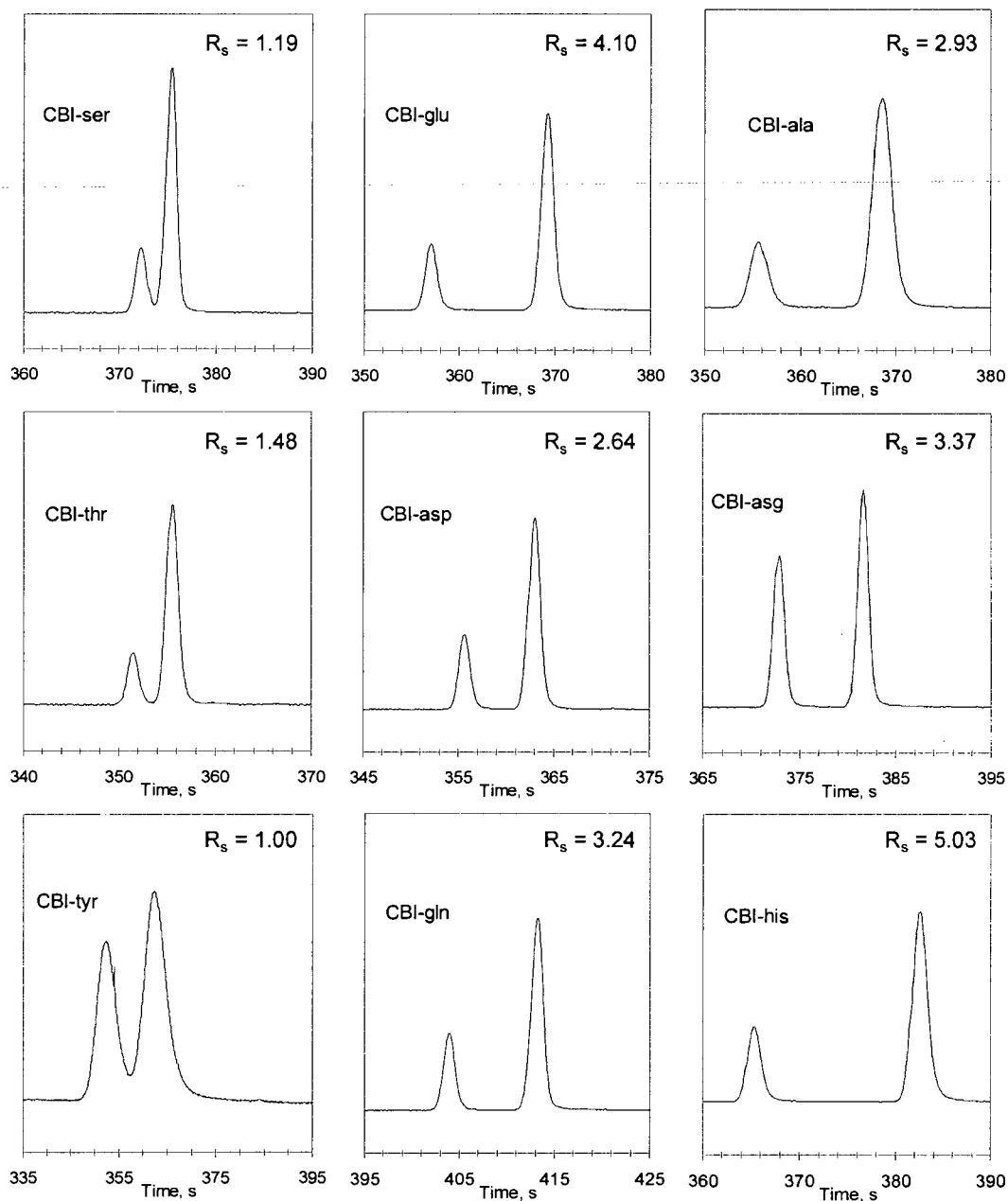


Figure 4.2. Chiral separation of 9 CBI-amino acids using KSPDM-β-CD. Conditions: 25 mM phosphate, pH 2.15 with 0.8 mM (~ 0.20 wt %) KSPDM-β-CD.

KSPDM-β-CD resolves a large number of CBI-amino acids in less than 7 min at low pH reverse polarity despite [KSPDM-β-CD] being < 1mM in the BGE. In fact, a

concentration ~10-fold less than that optimized for CBI-amino acids with S- β -CD is used here with KSPDM- β -CD. Several important conclusions can be drawn from these separations. Firstly, KSPDM- β -CD appears to be an excellent new chiral resolving agent for capillary electrophoresis which forms strong interactions with hydrophobic species like CBI-amino acids. Importantly, Figure 4.2 demonstrates that several D-amino acids of biological significance can easily be resolved with KSPDM- β -CD. This result is significant in consideration of future application of this new resolving agent for bioanalytical separations of amino acids. While separation efficiency remains high with this CD (>300,000 plates) despite low concentrations, chiral recognition is a result of enhanced selective chiral interaction rather than simply increased plate counts. However, while CBI-glu, CBI-asp, and CBI-ala are all baseline resolved, complete baseline resolution is not achieved for CBI-ser at the concentration used above ($R_s = 1.19$). An investigation of the role of concentration of KSPDM- β -CD on chiral separation of CBI-glu, CBI-asp, CBI-ala, CBI-thr, CBI-his, and CBI-ser is summarized in Figure 4.3.

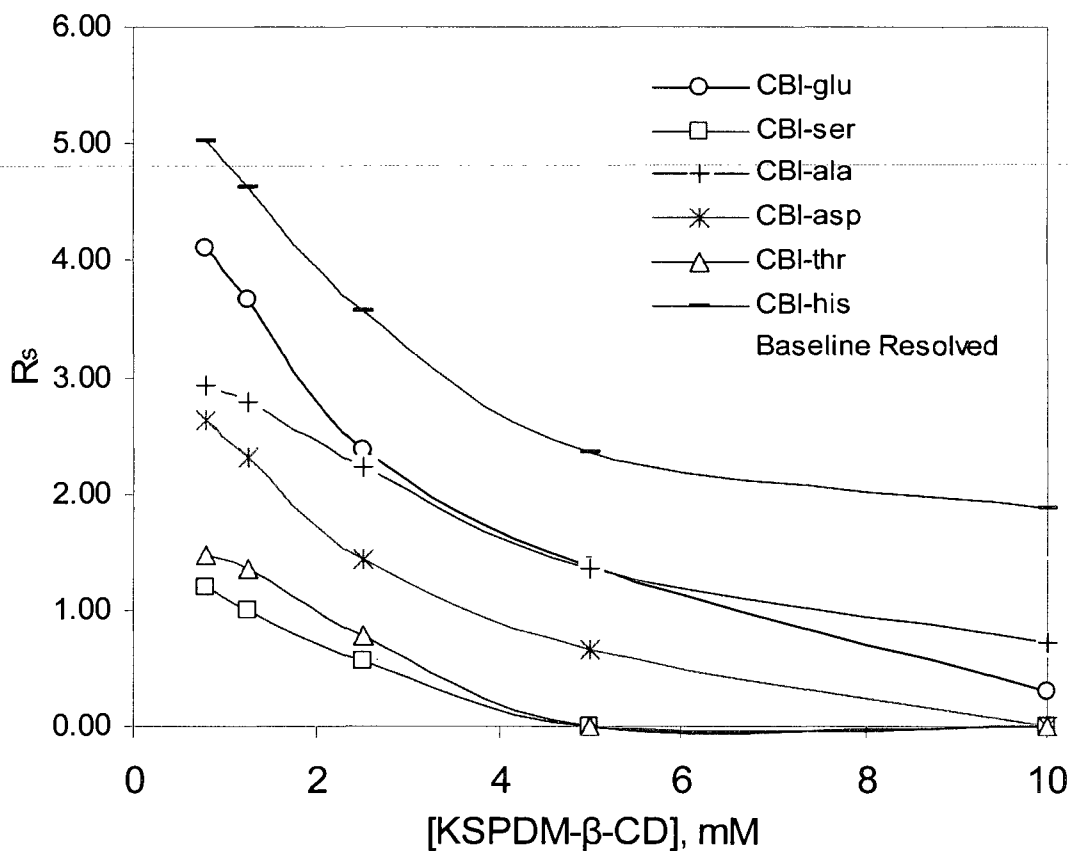


Figure 4.3. Effect of KSPDM-β-CD concentration on chiral resolution of CBI-amino acids at low pH reversed polarity.

Increasing KSPDM-β-CD concentration in the BGE beyond 0.8 mM results in decreased resolution of CBI-amino acids, in spite of a slight increase in separation efficiency (328,000 theoretical plates for CBI-ser at 0.8 mM versus 355,000 plates at 10 mM). It is apparent from the trend in this data that a chiral selector concentration below 0.8 mM may indeed continue to improve resolution of CBI-amino acids. The optimum concentration was not pursued in the current study with KSPDM-β-CD but may be between 0.1-0.8 mM for the CBI-amino acids investigated. Eventually it is expected that migration times will significantly increase with attendant peak broadening with

decreasing KSPDM- β -CD concentration, thus reducing overall resolution and separation efficiency. CBI-ser alone was investigated beyond concentrations used in Figure 4.3 and an electropherogram for the separation carried out at 0.20 mM KSPDM- β -CD is given in Figure 4.4.

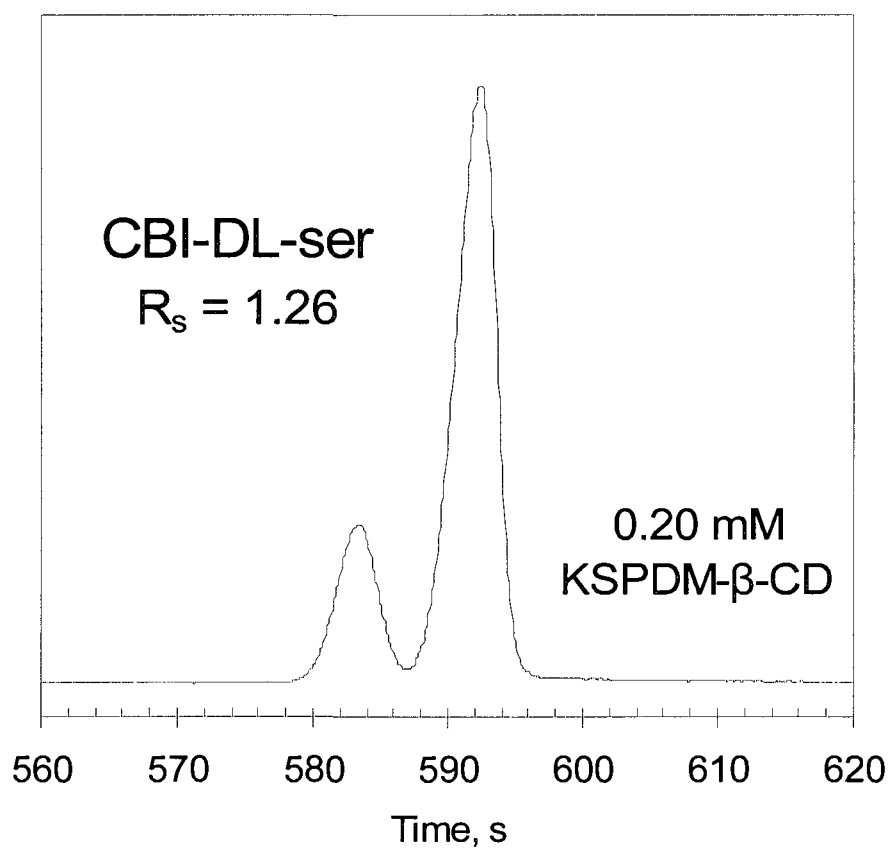


Figure 4.4. Chiral separation of CBI-ser at 0.2 mM (\sim 0.05 wt %) KSPDM- β -CD in the BGE.

A 4-fold decrease of KSPDM- β -CD from the minimum in Figure 4.3 still allows for excellent resolution of CBI-ser enantiomers in < 10 min with no loss in resolution. Indeed, CBI-DL-ser separation may be slightly better (R_s 1.26 versus 1.19) at 0.2 mM though statistical analysis of a larger data set was not examined. Either way, the migration time of CBI-ser enantiomers is increased at 0.2 mM KSPDM- β -CD (~ 588 s enantiomeric pair migration time) compared with higher concentrations (384 s enantiomeric pair migration time for 0.8 mM CD) suggesting that further decreases in chiral selector will continue to result in longer migration eventually leading to a decrease in resolution. In comparison to S- β -CD optimized in Chapter 3, the data shown here suggests CBI-ser can be resolved with KSPDM- β -CD using ~ 40 -fold reduction (~ 0.5 mg/mL versus 20 mg/mL) in mass per volume of chiral selector.

A qualitative comparison of migration times for amino acids in Figure 4.2 reveals that the cationic CBI-his does not have a unique migration time compared to other CBI-amino acids. This result is in contrast to that using S- β -CD (Chapter 2) for the cationic CBI-amino acids arginine and histidine, which form strong electrostatic interactions with S- β -CD and result in drastically reduced migration times (see Figures 2.7, 2.8, and 2.11 in Chapter 2). Indeed, it appears that, based on migration times in Figure 4.2, CBI-his does not display significant electrostatic interactions with KSPDM- β -CD. This suggests that the mechanism of chiral resolution for CBI-his is different for KSPDM- β -CD compared to S- β -CD. From a structure activity relationship, this has important implications. The sulfoalkyl groups on KSPDM- β -CD are selectively positioned on the primary face of the cavity and extend away from the CD torus by 3 methylene units.

Inclusion complex formation of CBI-amino acids with KSPDM- β -CD demonstrated by ROESY NMR (Chapter 3.5) provides evidence that the naphthalene inserts into the CD annulus from the secondary methylated face. Taken together, the data suggests that the cationic CBI-his imidazole group is too far extended from anionic sulfates during inclusion complexation to allow for any significant electrostatic interaction. In contrast, the sulfato groups of S- β -CD are positioned on both primary and secondary hydroxyl faces allowing for significant electrostatic interaction with cationic substrates. The results of future investigation on additional cationic species will have important implications in potential application of KSPDM- β -CD to chiral separation under reversed polarity of cationic drugs and metabolites which are widely analyzed with sulfato CDs (Stalcup and Gahm, 1996; Vincent et al., 1997b).

The second structural analog to KSPDM- β -CD, KSBDM- β -CD has also been investigated initially for chiral separation of CBI-amino acids and the results for the series of analytes investigated above are summarized in Figure 4.5 for 0.8 mM KSBDM- β -CD.

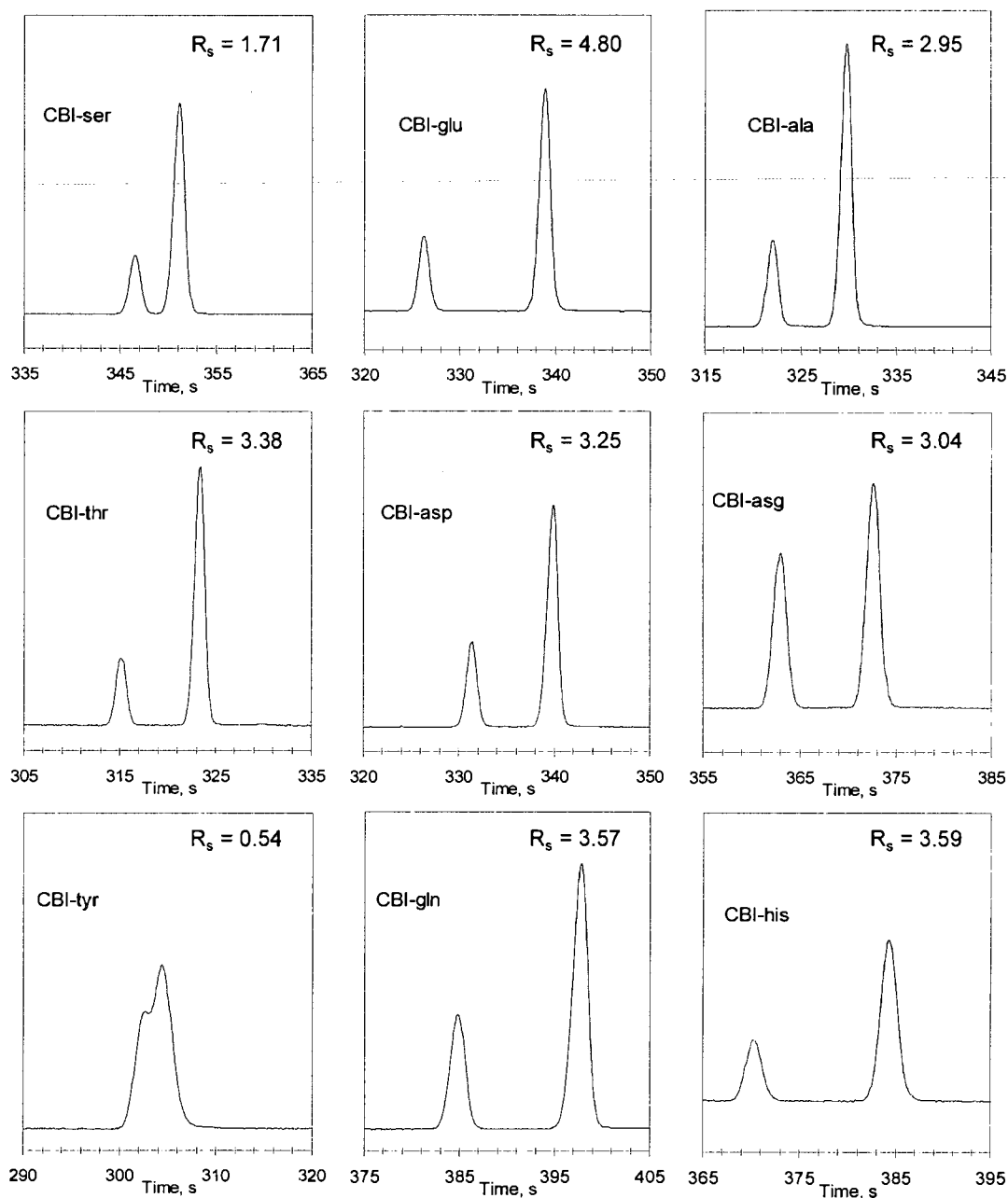


Figure 4.5. Chiral separation of 9 CBI-amino acids using KSBDM-β-CD. Conditions: 25 mM phosphate, pH 2.15 with 0.8 mM (~ 0.20 wt %) KSBDM-β-CD.

The sulfobutyl single isomer derivative is an excellent new chiral resolving agent for amino acids. In fact, KSBDM-β-CD offers significantly better resolution compared to

KSPDM- β -CD for the most biologically relevant DL-amino acids which are baseline resolved including CBI-ser (R_s 1.71 verses 1.19), CBI-glu (R_s 4.80 verses 4.10), and CBI-asp (R_s 3.25 verses 2.64) with no change in resolution of CBI-ala (R_s 2.95 verses 2.93) compared to KSPDM- β -CD. Interestingly, CBI-thr demonstrates greater than 2-fold increase in resolution with this chiral selector (R_s 3.38 verses 1.48). Furthermore, the average chiral pair migration time is significantly reduced for KSBDM- β -CD separations compared to KSPDM- β -CD for all CBI-amino acids at 0.8 mM CD except CBI-his which is unchanged. The reduced migration time suggests that a significant increase in the binding potential occurs when increasing the alkyl spacer group from sulfopropyl to sulfobutyl. This could be explained mechanistically by extension of sulfate charge density further from the CD torus with sulfobutyl CDs compared to sulfopropyl resulting in deeper penetration of the hydrophobic naphthalene group into the hydrophobic cavity. The resolution of CBI-tyr and CBI-his decreased for this CD though it is of note that CBI-his is still well resolved (R_s 3.59). Due to the near identical structural features of KSPDM- β -CD and KSBDM- β -CD, it is expected that increased KSBDM- β -CD concentration in the BGE beyond 0.8 mM will result in reduced chiral resolution as demonstrated for KSPDM- β -CD in Figure 4.3 above. Overall, it would appear that KSBDM- β -CD may be the better choice for development of a CE bioanalytical separation using charged chiral selectors that emphasizes separation of CBI-ser enantiomers since CBI-ser is well resolved.

While the concentration of KSBDM- β -CD was not investigated above 0.8 mM, the effect of reduced concentration of this chiral selector in the BGE on resolution of CBI-amino acids was deemed important to determine the minimum concentration of this new chiral selector capable of offering maximal resolution of biologically relevant amino acid enantiomers. The results are summarized in Figure 4.6 for concentrations ranging from 0.05-0.8 mM KSBDM- β -CD.

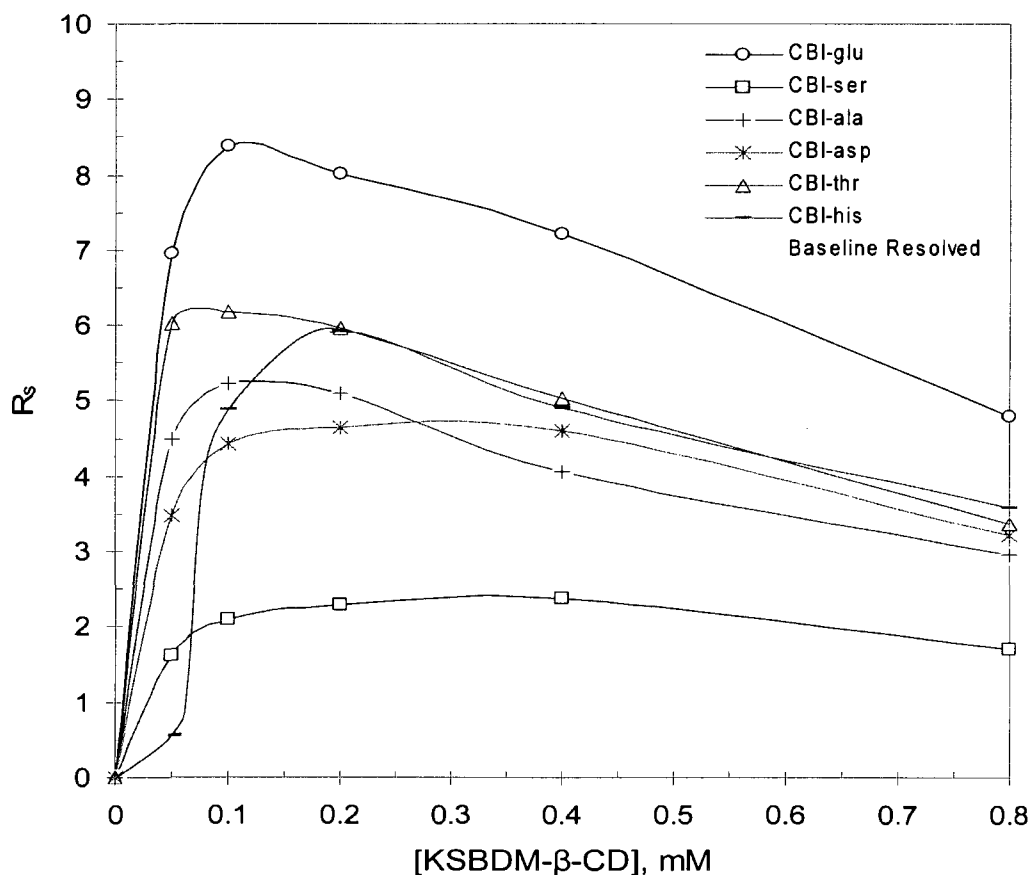


Figure 4.6. Effect of decreasing concentration of KSBDM- β -CD in the BGE on chiral resolution of CBI-amino acids at low pH reversed polarity.

Decreasing concentrations of KSBDM- β -CD below 0.8 mM results in enhanced enantioresolution of all CBI-amino acids investigated. Resolution reached a plateau for CBI-amino acid in the range of 0.10-0.40 mM CD. At concentrations of CD below \sim 0.10 mM, CBI-amino acid resolution rapidly decreases. Despite the \sim 16-fold reduction in BGE CD concentration compared to the 0.8 mM used for separations in Figure 4.5, all CBI-amino acids (except CBI-his) were baseline resolved at 50 μ M (\sim 0.013 wt %) KSBDM- β -CD in $<$ 17 min. A summary of the enhanced enantioresolution of CBI-amino acids demonstrated in Figure 4.6 is given in Table 4.1.

Table 4.1. Summary of enhanced enantioresolution of CBI-amino acids at low ($<$ 0.8 mM) concentrations of KSBDM- β -CD in the BGE.

	CBI-glu	CBI-ser	CBI-ala	CBI-asp	CBI-thr	CBI-his
% max R_s enhancement (from 0.8 mM)	74.7	40	76.9	87	83.1	65.9
R_s at optimal [KSBDM- β -CD]	8.37	2.38	5.22	4.65	6.17	5.92
[KSBDM] at max R_s , mM	0.1	0.4	0.1	0.2	0.1	0.2
D-isomer mobility at 50 μ M CD, min	15.35	15.53	14.99	13.77	14.26	34.05

All CBI-amino acids exhibit a $>$ 60 % increase in resolution when decreasing KSBDM- β -CD below 0.8 mM except CBI-ser which shows a 40 % increase. The best resolution for this series of CBI-amino acids is realized for CBI-glu enantiomers at 0.10 mM KSBDM- β -CD ($R_s = 8.37$). Despite this low concentration, CBI-D-glu has an apparent mobility of 15.35 min with 50 μ M KSBDM- β -CD, which, according to Figure 4.7 below, indicates significant interaction of KSBDM- β -CD with CBI-glu.

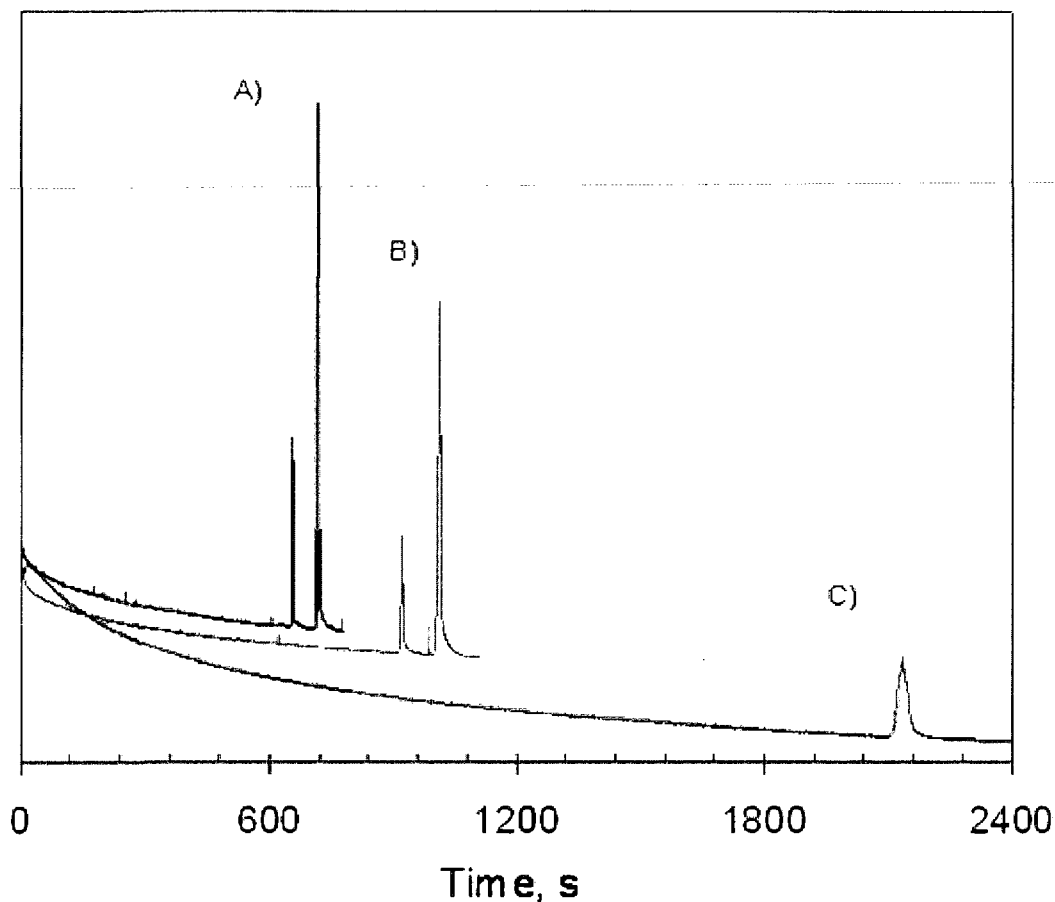


Figure 4.7. Comparison of CBI-glu enantioseparation in the presence and absence ≤ 100 μM KSBDM- β -CD in the BGE. (A) CBI-DL-glu separation with 100 μM KSBDM- β -CD; $R_s = 8.37$. (B) CBI-DL-glu separation with 50 μM KSBDM- β -CD. $R_s = 6.9$ (C) CBI-DL-glu without CD in the BGE. The comparison demonstrates that 50 μM CD dramatically alters CBI-glu mobility. Conditions: 25 mM phosphate, pH 2.15. The slight tailing for CBI-glu is an instrumental artifact caused by unequal buffer reservoirs.

A comparison of the migration time of the cationic CBI-his with the weakly acidic CBI-amino acids is shown in Figure 4.8 using 50 μM KSBDM- β -CD in the BGE.

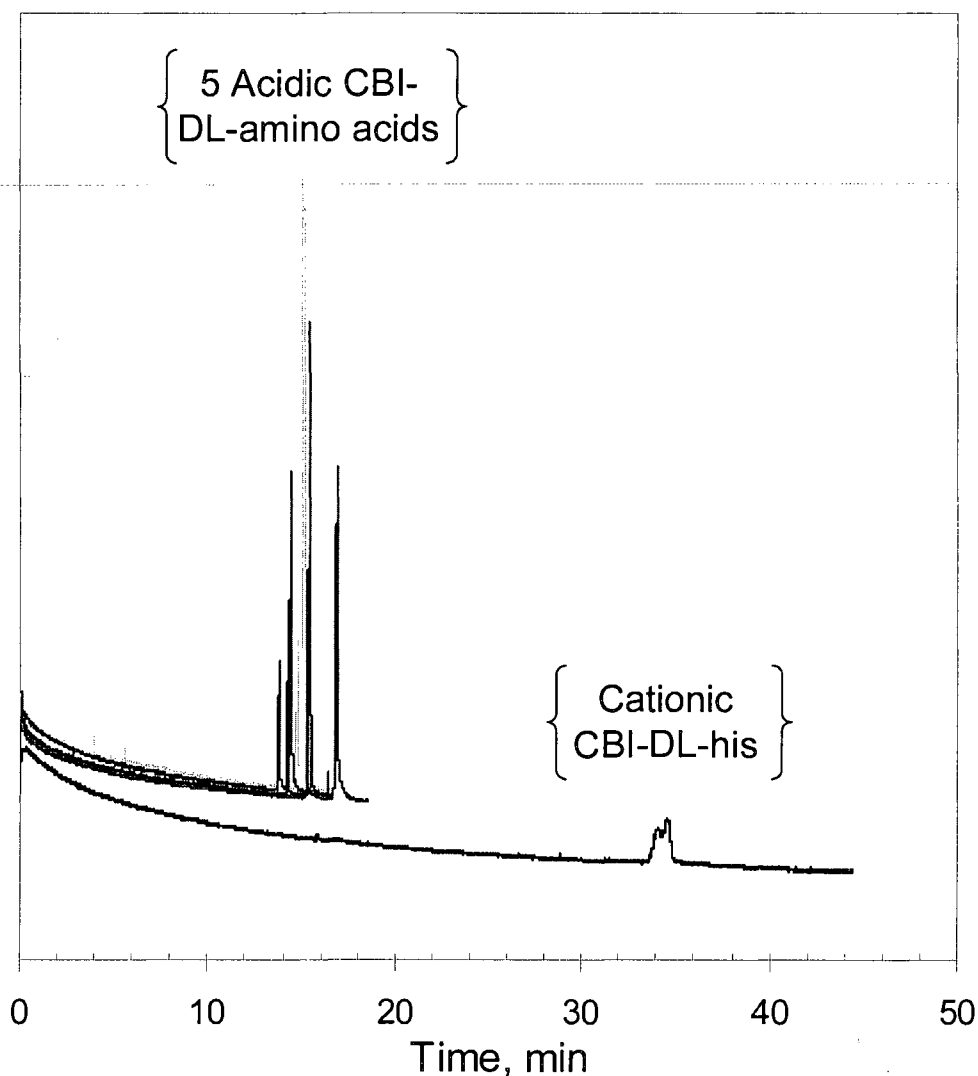


Figure 4.8. Comparison of cationic CBI-his migration time with weakly acidic anionic CBI-amino acids. BGE: 25 mM phosphate, pH 2.15 with 50 μ M KSBDM- β -CD in the BGE. For R_s values for acidic CBI-amino acids see Figure 4.6.

A \sim 2-fold difference in migration time is observed between weakly acidic CBI-amino acids and the cationic CBI-his. The cationic CBI-his has a net mobility in the absence of CD directed toward the cathode; it is likely that the longer migration time is a result of a greater proportion of free/bound CBI-his in solution. Importantly, it can be concluded

from Figure 4.8 that CBI-his does not form any significant electrostatic interaction with KSBDM- β -CD since the apparent mobility of CBI-his is greater than (Figure 4.8) or equivalent to (Figure 4.5) other derivatives which do not possess cationic functional groups capable of forming positive charge interactions. Overall, the comparison in Figure 4.8 strongly argues that electrostatic interaction between cationic analytes and the selectively modified single isomer anionic sulfobutyl CD is insignificant. Interestingly, the data presented in Figure 4.8 for KSBDM- β -CD interaction with CBI-his is nearly opposite to that presented for commercial S- β -CD in Figure 2.11 of Chapter 2 which illustrated strong electrostatic interactions between CBI-amino acids and S- β -CD.

Another important factor affecting resolution of CBI-amino acids is the BGE pH as mentioned in Chapter 2. Therein it was demonstrated that CBI-ser is significantly ionized when pH is raised from 2 to 3, leading to a loss of chiral resolution due to electrostatic repulsion with the S- β -CD. We speculated that this loss of resolution was likely due to reduced depth of penetration of the CBI-amino acid into the hydrophobic cavity of the anionic CD because of charge repulsion.

A comparison of chiral resolution of CBI-ser using 2 wt % S- β -CD and ~0.2 wt % KSBDM- β -CD in nearly identical conditions for the pH range of 2-3 is given in Figure 4.9 below.

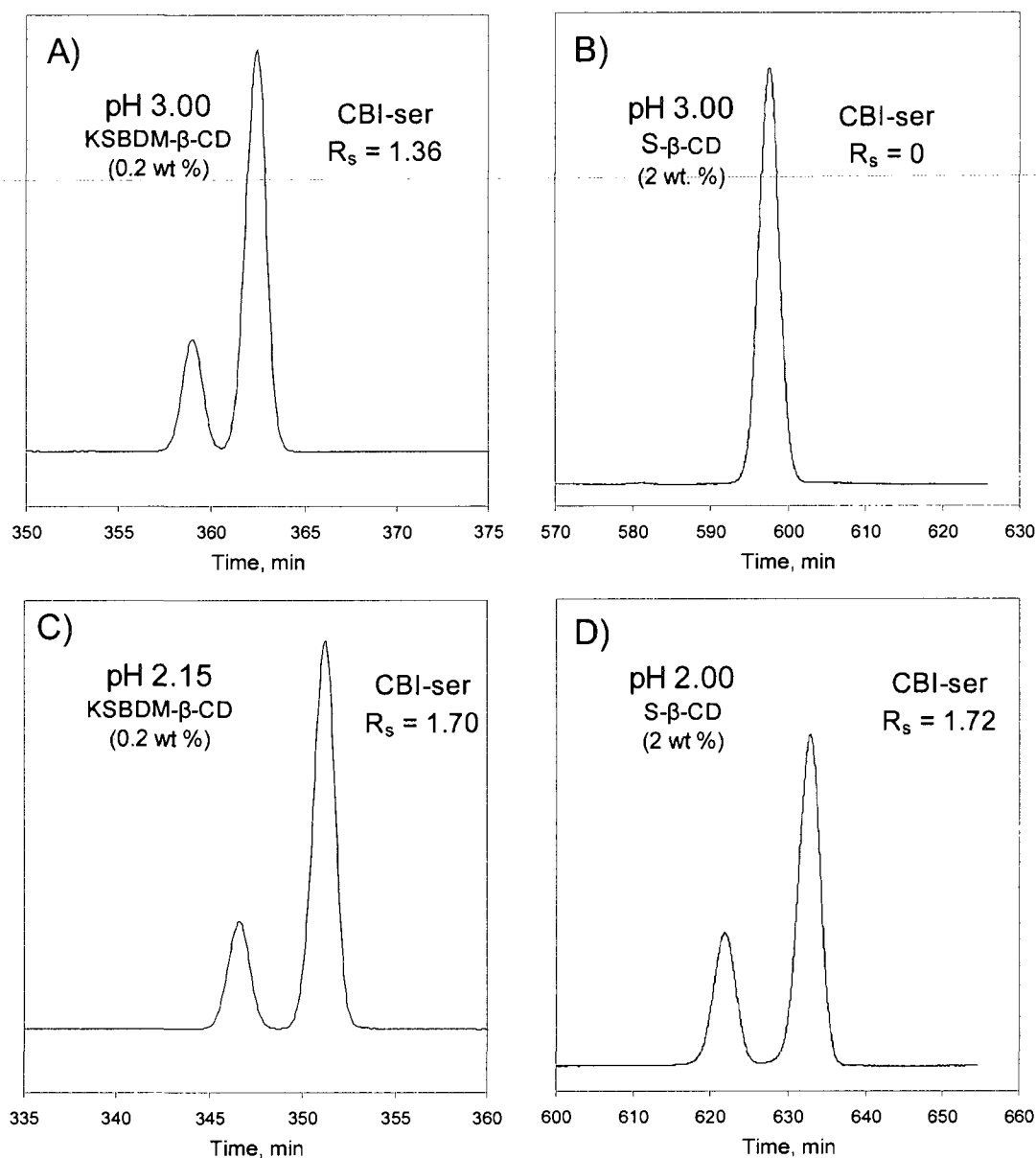


Figure 4.9. Effect of pH and anionic chiral selector on resolution of CBI-ser enantiomers. BGE is 25 mM phosphate with either 0.2 wt % KSBDM- β -CD or 2 wt % S- β -CD adjusted to pH through appropriate volume additions of equal molar NaH_2PO_4 and H_3PO_4 solutions. The separation shown in C and D are reproduced from Figure 2.3B in Chapter 2. The electric field was maintained at 430 V/cm in all separations.

As mentioned in Chapter 2, a change in the pH of the BGE from 2 to 3 for S- β -CD BGEs results in a complete loss of resolution of CBI-ser ($R_s = 1.72$ at pH 2.00, $R_s = 0$ at

pH 3.00) under reversed polarity. In comparison, a much more modest loss of chiral resolution is observed for similar pH changes with KSBDM- β -CD ($R_s = 1.70$ at pH 2.15, $R_s = 1.36$ at pH 3.00). Thus, it is apparent that chiral separation of CBI-ser with KSBDM- β -CD is much less dependent on the degree of ionization of the α -COOH of CBI-ser. From a mechanistic standpoint, and in concert with data presented above on CBI-his, this result is compelling evidence that the ionic sulfates of KSBDM- β -CD are significantly separated away from the hydrophobic CD torus such that charge interaction (positive or negative) does not dramatically alter binding affinity of guest molecules. Further studies on additional ionic guest species will be required to determine definitively if this is more or less a universal phenomenon with this new chiral selector. It is of note that the result for CBI-ser shown in Figure 4.8A,C was also reproduced in an identical experiment for CBI-glu enantiomers though, interestingly, CBI-glu enantiomers are better resolved with KSBDM- β -CD at higher pH (S- β -CD; $R_s = 3.26$ at pH 2.00, $R_s = 1.46$ at pH 3.00. KSBDM- β -CD; $R_s = 4.79$ at pH 2.15, $R_s = 5.37$ at pH 3.00).

The third single isomer sulfoalkyl β -CD derivative, KSPDE- β -CD, shows a uniquely different pattern of chiral recognition compared with the above di-O-methyl derivatives as shown in Figure 4.10 for the separation of a series of CBI-amino acids at 0.80 mM KSPDE- β -CD in the BGE.

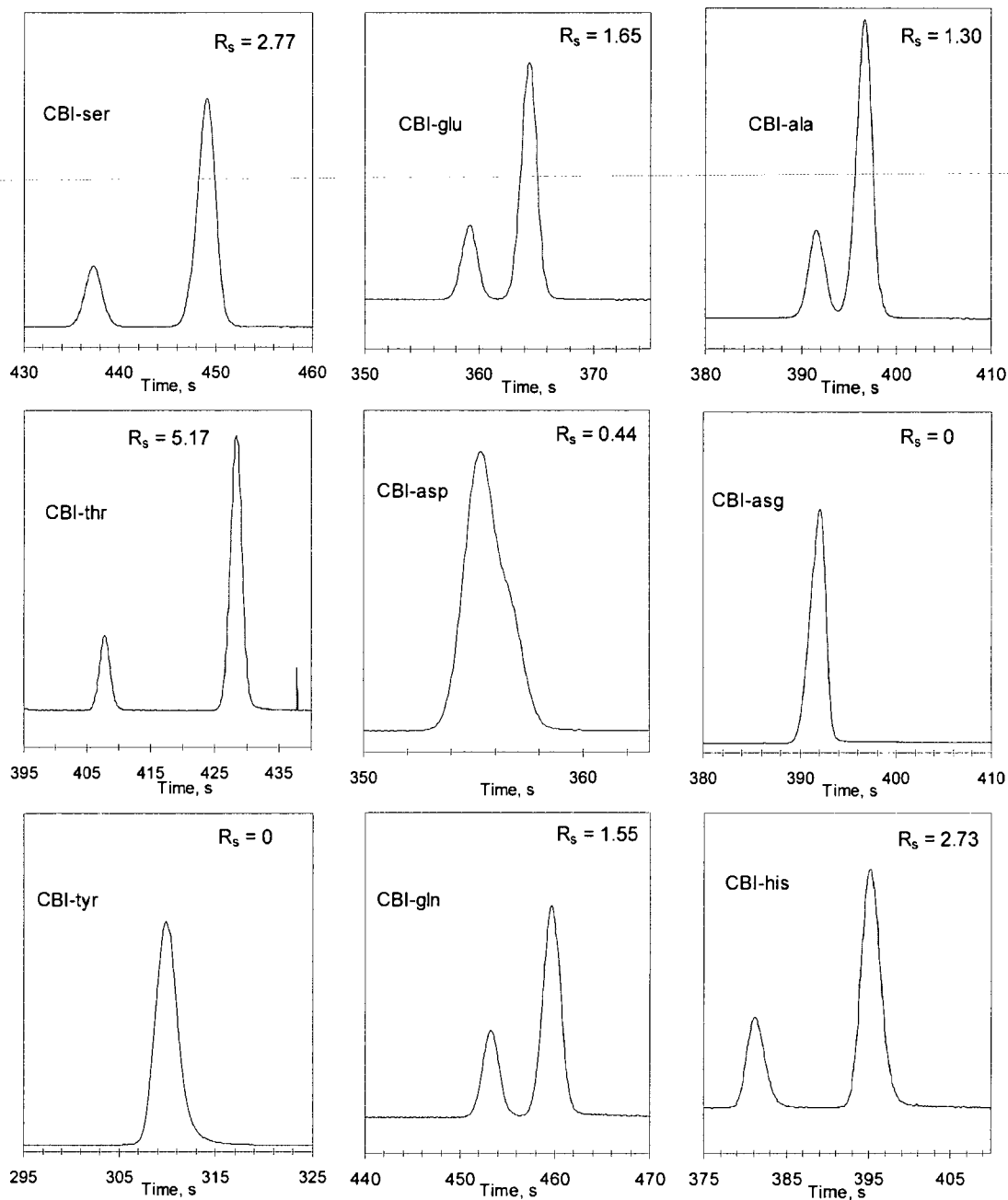


Figure 4.10. Chiral separation of 9 CBI-amino acids using KSPDE-β-CD. Conditions: 25 mM phosphate, pH 2.15 with 0.8 mM (~ 0.20 wt %) KSPDE-β-CD.

KSPDE-β-CD is the best resolving agent of this series of derivatives at 0.8 mM CD for CBI-ser and CBI-thr with resolution values of 2.77 and 5.17 respectively. This suggests

that this chiral selector would be a complimentary choice to KSBDM- β -CD for development of bioanalytical separation of CBI-ser enantiomers in this concentration range. Since it is a structural analog of KSBDM- β -CD, it is possible to speculate (see Figure 4.6) that CBI-ser and CBI-thr resolution may continue to increase with decreasing KSPDE- β -CD concentration though future studies will be required for validate this proposed similarity. Interestingly, the selectivity of this chiral selector is quite different from other CDs developed here. In fact, resolution of CBI-asp and its amide analog CBI-asp, as well as CBI-glu and its amide analog CBI-gln, is significantly diminished with KSPDE- β -CD at 0.8 mM compared with KSPDM- β -CD (Figure 4.2) and KSBDM- β -CD (Figure 4.5) which were both excellent resolving agents for these derivatives. An explanation for the loss of resolution and significant difference in chiral recognition may require a combination of molecular modeling and NMR binding studies. One of the advantages of this single isomer CD is that such future studies can be carried out which would be impossible with heterogeneous CDs such as S- β -CD due to their complex isomeric nature. The 2-D ROESY NMR approach using conditions that mimic the electrophoresis BGE may be valuable for determining a change in orientation and binding of the CBI-amino acids with KSPDE- β -CD. For example, CBI-glu and CBI-asp differ by one methylene unit, and a comparison of chiral separation of these amino acids using 5.0 mM KSPDE- β -CD presents some striking differences in binding interactions with this CD (Figure 4.11).

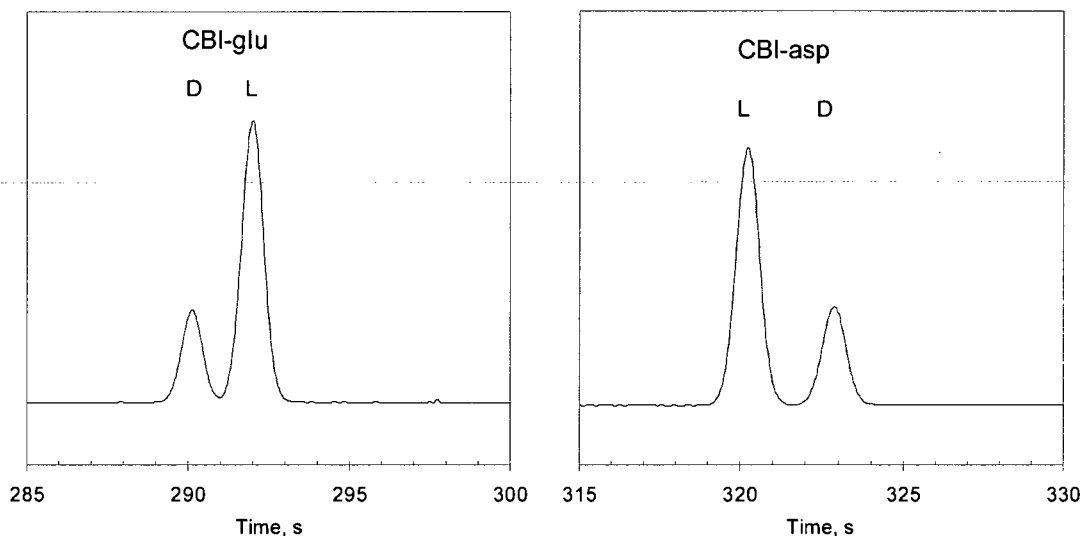


Figure 4.11. Comparison of chiral separation of CBI-glu and CBI-asp at pH 2.15 with 5.0 mM KSPDE- β -CD in the BGE.

For the chiral pair, KSPDE- β -CD interacts more strongly with the D-isomer of CBI-glu resulting in faster migration of this enantiomer. This is the typical migration order result observed for interactions of CBI-amino acids with KSBDM- β -CD and KSPDM- β -CD. In contrast, however, the D-isomer of CBI-asp has a longer migration time than its L-enantiomer, suggesting a weaker interaction. In fact, while CBI-glu resolution increases with decreasing KSPDE- β -CD ($R_s = 1.23$ at 5.0 mM, $R_s = 1.65$ at 0.8 mM), the opposite is true for CBI-asp ($R_s = 1.61$ at 5.0 mM, $R_s = 0.44$ at 0.8 mM). Furthermore, this suggests that ethyl groups on the secondary rim which possibly alter cavity size play a uniquely different functional role in chiral selectivity than methyl derivatives.

The order of elution of the respective enantiomers of CBI-glu and CBI-asp using KSPDE- β -CD, as shown in Figure 4.11, is exactly opposite that observed using S- β -CD (Chapter 2). A mechanistic understanding of this is presently lacking, and further studies are required. However, recall that S- β -CD is a mixture of many positional and regional isomers with a range of substitution due to nonselective synthesis. This heterogeneity greatly complicates any mechanistic understanding of the fundamental interactions responsible for change in binding order. In contrast, KSBDM- β -CD is well characterized and intricate investigations on inclusion complexes and binding potentials could more easily reveal information pertinent to understanding these fundamental interactions.

A reversal of enantiomer migration order (EMO) was observed for CBI-ala dependent on concentration of KSPDE- β -CD in the BGE as shown in Figure 4.12.

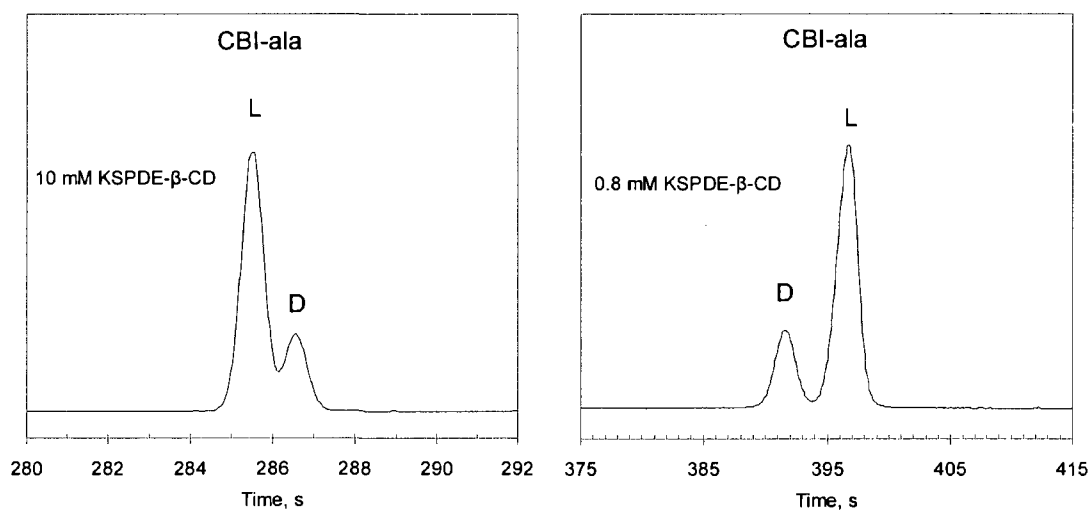


Figure 4.12. Reversal of EMO for 22:78 CBI-ala dependent on concentration of KSPDE- β -CD in the BGE.

CBI-ala is partially resolved at 10 mM KSPDE- β -CD with the L-enantiomer migrating first. Lowering the concentration to 0.8 mM results in complete reversal of migration order with near baseline resolution of CBI-ala. To account for this change in EMO there must be a concentration dependent change in the nature of the inclusion complex formed.

Rizzi and Kremser have investigated complexation induced reversal of EMO of dansylated amino acids (DNS-amino acids) dependent on the concentration of chiral selector (Rizzi and Kremser, 1999). While they suggest this observation to be an uncommon event, they provide compelling evidence that when the pH of the BGE approaches the pK_a range of some analytes (as occurs herein), a possibility exists for complex induced alteration of the pK_a (and thus charge and net mobility) of the guest species simply by altering the chiral selector concentration. Thus, rather than a change in strength of interaction for each enantiomer with the CD host resulting in differential migration times of enantiomers, there can be a change in the ionization of the guest resulting in enhanced electromigration of one enantiomer over the other. Rizzi and colleagues demonstrate that enantiomer migration order for DNS-phe and DNS-trp is dependent on the concentration of HP- β -CD in the BGE and rationalized this data by evidence demonstrating that one weakly acidic enantiomer exhibits a greater complexation induced pK_a shift than the other, resulting in a change of electrophoretic mobility of the enantiomer independent of differences in binding affinity.

The data provided by Rizzi et al. would argue that CBI-ala enantiomers studied herein exhibit a KSPDE- β -CD concentration dependent alteration in pK_a during complexation

resulting in the observed reversal of migration order. The determination of binding affinities of CBI-ala enantiomers with KSPDE- β -CD as well as any complex induced pK_a alterations under the current separation conditions will be required in future studies to verify the proposed mechanism of EMO reversal. Furthermore, the dimethyl CD derivatives (KSPDM- β -CD, KSBDM- β -CD) did not exhibit any concentration dependent reversal of EMO when resolving amino acids at the concentrations investigated. It is of note that the concentrations of single isomer sulfoalkyl CDs used in the experiments above did not exceed 10 mM. An investigation of higher CD concentrations in the BGE for all three of these derivatives may reveal complexation induced pK_a changes for additional amino acids which are not observed in the limited range studied here. This will verify whether this effect can be achieved with selectively modified sulfoalkyl CDs bearing methyl groups on the secondary rim. Studies by the Vigh group with single isomer sulfato CDs at low pH typically investigate sulfato CD concentrations as high as 50 mM in the BGE (Cai et al., 1998). Similar high levels should be studied in future experiments with single isomer sulfoalkyl CDs.

4.4 Summary of enantioselectivity for KSPDM- β -CD, KSBDM- β -CD, and KSPDE- β -CD

Single isomer sulfoalkyl β -CD derivatives form inclusion complexes with CBI-amino acids and were found to be excellent new chiral resolving agents for a series of CBI-amino acids at low pH reversed polarity. Biologically significant DL-amino acids including CBI-ser, CBI-glu, CBI-ala, and CBI-asp could be baseline resolved with these

chiral selectors. KSPDM- β -CD, KSBDM- β -CD, and KSPDE- β -CD form strong inclusion complexes with CBI-amino acids demonstrated by enhanced apparent mobility of CBI-amino acids which dramatically surpasses that of S- β -CD and allows for chiral analysis at much lower concentrations. Single isomer sulfoalkyl CDs do not form significant electrostatic interactions, either attractive or repulsive, with CBI-amino acids as demonstrated by comparison of mobility of cationic and anionic CBI-amino acids, and also by comparison of pH effects with these selectors. In addition, different selectivity is observed for these CDs with various chiral guests. KSBDM- β -CD and KSPDE- β -CD are the best resolving agents for CBI-ser enantiomers. While the dimethyl derivatives offer similar selectivity for biologically important amino acids (though sulfobutyl derivatives are superior in this respect), the selectivity was found to be quite different for KSPDE- β -CD. A KSPDE- β -CD concentration dependent reversal of EMO was observed for CBI-ala that may be the result of complex induced alteration in the pK_a .

Chapter 5

Simultaneous efflux of endogenous D-ser and L-glu from single acute hippocampus slices during oxygen glucose deprivation

5.1 Overview of study

Stroke is the third leading cause of death in the United States and the leading cause of adult long term disability (Rosamond et al., 2008). Much of the resulting brain damage caused by stroke is due to a cascade of excitotoxic events which occur as a result of insufficient blood supply to the brain. Similar excitotoxicity is responsible for much of the high morbidity and mortality in patients suffering from post cardiac arrest syndrome (Neumar et al., 2008). In the central nervous system (CNS), the excitotoxic cascade is initiated by the onset of energy deficit, which forces cell depolarization and subsequent neurotransmitter release. High levels of L-glu, the dominant excitatory neurotransmitter in the CNS, efflux from neurons and glia, resulting in excitotoxicity (Lipton, 1999). The N-methyl-D-aspartate receptor (NMDAR) is a glutamatergic ligand gated calcium/sodium ion channel that is responsible for the majority of excitotoxic cell death that occurs as a result of L-glu released during cerebral ischemia (Arundine and Tymianski, 2004).

The NMDAR is unique among neurotransmitter receptors in its requirement for coagonist activation (Kleckner and Dingledine, 1988; Curras and Pallotta, 1996). D-ser, an endogenous amino acid, is synthesized and released from neurons (Kartvelishvily et al., 2006) and glia (Oliet and Mothet, 2006) and is co-localized in brain regions having

high concentrations of NMDAR. D-ser binds with high nanomolar affinity to the strychnine insensitive binding domain (coagonist site, “glycine site”) on the obligatory NR1 subunit of the NMDAR. Recent evidence implicates D-ser as the essential coagonist of NMDA receptor-induced neurotoxicity in several brain regions (Katsuki et al., 2004; Shleper et al., 2005).

L-glu is released rapidly within the first few minutes of cerebral ischemia *in vivo* and *in vitro* suggesting it is an early event in the neuroxic cascade. Simultaneous efflux of D-ser would be necessary for excitotoxicity via NMDAR activation but little is known about the early time course of D-ser release. Lo and colleagues quantified several transmitters including D-ser during 2h focal ischemia with 10 min temporal resolution *in vivo* (Lo et al., 1998). In Chapter 2 of this dissertation the development of a sensitive enantioselective capillary electrophoresis laser induced fluorescence (CE-LIF) technique to assay D-ser, L-glu, and several other amino acids in biological samples using charged chiral selectors is described (Kirschner et al., 2007). The focus of this dissertation research was to couple the CE-LIF approach to a newly-designed *in vitro* microperfusion device described herein that would allow for more rapid monitoring of dynamic changes in D-ser and L-glu efflux from single acute hippocampus slices in response to modeled ischemia. Here we (Kirschner et al., 2009) apply our microperfusion technique to study L-glu and D-ser temporal response with 2 min sampling during oxygen glucose deprivation (OGD), an *in vitro* model of cerebral ischemia. Using the microperfusion/CE-LIF technique, we demonstrate parallel increases in D-ser and L-glu

efflux during OGD. To our knowledge, our data represents the fastest temporal resolution of endogenous D-ser efflux during modeled cerebral ischemia.

5.2. Methods

5.2.1 General

All chemicals were purchased from Aldrich Chemical Company unless otherwise noted. Sulfated β -cyclodextrin was purchased from Fluka (Lot# 1148973) and is the same lot as optimized for separation described in Chapter 2. Naphthalene-2,3-dicarboxaldehyde was obtained from Invitrogen. Buffers and reagents were prepared regularly every 1-2 weeks and stored at 4°C when not in use. Microchambers were soaked and perfusion tubing flushed for 1hr with 70% ethanol prior to each experiment.

5.2.2 Microperfusion chamber

Acute slice chambers were constructed in-house at the University of Alaska Fairbanks Engineering machine shop (Figure 5.1A-D).

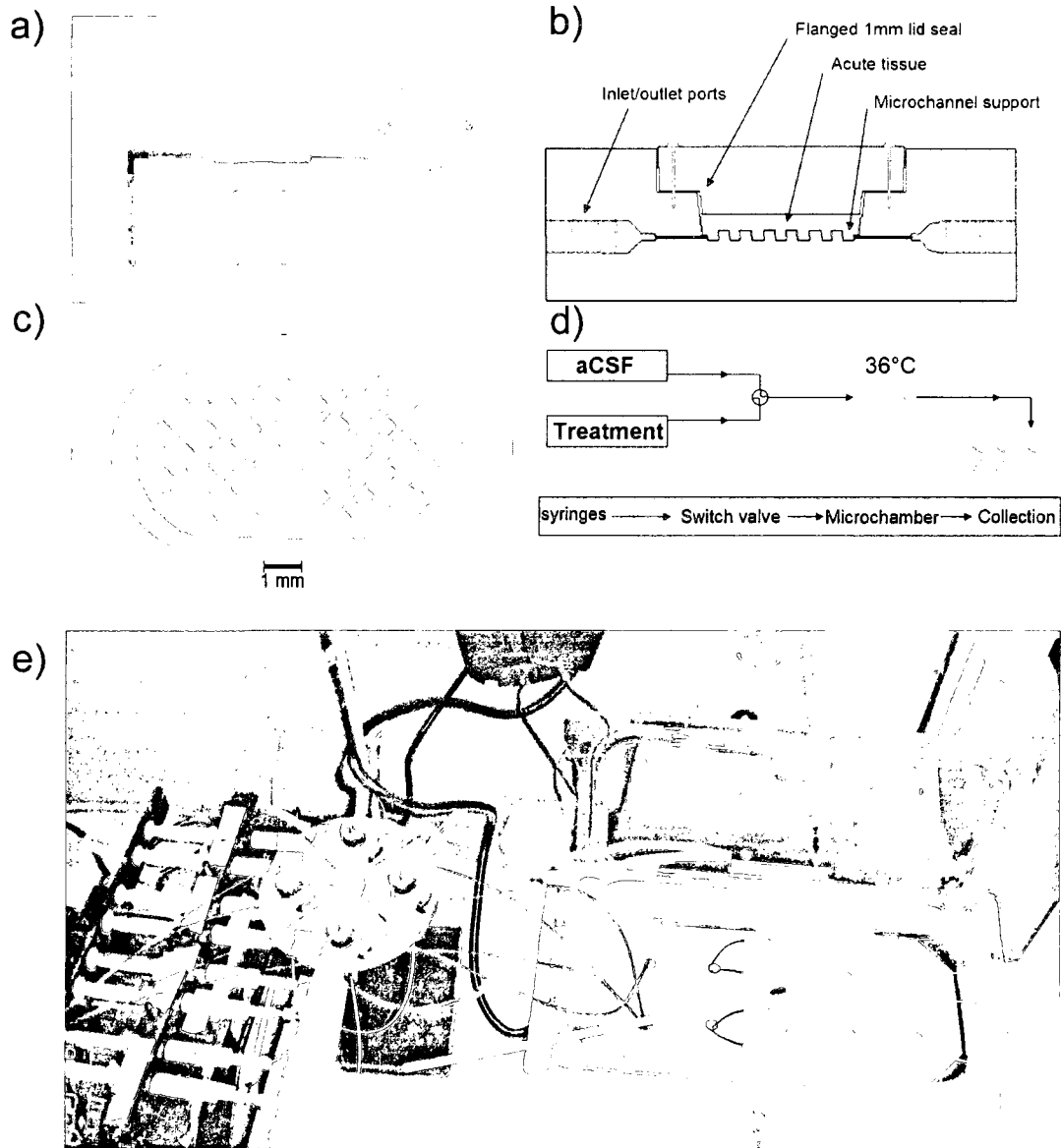


Figure 5.1. Custom Microperfusion chamber for single acute brain slices. (A) polycarbonate microperfusion chamber, (B) schematic diagram of major components of microchamber (actual chamber dimensions LxWxH ~9x5x0.7mm with additional 0.3 mm deep microchannel support), (C) magnification of microchamber well illustrating microchannel support designed to increase fluid flow around slice, (D) schematic of microperfusion setup from syringe pump to fraction collection, (E) actual instrument setup showing (from left to right) syringe pump, switching valve manifold, warming bath with sealed microchambers, and outlet tubing. The 150 mm thermometer is shown to illustrate chamber size and was not used for absolute determination of temperature

during experiments. Temperature was maintained by the proportional integral derivative (PID) controller built into the digital water bath (± 0.2 °C at 37 °C).

The chambers were machined from polycarbonate and incorporate a beveled leak-free lid and chamber body. The chamber body houses inlet and outlet ports connected via a small channel to an oval 2mm deep recessed, microchamber (dimensions $\sim 9 \times 5$ mm) specifically designed to accommodate 400 μm thick acute hippocampus slices from rats. The microchambers were engineered with a microchannel support in the well bottom to increase fluid exchange around the acute tissue preparation. The microchannels were machined ~ 400 μm wide, 300 μm deep in a waffle pattern shown in Figure 5.1c. A polycarbonate lid was machined with a 1 mm deep beveled oval flange to form a watertight (O-ring free) seal with the chamber body. This design yields a sealed chamber 700 μm deep with an additional 300 μm microchannel support. The sealed chamber has an estimated volume of ~ 35 μL without tissue in place. The lid is secured to the base using 4 stainless screws. Four chambers were mounted in parallel to a stainless steel tray submerged in a thermistor-controlled StableTemp water bath (Cole Parmer Instrument Company, Vernon Hills, Illinois, USA) kept at a constant temperature. All connections were made using 1/16-in O.D. 100 μm I.D. PEEK tubing with flanged fittings (outlet port used 150 μm I.D. PEEK tubing). Perfusion medium for each chamber was administered via a 10-stage syringe pump (Harvard Apparatus, Holliston, MA, USA), with medium passing first through a 4-port diagonal flow switching valve (#V101D, Upchurch Scientific, Oak Harbor, WA, USA) for administering treatments, before entering the water bath where it was preheated prior to

passing through the microchamber inlets. The chamber outlet tubing exited the water bath where samples were manually collected dropwise.

5.2.3 Acute hippocampus slices

Adult Male Sprague Dawley rats (Simonson labs, Gilroy, CA; age 3-4 months, 250-400g) were used for all experiments. Procedures were in accordance with The Institutional Animal Care and Use Committee of the University of Alaska Fairbanks. Transverse 400 μm acute hippocampus slices were prepared as follows. Rapidly dissected hippocampi were embedded in agar and sliced using a Vibratome 1000 plus sectioning system (The Vibratome Company, St. Louis, Missouri, USA). Slicing was performed at $\sim 2^{\circ}\text{C}$ in oxygenated HEPES buffered artificial cerebral spinal fluid (HEPES aCSF containing in mM: 120 NaCl, 20 NaHCO_3 , 6.88 HEPES acid, 3.3 HEPES sodium salt, 5.0 KCl, 2.0 MgSO_4 (pH 7.30-7.40)). Slices were transferred from HEPES buffered aCSF to a Brain Slice Keeper (Scientific Systems Design Inc, Mississauga, Ontario, CA) and allowed to recover in oxygenated aCSF (aCSF continuously bubbled with 95% O_2 , 5% CO_2 containing in mM: 120 NaCl, 25 NaHCO_3 , 10 glucose, 3.3 KCl, 1.2 NaH_2PO_4 , 2.4 MgSO_4 , 1.8 CaCl_2 , pH 7.30-7.40) for 1 h at room temperature prior to placement in individual microchambers. Slices were then transferred individually to chambers and lids sealed. The apparatus containing 4 parallel chambers was submerged in a bath at 36°C ($\pm 0.2^{\circ}\text{C}$) and acute slices were perfused at a flow rate of 7 μL /min. Sampling began 20 min after submerging the sealed chambers to allow adequate time for stabilization of neurochemical efflux. Perfusate was collected at 2 min intervals during

pre-treatment (basal), treatment, and the first 20 min of reperfusion. After 20 min reperfusion, samples were collected every 3 min. Treatment consisted of a 24 min exposure to oxygen glucose deprivation (OGD) solution (glucose-free aCSF equilibrated with 95% N₂ 5% CO₂ for a minimum of 1 h until pH stabilized in the range of 7.3-7.4). The PO₂ in OGD solution varied from 0-2.9 mmHg with an average for 6 determinations of 1.1 mmHg as measured using a miniature Clark-style electrode (Instech Laboratories, Plymouth Meeting, PA, USA). In control slices treatment was administered by switching to standard aCSF. Collected fractions were kept at -80 °C until they were analyzed by chiral CE-LIF.

5.2.4 CE-LIF analysis

Perfusate was derivatized with slight modification to the procedure described previously in Section 2.25 of Chapter 2 to form highly fluorescent CBI-amino acids. Briefly, 1 µL thawed perfusate was reacted with 1 µL 2 mM naphthalene-2,3-dicarboxaldehyde (NDA) in methanol and 1 µL NaCN (5.5 mM) in 60 mM sodium tetraborate. Cyanide solution contained 3 µM D-amino adipic acid as internal standard (IS) which was superior to L-homoarginine as IS due to its similar migration time to quantified amino acids (*vida infra*). Samples were reacted at room temperature for 20 min prior to analysis. CE-LIF was performed on a custom in-house built instrument as described in Section 2.2 of Chapter 2. Samples were injected onto a bare fused silica capillary of dimensions 48 x 45 cm x 25 µm for 1s at 380 mbar vacuum, and separated using negative polarity (-21 kV). Separation buffer optimized for analysis of D-ser and L-glu

is a 25 mM phosphate background electrolyte (BGE) adjusted to pH 2.15 using equal molar additions of H_3PO_4 and NaH_2PO_4 . BGE additionally contained 20 g/L (2 wt %) S- β -CD as chiral selector. PeakFit[®] software was used to process raw data and quantify peak areas in all experiments based on a Gaussian peak shape for each analyte. Linear calibration curves were constructed for analytes as a function of concentration versus the peak area ratio (analyte area / Internal Standard area). Efflux of analytes is expressed as percent of baseline, where baseline is defined as the average value of 10 samples collected prior to onset of treatment, a period of sampling in which analyte levels were stable.

5.2.5 Monitoring treatment profile

Monitoring actual treatment exposure is critical for precise timing of transmitter efflux. The actual treatment exposure time in perfusion experiments is influenced by multiple of factors including flow rate, chamber dimensions, lag time between pump and chamber, and lag time between chamber and sample collection and properties of flow within the chamber. Flow profile was monitored using different concentrations of D-glu as a marker of aCSF and OGD solutions. D-glu was conveniently quantified with endogenous amino acids in our chiral CE-LIF preparation which utilizes the remarkable chiral resolving properties of S- β -CD. D-glu does not have any known biological roles in the CNS, and is reportedly found in only trace levels in a few brain regions (Quan and Liu, 2003; Mangas et al., 2007). In our preparations, we detected no D-glu in

hippocampus slice perfusates. We therefore used 0.5 μM D-glu in aCSF solutions and 3.0 μM D-glu in treatment solutions.

5.2.6 Statistics

Data was analyzed using SAS[®] v9.1 software (SAS Institute Inc., Cary, NC, USA) by 2-way ANOVA with treatment analyzed as a between subjects variable and time analyzed as a repeated measures variable. Tukey post-hoc comparisons were used to compare OGD and control groups at specific time points. Significance was indicated by $p < 0.05$. Data are shown as mean \pm standard error mean (SEM).

5.3 Results

An optimized narrow pH range of 2.15-2.20 for the CE-LIF run buffer with 2 wt % S- β -CD allowed for baseline separation of D-ser, L-glu, L-asp, and L-gln CBI-amino acids as shown in Figure 5.2 in addition to an internal standard D-amino adipic acid.

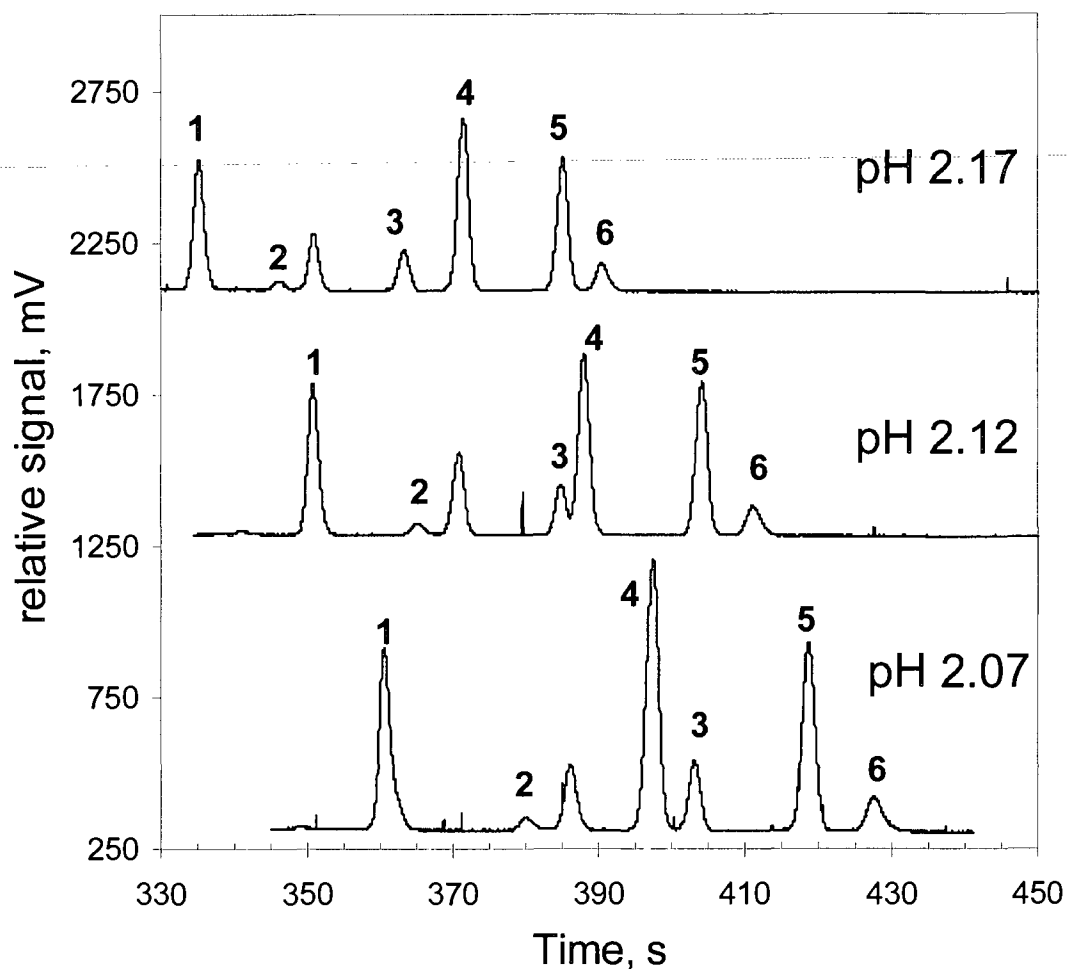


Figure 5.2. Impact of narrow pH range on migration order and run time for CBI-amino acids for bioanalysis with S- β -CD. Peak identities for CBI-amino acid standards: (1) CBI-L-gln; (2) CBI-D-ser; (3) CBI-L-asp; (4) CBI-D-amino adipic acid; (5) CBI-L-asp; (6) CBI-L-glu; (6) CBI-L-thr. Conditions: 25 mM phosphate with 2 wt % S- β -CD.

Exogenously applied D-glu partially overlapped with L-thr. The partial overlap of L-thr and D-glu was resolved using Gaussian peak fitting software (PeakFit[®] v4.12, SeaSolve Software Inc., Framingham, MA, USA).

Calibration curves using a weighted least squares linear regression for CBI-amino acids were obtained and the equations, R^2 values, linear dynamic range

investigated, and estimated concentration limits of detection (CLOD) for each analyte are given in Table 5.1. Larger dynamic ranges were calibrated for L-glu, L-asp and L-gln compared to other CBI-amino acids since preliminary results suggested these transmitters could fluctuate markedly during treatment with OGD.

Table 5.1. Linear regression results for concentration determinations of amino acids in perfusate medium. Shown are weighted standard curve equations ($y = mx + b$; CBI-AA/internal standard = $m[\text{CBI-AA}] + b$), square of correlation coefficient (R^2), calibrated range, and estimated CLOD. Curves were generated from weighted linear regression of ≥ 6 standard solutions with $N=5$ for each standard. *CLOD calculated from response of a low-concentration standard ($N=5$) assuming $S/N = 3$.

Analyte	Equation	R^2	Calibrated range, μM	CLOD*, nM
L-glu	$y = 0.388x - 0.032$	0.997	0-63.0	14.7 ± 3.8
L-asp	$y = 0.308x + 0.002$	0.999	0-25.2	16.0 ± 2.1
D-ser	$y = 0.260x - 0.001$	0.9961	0-1.80	19.3 ± 4.4
L-thr	$y = 0.247x - 0.005$	0.9995	0-7.20	26.2 ± 8.8
L-gln	$y = 0.357x - 0.031$	0.9968	0-36.0	12.5 ± 1.5

A stepwise change in D-glu produced a 6-fold higher concentration of D-glu in treatment compared to aCSF. The resultant profile was used to establish the timing of OGD treatment (Figure 5.3). D-glu profiles were conveniently quantified by CE-LIF which chirally resolves exogenous D-glu from endogenous L-glu in perfusate samples.

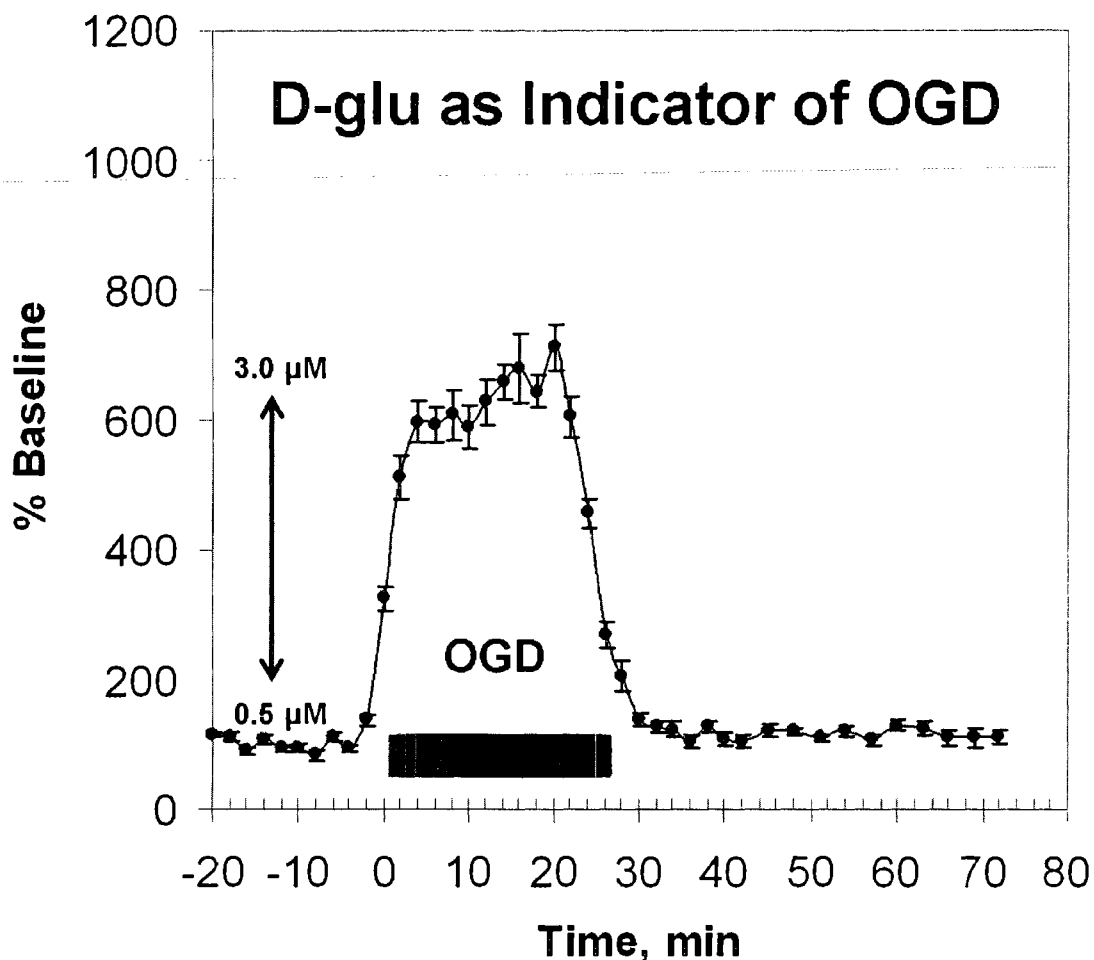


Figure 5.3. OGD treatment profile determined using trace D-glu perfusion across slices. A stepwise change in D-glu levels ($0.5 \mu\text{M}$ switched to $3.0 \mu\text{M}$) occurs in ~ 4.5 min which establishes the turnover rate of the microchamber and allows for precise monitoring of the treatment profile. A 24 min OGD exposure is equivalent at the reported perfusion flow rate to ~ 20 min of 100% OGD (based on time D-glu response is at maximal level) and 24 min of $\geq 80\%$ OGD solution, $n = 8$ slices.

OGD induced a significant increase in all amino acids investigated except L-gln as demonstrated by a comparison of CE electropherograms of basal and OGD perfusates (Figure 5.4). Average basal concentrations of analytes in slice perfusates, including both control ($n = 5$) and OGD ($n = 8$) slices, are as follows: D-ser ($0.34 \pm 0.03 \mu\text{M}$ OGD, 0.34

$\pm 0.03 \mu\text{M}$ CTL), L-glu ($0.93 \pm 0.19 \mu\text{M}$ OGD, $1.07 \pm 0.18 \mu\text{M}$ CTL), L-asp ($0.66 \pm 0.20 \mu\text{M}$ OGD, $0.80 \pm 0.15 \mu\text{M}$ CTL), L-gln ($10.68 \pm 1.20 \mu\text{M}$ OGD, $9.83 \pm 0.74 \mu\text{M}$ CTL), L-thr ($1.64 \pm 0.14 \mu\text{M}$ OGD, $2.00 \pm 0.21 \mu\text{M}$ CTL).

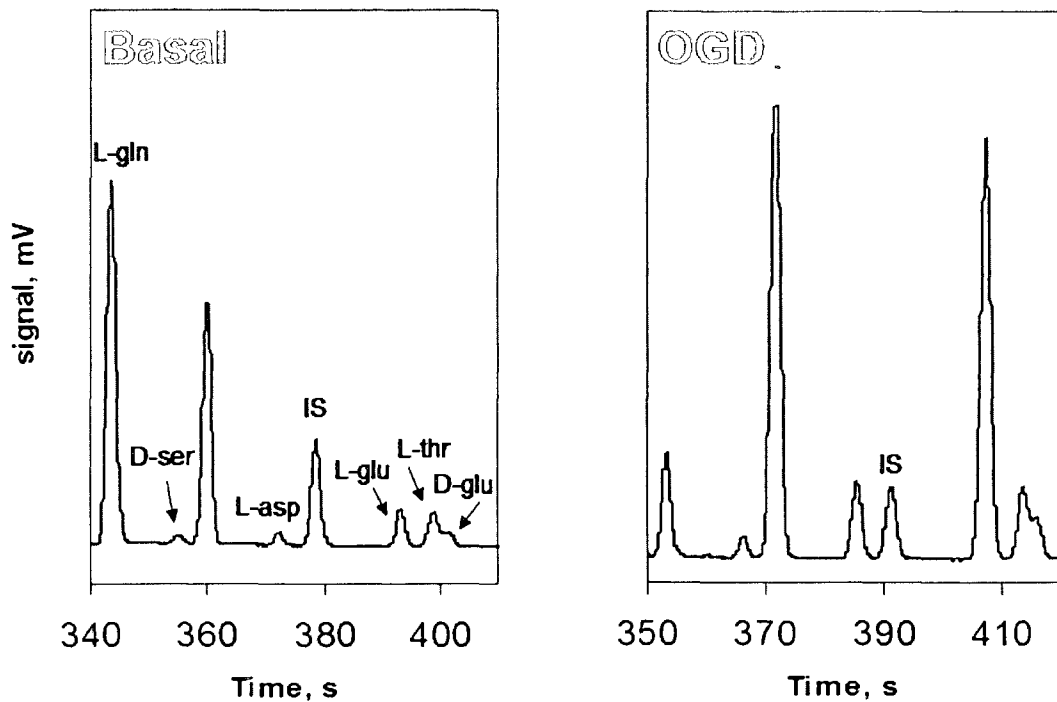


Figure 5.4. Comparison of typical electropherograms from basal and OGD perfusate samples. A change in analyte peak height relative to internal standard, IS, is observed for labeled amino acid peaks. Basal sample shown is from perfusate collected 10 min prior to OGD treatment whereas OGD sample shown was collected 24 min into OGD treatment. Both basal and OGD samples were obtained from the same acute slice experiment.

Within a few minutes after the onset of OGD treatment, there is a significant, rapid increase in all amino acids except L-gln (Figure 5.5a-e).

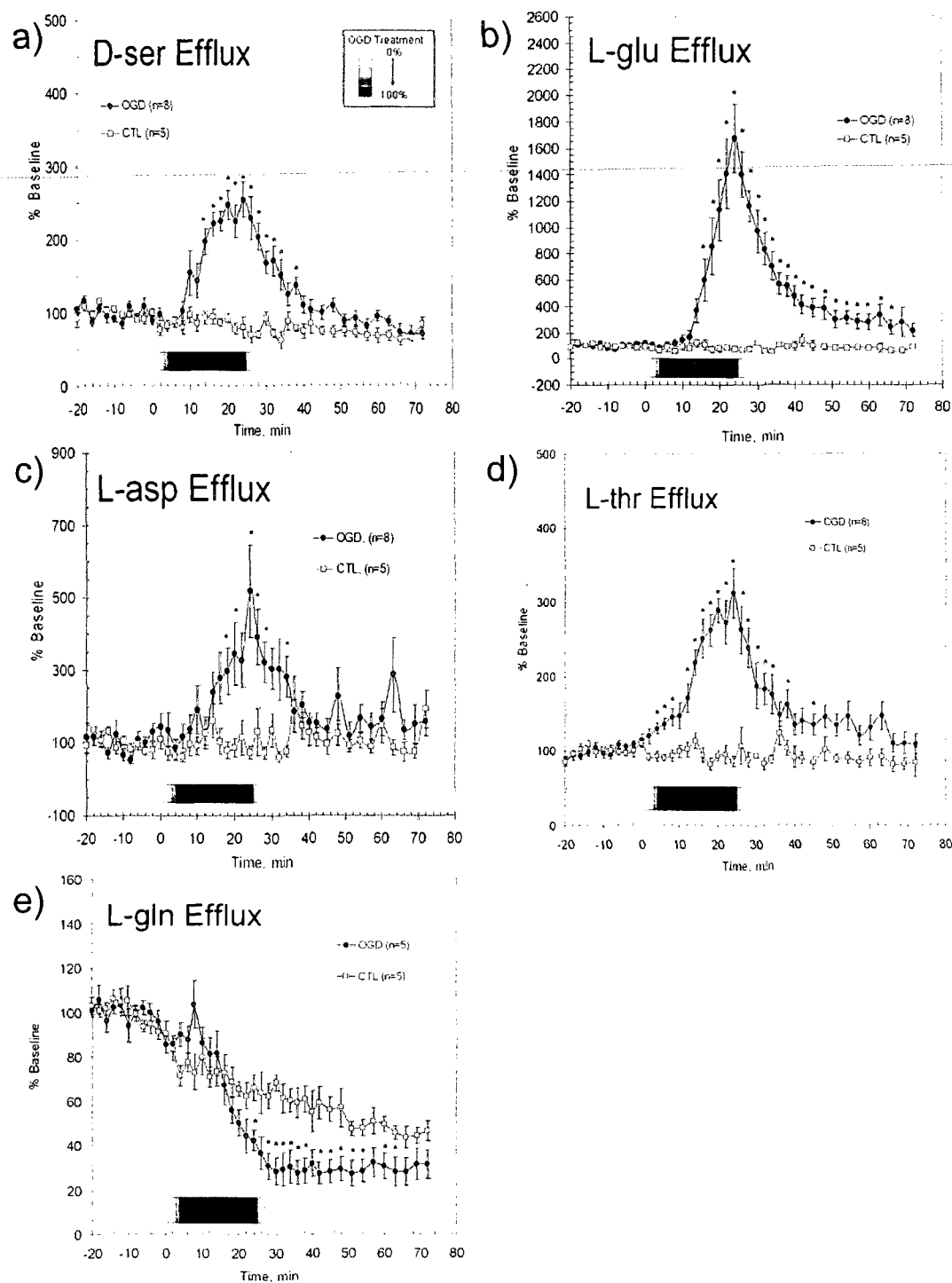


Figure 5.5. Efflux profiles for amino acids from single acute hippocampus slices in response to OGD. Efflux of D-ser occurs in parallel with efflux of L-glu during OGD in acute hippocampal slices. Percent change in endogenous amino acid concentrations

relative to average of last 10 pre-treatment samples are shown: a) D-ser, b) L-glu, c) L-asp, d) L-thr, and e) L-gln. Sampling and analysis was carried out using the newly developed microperfusion/CE-LIF strategy. Temperature was maintained at 36°C throughout perfusion. In control experiments, perfusate treatment was administered by switching to standard oxygenated aCSF medium. Data points represent average \pm SEM of n slices as indicated. * $p < 0.05$, OGD vs. CTL (Tukey post-hoc comparison).

Stable, pretreatment D-ser efflux rapidly increases during OGD and is significantly different from CTL values within 14 min of onset of OGD ($p < 0.05$; Tukey post-hoc comparison). D-ser efflux increases to $254 \pm 24\%$ of baseline levels then decreases within the first few minutes of reperfusion (reintroduction of oxygenated aCSF) returning to near pre-treatment values within 12 min. D-ser remains at pre-treatment levels throughout the remainder of the reperfusion phase (Figure 5.5a).

Likewise, efflux of L-glu is rapid and the timing of efflux is similar to D-ser. Stable, pretreatment, L-glu efflux increases and is statistically different from CTL levels within 16 min of onset of OGD ($p < 0.05$; Tukey post-hoc comparison) and reaches a maximum of $1675 \pm 259\%$ of baseline 24 min after onset of OGD. Within the first 2-4 min of reperfusion L-glu begins to slowly decline and this decline continues over the course of the 50 min reperfusion. The magnitude of L-glu efflux is larger than D-ser and unlike D-ser, L-glu remains significantly higher ($244 \pm 56\%$ of baseline values) for up to 46 min after onset of reperfusion ($p < 0.05$; Figure 5.5b).

Stable, baseline L-asp efflux increases rapidly and is statistically different from CTL levels within 18 min of onset of OGD ($p < 0.05$; Tukey post-hoc comparison). L-asp levels increase significantly to $519 \pm 128\%$ of baseline shortly after OGD with maximal

efflux corresponding to that of L-glu at 24 min from onset of OGD. L-asp returns to basal values within 10-12 min of reperfusion (Figure 5.5c). Stable, pretreatment, L-thr efflux initially increases from CTL levels modestly and is statistically significant by 4 min after onset of OGD ($p < 0.05$; Tukey post-hoc comparison). After 12-14 min treatment, L-thr efflux rises more rapidly with maximum efflux at 24 min from onset with magnitude of $313 \pm 33\%$ basal values. L-thr returns to near baseline within 12 min of reperfusion (Figure 5.5d).

Interestingly, the effect of OGD on L-gln efflux is markedly different from the other amino acids investigated here (Figure 5.5e). Firstly, in control slices, L-gln efflux slowly decreases throughout the entire experiment ($46.3 \pm 4.6\%$ basal values after 94 min of perfusion). Initially it appears that L-gln efflux increases briefly and early on during OGD however statistical analysis of these early events does not support this conclusion ($p > 0.05$; Tukey post-hoc comparison, time periods 6, 8, and 10 min). OGD then produces a further significant drop in L-gln efflux that reaches statistical significance compared to CTL at 24 min from onset ($p < 0.05$; Tukey post-hoc comparison). Ultimately, L-gln efflux reaches a minimum of $30.7 \pm 6.0\%$ baseline after 4 min reperfusion (versus $62.3 \pm 5.8\%$ at the same time point in control slices). L-gln does not significantly recover to baseline levels over the next 30 min of reperfusion.

5.4 Discussion

5.4.1 D-ser efflux from hippocampal slices during OGD

We demonstrate that D-ser, the endogenous coagonist of NMDAR, increases 2.5-fold during 24 min of *in vitro* modeled ischemia in hippocampus and, for the first time with 2 min temporal resolution, show that the timing of the rise and fall of D-ser precedes or parallels that of L-glu. These results therefore demonstrate that both co-agonists are available to activate NMDAR and contribute to excitotoxicity. Endogenous D-ser is essential for NMDA-induced excitotoxicity while endogenous levels of glycine are not sufficient to support excitotoxicity (Shleper et al., 2005). D-ser release is therefore expected to enhance excitotoxicity and, indeed, antagonists of the D-ser (“gly”) binding site are neuroprotective in animal models of stroke (Wasterlain et al., 1996; Ohtani et al., 2000; Ohtani et al., 2003).

To our knowledge, there is only one other report of a temporal response of D-ser to model ischemia. Lo and colleagues using *in vivo* microdialysis with HPLC and fluorescence detection investigated efflux of D-ser with 10 min temporal resolution in response to 2 hr focal ischemia in rabbit cortex (Lo et al., 1998). As supported by our study, they found D-ser efflux was significantly elevated throughout the ischemic period but did not have sufficient time resolution to address if D-ser and L-glu release occurred within the same functional time window. Additionally, this is the first report of D-ser efflux from hippocampus during modeled ischemia. Hippocampus is highly susceptible to global cerebral ischemia experienced during cardiac arrest (Schmidt-Kastner and

Freund, 1991; Kirino, 2000) and hippocampal tissue is shown to have particularly high concentrations of both D-ser and NMDAR (Hashimoto and Oka, 1997).

5.4.2 Validity of microperfusion chamber

Similarities between results reported here in acute hippocampal slices and results reported during cerebral ischemia *in vivo* support the validity of the microperfusion technique. We demonstrate that L-glu increases ~17-fold from baseline during 24 min *in vitro* ischemia (Figure 5.5b). In support of our data, Mitani and Tanaka show that during 20 min of bilateral occlusion of the common carotid artery in mouse hippocampus glu levels, sampled by microdialysis from probes placed in the CA1 region, rose ~14-fold and did not return to basal values after 40 min of reperfusion (Mitani and Tanaka, 2003). Using the microperfusion chamber in the present study L-asp increases ~6-fold during 24 min OGD and returns to basal values soon after reperfusion. Similarly, L-asp increases in response to ischemia *in vivo* (Benveniste et al., 1984; Dawson et al., 2000).

Three points of evidence in our current data support slice viability despite low flow rates. First, we demonstrate stable basal levels of glutamate and other transmitters over the course of 2 hours in the microchamber. Second, treatment of stable basal slices with OGD results in robust efflux of L-glu which is compelling evidence that slices are viable prior to switching to treatment since it demonstrates that cells maintain Na⁺ gradients and that these are reversed during OGD. The capacity for slices to recover basal levels of glu that persist at a slightly higher level than basal levels as demonstrated following *in vivo* ischemia further demonstrate that slices are able to recover ion

homeostasis post-OGD. Furthermore, the magnitude of maximal evoked L-glu release and levels during recovery demonstrated here is similar to reported magnitudes for hippocampus *in vivo* during cerebral ischemia. Taken together, these results suggest that slices are viable in this microperfusion preparation. This validates the microperfusion device for hippocampal slice OGD experiments.

In our 24 min OGD exposure several factors likely contribute to the delayed glu response seen in these hippocampal slices. Firstly, several minutes are likely required for significant depletion of ATP from the slice preparation. Mitani et al. demonstrated that over 3 min were required for ~80 % ATP depletion in acute hippocampal slices exposed to OGD in a flow through chamber at 33 °C (Mitani et al., 1994). Secondly, the temporal response of our slice chamber is around 4.5 min for a complete turnover. This response may have the effect of further delaying total ATP depletion and initial chemical response, since it takes longer for tissue to be exposed to the full 100 % OGD solution. Thirdly, we expect that chemical diffusion from synaptic regions in the tissue matrix to the bulk medium may limit overall temporal response in 400 µm thick slices during perfusion experiments.

5.4.3 Significance of L-thr efflux

L-thr increases significantly in response to OGD in a manner similar to that of D-ser with the exception that we note a small but significant elevation of L-thr earlier on in the OGD time course as compared to D-ser. The chemical similarity between L-thr and D-ser suggests that these two amino acids use similar transport mechanisms. The sodium

dependent neutral amino acid transporter alanine serine cysteine transporter-2 (ASCT-2) has indeed been demonstrated to show high micromolar affinity for both L-thr and D-ser (Ribeiro et al., 2002; Rutter et al., 2007). ASCT-2 is therefore an attractive candidate for efflux of these amino acids during OGD when transmembrane sodium ion gradients are reversed. Unfortunately selective inhibitors of ASCT-2 have not yet been developed thus the relative contribution of this Na⁺ dependent mechanism to L-thr and D-ser efflux during OGD remains to be determined.

5.4.4 Significance of L-gln efflux

L-gln response to 24 min OGD treatment is different from other amino acids investigated here. The basal level of L-gln steadily decreases in control slices. This result is similar to that of Kapetanovic and colleagues who demonstrated a dramatic, time-dependent loss of L-gln in mouse and rat acute hippocampal slices under static (no flow) and superfused (3 mL/min, constant flow) conditions (Kapetanovic et al., 1993). Several studies have demonstrated a similar drop in L-gln during cerebral ischemia *in vivo*, though never with the same temporal resolution as shown here during OGD (Benveniste et al., 1984; Silverstein et al., 1991; Uchiyama-Tsuyuki et al., 1994; Van Hemelrijck et al., 2005). Many studies have postulated that the decrease of L-gln during ischemia may be due to loss as L-glu via the Gln-Glu cycle (Silverstein et al., 1991; Uchiyama-Tsuyuki et al., 1994; Huang and Hertz, 1995a, b; Phillis et al., 2001; Shen et al., 2009). The particular role of L-gln in excitotoxicity has not been investigated; however, L-gln may enhance excitotoxicity by serving as a source for L-glu.

5.4.5 Advantages of microperfusion/CE-LIF technique

The importance of D-ser in the mammalian brain and its relationship to L-glu via NMDA receptor coactivation has led to the need for robust and sensitive approaches for quantifying this transmitter with L-glu in various brain preparations. Chiral HPLC assays have been extensively utilized for D-ser quantification from brain homogenates and *in vivo* microdialysis samples (Hashimoto et al., 1995; Fukushima et al., 2004; Grant et al., 2006). HPLC assays typically suffer from long migration times (30-60min) and expensive chiral columns and column switching protocols. Recently, Bowser and colleagues developed powerful online capillary electrophoresis microdialysis assays for monitoring D-ser, L-glu, and other amines *in vivo* (Ciriacks and Bowser, 2006; Klinker and Bowser, 2007) and *in vitro* (O'Brien et al., 2004; O'Brien and Bowser, 2006). The latter studies involved assaying D-ser and L-glu in single excised retina and acute cortical tissue using a microliter sized retinal perfusion chamber coupled online to microdialysis CE-LIF. To our knowledge these were the first reports of monitoring rapid dynamic release of endogenous D-ser from an *in vitro* preparation. Their unique system was capable of monitoring efflux of D-ser and L-glu every 15 s, although temporal resolution (time required to detect an instantaneous stepwise change in analyte concentration) of the transmitter response was limited by the turnover rate of the chamber (turnover every 4 min), not by sampling rate. Furthermore the practical limitation of this online CE-LIF approach for routine studies *in vitro* relates to the fact that multiple CE-LIF platforms would be required for each chamber run in parallel, thus

limiting throughput. In addition, the prerequisite for microdialysis sampling of the perfusion medium as it exits the chamber adds unwanted complexity and costs for *in vitro* studies, and compromises quantitative recovery of analyte. Overall, we demonstrate that the microperfusion/CE-LIF technique described here offers several inherent advantages including (1) the ability to simultaneously sample from multiple brain slices from a single animal, (2) complete recovery of neurotransmitter since microdialysis is not required, (3) high temporal *in vitro* response of neurotransmitter efflux and (4) ability to simultaneously monitor multiple analytes by CE-LIF with high sensitivity.

Temporal response using the microperfusion approach could be increased further than reported here in future work by increasing perfusion flow rate and sampling frequency. Indeed one of the advantages of the microperfusion approach in combination with sensitive CE-LIF is the potential to realize these improvements. Our CE-LIF technique utilizes minute volumes of perfusion media and based on S/N shown in Figure 5.4 for CBI-amino acids, would likely allow for doubling of flow rate without loss in capacity to detect the amino acids of interest.

5.5 Summary on microperfusion sampling with CE-LIF

In summary, we show that OGD-induces D-ser and L-glu efflux from acute slices with similar timing of release which is important when considering that both are required for NMDAR excitotoxicity. In addition, our data represents the first temporal monitoring of both excitotoxic chemicals D-ser and L-glu in hippocampus. We describe a new microperfusion technique that is coupled to offline chiral CE-LIF to investigate ischemia

evoked efflux of neurochemicals. The use of CE-LIF utilizing S- β -CD as described in Chapter 2 allowed for monitoring efflux profiles of L-asp, L-thr, and L-gln in addition to the targeted excitotoxic chemicals D-ser and L-glu with 2 min temporal resolution. We speculate that this new approach will be valuable for future studies investigating mechanisms of neurochemical regulation.

Chapter 6

Conclusions

6.1 Overview

Several D-amino acids including D-ser and D-asp are important metabolites in the mammalian brain; studies on function and distribution of D-amino acids require the development of bioanalytical tools capable of sensitive enantioselective analysis in complex biological matrices. Capillary electrokinetic chromatography has emerged as a powerful, yet simple tool for chiral recognition; the approach is well validated for bioanalysis and offers many advantages for analyzing trace samples in complex biological matrices.

The primary focus of this dissertation was to demonstrate the capabilities of anionic CDs in cEKC for bioanalysis of amino acids for the first time and take advantage of sensitive bioanalytical approaches with these chiral selectors for quantifying D-amino acids in the CNS. This research represents the first application of an ionic CD for bioanalysis of a chiral amino acid. Selective separation and sensitive detection of D-ser, the dominant coagonist of the NMDAR, in CNS samples, was a central focus of this work. Studies over the past few years stress the importance of single isomer CDs for robust chiral separations; this thesis research also focuses on design and synthesis of a new family of single isomer selectively modified sulfoalkyl anionic CDs and investigations on their application for D-amino acid analysis. Sensitive separation and quantification is only one aspect of bioanalytical chemistry. This dissertation also focused on the development

of a novel microperfusion brain slice chamber for rapid sampling of neurochemical efflux dynamics including D-ser and L-glu from single acute hippocampus slices. Studies with this approach coupled to anionic CD based chiral separations were carried out for investigating timing and magnitude of D-ser and L-glu efflux in response to modeled cerebral ischemia.

6.2 Conclusions on reverse polarity CD-cEKC with S- β -CD

Anionic commercially available S- β -CD was shown for the first time to be a powerful chiral selector for CBI-amino acids and was capable of resolving as many as 14 CBI-amino acids with a single buffer formulation. The anionic CD derivative was found to be highly sensitive to the ionic nature of the CBI-amino acid; significant electrostatic interactions drastically altered resolution using reverse polarity CD-cEKC. BGE pH was established as the most important factor for chiral resolution of CBI-ser as well as other weakly acidic CBI-derivatives due to this electrostatic interaction. Data was provided demonstrating significant ionization of CBI-amino acids around pH 3 which results in significant electrostatic repulsion between anionic CD and anionic amino acid derivative and also significant electrostatic attraction at low pH between cationic CBI-amino acids and anionic CDs. RP-CD-cEKC with S- β -CD was applied to dilute samples of CBI-amino acids to investigate an observed stacking phenomenon. We found that S- β -CD could be used for pH mediated stacking and sweeping of dilute enantiomers of CBI-amino acids resulting in ~100-fold improvements in S/N without loss in chiral resolution. S- β -CD was developed for the first time as a bioanalytical method for amino

acids. The approach was used for analysis of D-ser, D-asp, L-asp, D-glu, and L-glu in microdialysates from hippocampus of arctic ground squirrel. The bioanalytical method offered sufficient sensitivity for biological samples and was the first CE-LIF method for analysis of all three of these D-isomers simultaneously.

6.3 Conclusions on synthesis of selectively modified sulfoalkyl CDs

The poor batch to batch reproducibility of most commercially available anionic CDs (including S- β -CD) stimulated interests to develop a new class of selectively modified single isomer sulfoalkyl cyclodextrins. These CDs were expected to have increased binding affinity with hydrophobic guest species compared to S- β -CD due to an increase in the separation of the charged sulfonate from the CD torus.

Six new members of the first family of selectively modified sulfoalkyl CDs, including α - and β -CD derivatives, were fully synthesized and characterized. The CDs were designed to incorporate hydrophobic methyl or ethyl groups on the wider secondary hydroxyl rim of the CD torus. The primary hydroxyl rim was selectively modified with either sulfopropyl or sulfobutyl groups. A 4-step synthesis for each single isomer was required in order to selectively react both primary and secondary hydroxyls of the native CDs. The first 3-steps were primary hydroxyl protection, secondary hydroxyl alkylation, and primary hydroxyl deprotection reactions, and were reproduced from literature with only minor modifications. The sulfoalkylation step had to be developed within this thesis using nonaqueous reaction chemistry.

We found that hexakis- and heptakis(2,3-di-O-alkyl)cyclodextrins could be reacted to produce single isomer 6-O-sulfoalkyl derivatives using 1,3-propanesultone or 1,4-butanedisultone in THF in the presence of 18-crown-6/KH as base. Without crown ether, the reaction produced only poorly substituted product mixtures characterized by a low average DS. Full substitution was accomplished using high molar excess of crown ether compared to CD. After purification to remove various byproducts, reactants, and catalyst, CDs were characterized by NMR, elemental analysis, inverse detection capillary electrophoresis and MALDI-MS. All CDs were highly substituted with a composition of at least 95 % of the single isomer heptasulfoalkyl (β -CDs) or hexasulfoalkyl (α -CDs) products. KSPDM- β -CD was additionally demonstrated to form an inclusion complex in solution using ROESY NMR with CBI-D-ser.

6.4 Conclusion on single isomer CDs as resolving agents for CBI-amino acids

Single isomer CDs are structurally superior buffer additives for robust chiral analytical assays compared to commercially available randomly substituted CDs. The initial study on single isomer sulfoalkyl CDs developed here for CBI-DL-amino acid analysis using RP-CD-cEKC was promising and suggests that KSPDM- β -CD, KSBDM- β -CD, and KSBDE- β -CD are excellent new resolving agents for chiral capillary electrophoresis. Additionally these CDs may be valuable for bioanalysis of chiral amino acids. Single isomer sulfoalkyl CDs form much stronger interactions with CBI-amino acids than S- β -CD and are not as sensitive to the ionic nature of the guest molecule. This latter observation was in accordance with the structure of these selectively modified

derivatives compared to S- β -CD in that the extended alkyl spacer group separates the charged sulfonates too far from the CD torus to allow for significant electrostatic interaction with guest species for sulfoalkyl CDs. Thus the significant pH effects on resolution of CBI-amino acids with S- β -CD are not observed to anywhere near the same magnitude with KSBDM- β -CD suggesting for the latter that the complexation potential is not as greatly affected by increased ionization of CBI-amino acid. Further, CBI-his migration was actually ~2-fold longer than weakly acidic amino acids at low KSBDM- β -CD concentration illustrating that CBI-his migration is not greatly influenced by any significant electrostatic attraction to this CD. The strong interaction between weakly acidic CBI-derivatives and single isomer sulfoalkyl CDs allowed for chiral resolution at remarkably lower concentrations of selector while maintaining high separation efficiencies. Thus CBI-DL-ser, CBI-DL-asp, CBI-DL-glu, CBI-DL-ala, and CBI-DL-thr were all baseline resolved in less than <17 min using 50 μ M of KSBDM- β -CD as the only chiral selector in the BGE. The diethyl derivative, KSPDE- β -CD, offered unique selectivity compared to the similar chiral recognition behavior of dimethyl derivatives. KSPDE- β -CD was the best resolving agent of the series investigated for CBI-ser enantiomers at low CD concentrations though it displayed poorer selectivity at these levels for several other CBI-derivatives. A notable observation was a KSPDE- β -CD concentration dependent change in enantiomer migration order which may be the result of complex induced alterations in CBI-amino acid pK_a values.

6.5 Conclusions on microperfusion/CE-LIF for D-ser and L-glu analysis during oxygen glucose deprivation.

D-ser and L-glu play crucial roles in excitotoxicity through N-methyl-D-aspartate receptor coactivation but little is known about the temporal profile of efflux during cerebral ischemia. To investigate, this dissertation describes a newly designed brain slice microperfusion device coupled offline to chiral CE-LIF with S- β -CD as chiral selector to monitor dynamic efflux of endogenous D-ser and L-glu in response to oxygen glucose deprivation in single acute hippocampus slices. Efflux profiles with 2 min temporal resolution in response to 24 min OGD show that efflux of D-ser slightly precedes efflux of L-glu by one, 2-min sampling interval. Thus both coagonists are available to activate NMDA receptors by the time glu is released. The magnitude of D-ser efflux relative to baseline values is, however, less than for L-glu. This microperfusion approach coupled with CE-LIF represents the fastest temporal monitoring of D-ser during modeled ischemia to date, and was the first study to investigate D-ser and L-glu efflux simultaneously in acute hippocampus. Several other endogenous amino acids were also simultaneously analyzed in perfusate media using CE-LIF including L-thr, L-gln, and L-asp. Advantages of the microperfusion device included (1) the ability to simultaneously sample from multiple brain slices from a single animal, (2) complete recovery of neurotransmitter since microdialysis is not required, (3) high temporal *in vitro* response of neurotransmitter efflux, and (4) ability to simultaneously monitor multiple analytes by CE-LIF with high sensitivity. We

speculate that this new approach will be valuable for future studies investigating mechanisms of neurochemical regulation.

6.6 Final remarks

To summarize, this dissertation argues that anionic CDs are powerful chiral selectors for fluorescently labeled amino acids and can be applied for sensitive bioanalysis of D-amino acids including D-ser, D-glu, and D-asp in brain samples. It is anticipated that the single isomer sulfoalkyl CD derivatives which were synthesized and characterized here for the first time, and initially studied for separation of CBI-amino acids, will be valuable reagents for future bioanalytical separations of these important metabolites. Due to excellent batch-to-batch reproducibility, these CDs will likely replace bioanalytical methods using heterogeneous CD mixtures despite excellent resolving power demonstrated for these latter CDs. These new single isomer sulfoalkyl CDs are powerful chiral selectors capable of chiral recognition at very low concentrations of selector. Their unique structure allows for significant interaction between the CD torus and the hydrophobic guest of both weakly acidic and cationic CBI-amino acid derivatives which is a rather unique feature of anionic CD selectors reported thus far. The single isomer sulfoalkyl α -CD derivatives await further application to analytical chemistry. It is anticipated that they will additionally show similar unique inclusion complexing behavior which may be characteristic of this broader family of sulfoalkyl CDs. This dissertation describes a new *in vitro* tissue perfusion approach which allows for rapid dynamic changes in neurochemicals from acute tissue to be evaluated. The

approach was applied to investigate magnitude and timing of D-ser and L-glu efflux during modeled ischemia in hippocampus and evidence suggests that these neurochemicals are released with similar timing but differing magnitudes. Future studies with this new *in vitro* approach are expected which may reflect investigative studies on mechanisms of neurochemical regulation in the CNS.

Future studies in molecular recognition with single isomer CDs will seek to understand more clearly the mechanisms of chiral interaction of selectively modified sulfoalkyl CDs with guest molecules and especially verify the novel data presented here suggesting weak to nonexistent electrostatic interaction with acidic and basic guest species despite the heptasulfato nature of these new single isomer CD derivatives. The development of robust bioanalytical separations of CBI-ser and additional CBI-amino acid enantiomers is expected in future studies with these powerful new chiral resolving agents. These CDs may prove valuable for additional chiral separations; perhaps including analysis of pharmaceutical weak bases, acids, and neutral chiral drugs and intermediates. Their ability to offer excellent enantioselectivity, high batch to batch reproducibility, narrow peak widths, and high separation efficiencies at reduced concentrations are all features that will be utilized in future robust analytical separations.

References

- Albanese D, Landini D, Maia A (2001) Dramatic Effect of the Metal Cation in Dealkylation Reactions of Phosphinic Esters Promoted by Complexes of Polyether Ligands with Metal Iodides. *J Org Chem* 66:3249-3252.
- Arundine M, Tymianski M (2004) Molecular mechanisms of glutamate-dependent neurodegeneration in ischemia and traumatic brain injury. *Cell Mol Life Sci* 61:657-668.
- Benveniste H, Drejer J, Schousboe A, Diemer NH (1984) Elevation of the extracellular concentrations of glutamate and aspartate in rat hippocampus during transient cerebral ischemia monitored by intracerebral microdialysis. *J Neurochem* 43:1369-1374.
- Berna MJ, Ackermann BL (2007) Quantification of serine enantiomers in rat brain microdialysate using Marfey's reagent and LC/MS/MS. *J Chromatogr* 846:359-363.
- Bhattacharyya SK, Banerjee AB (1974) D-amino acids in the cell pool of bacteria *Fol Microbiol* 19:43-50.
- Broer A, Wagner C, Lang F, Broer S (2000) Neutral amino acid transporter ASCT2 displays substrate-induced Na⁺ exchange and a substrate-gated anion conductance. *Biochem J* 346 Pt 3:705-710.
- Bruckner H, Hausch M (1993) Gas chromatographic characterization of free D-amino acids in the blood serum of patients with renal disorders and of healthy volunteers. *J Chromatogr* 614:7-17.
- Bruckner H, Schieber A (2001) Ascertainment of D-amino acids in germ-free, gnotobiotic and normal laboratory rats. *Biomed Chromatogr* 15:257-262.
- Busby MB, Vigh G (2005a) Synthesis of heptakis(2-O-methyl-3-O-acetyl-6-O-sulfo)-cyclomaltoheptaose, a single-isomer, sulfated beta-cyclodextrin carrying nonidentical substituents at all the C2, C3, and C6 positions and its use for the capillary electrophoretic separation of enantiomers in acidic aqueous and methanolic background electrolytes. *Electrophoresis* 26:1978-1987.

- Busby MB, Vigh G (2005b) Synthesis of a single-isomer sulfated beta-cyclodextrin carrying nonidentical substituents at all of the C2, C3, and C6 positions and its use for the electrophoretic separation of enantiomers in acidic aqueous and methanolic background electrolytes. Part 2: Heptakis(2-O-methyl-6-O-sulfo)cyclomaltoheptaose. *Electrophoresis* 26:3849-3860.
- Busby MB, Lim P, Vigh G (2003) Synthesis, analytical characterization and use of octakis(2,3-di-O-methyl-6-O-sulfo)-gamma-cyclodextrin, a novel, single-isomer, chiral resolving agent in low-pH background electrolytes. *Electrophoresis* 24:351-362.
- Cai H, Vigh G (1998) Capillary electrophoretic separation of weak base enantiomers using the single-isomer heptakis-(2,3-dimethyl-6-sulfo)-beta-cyclodextrin as resolving agent and methanol as background electrolyte solvent. *J Pharm Biomed Anal* 18:615-621.
- Cai H, Nguyen TV, Vigh G (1998) A Family of Single-Isomer Chiral Resolving Agents for Capillary Electrophoresis. 3. Heptakis(2,3-dimethyl-6-sulfo)-beta-cyclodextrin. *Anal Chem* 70:580-589.
- Chankvetadze B (2007) Enantioseparations by using capillary electrophoretic techniques. The story of 20 and a few more years. *J Chromatogr A* 1168:45-70; discussion 44.
- Chankvetadze B, Lomsadze K, Bergenthal, D, Breitkruetz J, Bergander K, Blaschke G (2001) Mechanistic study on the opposite migration order of clenbuterol enantiomers in capillary electrophoresis with beta-cyclodextrin and single-isomer heptakis(2,3-diacetyl-6-sulfo)-beta-cyclodextrin. *Electrophoresis* 22:3178-3184.
- Chankvetadze B, Endresz G, Blaschke G (1995) Capillary electrophoresis enantioseparation of noncharged and anionic chiral compounds using anionic cyclodextrin derivatives as chiral selectors. *J Capillary Electrophor* 2:235-240.
- Chatterton JE, Awobuluyi M, Premkumar LS, Takahashi H, Talantova M, Shin Y, Cui J, Tu S, Sevarino KA, Nakanishi N, Tong G, Lipton SA, Zhang D (2002) Excitatory glycine receptors containing the NR3 family of NMDA receptor subunits. *Nature* 415:793-798.
- Chen FT, Shen G, Evangelista RA (2001) Characterization of highly sulfated cyclodextrins. *J Chromatogr A* 924:523-532.
- Ciriacks CM, Bowser MT (2006) Measuring the effect of glutamate receptor agonists on extracellular D-serine concentrations in the rat striatum using online microdialysis-capillary electrophoresis. *Neurosci Lett* 393:200-205.

- Corrigan JJ (1969) D-amino acids in animals. *Science* (New York, NY) 164:142-149.
- Curras MC, Pallotta BS (1996) Single-channel evidence for glycine and NMDA requirement in NMDA receptor activation. *Brain Res* 740:27-40.
- D'Aniello A (2007) D-Aspartic acid: an endogenous amino acid with an important neuroendocrine role. *Brain Res Rev* 53:215-234.
- Dawson LA, Djali S, Gonzales C, Vinegra MA, Zaleska MM (2000) Characterization of transient focal ischemia-induced increases in extracellular glutamate and aspartate in spontaneously hypertensive rats. *Brain Res Bull* 53:767-776.
- De Miranda J, Panizzutti R, Foltyn VN, Wolosker H (2002) Cofactors of serine racemase that physiologically stimulate the synthesis of the N-methyl-D-aspartate (NMDA) receptor coagonist D-serine. *Proc Natl Acad Sci U S A* 99:14542-14547.
- De Montigny P, Stobaugh JF, Givens RS, Carlson RG, Srinivasachar K, Sternson LA, Higuchi T (1987) Naphthalene-2,3-dicarboxyaldehyde/cyanide ion: a rationally designed fluorogenic reagent for primary amines. *Anal Chem* 59:1096-1101.
- DeSilva K, Kuwana T (1997) Separation of chiral amino acids by micellar electrokinetic chromatography with derivatized cyclodextrins. *Biomed Chromatogr* 11:230-235.
- Dingledine R, Kleckner NW, McBain CJ (1990) The glycine coagonist site of the NMDA receptor. *Adv Exp Med Biol* 268:17-26.
- Dong MW (2006) *Modern HPLC for practicing scientists*. Hoboken, N.J.: Wiley-Interscience.
- Duchateau A, Heemels G, L. M, De Vries N (1992) Separation of benz[f]isoindole derivatives of amino acid and amino acid amide enantiomers on a β -cyclodextrin bonded phase. *J Chromatogr A* 603:151-156.
- Dunlop DS, Neidle A (1997) The origin and turnover of D-serine in brain. *Biochem Biophys Res Commun* 235:26-30.
- Dunlop DS, Neidle A, McHale D, Dunlop DM, Lajtha A (1986) The presence of free D-aspartic acid in rodents and man. *Biochem Biophys Res Commun* 141:27-32.
- Easton CJ, Lincoln SF (1999) *Modified cyclodextrins : scaffolds and templates for supramolecular chemistry*. London ; River Edge, N.J.: Imperial College Press.

- Fuchs SA, de Sain-van der Velden MG, de Barse MM, Roeleveld MW, Hendriks M, Dorland L, Klomp LW, Berger R, de Koning TJ (2008) Two Mass-Spectrometric Techniques for Quantifying Serine Enantiomers and Glycine in Cerebrospinal Fluid: Potential Confounders and Age-Dependent Ranges. *Clin Chem* 54:1443-1450.
- Fukushima T, Kato M, Santa T, Imai K (1995) Enantiomeric separation and sensitive determination of D,L-amino acids derivatized with fluorogenic benzofurazan reagents on Pirkle type stationary phases. *Biomed Chromatogr* 9:10-17.
- Fukushima T, Kawai J, Imai K, Toyooka T (2004) Simultaneous determination of D- and L-serine in rat brain microdialysis sample using a column-switching HPLC with fluorimetric detection. *Biomed Chromatogr* 18:813-819.
- Furuchi T, Homma H (2005) Free D-aspartate in mammals. *Biol Pharm Bull* 28:1566-1570.
- Gillogly JA, Lunte CE (2005) pH-mediated acid stacking with reverse pressure for the analysis of cationic pharmaceuticals in capillary electrophoresis. *Electrophoresis* 26:633-639.
- Gobbi A, Landini D, Maia A, Secci D (1995) Metal Ion Catalysis in Nucleophilic Substitution Reactions Promoted by Complexes of Polyether Ligands with Alkali Metal Salts. *J Org Chem* 60:5954-5957.
- Gozel P, Gassmann E, Michelsen H, Zare RN (1987) Electrokinetic resolution of amino acid enantiomers with copper(II)-aspartate support electrolyte. *Anal Chem* 59:44-49.
- Grant SL, Shulman Y, Tibbo P, Hampson DR, Baker GB (2006) Determination of d-serine and related neuroactive amino acids in human plasma by high-performance liquid chromatography with fluorimetric detection. *J Chromatogr* 844:278-282.
- Gubitz G, Schmid MG (2001) Chiral separation by chromatographic and electromigration techniques. A review. *Biopharm Drug Dispos* 22:291-336.
- Gubitz G, Schmid MG (2008) Chiral separation by capillary electromigration techniques. *J Chromatogr A* 1204:140-156.
- Hamase K (2007) Sensitive two-dimensional determination of small amounts of D-amino acids in mammals and the study on their functions. *Chem Pharm Bull (Tokyo)* 55:503-510.

- Hamase K, Inoue T, Morikawa A, Konno R, Zaitso K (2001) Determination of free D-proline and D-leucine in the brains of mutant mice lacking D-amino acid oxidase activity. *Anal Biochem* 298:253-258.
- Hamase K, Morikawa A, Ohgusu T, Lindner W, Zaitso K (2007) Comprehensive analysis of branched aliphatic D-amino acids in mammals using an integrated multi-loop two-dimensional column-switching high-performance liquid chromatographic system combining reversed-phase and enantioselective columns. *J Chromatogr A* 1143:105-111.
- Hamase K, Takagi S, Morikawa A, Konno R, Niwa A, Zaitso K (2006) Presence and origin of large amounts of D-proline in the urine of mutant mice lacking D-amino acid oxidase activity. *Anal Bioanal Chem* 386:705-711.
- Hapitot F, Lyskawa J, Bricout H, Tilloy S, Monflier E (2004) Cyclodextrins or Calixarenes: What is the Best Mass Transfer Promoter for Suzuki Cross-Coupling Reactions in Water? *Adv Syn Catal* 346:83-89.
- Hashimoto A, Oka T (1997) Free D-aspartate and D-serine in the mammalian brain and periphery. *Prog Neurobiol* 52:325-353.
- Hashimoto A, Oka T, Nishikawa T (1995) Anatomical distribution and postnatal changes in endogenous free D-aspartate and D-serine in rat brain and periphery. *Eur J Neurosci* 7:1657-1663.
- Hashimoto A, Nishikawa T, Oka T, Takahashi K (1993a) Endogenous D-serine in rat brain: N-methyl-D-aspartate receptor-related distribution and aging. *J Neurochem* 60:783-786.
- Hashimoto A, Nishikawa T, Oka T, Takahashi K, Hayashi T (1992a) Determination of free amino acid enantiomers in rat brain and serum by high-performance liquid chromatography after derivatization with N-tert.-butyloxycarbonyl-L-cysteine and o-phthaldialdehyde. *J Chromatogr* 582:41-48.
- Hashimoto A, Nishikawa T, Hayashi T, Fujii N, Harada K, Oka T, Takahashi K (1992b) The presence of free D-serine in rat brain. *FEBS Lett* 296:33-36.
- Hashimoto A, Kumashiro S, Nishikawa T, Oka T, Takahashi K, Mito T, Takashima S, Doi N, Mizutani Y, Yamazaki T, et al. (1993b) Embryonic development and postnatal changes in free D-aspartate and D-serine in the human prefrontal cortex. *J Neurochem* 61:348-351.
- Helboe L, Egebjerg J, Moller M, Thomsen C (2003) Distribution and pharmacology of alanine-serine-cysteine transporter 1 (asc-1) in rodent brain. *Eur J Neurosci* 18:2227-2238.

- Hille B (2001) Ion channels of excitable membranes, 3rd Edition. Sunderland, Mass.: Sinauer.
- Horiike K, Tojo H, Arai R, Nozaki M, Maeda T (1994) D-amino-acid oxidase is confined to the lower brain stem and cerebellum in rat brain: regional differentiation of astrocytes. *Brain Res* 652:297-303.
- Huang R, Hertz L (1995a) Potentiation by K⁺ of anoxic release of newly synthesized neuronal glutamate. *Neuroreport* 6:2404-2408.
- Huang R, Hertz L (1995b) Neuroprotective effect of phenylsuccinate, an inhibitor of cytosolic glutamate formation from glutamine, under anoxic conditions but not during exposure to exogenous glutamate. *Neurosci Lett* 183:22-26.
- Iadarola P, Ferrari F, Fumagalli M, Viglio S (2008) Determination of amino acids by micellar EKC: recent advances in method development and novel applications to different matrices. *Electrophoresis* 29:224-236.
- Iino M, Ozawa S, Tsuzuki K (1990) Permeation of calcium through excitatory amino acid receptor channels in cultured rat hippocampal neurones. *J Physiol* 424:151-165.
- Inoue T, Hamase K, Morikawa A, Zaitzu K (2000) Determination of minute amounts of D-leucine in various brain regions of rat and mouse using column-switching high-performance liquid chromatography. *J Chromatogr B Biomed Sci Appl* 744:213-219.
- Jacobs WA, Leburg MW, Madaj EJ (1986) Stability of o-phthalaldehyde-derived isoindoles. *Anal Biochem* 156:334-340.
- Jin LJ, Rodriguez I, Li SF (1999) Enantiomeric separation of amino acids derivatized with fluoresceine isothiocyanate isomer I by micellar electrokinetic chromatography using beta- and gamma-cyclodextrins as chiral selectors. *Electrophoresis* 20:1538-1545.
- Jonas P (1993) AMPA-type glutamate receptors--nonselective cation channels mediating fast excitatory transmission in the CNS. *EXS* 66:61-76.
- Juvancz Z, Kendrovics RB, Ivanyi R, Szenté L (2008) The role of cyclodextrins in chiral capillary electrophoresis. *Electrophoresis* 29:1701-1712.
- Kahle C, Deubner R, Schollmayer C, Scheiber J, Holzgrabe U (2005) NMR Spectroscopic and Molecular Modelling Studies on Cyclodextrin-Dipeptide Inclusion Complexes. *Eur J Org Chem* 2005:1578-1589

- Kapetanovic IM, Yonekawa WD, Kupferberg HJ (1993) Time-related loss of glutamine from hippocampal slices and concomitant changes in neurotransmitter amino acids. *J Neurochem* 61:865-872.
- Kartvelishvily E, Shleper M, Balan L, Dumin E, Wolosker H (2006) Neuron-derived D-serine release provides a novel means to activate N-methyl-D-aspartate receptors. *J Biol Chem* 281:14151-14162.
- Katsuki H, Nonaka M, Shirakawa H, Kume T, Akaike A (2004) Endogenous D-serine is involved in induction of neuronal death by N-methyl-D-aspartate and simulated ischemia in rat cerebrocortical slices. *J Pharmacol Exp Ther* 311:836-844.
- Khaledi MG (1998) High-performance capillary electrophoresis : theory, techniques, and applications. New York: John Wiley.
- Kirino T (2000) Delayed neuronal death. *Neuropathology* 20 Suppl:S95-97.
- Kirschner D, Wilson A, Green T, Drew K (2009) Simultaneous efflux of endogenous D-ser and L-glu from single acute hippocampus slices during oxygen glucose deprivation. *J Neurosci Res* (In Press).
- Kirschner D, Jaramillo M, Green T, Hapiot F, Leclercq L, Bricout H, Monflier E (2008) Fine tuning of sulfoalkylated cyclodextrin structures to improve their mass-transfer properties in an aqueous biphasic hydroformylation reaction. *J Mol Catal A* 286:11-20.
- Kirschner DL, Green TK (2005) Nonaqueous synthesis of a selectively modified, highly anionic sulfopropyl ether derivative of cyclomaltoheptaose (beta-cyclodextrin) in the presence of 18-crown-6. *Carbohydr Res* 340:1773-1779.
- Kirschner DL, Jaramillo M, Green TK (2007) Enantioseparation and stacking of Cyanobenz[f]isoindole-amino acids by reverse polarity capillary electrophoresis and sulfated beta-cyclodextrin. *Anal Chem* 79:736-743.
- Kleckner NW, Dingledine R (1988) Requirement for glycine in activation of NMDA-receptors expressed in *Xenopus* oocytes. *Science* (New York, NY) 241:835-837.
- Klinker CC, Bowser MT (2007) 4-fluoro-7-nitro-2,1,3-benzoxadiazole as a fluorogenic labeling reagent for the in vivo analysis of amino acid neurotransmitters using online microdialysis-capillary electrophoresis. *Anal Chem* 79:8747-8754.
- Krebs HA (1935) Metabolism of amino-acids: Deamination of amino-acids. *Biochem J* 29:1620-1644.

- Lada MW, Vickroy TW, Kennedy RT (1997) High temporal resolution monitoring of glutamate and aspartate in vivo using microdialysis on-line with capillary electrophoresis with laser-induced fluorescence detection. *Anal Chem* 69:4560-4565.
- Li S, Vigh G (2003) Synthesis, analytical characterization and initial capillary electrophoretic use in acidic background electrolytes of a new, single-isomer chiral resolving agent: hexakis(2,3-di-O-acetyl-6-O-sulfo)-alpha-cyclodextrin. *Electrophoresis* 24:2487-2498.
- Li S, Vigh G (2004a) Single-isomer sulfated alpha-cyclodextrins for capillary electrophoresis: hexakis(2,3-di-O-methyl-6-O-sulfo)-alpha-cyclodextrin, synthesis, analytical characterization, and initial screening tests. *Electrophoresis* 25:2657-2670.
- Li S, Vigh G (2004b) Single-isomer sulfated alpha-cyclodextrins for capillary electrophoresis. Part 2. Hexakis(6-O-sulfo)-alpha-cyclodextrin: synthesis, analytical characterization, and initial screening tests. *Electrophoresis* 25:1201-1210.
- Lipton P (1999) Ischemic cell death in brain neurons. *Physiol Rev* 79:1431-1568.
- Lo EH, Pierce AR, Matsumoto K, Kano T, Evans CJ, Newcomb R (1998) Alterations in K⁺ evoked profiles of neurotransmitter and neuromodulator amino acids after focal ischemia-reperfusion. *Neuroscience* 83:449-458.
- Long Z, Nimura N, Adachi M, Sekine M, Hanai T, Kubo H, Homma H (2001) Determination of D- and L-aspartate in cell culturing medium, within cells of MPT1 cell line and in rat blood by a column-switching high-performance liquid chromatographic method. *J Chromatogr B Biomed Sci Appl* 761:99-106.
- Lu X, Chen Y (2002) Chiral separation of amino acids derivatized with fluoresceine-5isothiocyanate by capillary electrophoresis and laser-induced fluorescence detection using mixed selectors of beta-cyclodextrin and sodium taurocholate. *J Chromatogr A* 955:133-140.
- Luna EA, Bornancini ER, Thompson DO, Rajewski RA, Stella VJ (1997a) Fractionation and characterization of 4-sulfobutyl ether derivatives of cyclomaltoheptaose (beta-cyclodextrin). *Carbohydr Res* 299:103-110.
- Luna EA, Vander Velde DG, Tait RJ, Thompson DO, Rajewski RA, Stella VJ (1997b) Isolation and characterization by NMR spectroscopy of three monosubstituted 4-sulfobutyl ether derivatives of cyclomaltoheptaose (beta-cyclodextrin). *Carbohydr Res* 299:111-118.

- Luna EA, Bornancini ER, Tait RJ, Thompson DO, Stobaugh JF, Rajewski RA, Stella VJ (1996) Evaluation of the utility of capillary electrophoresis for the analysis of sulfobutyl ether beta-cyclodextrin mixtures. *J Pharm Biomed Anal* 15:63-71.
- Man EH, Fisher GH, Payan IL, Cadilla-Perezrios R, Garcia NM, Chemburkar R, Arends G, Frey WH (1987) d-Aspartate in Human Brain. *J Neurochem* 48:510-515.
- Mangas A, Covenas R, Bodet D, Geffard M, Aguilar LA, Yajeya J (2007) Immunocytochemical visualization of D-glutamate in the rat brain. *Neuroscience* 144:654-664.
- Martineau M, Galli T, Baux G, Mothet JP (2008) Confocal imaging and tracking of the exocytotic routes for D-serine-mediated gliotransmission. *Glia* 56:1271-1284.
- Matsuo H, Kanai Y, Tokunaga M, Nakata T, Chairoungdua A, Ishimine H, Tsukada S, Ooigawa H, Nawashiro H, Kobayashi Y, Fukuda J, Endou H (2004) High affinity D- and L-serine transporter Asc-1: cloning and dendritic localization in the rat cerebral and cerebellar cortices. *Neurosci Lett* 358:123-126.
- Maynard DK, Vigh G (2000) Synthesis and analytical characterization of the sodium salt of heptakis(2-O-methyl-3,6-di-O-sulfo)cyclomaltoheptaose, a chiral resolving agent candidate for capillary electrophoresis. *Carbohydr Res* 328:277-285.
- Maynard DK, Vigh G (2001) Heptakis(2-O-methyl-3,6-di-O-sulfo)-beta-cyclodextrin: a single isomer, 14-sulfated beta-cyclodextrin for use as a chiral resolving agent in capillary electrophoresis. *Electrophoresis* 22:3152-3162.
- McBain CJ, Kleckner NW, Wyrick S, Dingledine R (1989) Structural requirements for activation of the glycine coagonist site of N-methyl-D-aspartate receptors expressed in *Xenopus* oocytes. *Mol Pharmacol* 36:556-565.
- Miao H, Rubakhin SS, Sweedler JV (2005) Subcellular analysis of D-aspartate. *Anal Chem* 77:7190-7194.
- Miao H, Rubakhin SS, Scanlan CR, Wang L, Sweedler JV (2006) D-Aspartate as a putative cell-cell signaling molecule in the *Aplysia californica* central nervous system. *J Neurochem* 97:595-606.
- Mitani A, Tanaka K (2003) Functional changes of glial glutamate transporter GLT-1 during ischemia: an in vivo study in the hippocampal CA1 of normal mice and mutant mice lacking GLT-1. *J Neurosci* 23:7176-7182.
- Mitani A, Takeyasu S, Yanase H, Nakamura Y, Kataoka K (1994) Changes in intracellular Ca²⁺ and energy levels during in vitro ischemia in the gerbil hippocampal slice. *J Neurochem* 62:626-634.

- Miya K, Inoue R, Takata Y, Abe M, Natsume R, Sakimura K, Hongou K, Miyawaki T, Mori H (2008) Serine racemase is predominantly localized in neurons in mouse brain. *J Comp Neurol* 510:641-654.
- Morikawa A, Hamase K, Zaitso K (2003) Determination of D-alanine in the rat central nervous system and periphery using column-switching high-performance liquid chromatography. *Anal Biochem* 312:66-72.
- Morikawa A, Hamase K, Inoue T, Konno R, Niwa A, Zaitso K (2001) Determination of free D-aspartic acid, D-serine and D-alanine in the brain of mutant mice lacking D-amino acid oxidase activity. *J Chromatogr B Biomed Sci Appl* 757:119-125.
- Morikawa A, Hamase K, Miyoshi Y, Koyanagi S, Ohdo S, Zaitso K (2008) Circadian changes of D-alanine and related compounds in rats and the effect of restricted feeding on their amounts. *J Chromatogr B Analyt Technol Biomed Life Sci*. 875:168-173.
- Mothet JP, Pollegioni L, Ouanounou G, Martineau M, Fossier P, Baux G (2005) Glutamate receptor activation triggers a calcium-dependent and SNARE protein-dependent release of the gliotransmitter D-serine. *Proc Natl Acad Sci U S A* 102:5606-5611.
- Nagata Y, Konno R, Niwa A (1994) Amino acid levels in D-alanine-administered mutant mice lacking D-amino acid oxidase. *Metabolism* 43:1153-1157.
- Neidle A, Dunlop DS (1990) Developmental changes in free D-aspartic acid in the chicken embryo and in the neonatal rat. *Life Sci* 46:1517-1522.
- Neumar RW et al. (2008) Post-Cardiac Arrest Syndrome. Epidemiology, Pathophysiology, Treatment, and Prognostication A Consensus Statement From the International Liaison Committee on Resuscitation (American Heart Association, Australian and New Zealand Council on Resuscitation, European Resuscitation Council, Heart and Stroke Foundation of Canada, InterAmerican Heart Foundation, Resuscitation Council of Asia, and the Resuscitation Council of Southern Africa); the American Heart Association Emergency Cardiovascular Care Committee; the Council on Cardiovascular Surgery and Anesthesia; the Council on Cardiopulmonary, Perioperative, and Critical Care; the Council on Clinical Cardiology; and the Stroke Council. *Circulation*.
- Nilsson A, Duan J, Mo-Boquist LL, Benedikz E, Sundstrom E (2007) Characterisation of the human NMDA receptor subunit NR3A glycine binding site. *Neuropharmacology* 52:1151-1159.

- North RY, Vigh G (2008) Determination of the operational pH value of a buffering membrane by an isoelectric trapping separation of a carrier ampholyte mixture. *Electrophoresis* 29:1077-1081.
- O'Brien KB, Bowser MT (2006) Measuring D-serine efflux from mouse cortical brain slices using online microdialysis-capillary electrophoresis. *Electrophoresis* 27:1949-1956.
- O'Brien KB, Miller RF, Bowser MT (2005) D-Serine uptake by isolated retinas is consistent with ASCT-mediated transport. *Neurosci Lett* 385:58-63.
- O'Brien KB, Esguerra M, Miller RF, Bowser MT (2004) Monitoring neurotransmitter release from isolated retinas using online microdialysis-capillary electrophoresis. *Anal Chem* 76:5069-5074.
- O'Brien KB, Esguerra M, Klug CT, Miller RF, Bowser MT (2003) A high-throughput on-line microdialysis-capillary assay for D-serine. *Electrophoresis* 24:1227-1235.
- Ohtani K, Tanaka H, Ohno Y (2003) SM-31900, a novel NMDA receptor glycine-binding site antagonist, reduces infarct volume induced by permanent middle cerebral artery occlusion in spontaneously hypertensive rats. *Neurochem Int* 42:375-384.
- Ohtani K, Tanaka H, Yasuda H, Maruoka Y, Kawabe A, Nakamura M (2000) Blocking the glycine-binding site of NMDA receptors prevents the progression of ischemic pathology induced by bilateral carotid artery occlusion in spontaneously hypertensive rats. *Brain Res* 871:311-318.
- Oliet SH, Mothet JP (2006) Molecular determinants of D-serine-mediated gliotransmission: from release to function. *Glia* 54:726-737.
- Panizzutti R, de Souza Leite M, Pinheiro CM, Meyer-Fernandes JR (2006) The occurrence of free D-alanine and an alanine racemase activity in *Leishmania amazonensis*. *FEMS Microbiol Lett* 256:16-21.
- Patzold R, Schieber A, Bruckner H (2005) Gas chromatographic quantification of free D-amino acids in higher vertebrates. *Biomed Chromatogr* 19:466-473.
- Pernot P, Mothet JP, Schuvailo O, Soldatkin A, Pollegioni L, Pilone M, Adeline MT, Cespuglio R, Marinesco S (2008) Characterization of a yeast D-amino acid oxidase microbiosensor for D-serine detection in the central nervous system. *Anal Chem* 80:1589-1597.

- Phillis JW, Ren J, O'Regan MH (2001) Studies on the effects of lactate transport inhibition, pyruvate, glucose and glutamine on amino acid, lactate and glucose release from the ischemic rat cerebral cortex. *J Neurochem* 76:247-257.
- Piehl N, Ludwig M, Belder D (2004) Subsecond chiral separations on a microchip. *Electrophoresis* 25:3848-3852.
- Quan Z, Liu YM (2003) Capillary electrophoretic separation of glutamate enantiomers in neural samples. *Electrophoresis* 24:1092-1096.
- Quan Z, Songa Y, Fengc Y, LeBlanc M, Liua Y (2005) Detection of d-serine in neural samples by saccharide enhanced chiral capillary electrophoresis. *Anal Chim Acta* 528:101-106.
- Rajewski RA (1990) Development and evaluation of the usefulness and parenteral safety of modified cyclodextrins. In: Department of Pharmaceutical Chemistry. Lawrence: University of Kansas.
- Rammouz G, Lacroix M, Garrigues JC, Poinot V, Couderc F (2007) The use of naphthalene-2,3-dicarboxaldehyde for the analysis of primary amines using high-performance liquid chromatography and capillary electrophoresis. *Biomed Chromatogr* 21:1223-1239.
- Ribeiro CS, Reis M, Panizzutti R, de Miranda J, Wolosker H (2002) Glial transport of the neuromodulator D-serine. *Brain Res* 929:202-209.
- Rizzi AM, Kremser L (1999) pKa shift-associated effects in enantioseparations by cyclodextrin-mediated capillary zone electrophoresis. *Electrophoresis* 20:2715-2722.
- Rosamond W et al. (2008) Heart disease and stroke statistics--2008 update: a report from the American Heart Association Statistics Committee and Stroke Statistics Subcommittee. *Circulation* 117:e25-146.
- Rutter AR, Fradley RL, Garrett EM, Chapman KL, Lawrence JM, Rosahl TW, Patel S (2007) Evidence from gene knockout studies implicates Asc-1 as the primary transporter mediating d-serine reuptake in the mouse CNS. *Eur J Neurosci* 25:1757-1766.
- Schell MJ, Molliver ME, Snyder SH (1995) D-serine, an endogenous synaptic modulator: localization to astrocytes and glutamate-stimulated release. *Proc Natl Acad Sci U S A* 92:3948-3952.
- Schell MJ, Cooper OB, Snyder SH (1997a) D-aspartate localizations imply neuronal and neuroendocrine roles. *Proc Natl Acad Sci U S A* 94:2013-2018.

- Schell MJ, Brady RO, Jr., Molliver ME, Snyder SH (1997b) D-serine as a neuromodulator: regional and developmental localizations in rat brain glia resemble NMDA receptors. *J Neurosci* 17:1604-1615.
- Schieber A, Bruckner H, Rupp-Classen M, Specht W, Nowitzki-Grimm S, Classen HG (1997) Evaluation of D-amino acid levels in rat by gas chromatography-selected ion monitoring mass spectrometry: no evidence for subacute toxicity of orally fed D-proline and D-aspartic acid. *J Chromatogr B Biomed Sci Appl* 691:1-12.
- Schmidt-Kastner R, Freund TF (1991) Selective vulnerability of the hippocampus in brain ischemia. *Neuroscience* 40:599-636.
- Schurig V (2001) Separation of enantiomers by gas chromatography. *J Chromatogr A* 906:275-299.
- Shen J, Rothman DL, Behar KL, Xu S (2009) Determination of the glutamate-glutamine cycling flux using two-compartment dynamic metabolic modeling is sensitive to astroglial dilution. *J Cereb Blood Flow Metab* 29:108-118.
- Shih CM, Lin CH (2005) Full-capillary sample stacking/sweeping-MEKC for the separation of naphthalene-2,3-dicarboxaldehyde-derivatized tryptophan and isoleucine. *Electrophoresis* 26:3495-3499.
- Shleper M, Kartvelishvily E, Wolosker H (2005) D-serine is the dominant endogenous coagonist for NMDA receptor neurotoxicity in organotypic hippocampal slices. *J Neurosci* 25:9413-9417.
- Silverstein FS, Naik B, Simpson J (1991) Hypoxia-ischemia stimulates hippocampal glutamate efflux in perinatal rat brain: an in vivo microdialysis study. *Pediatr Res* 30:587-590.
- Skanchy DJ, Xie GH, Tait RJ, Luna E, Demarest C, Stobaugh JF (1999) Application of sulfobutylether-beta-cyclodextrin with specific degrees of substitution for the enantioseparation of pharmaceutical mixtures by capillary electrophoresis. *Electrophoresis* 20:2638-2649.
- Song Y, Liang F, Liu YM (2007) Quantification of D-amino acids in the central nervous system of *Aplysia californica* by liquid chromatography/tandem mass spectrometry. *Rapid Commun Mass Spectrom* 21:73-77.
- Song Y, Feng Y, LeBlanc MH, Zhao S, Liu YM (2006) Assay of trace D-amino acids in neural tissue samples by capillary liquid chromatography/tandem mass spectrometry. *Anal Chem* 78:8121-8128.

- Song Y, Feng Y, Lu X, Zhao S, Liu C-W, Liu Y-M (2008) d-Amino acids in rat brain measured by liquid chromatography/tandem mass spectrometry. *Neurosci Lett* 445:53-57.
- Stalcup AM, Gahm KH (1996) Application of sulfated cyclodextrins to chiral separations by capillary zone electrophoresis. *Anal Chem* 68:1360-1368.
- Tait R, Skanchy D, Thompson D, Chetwyn N, Dunshee D, Rajewski R, Stella V, Stobaugh J (1992) Characterization of sulphoalkyl ether derivatives of β -cyclodextrin by capillary electrophoresis with indirect UV detection. *J Pharm Biomed Anal* 10:615-622.
- Takahashi K, Hayashi F, Nishikawa T (1997) In vivo evidence for the link between L- and D-serine metabolism in rat cerebral cortex. *J Neurochem* 69:1286-1290.
- Takeo K, Mitoh H, Uemura K (1989) Selective Chemical Modification of Cyclomalto-oligo-saccharides via tert-Butylmethylsilylation. *Carbohydr Res* 187:203-221.
- Takeo KI, Ueraura K, Mitoh H (1988) Derivatives Of alpha-Cyclodextrin and the Synthesis of 6-O-alpha-D-Glucopyranosyl-alpha-Cyclodextrin. *J Carbohydr Chem* 7:293-308.
- Thompson JE, Vickroy TW, Kennedy RT (1999) Rapid determination of aspartate enantiomers in tissue samples by microdialysis coupled on-line with capillary electrophoresis. *Anal Chem* 71:2379-2384.
- Thongkhao-On K, Kottegoda S, Pulido JS, Shippy SA (2004) Determination of amino acids in rat vitreous perfusates by capillary electrophoresis. *Electrophoresis* 25:2978-2984.
- Thorsen G, Bergquist J (2000) Chiral separation of amino acids in biological fluids by micellar electrokinetic chromatography with laser-induced fluorescence detection. *J Chromatogr B Biomed Sci Appl* 745:389-397.
- Thorsen G, Engstrom A, Josefsson B (1997) Enantiomeric determination of amino compounds with high sensitivity using the chiral reagents (+)- and (-)-1-(9-anthryl)-2-propyl chloroformate. *J Chromatogr A* 786:347-354.
- Tivesten A, Folestad S (1995) Separation of precolumn-labeled derivatization of D- and L-amino acids by micellar electrokinetic chromatography and UV and fluorescence detection. *J Chromatogr A* 708:323-337.
- Tivesten A, Folestad S (1997) Chiral o-phthaldialdehyde reagents for fluorogenic on-column labeling of D- and L-amino acids in micellar electrokinetic chromatography. *Electrophoresis* 18:970-977.

- Tojo Y, Hamase K, Nakata M, Morikawa A, Mita M, Ashida Y, Lindner W, Zaitso K (2008) Automated and simultaneous two-dimensional micro-high-performance liquid chromatographic determination of proline and hydroxyproline enantiomers in mammals. *J Chromatogr B Analyt Technol Biomed Life Sci* 875:174-179.
- Tsunoda M, Kato M, Fukushima T, Santa T, Homma H, Yanai H, Soga T, Imai K (1999) Determination of aspartic acid enantiomers in bio-samples by capillary electrophoresis. *Biomed Chromatogr* 13:335-339.
- Uchiyama-Tsuyuki Y, Araki H, Yae T, Otomo S (1994) Changes in the extracellular concentrations of amino acids in the rat striatum during transient focal cerebral ischemia. *J Neurochem* 62:1074-1078.
- Ueda T, Kitamura F, Mitchell R, Metcalf T, Kuwana T, Nakamoto A (1991) Chiral separation of naphthalene-2,3-dicarboxaldehyde-labeled amino acid enantiomers by cyclodextrin-modified micellar electrokinetic chromatography with laser-induced fluorescence detection. *Anal Chem* 63:2979-2981.
- Utsunomiya-Tate N, Endou H, Kanai Y (1996) Cloning and functional characterization of a system ASC-like Na⁺-dependent neutral amino acid transporter. *J Biol Chem* 271:14883-14890.
- Van Hemelrijck A, Sarre S, Smolders I, Michotte Y (2005) Determination of amino acids associated with cerebral ischaemia in rat brain microdialysates using narrowbore liquid chromatography and fluorescence detection. *J Neurosci Methods* 144:63-71.
- Vincent JB, Kirby DM, Nguyen TV, Vigh G (1997a) A Family of Single-Isomer Chiral Resolving Agents for Capillary Electrophoresis. 2. Hepta-6-sulfato-beta-cyclodextrin. *Anal Chem* 69:4419-4428.
- Vincent JB, Sokolowski AD, Nguyen TV, Vigh G (1997b) A Family of Single-Isomer Chiral Resolving Agents for Capillary Electrophoresis. 1. Heptakis(2,3-diacetyl-6-sulfato)-beta-cyclodextrin. *Anal Chem* 69:4226-4233.
- Wasterlain CG, Adams LM, Wichmann JK, Sofia RD (1996) Felbamate protects CA1 neurons from apoptosis in a gerbil model of global ischemia. *Stroke* 27:1236-1240.
- Weinberger R (2000) *Practical capillary electrophoresis*, 2nd Edition. San Diego, CA: Academic Press.

- Williams SM, Diaz CM, Macnab LT, Sullivan RK, Pow DV (2006) Immunocytochemical analysis of D-serine distribution in the mammalian brain reveals novel anatomical compartmentalizations in glia and neurons. *Glia* 53:401-411.
- Wolosker H (2007) NMDA receptor regulation by D-serine: new findings and perspectives. *Mol Neurobiol* 36:152-164.
- Wolosker H, Blackshaw S, Snyder SH (1999a) Serine racemase: a glial enzyme synthesizing D-serine to regulate glutamate-N-methyl-D-aspartate neurotransmission. *Proc Natl Acad Sci U S A* 96:13409-13414.
- Wolosker H, Sheth KN, Takahashi M, Mothet JP, Brady RO, Jr., Ferris CD, Snyder SH (1999b) Purification of serine racemase: biosynthesis of the neuromodulator D-serine. *Proc Natl Acad Sci U S A* 96:721-725.
- Wroblewski JT, Fadda E, Mazzetta J, Lazarewicz JW, Costa E (1989) Glycine and D-serine act as positive modulators of signal transduction at N-methyl-D-aspartate sensitive glutamate receptors in cultured cerebellar granule cells. *Neuropharmacology* 28:447-452.
- Xie X, Dumas T, Tang L, Brennan T, Reeder T, Thomas W, Klein RD, Flores J, O'Hara BF, Heller HC, Franken P (2005) Lack of the alanine-serine-cysteine transporter 1 causes tremors, seizures, and early postnatal death in mice. *Brain Res* 1052:212-221.
- Yang L, Yuan Z (1999) Comparison of enantioseparation of amino acid derivatives in aqueous and mixed aqueous-organic media by capillary zone electrophoresis. *Fresenius J Anal Chem* 365:541-544.
- Yang L, Zhang D, Yuan Z (2001) Enantioseparation of o-phthalaldehyde derivatized amino acids using β -CD-modified micellar electrokinetic chromatography in the mixed aqueous-organic media. *Anal Chim Acta* 433:23-30.
- Yao Y, Harrison CB, Freddolino PL, Schulten K, Mayer ML (2008) Molecular mechanism of ligand recognition by NR3 subtype glutamate receptors. *The EMBO J* 27:2158-2170.
- Zhao H, Hamase K, Morikawa A, Qiu Z, Zaitso K (2004) Determination of D- and L-enantiomers of threonine and allo-threonine in mammals using two-step high-performance liquid chromatography. *J Chromatogr B Analyt Technol Biomed Life Sci* 810:245-250.
- Zhao S, Liu YM (2001) Electrophoretic separation of tryptophan enantiomers in biological samples. *Electrophoresis* 22:2769-2774.

- Zhao S, Lifu Ym (2001) Quantification of amino acid enantiomers in single cells by capillary electrophoresis. *Cell Mol Biol (Noisy-le-Grand)* 47:1217-1222.
- Zhao S, Song Y, Liu YM (2005a) A novel capillary electrophoresis method for the determination of d-serine in neural samples. *Talanta* 67:212-216.
- Zhao S, Yuan H, Xiao D (2005b) Detection of D-Serine in rat brain by capillary electrophoresis with laser induced fluorescence detection. *J Chromatogr B Analyt Technol Biomed Life Sci* 822:334-338.
- Zhao S, Feng Y, LeBlanc MH, Liu YM (2001) Determination of free aspartic acid enantiomers in rat brain by capillary electrophoresis with laser-induced fluorescence detection. *J Chromatogr B Biomed Sci Appl* 762:97-101.
- Zhao S, Wang B, He M, Bai W, Chen L (2006) Determination of free D-alanine in the human plasma by capillary electrophoresis with optical fiber light-emitting diode-induced fluorescence detection. *Anal Chim Acta* 569:182-187.
- Zhu W, Vigh G (2000) A family of single-isomer, sulfated gamma-cyclodextrin chiral resolving agents for capillary electrophoresis. 1. Octakis(2,3-diacetyl-6-sulfato)-gamma-cyclodextrin. *Anal Chem* 72:310-317.
- Zhu W, Vigh G (2003) A family of single-isomer, sulfated gamma-cyclodextrin chiral resolving agents for capillary electrophoresis: octa(6-O-sulfo)-gamma-cyclodextrin. *Electrophoresis* 24:130-138.
- Zia V, Rajewski RA, Bornancini ER, Luna EA, Stella VJ (1997) Effect of alkyl chain length and degree of substitution on the complexation of sulfoalkyl ether beta-cyclodextrins with steroids. *J Pharm Sci* 86:220-224.